



National Library
of Canada

Bibliothèque nationale
du Canada

Canadian Theses Service Service des thèses canadiennes

Ottawa, Canada
K1A 0N4

NOTICE

The quality of this microform is heavily dependent upon the quality of the original thesis submitted for microfilming. Every effort has been made to ensure the highest quality of reproduction possible.

If pages are missing, contact the university which granted the degree.

Some pages may have indistinct print especially if the original pages were typed with a poor typewriter ribbon or if the university sent us an inferior photocopy.

Previously copyrighted materials (journal articles, published tests, etc.) are not filmed.

Reproduction in full or in part of this microform is governed by the Canadian Copyright Act, R.S.C. 1970, c. C-30.

AVIS

La qualité de cette microforme dépend grandement de la qualité de la thèse soumise au microfilmage. Nous avons tout fait pour assurer une qualité supérieure de reproduction.

S'il manque des pages, veuillez communiquer avec l'université qui a conféré le grade.

La qualité d'impression de certaines pages peut laisser à désirer, surtout si les pages originales ont été dactylographiées à l'aide d'un ruban usé ou si l'université nous a fait parvenir une photocopie de qualité inférieure.

Les documents qui font déjà l'objet d'un droit d'auteur (articles de revue, tests publiés, etc.) ne sont pas microfilmés.

La reproduction, même partielle, de cette microforme est soumise à la Loi canadienne sur le droit d'auteur, SRC 1970, c. C-30.

THE UNIVERSITY OF ALBERTA

GLACIAL GEOMORPHOLOGY AND LATE QUATERNARY HISTORY OF PHILLIPS
INLET AND THE WOOTTON PENINSULA, NORTHWEST ELLESMERE ISLAND,
CANADA.

©

by

DAVID J.A. EVANS B.A. HONS., M.SC.

A THESIS SUBMITTED TO THE FACULTY OF GRADUATE STUDIES
AND RESEARCH IN PARTIAL FULFILMENT OF THE REQUIREMENTS
FOR THE DEGREE OF DOCTOR OF PHILOSOPHY

DEPARTMENT OF GEOGRAPHY

EDMONTON, ALBERTA

FALL 1988

Permission has been granted to the National Library of Canada to microfilm this thesis and to lend or sell copies of the film.

The author (copyright owner) has reserved other publication rights, and neither the thesis nor extensive extracts from it may be printed or otherwise reproduced without his/her written permission.

L'autorisation a été accordée à la Bibliothèque nationale du Canada de microfilmer cette thèse et de prêter ou de vendre des exemplaires du film.

L'auteur (titulaire du droit d'auteur) se réserve les autres droits de publication; ni la thèse ni de longs extraits de celle-ci ne doivent être imprimés ou autrement reproduits sans son autorisation écrite.

ISBN 0-315-45669-8

National Library
of Canada

Canadian Theses Service

Bibliothèque nationale
du Canada

Service des thèses canadiennes

NOTICE

THE QUALITY OF THIS MICROFICHE IS HEAVILY DEPENDENT UPON THE QUALITY OF THE THESIS SUBMITTED FOR MICROFILMING.

UNFORTUNATELY THE COLOURED ILLUSTRATIONS OF THIS THESIS CAN ONLY YIELD DIFFERENT TONES OF GREY.

AVIS

LA QUALITE DE CETTE MICROFICHE DEPEND GRANDEMENT DE LA QUALITE DE LA THESE SOUMISE AU MICROFILMAGE.

MALHEUREUSEMENT, LES DIFFERENTES ILLUSTRATIONS EN COULEURS DE CETTE THESE NE PEUVENT DONNER QUE DES TEINTES DE GRIS.

THE UNIVERSITY OF ALBERTA

RELEASE FORM

NAME OF AUTHOR: DAVID J. A. EVANS

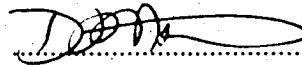
TITLE OF THESIS: GLACIAL GEOMORPHOLOGY AND LATE
QUATERNARY HISTORY OF PHILLIPS INLET AND THE
WOOTTON PENINSULA, NORTHWEST ELLESMEERE ISLAND,
CANADA.

DEGREE: DOCTOR OF PHILOSOPHY

YEAR THIS DEGREE GRANTED: 1988

Permission is hereby granted to THE UNIVERSITY OF ALBERTA
LIBRARY to reproduce single copies of this thesis and to lend or sell
such copies for private, scholarly or scientific purposes only.

The author reserves other publication rights, and neither the thesis
nor extensive extracts from it may be printed or otherwise reproduced without
the author's written permission.

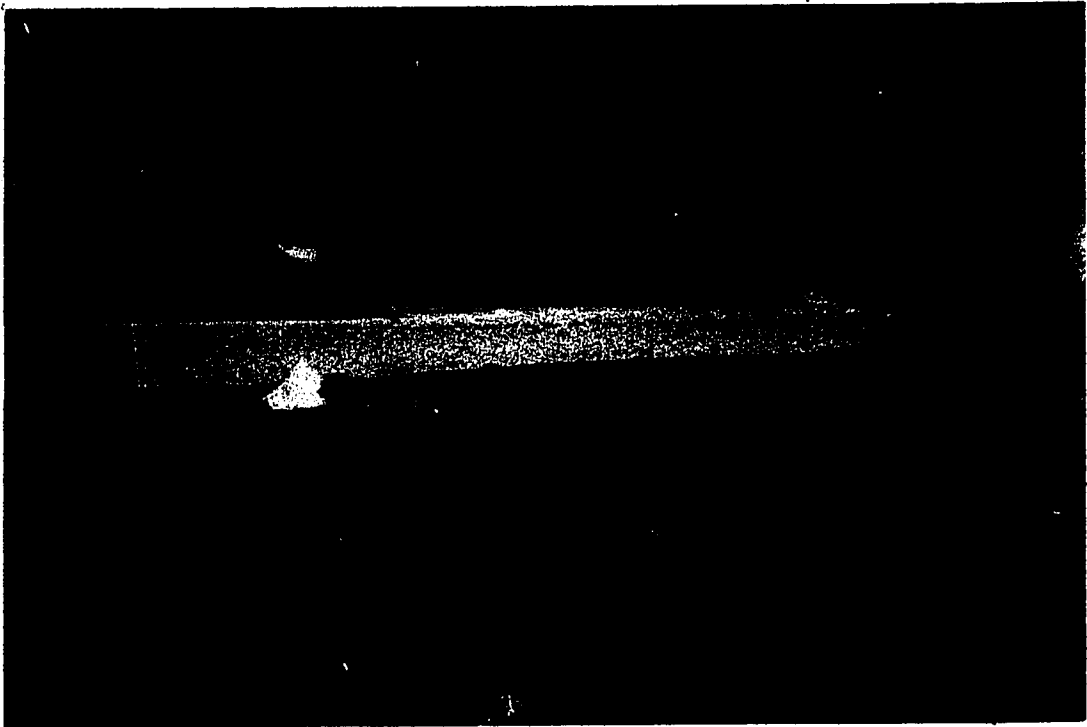


(Student's signature)

2 SOMERS ROAD
NORTH MYMMST
HATFIELD,
HERTFORDSHIRE,
AL9 7PL U.K.

(Student's permanent address)

Date: 10 JUNE 1988



*Little minds have only room for
thoughts of bread and butter.*
Roald Amundsen.

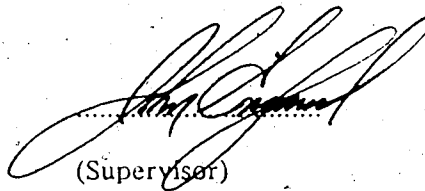
THE UNIVERSITY OF ALBERTA

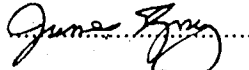
FACULTY OF GRADUATE STUDIES AND RESEARCH

The undersigned certify that they have read, and recommend to the Faculty of Graduate Studies and Research for acceptance, a thesis entitled
GLACIAL GEOMORPHOLOGY AND LATE QUATERNARY HISTORY OF
PHILLIPS INLET AND THE WOOTTON PENINSULA, NORTHWEST
ELLESMERE ISLAND, CANADA

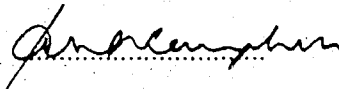
submitted by DAVID J.A. EVANS

in partial fulfilment of the requirements for the degree of DOCTOR OF
PHILOSOPHY.


.....
(Supervisor)


.....


.....


.....


.....

Date: 10 JUNE 1988

This thesis is for mum and dad, the keepers of the sacred,
infallible logic *once its gone its gone* and *I've had*
one out of that "packet".

ABSTRACT

Phillips Inlet and the Wootton Peninsula (2500km²) are located on the northwest coast of Ellesmere Island. From south to north there are three geologically controlled physiographic zones: 1) a 900m undulating plateau dissected by fiords; 2) a deeply fretted cirque terrain (>1200m); and 3) a 300m plateau bounded by coastal cliffs.

A 1:125,000 surficial geology and geomorphology map is compiled for the field area. Extensive surveying and dating (26 ¹⁴C dates) of raised marine sediments and shorelines provide a chronologic framework for the pattern of ice retreat and information on former ice configuration. Stratigraphic logs of ancient sediments and observations on contemporary glaciers are used to construct subclassifications of a glaciated valley landsystem.

Older, more extensive glaciers deposited erratics up to 660m asl and tills with shell fragments up to 450m asl. Raised marine sediments from earlier glaciations are rare. Some speculations on ancient topography and palaeoglaciology are formulated.

A subfossil peat dating 39ka BP provides a maximum age on the onset of the last glaciation. During the last glaciation glaciers advanced <10km from present margins. Moraines demarcate glacier margins at the fiord heads where piedmont lobes coalesced and floated in the sea. Morainal banks were deposited at the grounding lines of these glaciers and, where debris-charged basal ice occurred, subaqueous fans were deposited upon deglaciation. A palaeo-ELA of ca.300m asl is derived for the centre of the field area. Shells dating 20.2ka BP (<2km from present ice margin) and 14.9ka BP (from a morainal bank) document full glacial marine fauna. The restricted nature of the grounding lines suggests that extensive permanent landfast sea-ice and glacier and sea-ice shelves existed offshore.

An equidistant shoreline diagram is constructed using the 8.5ka BP shoreline as a guide. Tilts from 0.73m/km to 0.85m/km are calculated for this

shoreline. Using shoreline tilts from elsewhere on northern Ellesmere Island the 10.1ka BP marine limit descends from 112-117m asl at the fiord heads to 63-66m asl at the north coast.

Deglaciation started with a catastrophic calving phase throughout the field area between 10.1ka and 7.8ka BP. This chronology is similar to that from Clements Markham Inlet on the northeast coast and attests to the early Holocene warming trend recorded in high Arctic ice cores. A maximum lag of 2.1ka exists between the field area and Greely Fiord, lending further support to the previously postulated differences in glacioclimatic regimes on either side of the Grant Land Mountains.

ACKNOWLEDGEMENTS

The construction of a PhD thesis is a daunting task, one that can be achieved only with the help and encouragement of a lot of people. Firstly, I would like to thank my intrepid supervisor John "Greenshirt" England who characteristically has gone many steps beyond plain supervision. John has never been anything less than a good friend and a colleague throughout my three and a half years at the U. of A.. His honesty and unfailing barrage of masterful analogies have ensured that my own research has been critically evaluated from inception to binding. I have had many happy times at the U. of A. and John has been at the centre of many "magic moments in science". Impersonations of famous glacial geomorphologists will always be one of my favourites.

It seems like only last week that I failed A-level Geography and this is the ideal place to mention my mentor Mr J.E. Boden who sent me on my way back in 1979. Not only did Mr Boden's diligence help me to get a place at university but his keen interest in my later progress has assured me that this PhD means as much to him as it does to me. The success of any research programme relies heavily upon interaction and at the U. of A. I was privileged to share insights, discussions, harsh realities, seminars, doughnuts and uncontrollable giggles with the "scientists"; Don Lemmen, Tom Morris, Tom Stewart, Jan Bednarski, Hector Beaudet and Trevor Bell. Thanks to Dirk de Boer and Francien Niekus for the many light-hearted debates on real science and geomorphology and the world beyond candidacy exams. Thanks also to my committee members: Drs J.T. Gray; I.A. Campbell; R.B. Rains; and N.W. Rutter.

This thesis reports the findings of three very successful arctic field seasons in one of the most inaccessible areas of north America. The research would have been impossible without financial support from the Boreal Institute

of Northern Studies at the U. of A.. Invaluable logistical support was provided by the Polar Continental Shelf Project and funding for my final year of research came from the Department of Energy, Mines and Resources in Ottawa (Research Agreement No.88). NSERC grant no.A6680 awarded to John England and a grant from Atmospheric Environment Services, Canada have also contributed to financing this study. I would personally like to thank the people of Canada for funding my five year academic stay during a period when the government of the United Kingdom had fallen woefully short of its responsibilities to the scientific and academic community.

Working in the high Arctic requires a special breed of cultivated insanity and in this realm I would like to acknowledge my field assistants Tim (Aviator) Fisher 1985-1986 and Ulrika (Chocolate Sloth) Hawkins 1986-1987. Throughout my three field seasons Tim and Ulrika freely participated in my longest "mynds" and ski traverses, were cruelly subjected to hours of Billy Connolly and Monty Python and through their unfailing support and humour in uncomfortable weather (the eight day wind storm in Drift Pass will never be forgotten) contributed greatly to the success of the project. Together we have immortalized Logan pizzas, outrageously challenging golf courses, electrifying high latitude frisbee, head boiling, ridiculous river crossings and the bottomless tea pot. Philip (lobe monster) Friend delighted us with his own brand of river crossing in 1985. Mention also should be made to the pilots of Bradley Air Services and Quasar and Okanagan Helicopters; especially Karl Z'berg for landing us on a frighteningly short delta terrace in 1985 and John Pridie for showing us what it was like to have a helicopter pilot in the field who was genuinely interested in our science and insanity and who would take the calculated risks that insured our ultimate success.

Finally I would like to mention Sarah O'Hara who has shared with me the long months of separation and the mutual encouragement that have been part and parcel of the career building process. It must be worth it!

CONTENTS

	Page
CHAPTER ONE	
Introduction	1
1.1: Preface	1
1.2: General problems and objectives	2
1.3: Physiography and glaciology of northern Ellesmere Island	6
1.4: Past research and the present status of the glacial history of northern Ellesmere Island	11
1.4.1: Regional physiography and the development of a high latitude ice sheet	11
1.4.2: Events predating the last glaciation	13
1.4.3: The last glaciation	15
1.4.4: Holocene history	22
CHAPTER TWO	
The study area	26
2.1: General physiography of Phillips Inlet and the Wootton Peninsula	26
2.2: Geology of northern Ellesmere Island	31
2.3: Geology of Phillips Inlet and the Wootton Peninsula	34
2.3.1: Pearya	34
2.3.2: Clements Markham Fold Belt	34
2.3.3: Sverdrup Basin	35
2.3.4: Intrusions	35
2.3.5: Tectonics and structure	35

2.4: Climate	36
2.4.1: Regional climate	36
2.4.2: Local climate and ice cover	37
2.4.3: Glaciation level	40
2.4.4: Ice shelves and sea ice	42

CHAPTER THREE

Theory and methods	45
3.1: Introduction	45
3.2: Glacial geology and geomorphology	45
3.2.1: The landsystems approach	47
3.3: Glacimarine sediments	49
3.3.1: Introduction	49
3.3.2: Controls on glacimarine sedimentation	50
3.3.3: Glacimarine stratigraphy	53
3.4: Glacioisostasy	55
3.4.1: Introduction	57
3.4.2: Methodology for reconstructing deglacial and sea level history	57
3.4.2.1: Landforms	57
3.4.2.2: Surveying	58
3.4.2.3: Determining postglacial emergence	59

CHAPTER FOUR

Glacial geologic processes and a landsystems model for Phillips Inlet and the Wootton Peninsula	62
4.1: Introduction and glacier classifications	62
4.2: Observations on glacial geologic processes	62
4.2.1: The supraglacial system	65

4.2.2: Debris patterns within glacier margins	67
4.2.3: Contemporary proglacial processes	71
4.2.4: Contemporary glaci-tectonic structures and associated sediments	75
4.2.4.1: Definitions	75
4.2.4.2: Processes	78
4.2.4.3: Observations	79
4.3: Interpretations of glacial geologic processes and a landsystem model	90
4.3.1: Debris entrainment	90
4.3.2: Glacial tectonic processes and sediments	98
4.3.3: A landsystems model for Phillips Inlet and the Wootton Peninsula	106
4.3.3.1: General model	106
4.3.3.2: Depositional sequences	112
 CHAPTER FIVE	
Surface geology, geomorphology and stratigraphy	117
5.1: Introduction	117
5.2: Surficial geology map	117
5.2.1: Bedrock	119
5.2.2: Residuum	119
5.2.3: Till	119
5.2.4: Glacifluvial sediments	120
5.2.5: Glacilacustrine sediments	121
5.2.6: Raised marine sediments	121
5.2.7: Inactive alluvium	122
5.2.8: Active alluvium	122
5.2.9: Colluvium	122

5.3: Geomorphic and stratigraphic data	122
5.3.1: Introduction	122
5.3.2: Sector 1: Western Wootton Peninsula	123
5.3.2.1: General description	123
5.3.2.2: Geomorphology and stratigraphy	123
5.3.2.3: Interpretation	134
5.3.3: Sector 2: The Cape Wood coast	138
5.3.3.1: General description	138
5.3.3.2: Geomorphology and stratigraphy	138
5.3.3.3: Interpretation	144
5.3.4: Sector 3: Cape Armstrong and the Armstrong River valley	146
5.3.4.1: General description	146
5.3.4.2: Geomorphology and stratigraphy	148
5.3.4.3: Interpretation	151
5.3.5: Sector 4: Bushmill Pass/Ice Alley Fiord	153
5.3.5.1: General description	153
5.3.5.2: Geomorphology and stratigraphy	155
5.3.5.3: Interpretation	159
5.3.6: Sector 5: Drift Pass/Muskox River/Desperation Bay	163
5.3.6.1: General description	163
5.3.6.2: Geomorphology and stratigraphy	163
5.3.6.3: Interpretation	175
5.3.7: Sector 6: Bridge Street and Ice Alley Fiord	179
5.3.7.1: General description	180
5.3.7.2: Geomorphology and stratigraphy	180
5.3.7.3: Interpretation	185
5.3.8: Sector 7: Cache Head Fiord, Cache River and Garden Plateau	189

5.3.8.1: General description	189
5.3.8.2: Geomorphology and stratigraphy	192
5.3.8.3: Interpretation	199
5.3.9: Sector 8: Transition Fiord and The Promontory	203
5.3.9.1: General description	203
5.3.9.2: Geomorphology and stratigraphy	205
5.3.9.3: Interpretation	206
5.3.10: Sector 9: Phillips River and Berg Bay Fiord	208
5.3.10.1: General description	208
5.3.10.2: Geomorphology and stratigraphy	210
5.3.10.3: Interpretation	213
5.3.11: Sector 10: Wind Gap, Valley of the Blocks and Mymmshall Delta	214
5.3.11.1: General description	214
5.3.11.2: Geomorphology and stratigraphy	216
5.3.11.3: Interpretation	218
5.3.12: Summary	219
5.3.12.1: Sector 1	219
5.3.12.2: Sector 2	220
5.3.12.3: Sector 3	220
5.3.12.4: Sector 4	220
5.3.12.5: Sector 5	221
5.3.12.6: Sector 6	221
5.3.12.7: Sector 7	221
5.3.12.8: Sector 8	222
5.3.12.9: Sector 9	222
5.3.12.10: Sector 10	222

CHAPTER SIX

Discussion	224
6.1: Introduction	224
6.2: Events predating the last glaciation	224
6.3: The last glaciation	228
6.4: Sea level history	240
6.5: Holocene history	246
CHAPTER SEVEN	
Conclusions and future research	250
BIBLIOGRAPHY	254
APPENDIX 1	
Radiocarbon dating	267
APPENDIX 2	
Clast analyses	269
APPENDIX 3	
Glossary of glacioisostatic terms	278

LIST OF TABLES

Table	Description	Page
1.1:	Chronology of events from localized research on northern Ellesmere Island.	14
6.1:	Radiocarbon dates from the Phillips Inlet/Wootton Peninsula area.	234
6.2:	Chronology of Holocene geomorphic events from around the field area.	248

LIST OF FIGURES

Figure	Description	Page
1.1:	Northern Ellesmere Island official place names. ✓	7
1.2:	Northern Ellesmere Island geology.	8
1.3:	Northernmost Ellesmere Island physiographic zones and glaciology.	10
1.4:	Regional isobase maps from England and Bednarski (1986) for northeast Ellesmere Island and northwest Greenland.	18
1.5:	The emergence curve from the full glacial sea on northeast Ellesmere Island and patterns of emergence in a glaciated and partially glaciated reentrant.	20
1.6:	Map of northern Ellesmere Island and northwest Greenland showing the extent of the full glacial sea and the extent of the last glaciation (from England 1987b).	21
2.1a:	Place names of northern Phillips Inlet and the Wootton Peninsula.	27
2.1b:	Place names of southern Phillips Inlet.	28
2.2:	Air photograph of field area and physiographic zones 1, 1A and 2.	29
2.3:	Air photograph of physiographic zones 2 and 3.	30
2.4:	Geology of Phillips Inlet and the Wootton Peninsula.	33
2.5:	The glaciation level depicted along a transect X1-X4 on Figure 2.6.	38
2.6:	Glaciation level for Phillips Inlet and the Wootton Peninsula and generalized topography.	41
2.7:	The Cape Alfred Ernest Ice Shelf and the Alert Point Ice	

Cap air photograph mosaic from 1959.	44
3.1: Lithofacies characteristics at the margin of a floating glacier/ice shelf (after Drewry 1986).	51
3.2: Transgression and regression classifications from Curray (1964) and associated sedimentary facies successions as applied to an Arctic fiord by Bednarski (1984).	54
3.3: Depositional sequence resulting from the last glacial cycle in Clements Markham Inlet at 11-10ka BP (from Bednarski 1984).	56
4.1: Map of glaciers used in the analysis of glacial geologic processes and the construction of a landsystem model.	64
4.2: Above; part of air photograph no. A 16724-76 illustrating Tidewater Glacier, its tributary and resulting medial moraine. Below; stratified sands and gravels deposited in crevasse in medial moraine.	66
4.3: Supraglacial stream cutting down through the snout of Pudding Glacier in series of tight meanders.	68
4.4: Idealized sketch of a piedmont lobe with no proglacial thrusting.	70
4.5: Augen structures in Pudding Glacier.	72
4.6: Augen structure containing gravels and sands at the margin of Muskox Glacier.	73
4.7: Reentrained ice blocks from a former apron at the base of Pudding Glacier.	74
4.8: Lateral incision and ice block collapse over ice-cored gravel terraces at the margin of Terrible Glacier.	74

4.9: Sand/silt drape over stagnant ice at the margin of Muskox Glacier.	76
4.10: An ice-cored debris cone in a position of partial entrainment at the margin of Muskox Glacier.	76
4.11: Stagnant ice displaying recumbent folds and buried by alluvium at the margin of Endeavour Glacier.	77
4.12: Map of thrust block moraine and associated geomorphic features around the margin of Alfreds Glacier.	81
4.13: Dogleg Glacier and its thrust block moraine in Wind Gap.	83
4.14: Map of thrust block moraine and associated geomorphic features around the margin of Muskox Glacier as in 1959 and 1985/86.	84
4.15: Photograph of Muskox Glacier and its thrust block moraine from the air.	85
4.16a: Thrusted slice of marine silt, including shells in life position, at the base of Pudding Glacier.	87
4.16b: A possible explanation for the occurrence of such thrust slices in the basal debris-rich ice.	88
4.17: Intense folding in the basal debris-rich ice of Pudding Glacier.	89
4.18: Histograms of clast analyses from Terrible Glacier (5 samples) and from the marginal sediments (6 samples).	92
4.19: Cone of coarse, angular slate with rising folia at the snout of Muskox Glacier.	94
4.20: An explanation for the origin of gravel augens in the face of Endeavour Glacier.	97
4.21: Simplified time-sequence diagram of lateral entrainment of marginal stream bedload.	100

4.22: Landsystem model of piedmont lobe with thrust block moraine.	102
4.23: Composite of thrust block moraine, erosional and depositional processes and debris entrainment patterns at the snout of Pudding Glacier.	105
4.24: Map of present sublandsystems in Phillips Inlet/Wootton Peninsula.	107
4.25: Lithofacies codes from Miall (1977) and Eyles et al. (1983).	108
4.26: Coded vertical profiles showing diamicts and sediments associated with glacial landsystems and principal till types (from Eyles 1983 and Eyles et al. 1983).	109
4.27: The snout cliff of Kipper Glacier illustrating clean ice overriding an alluvial fan without initiating proglacial thrusting.	111
5.1: Surficial geology map.	Pocket
5.2: Sectors of the field area as discussed in Chapter 5.	118
5.3a: Place names of northern Phillips Inlet and the Wootton Peninsula.	124
5.3b: Place names of southern Phillips Inlet.	125
5.4: Map of glaciers mentioned in Chapter 5.	126
5.5: Map of radiocarbon dates from Phillips Inlet and the Wootton Peninsula.	127
5.6: View from the air of the coastal cliffs and calcareous plateau of sector 1, west Wootton Peninsula.	128
5.7: Air photograph no.17456-10 of the west Wootton Peninsula, illustrating major geomorphic features.	130
5.8: Thrust block (hummocky) moraines on south Cairn	

Peninsula.	131
5.9: Sea-ice push ridges up to 5m in height on Bumblebird Beacon.	131
5.10: Principal units of the stratigraphic section south of Alert Point.	133
5.11: Air photographs A16760-88 and 93 of the Cape Woods coast illustrating major geomorphic features.	139
5.12: The Cape Woods coastal cliff looking east.	140
5.13: The poorly lithified sandstone and gravel conglomerate bedrock with well lithified corestones outcropping below the gently undulating coastal piedmont to the west of the Cape Woods sector.	140
5.14: Kames on the cliff top of the eastern half of the Cape Woods coast.	142
5.15: Diamicton/boulder benches and ridges along the narrowest coastal strip below the cliff to the west of sector 2.	142
5.16: A quartz monzonite mega-block ($>5m^3$) lying on the low coastal strip of Cape Woods. The main cliff, from which sand and gravel deltas emanate, is visible in the background.	143
5.17: The small raised embayment to the west of Woods Glacier viewed from the lateral morainic ridge that seals it off from the coastal strip.	143
5.18: Air photograph no. A17456-27 of Cape Armstrong, the west Idris Peaks and Armstrong River illustrating major geomorphic features.	147
5.19: Looking south from the incipient felsenmeer of the northern Cache Plateau.	149

5.20: Air photograph no. A16858-91 of Bushmill Pass, the south Idris Peaks and Ice Alley Fiord illustrating major geomorphic features.	154
5.21: The Dodger Ice Cap and its outlet, Terrible Glacier from the north.	156
5.22: The north Idris Peaks and ice caps from the summit of one of the south Idris Peaks looking northwest out to the Arctic Ocean.	156
5.23: Well rounded erratics at 550m on a broad lower summit of the south Idris Peaks.	157
5.24: Looking north along the lateral moraine and 222m kame delta (arrowed) towards the Idris Peaks.	157
5.25a: Part of air photograph A 16866-63 illustrating Drift and lower Muskox River and the major geomorphic features of the area.	164
5.25b: Part of air photograph A 16760-83 illustrating Desperation Bay and the major geomorphic features of the area.	165
5.26: View to the northeast from the highest summit of the Western Pikes (915m) looking over the tors and felsenmeer developed in the granitic bedrock.	167
5.27: Deep meltwater channel cut into till veneer and bedrock along the southeast margin of Drift Pass.	167
5.28: The medial moraine/kame ridge as it grades into the diamicton moraine loop at the northeast end of Drift Pass.	168
5.29: Thrust block of shallow lacustrine sediments displaying 50° dip angle.	168
5.30: The upper outcrop of lacustrine sediments in central	

Muskox River valley.	170
5.31: Intense folding and faulting in the lacustrine sediments of the central Muskox River valley.	170
5.32: The moraine marking the margin of the lacustrine sediments in central Muskox River valley.	171
5.33: Composite stratigraphic log from the bluffs at the southwest end of Drift Pass.	172
5.34: The marine limit ice contact delta at 89m at the northeast end of Drift Pass.	174
5.35: Geomorphology of the headland to the north of outer Desperation Bay viewed from the Idris Peaks.	174
5.36: A prominent trimline in the Western Pikes representative of the extensive retreat of local cirque glaciers.	176
5.37: Air photograph no. A 16760-101 of Bridge Street and the head of Ice Alley Fiord illustrating major geomorphic features.	181
5.38: View of upper Bridge Street from the west illustrating the large number of terraces cut into alluvium and lacustrine sediments.	182
5.39: Heavily contorted and faulted braided outwash deposits on the north side of Bridge Street.	182
5.40: The section 750m from the Ice Alley Fiord shoreline exhibiting folded and contorted marine silts with occasional beds of gravelly diamicton overlying morainal bank.	184
5.41: The section at the margin of Pudding Glacier and the undulating fan through which the section is cut.	184
5.42: Stratigraphy of the section adjacent to the snout of	

Pudding Glacier.	186
5.43: Air photograph A 16724-81 of Cache Head Fiord, Cache River and surrounding highlands with major geomorphic features.	190
5.44: Well developed felsenmeer and tors of the Castle Range.	191
5.45: Looking east-southeast across the discontinuous till veneer of Garden Plateau towards Endeavour Glacier and the 600m ridge overlooking Cache River.	191
5.46: View to the north along Cache River from Garden Plateau illustrating the till veneer/blanket on the east side of the valley.	194
5.47: View of the east fiord head from the southwest.	194
5.48: Detailed stratigraphic logs along the east bank of the Cache River.	196
5.49: Faulted and contorted silts and sands at the base of section E-8 on the east bank of the upper Cache River.	198
5.50: Steeply dipping gravels and sands forming subaqueous fans and draped by laminated silts with dropstones at Storm Delta.	198
5.51: Air photograph no. A16978-35 showing the southern half of sector 8; Transition Fiord and The Promontory with major geomorphic features.	204
5.52: Air photograph no. A16606-15 showing Berg Bay Fiord, Phillips River, Napes River and surrounding highlands with major geomorphic features.	209
5.53: Section logs from the north side of Phillips River sandur.	212
5.54: Air photograph no. A16978-38 of Wind Gap, Valley of the Blocks and Dogleg Glacier with major geomorphic	

features.	215
5.55: Valley of the Blocks from the east illustrating the valley-in-valley form, the steep drop into the inlet head and the transition from dissected plateau in the south to the fretted cirque landscape in the north.	217
5.56: Telephoto across Tidewater Glacier of the western end of the bedrock ridge separating Valley of the Blocks and Wind Gap.	217
6.1: Map of radiocarbon dates of Phillip Inlet and the Wootton Peninsula.	226
6.2: Map of marine limit altitudes of Phillips Inlet and the Wootton Peninsula.	229
6.3a: Palaeogeography of Phillips Inlet and Wootton Peninsula at full glacial.	230
6.3b: Palaeogeography of Phillips Inlet and Wootton Peninsula at 7ka BP.	231
6.4: Equidistant shoreline diagram from Phillips Inlet and Wootton Peninsula aligned from X-Y on Figures 6.1 and 6.2.	233
6.5: Isobase map for northern Ellesmere Island at 10.1ka BP.	243
6.6: Equidistant shoreline diagram with heights of all shorelines and deltas surveyed in the field area plotted on the X-Y axis on Figures 6.1 and 6.2.	245

CHAPTER ONE

Introduction

"... those who support minimum versions of late Quaternary ice sheets actually prefer a world in which there are no ice sheets at all, and never were any such things. It is much easier to deny the existence of an ice sheet that is now gone, than one that is still here. So their strategy is to push back one margin of a former ice sheet here, and push back another margin there, in the hope that in time their descendants will succeed in convincing themselves, if not the rest of us, that there were no ice sheets at all. Ever."

T.J. Hughes, Boreas, 1980.

1.1: Preface.

Because of its physiography, glaciology and proximity to the Arctic Ocean, northern Ellesmere Island provides an ideal opportunity to study climatic change at high latitudes. This is augmented by the increasing concern about global climatic change induced by the greenhouse gases (Idso 1980, 1982; Schneider et al. 1980). Given the important role of high latitude snow and ice in such changes, the onus is upon scientists to cultivate a better understanding of the climatically sensitive high Arctic regions (Kellogg 1975).

Since the early reconnaissance work on geology, glaciology/ice shelves and geomorphology of the 1950's and 1960's several localised studies have been undertaken on the Quaternary/Holocene palaeoenvironments on northern Ellesmere Island and adjacent Greenland. Detailed work has been conducted on the late Quaternary glacial history of northeast and northern Ellesmere Island (cf. England and Bednarski 1986; Retelle 1986), northwest Greenland (cf. England 1985a), central Ellesmere Island (cf. Hodgson 1985), Greely Fiord/Nansen Sound (cf. England 1986a, b and c) and Otto Fiord (Bednarski 1987). Comprehensive summaries of the earlier work are available in England et al. (1981b) and Bednarski (1984). Several studies have been aimed at understanding Holocene glacier fluctuations and climatic change (eg. Hattersley-Smith and Long 1967; Hattersley-Smith 1969, 1972; Lyons et al. 1972; Lyons and Mielke 1973; England and Bradley 1978; Bradley and England 1979; Stewart 1981; Stewart and England

1983; Koerner and Fisher 1985; Bradley and Serreze 1987).

The primary objective of this study is to extend the data base developed principally by the Department of Geography, University of Alberta, on northern Ellesmere Island and northwest Greenland. This research has now been extended as far north and west as Clements Markham Inlet (Stewart 1981; Stewart and England 1983; Bednarski 1984, 1986; England and Bednarski 1986) and Greely Fiord/Otto Fiord (England 1986a, b and c; Bednarski 1987). My research extends this work to Phillips Inlet and the Wootton Peninsula on the northwest corner of the island. This area was visited previously by Hattersley-Smith's sled party in 1954 (cf. Hattersley-Smith et al. 1955) and by H.P. Trettin, R.L. Christie, T. Frisch, R. Thorsteinsson, and E.T. Tozer of the Geological Survey of Canada whilst undertaking reconnaissance mapping since 1956. A study in this area represents an ideal opportunity to investigate both ancient and contemporary glacial environments adjacent to the Arctic Ocean. The area's topographic diversity and steep decline in glaciation level from north to south also provide an opportunity to study changes in different glacio-/topoclimatic regimes. This study was initiated during the summer of 1985 and complements a similar study conducted by D.S. Lemmen on the Marvin Peninsula, 150km to the east.

1.2: General problems and objectives.

This research will address a number of controversial topics that have developed over the last three decades. These are concerned with the extent and style of glaciation in the high Arctic (cf. Blake 1970, 1975, 1977a and b; England 1976a and b, 1983, 1987b; England and Bradley 1978; England et al. 1981a; Hughes et al. 1977, 1985; and Hodgson 1985). The models of restricted glacial style for the last glaciation are presented largely by field workers, whereas the models of all-pervasive ice sheets are presented by theoretical reconstructions which persist in the literature (Chorley et al. 1984, chaps.

17 and 19; Reeh 1982, 1984; Hughes et al. 1985; Selby 1985, chap. 16).

Specifically this thesis is concerned with two objectives:

1. Determining the style and extent of past glaciations in the Phillips Inlet/Wootton Peninsula area using a glacial landsystems approach to reconstruct landform and depositional sequences (Eyles 1983). The Arctic Ocean has been referred to as an important moisture source for the growth of high latitude ice sheets (Ewing and Donn 1956, 1958; Donn and Shaw 1965; Donn and Ewing 1966) and this has fostered much discussion (Hattersley-Smith 1960a; Hunkins et al. 1971; Herman and Hopkins 1980; Clark 1982). England (1987b) has suggested that northern Ellesmere Island was characterized by great aridity during at least the last glaciation. This implies that the Arctic Ocean had very little effect on ice sheet growth. Using cores from the central Arctic Ocean, Clark et al. (1980) have concluded that there has been more or less continuous ice rafting for the last 5ma. However, the resolution here is far too imprecise to compare with the Holocene terrestrial record. Holocene sea ice variations have been reported by Blake (1972), Haggblom (1982) and Stewart and England (1983) and reconstructions of regional climatic change have been attempted. However, local variations in the response of glaciers to Holocene climatic change are rarely documented (Hattersley-Smith 1969; Blake 1981; Stewart and England 1983; Evans and Lemmen 1987). Furthermore, very little is known about the characteristics and dynamics of ice shelves off the northern Ellesmere Island coast before the Holocene (England et al. 1978). Extensive ice shelves have been postulated by Denton and Hughes (1981), Hughes et al. (1985), Dawes (1986) and Hughes (1987) as part of northern hemisphere maximum ice sheet models during the last glaciation. Mercer (1970), Broecker (1975), Hughes et al. (1977) and Grosswald (1980) have even suggested an Arctic Ice sheet.

The collection of Arctic Ocean cores has enabled researchers to estimate sedimentation rates in the Arctic Ocean since the Plio-Pleistocene

boundary (Hunkins et al. 1971; Clark et al. 1980; Herman and Hopkins 1980; Morris et al. 1985). This has led to the correlation of the onshore and offshore stratigraphies (Clark et al. 1984; Dalrymple and Maass 1987). However, many of these interpretations are simplistic (cf. Brigham-Grette et al. 1987). The exact relationships between Arctic Ocean deep sea cores and terrestrial glacial-non glacial sequences are still poorly understood and further terrestrial studies bordering the Arctic Ocean are warranted.

Biological refugia (Ives 1974) during the last glaciation have been proposed for northern Ellesmere Island by Leech (1966) Brassard (1971) and Brown (1985). The identification of nunataks or unglaciated enclaves adds support but not proof of refugia. These remain based upon disjunctions of certain vascular and non-vascular plants and insects rather than *in situ* fossils of full glacial age.

Little is known about glacial processes in high Arctic environments. Many of the theories on erosion and deposition by glaciers remain untested at high latitudes (Boulton 1970, 1972a and b, 1974, 1979; Shaw 1977a and b; Sugden 1977, 1978; England 1986c). Eyles (1983) has introduced a landsystems approach for the mapping and interpretation of glaciated terrain. There are presently no landsystem models for high latitude areas and the dynamics and entrainment patterns of sub-polar and polar glaciers remain poorly understood.

Finally, England (1985b, 1987) attempted to explain the physiography of the Canadian Arctic archipelago without invoking a pervasive and erosive regional glaciation. England proposes that the Arctic islands are a Tertiary fluvial landscape later fractured by block faulting. This fracturing essentially terminated the possibility of a regional ice sheet through the creation of fiords and marine channels which now constitute a permanent impasse to glaciers. If faulting has continued throughout the Quaternary then it follows that glaciations would have become progressively more restricted in style. This not only questions the theoretical arguments of

selective linear erosion (Sugden 1977, 1978) but also demands a reconciliation of the Tertiary and Quaternary landscapes (cf. Linton 1955; Bird 1967; Chorley et al. 1984, chap.2). England (1987b) emphasizes that it is critical to the accuracy of palaeoenvironmental reconstructions that landform/sediment assemblages are not misattributed to a narrow view of pervasive late Quaternary glaciations. Therefore, it is essential that further efforts are made to understand glacial geologic processes at high latitudes and to deduce to what extent the present landscape is a determinant rather than a product of glacial style.

2. Extending the existing glacioisostatic data base for northern Ellesmere Island and relating this to former centres of ice dispersal, glacial sediments and landforms within the area. Patterns of postglacial emergence and sea level histories have been interpreted in two very different ways. Blake (1970) interpreted an apparent ridge of greater emergence (since 5ka BP) running from Bathurst Island to Eureka Sound as evidence for a pervasive late Wisconsinan "Innuitian" ice sheet. England (1974a and b, 1976a and b) reinterpreted this data and through later work suggested that northeastern Ellesmere Island was dominated by the unloading of the northwest Greenland ice sheet following the last glaciation (England 1978, 1982, 1983, 1985a, 1986d; England and Bradley 1978; England et al. 1981a; England and Bednarski, 1986). This interpretation reduces Blake's ridge of high emergence to a saddle of lower emergence between northeastern Ellesmere Island and the central Arctic islands (dominated by the north-central Laurentide Ice Sheet). Glacial geologic and glacial marine stratigraphic observations have led England to conclude that a full glacial sea, rather than ice, occupied most of the fiords and interisland channels of the high Arctic throughout the last glaciation. *In situ* marine fauna from the full glacial sea range in age from early Holocene to >33ka BP (England 1985a). However, the paucity of finite ¹⁴C dates >11ka BP (cf. Andrews 1975a) and a general uncertainty of the validity

of such "old" ^{14}C dates (cf. Appendix 1) has led other researchers to question the validity of the full glacial sea (Bennike et al. 1987).

High Arctic ice cores have been used to make palaeoenvironmental interpretations and to reconstruct former ice divides (Dansgaard et al. 1971, 1973; Koerner and Paterson 1974; Koerner 1977a and b, 1979; Paterson 1977; Fisher and Koerner 1980, 1983; Koerner and Fisher 1981, 1985; England et al. 1982; Gemmell et al. 1986; Koerner et al. 1987). Interpretations of former ice thickness using ice core evidence have accommodated both maximum and minimum ice sheet reconstructions (Paterson 1977) although recent papers have favoured restricted ice volumes, at least during the last glaciation (Koerner et al. 1987).

1.3: Physiography and glaciology of northern Ellesmere Island.

Northern Ellesmere Island is defined here as the area bounded by the Arctic Ocean to the north, Nares Strait to the east, the Victoria and Albert Mountains to the south and Nansen Sound to the west (Fig.1.1). The general physiography comprises the Grant Land Mountains (>2000m) to the north and northwest and the Hazen Plateau (300-1300m) to the southeast. The mountain ranges and the Hazen Plateau are part of the Innuitian Orogenic System which trends northeast-southwest (Trettin 1972). The north coast fiords are 40-90km long reentrants joining the ice fields of the Grant Land Mountains to the Arctic Ocean. Phillips Inlet is a composite made up of an east-west trending reentrant with four north-south trending tributary fiords. To the west, the Grant Land Mountains give way to the Hvitland and Svartfjeld Peninsula's (1000m). This general westward decline in the topography is broken to the northwest by the highlands of the Wootton Peninsula (2000m). The "Lake Hazen Fault Zone" forms the southern limit of the Grant Land Mountains on northern Ellesmere Island and is the northern boundary of the Hazen Plateau (Christie 1964; Trettin 1969, 1971; Fig.1.2). Across the Lake Hazen Fault the mountains

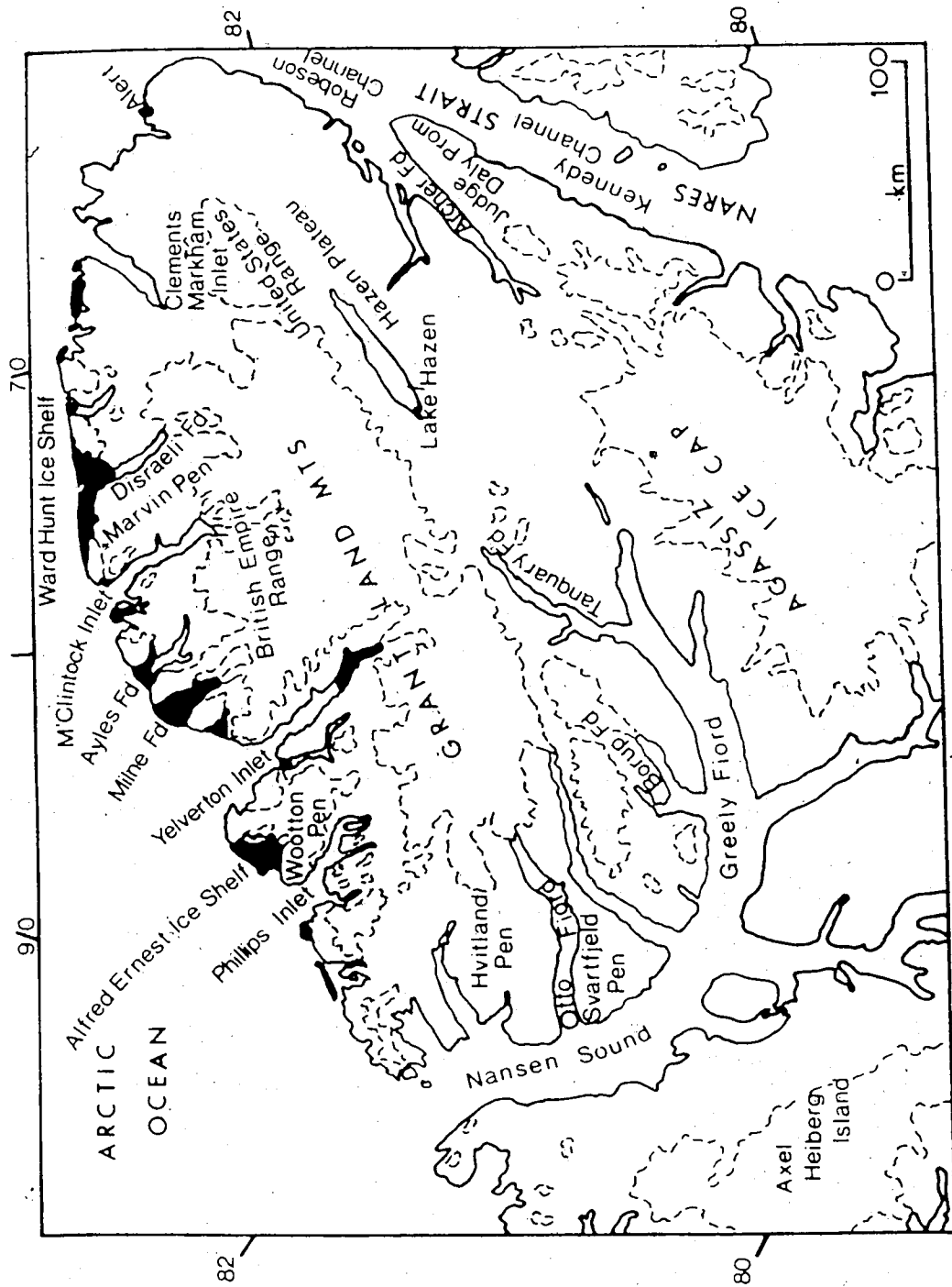


Figure 1.1: Northern Ellesmere Island official place names. Ice shelves in black and ice bodies outlined by broken line.

PAGE REMOVED DUE TO COPYRIGHT
RESTRICTIONS

Figure 1.2: Northern Ellesmere Island geology (from Trettin 1987).

descend from ca.2500m to ca.300m at Lake Hazen.

Although the geology is extremely complex, three general physiographic zones can be distinguished north of the Grant Land Mountains (Fig.1.3): 1. Parts of the northernmost coast of Ellesmere Island are deeply fretted terrains, with relief generally >1000m. These terrains are largely composed of coarse crystalline plutons of the Pearya geanticline (Frisch 1974; Trettin and Frisch 1981; Trettin 1987). In some areas, such as the north Wootton Peninsula, low coastal plains (1a) are composed of metamorphosed carbonates and Tertiary sandstones and mudrocks (Trettin and Frisch 1981; Trettin 1987); 2. South of zone 1 and north of the main Grant Land Mountains, clastic and carbonate sedimentary rocks of the Clements Markham Fold Belt (Trettin 1987) form an undulating plateau dissected by the north coast fiords and through-valleys. The largest of these fiords, Yelverton Inlet, is 90km long and penetrates the Grant Land Mountains to the south. A similar terrain within Pearya geanticline rocks exists between Markham and Ayles Fiords; 3. The northern Grant Land Mountains are composed of limestone, sandstone and conglomerate facies of the Sverdrup Basin (Christie 1964). This constitutes the highest relief in the field area.

The physiographic zones are most pronounced on northwest Ellesmere Island and largely control the distribution of ice. The Grant Land Mountains host a large icefield through which many peaks protrude as nunataks. The equilibrium line altitude (ELA) in this area is 1200m (Miller et al. 1975). These icefields feed major, north flowing trunk glaciers that either float in the larger fiords (Disraeli Fiord, M'Clintock Inlet, Milne Fiord, Yelverton Inlet) or terminate in the interior valleys leading to them (Phillips Inlet, Ayles Fiord, Clements Markham Inlet). The ice caps attain a maximum thickness of 900m whereas the maximum depths on major trunk glaciers range from 600-700m (Hattersley-Smith et al. 1969). The topography of zone 2 hosts a number of plateau ice caps (<400km²) whose outlet glaciers descend into fiords or fiord



Figure 1.3: Northernmost Ellesmere Island physiographic zones and glaciology.
1. north coast mountainous, cirque terrain; 1A. coastal lowlands; 2. central plateau with fjords; 3. northern Grant Land Mountains.

head valleys. Nonetheless, extensive areas of upland are ice-free. Zone 1 is an area of cirque and transection glaciers with an ice cover of >50%. This ice cover persists on the coastal lowlands of zone 1a where the ELA descends to sea level. Here the proximity of the Arctic Ocean with its frequent fog and pack ice has facilitated the growth of ice shelves which are often fed by outlet glaciers. Distinctions may be made between glacier ice shelves, which are essentially floating ice tongues, and sea-ice shelves which are composed of land-fast multi-year sea ice with a freeboard >2m (Hattersley-Smith et al. 1955; Marshall 1955; Hattersley-Smith 1957; Cray 1958, 1960; Lyons et al. 1972; Stewart and England 1983; Lemmen et al. 1988). A full discussion of ice shelves is available in England et al. (1981b) and Jeffries (1987).

1.4: Past research and the present status of the glacial history of northern Ellesmere Island.

1.4.1: Regional physiography and the development of a high latitude ice sheet.

The debate over a glacial versus tectonic origin for fiord landscapes is almost a century old. Gregory (1913) made a valid summary:

"It has been claimed that this controversy has been between the physiographers and the experts on glaciers. The physiographers, it is said, have been driven to attribute to glaciers great powers of erosion in order to explain otherwise puzzling physiographic features."

"Their position, according to Professor Fairchild (1905), shelters behind a bulwark of analogy and assumption..."

Fortier and Morley (1956), Horn (1963) and Pelletier (1966, 1979) proposed that the fiords and interisland channels of Arctic Canada were Tertiary river valleys that were overdeepened by glacial erosion. This view was supported by Blake (1970) who used the physiography of the Queen Elizabeth Islands, together with scattered erratics and an apparent ridge of greater

emergence over central Ellesmere Island, to support his Innuitian Ice Sheet concept. Indeed, more localised studies have invoked large-scale erosion by trunk glaciers to explain the overdeepened fiords (up to 800m) of northern Ellesmere Island (Crary 1956; Hattersley-Smith 1969). Others have identified areas of differential erosion by using the distribution of erratics and fiords (Taylor 1956; Smith 1959, 1961; Hattersley-Smith 1961). These views were given theoretical credibility by Sugden (1977, 1978) when he introduced the concept of selective linear erosion. In this model warm-based ice streams are channelled down existing drainage systems, overdeepening them and forming glacial troughs. Interfiord highlands are protected by inert cold-based ice. Large circumpolar ice sheets have thus been popularized in recent literature (CLIMAP 1976; Hughes et al. 1977, 1985; Denton and Hughes 1981; Selby 1985; Denton et al. 1986).

The tectonic evolution of the high Arctic has been largely ignored by those who favour highly erosive ice sheets. This continues despite many papers that show the interisland channels to be controlled by faulting (cf. Bornhold et al. 1976; Thorsteinsson and Tozer 1976; Kerr 1980; Sobczak 1982). As early as the turn of the century Schei (1904) and Gregory (1913) had favoured a tectonic origin. This has been addressed by England (1987b) who envisages the Arctic Islands as a set of horsts and grabens. The exact ages of these features are unknown but Kerr (1980) places the faulting at least as late as Miocene or Pliocene. England (1987b) suggests that the faulting postdates not only the late Tertiary regional drainage but possibly the maximum distribution of glacial erratics as well. He further proposed that before this event a contiguous land mass and a more temperate climate arising from an open Arctic Ocean (Funder et al. 1984) would have been more favourable to regional glaciation. Since that time the landscape has been progressively fractured, ending the possibility of regional ice sheets. Today the principal obstacles to glaciers in Arctic Canada are aridity and calving. For Ellesmere Island

England (1985b) suggests that a hierarchy of fiord ages may be appropriate.

This he bases upon glacial geomorphic evidence to be discussed in the following section.

1.4.2: Events predating the last glaciation.

Evidence that northern Ellesmere Island was once largely inundated by ice comes from glacial erratics and high-elevation meltwater channels (cf. England and Bednarski, in press). The first mapping of erratics was by Christie (1967), England (1974a and b, 1978) and England et al. (1981a) who delineated the maximum incursion of the Greenland ice sheet onto Ellesmere Island using granite and gneiss erratics. This oldest and most extensive glaciation advanced between 5-15km onto Judge Daly Promontory and was originally tentatively dated at >80ka BP using amino acid ratios on shells (England and Bradley 1978). This date has since been revised to between 500ka and 1ma BP based upon comparisons with amino acid ratios from elsewhere in the Arctic (England 1987b; Table 1.1). Retelle (1986) has mapped the maximum advance of Greenland ice onto Ellesmere Island in the Robeson Channel area and concludes that it extended at least 20km inland. This advance he tentatively dates 70ka BP based upon amino acid ratios.

The subsequent glaciation in this area was by Ellesmere Island ice which cross-cut the Greenland till and deposited ice-shelf moraines at the outer coast. Raised marine sediments up to 175m asl are associated with this advance and are dated >35ka BP (England and Bradley 1978; England et al. 1978; 1981a). Retelle (1986) considers the sediments associated with this Ellesmere advance as deglacial. During the retreat of the Greenland ice sheet from northeastern Ellesmere Island, fossiliferous marine sediments were deposited in contact with glacial lobes as they allowed the incursion of the sea to 286m asl. Retelle's interpretation is based upon local glacial geomorphology and stratigraphy and the clustering of shell samples into two groups; the Beaufort

Table 1.1: Chronology and events from localized research on northern Ellesmere Island

England 1974a,b 1978 & Bradley 1978 et al. 1978	Archer Fiord/Lady Franklin Bay, N. Judge Daly Prom.	Deglaciation 8.1-8.4ka M.L. 120m Last glaciation Hazen Moraines. Ice free corridor between Greenland and Ellesmere Is.	Deglaciation 28-30ka M.L. 105m Ellesmere advance >35ka M.L. 175m Zone II Greenland advance Zone IIIA >80ka Zone IIIB unglaciated.	England et al. 1981	Western Kennedy Channel	Ice marginal depression M.L. 100m 12.3-8ka	England 1983	NE Ellesmere NW Greenland	Rapid deglaciation and unloading <6.2ka Slow emergence 8-6.2ka Full glacial sea 11-8ka	England 1985	Hall Land	Unloading <8.2ka Glacial advance 40-60km Full glacial sea 8.2->33ka M.L. 150m	Tedrow 1970 Weidick 1976, 1978 Christie 1975. Davies 1972	NW Greenland	Late glacial re-advance 3 12-50km 6.1-3.7ka Deglaciation 10ka Marine sed. 19ka, not overridden Fluvial terrace 20.8ka Glacial 2 advance Glacial 1 advance ice reached Ellesmere Is.	Reille 1986	West Robeson Channel	Initial emergence 8.6-8ka Beaufort Aminozone Hazen Moraines M.L. 116m Robeson aminozone Deglaciation from Greenland advance with assoc. shoreline at 286m Greenland advance 70ka	Bednarski 1984 1986	Clements Markham Inlet	Deglaciation 9.8-8ka Last glaciation 40km advance M.L. 124m 9.8ka Old glaciation inundated Inlet	Bednarski 1987	Otto Fiord	Deglaciation 9.1ka Marine transgression to 116m 30.2ka Upper till Marine sediments Lower till	England 1987b	General	Zone IIIA Greenland advance 500ka-1ma	Hodgson 1985	West central Ellesmere Island	Advance to drift belt 10-60k.m 9-7ka Older till
--	---	--	--	---------------------------	-------------------------------	--	-----------------	------------------------------	--	-----------------	--------------	---	--	-----------------	--	----------------	----------------------------	---	---------------------------	------------------------------	--	-------------------	---------------	--	------------------	---------	--	-----------------	--	---

Aminozone (Holocene) and the Robeson Aminozone (pre-Holocene). If Retelle's interpretations are correct then the Ellesmere Island advance (dated >35ka BP by England 1974a and b, 1978; England and Bradley 1978; and England et al. 1978) would become a stillstand during general retreat of the Greenland ice sheet.

Older glaciations have also been documented on adjacent northwest Greenland. Tedrow (1970), Davies (1972), Christie (1975) and Weidick (1976) have all reported evidence of two older glacial advances. Tedrow (1970) suggests that during the oldest of these advances ice advanced onto northern Ellesmere Island. For Otto Fiord, west Ellesmere Island, Bednarski (1987) has reported two tills separated by marine sediments, all of which likely predate 30.2ka BP. Other than these localised studies the evidence for older glaciations is sparse and is usually restricted to high-elevation erratics, the origins of which are uncertain (England 1987b).

1.4.3: The last glaciation.

Some authors continue to propose models of all-pervasive ice sheets in the high Arctic during the last glaciation (eg. Blake 1970; CLIMAP 1976; Hughes et al. 1977, 1985; Denton and Hughes 1981). The debate of maximum versus minimum ice sheet coverage began at the turn of the century when Daly (1902) and Coleman (1920) suggested that large nunataks existed within the Torngat Mountains of northern Labrador during the maximum ice advance. This idea was refuted by Odell (1938) whose interpretations of complete inundation by ice were uncritically preferred by Flint (1971). Since that time the late Wisconsinan "maximum" school has persisted largely on the basis of theoretical reconstructions (Dansgaard et al. 1973; Sugden 1977, 1978; Reeh 1984). For a comprehensive review of the debate the reader is referred to Ives (1978).

The glacial geologic evidence cited in support of an all-pervasive ice sheet on Ellesmere Island during the last glaciation includes high elevation

erratics, well preserved striae and postglacial emergence patterns.

Specifically, Blake (1970) showed a ridge of greatest emergence running from central Ellesmere Island to Bathurst Island at 5ka BP which he ascribed to a preceding "Innuitian ice sheet". The Innuitian ice sheet was presumably responsible for the excavation of the fiords and interisland channels and served to join the Laurentide and Greenland Ice Sheets. The presence of the Innuitian Ice Sheet during the last glaciation has been questioned extensively by England (1976a and b, 1986a, c and d) and England et al. (1981a). England (1976a and b, 1982) reconstructed different postglacial isobases for the Queen Elizabeth Islands (7.5ka BP) which show the glacioisostatic dominance of the Greenland ice sheet to the east. In this reconstruction, Blake's (1970) ridge of emergence becomes a saddle joining the greatest emergence caused by the Laurentide ice sheet to the south with that of the Greenland Ice Sheet to the north. England proposed that a non-contiguous ice cover over the Queen Elizabeth Islands (termed the "Franklin Ice Complex"), together with the northwest Greenland Ice Sheet, was capable of producing the regional patterns of postglacial isobases.

England (1983), Bednarski (1984, 1986) and England and Bednarski (1986) have subsequently collected more emergence data from northern Ellesmere Island and northwest Greenland and connected this to specific ice margins. They concluded that a full glacial sea rather than glacial ice occupied numerous fiords and channels of northern Greenland and Ellesmere Island throughout the last glaciation. Isobases drawn on the limit of the full glacial sea (10ka BP) record the relative magnitude of the last glacial ice load. This had two centres: the largest coincides with the northwest coast of Greenland, whereas the second smaller centre represents an independent centre over the Grant Land Mountains (Fig.1.4). Furthermore, these isobases reveal a lag of 2ka between initial ice retreat on the north coast of Ellesmere Island versus the area of northern Nares Strait, separating Ellesmere Island and Greenland. This is

Figure 1.4: Regional isobase maps from England and Bednarski (1986) for northeast Ellesmere Island and northwest Greenland with site numbers from that paper in bold. A: isobases at 10ka. B: isobases at 8ka. C: isobases at 6ka.

PAGE REMOVED DUE TO COPYRIGHT
RESTRICTIONS

thought to reflect the difference in glacioclimatic regimes north and south of the Grant Land Mountains as well as the differential response rates between Greenland and Ellesmere Island ice.

Beyond the last glacial limit on northeast Ellesmere Island, emergence curves from the full glacial sea are characterized by: 1. an interval of stable relative sea level at the marine limit 11-8ka BP; 2. an interval of slow emergence from 8-6.2ka BP marked by slow retreat of the Ellesmere Island ice; and 3. a period of rapid emergence as a result of rapid glacial unloading after 6.2ka BP (England 1983; Fig.1.5). Along the west coast of Robeson Channel, the last glaciation was characterized by small plateau ice caps whose outlet glaciers contacted the sea in some embayments (Retelle 1986). Elsewhere on this coast the full glacial sea reached 116m and trimmed weathered deposits of previous glaciations. Initial emergence occurred between 8 and 8.6ka BP. On the adjacent coast of Hall Land, northwest Greenland, England (1985a) reports a 40-60km advance of the Petermann and Newmann Bay glaciers during the last glaciation (Fig.1.6). *In situ* shells from the full glacial sea date from 8.2 to >33ka BP. From these dates England suggests that the Greenland ice sheet must have reached its limit well before the attainment of isostatic equilibrium at 10ka BP. Initial retreat from the last ice limit on Hall Land occurred around 8.2ka BP coinciding with the initial emergence of northeast Ellesmere Island. Bednarski (1984, 1986) mapped the limits of a major trunk glacier and other outlet glaciers which left a full glacial sea occupying much of Clements Markham Inlet (Fig.1.6). In this area very slow retreat and emergence began at 9.8ka and lasted until 8ka BP after which the rates increased substantially.

On west-central Ellesmere Island, England (1987b) has mapped an advance of approximately 15km at the head of Greely Fiord (Fig.1.6) where glaciers formed ice shelves within the full glacial sea at 140m asl. Dates on *in situ* shells indicate that the full glacial sea remained at marine limit

PAGE REMOVED DUE TO COPYRIGHT
RESTRICTIONS

Figure 1.5: The emergence curve from the full glacial sea on northeast Ellesmere Island and patterns of emergence in a glaciated and partially glaciated reentrant. A period of stable sea level is followed by a period of slow emergence which is in turn followed by "normal" emergence (Andrews 1970) up to the present (from England 1983).

PAGE REMOVED DUE TO COPYRIGHT
RESTRICTIONS

Figure 1.6: Map of northern Ellesmere Island and northwest Greenland showing the extent of the full glacial sea and the extent of the last glaciation (from England 1987b).

from 9.1ka to 7.8ka BP. Deglaciation and emergence commenced at approximately 7.5ka BP. The limit of the full glacial sea in Greely Fiord trims weathered terrain which England (1987b) describes as a non-glacial landscape.

1.4.4: Holocene history.

Particularly good records of Holocene climatic change are available in the ice cores collected from the Greenland, Ellesmere, Meighen and Devon Ice Caps (Dansgaard et al. 1971; Koerner and Paterson 1974; Koerner 1977a and b, 1979; Paterson et al. 1977; Fisher and Koerner 1980, 1983; Koerner and Fisher 1985) and a good discussion of the technique is available in Bradley (1985, Chap.5). A period of maximum postglacial warmth between 8ka and 4ka BP has been proposed from the Camp Century ice core on Greenland (Dansgaard et al. 1971). The core reveals a variable cooling trend after 4ka. In contrast, Fisher and Koerner (1980) report a period of increasing postglacial warmth from 10ka to 8.3ka BP based on the Devon Island ice core. After 8.3ka BP temperatures reached a plateau about which they oscillated until 4.5ka to 5ka BP, the period of maximum postglacial warmth. From 4.5ka BP to the present there has been a progressive cooling at the Devon Island site. Furthermore, Koerner and Paterson (1974) report the formation of the Meighen Ice Cap between 3ka and 4.5ka BP, marking the end of the postglacial climatic optimum. The Little Ice Age, dating from approximately 100 to 400 years BP, is well represented in all cores (cf. Alt 1985).

Another important indicator of Holocene climatic change in the high Arctic is the abundance of driftwood through time (Blake 1972, 1987b; Haggblom 1982; Stewart and England 1983). Stewart and England (1983) have reconstructed three periods of driftwood abundance using all of the dates available from the Canadian and Greenland high Arctic. Their Period 1 extends from 8.9ka to 4.2ka BP during which driftwood penetration increases, with a period of greatest abundance between 6ka and 4.2ka BP. This is interpreted as the period with the

least summer sea ice. Period 2 dates from 4.2ka to 500 years BP when driftwood was sparse and summer sea ice had increased. In the time since 500 years BP (Period 3) driftwood penetration exceeds that of the previous periods and hence sea ice conditions had improved. Stewart and England (1983) also report 25 species of subfossil bryophytes and a disjunct marine pelycypod *Limatula subauriculata* (presently subarctic-boreal) dating 6.4ka BP from Clements Markham Inlet. These represent a period of increased plant productivity and of greater warmth and precipitation associated with a more open Arctic Ocean.

Driftwood has been used to date the formation of the northern Ellesmere Island ice shelves. Because increased open water would cause ice shelves to calve, their age of formation is a good indicator of climatic deterioration. Lyons and Mielke (1973) obtained dates of 3.4ka and 3ka BP on driftwood behind the Ward Hunt Ice Shelf. Because the wood may have penetrated a moat behind the ice shelf they suggested that the age of formation was >3.4ka BP. Basally accreted marine organics dated 3.3ka, 3.4ka, 3.6ka, 3.7ka and 4.5ka BP (Lyons and Mielke 1973). Blake (1987b) has published several dates between 3ka and 6ka BP on driftwood behind the Ward Hunt Ice Shelf. Twenty-five pieces of driftwood have been observed at 45-65cm above high tide behind the Ward Hunt Ice Shelf (Evans and Lemmen 1987).

There is less chronologic control on the response rates of the glacial systems of northern Ellesmere Island. From the evidence discussed above it is clear that a mid-Holocene climatic deterioration occurred during which the ice shelves (specifically the Ward Hunt) appear to have formed. From 100 to 400 years BP the Little Ice Age is recorded in the high Arctic ice caps as a period of accumulation. Glacial geologic evidence of the mid-Holocene cooling on northern Ellesmere Island comes from Tanquary Fiord, where Hattersley-Smith (1969) reports buried organics dating 4ka BP, and from the Eugene Glacier on the northern Hazen Plateau where similar material underlying till dates 4.9ka BP (Lowden and Blake 1979). Hattersley-Smith (1969) reported that many

glaciers on northern Ellesmere Island are advancing while smaller glaciers are retreating, indicating a predictable lag in glacier response rates (cf.

Andrews 1975b). Blake (1975, 1981) has reported glacier advances over Holocene beaches and peats on southern Ellesmere Island at 1ka and 100 years BP.

Hattersley-Smith et al. (1955), Christie (1967), Hattersley-Smith (1969),

Blake (1975) and Stewart and England (1983) have observed that many glaciers are at, or retreating from, their maximum postglacial positions. Stewart and

England (1983) have suggested that many glaciers on northern Ellesmere Island are still responding to the Little Ice Age but this alone does not account for

their maximum postglacial positions. They consider these large advances to

relate to the mid-Holocene climatic deterioration (post 4.5ka BP). Clearly

response rates would be much slower in the large trunk glaciers than the

smaller plateau ice caps. Therefore, Stewart and England's (1983) conclusion

is reasonable especially when they cite other radiocarbon dates from Greenland

and Ellesmere Island relating to ice advances from 4.2ka to 200 years BP (cf.

Dyck and Fyles 1963; Trautman 1963; Long 1967; Weidick 1977; Lowden and Blake 1979; Kelly 1980; Volk 1980; Blake 1981; King 1983).

The exact effect of the Little Ice Age on the northern Ellesmere Island glaciers and ice shelves is unclear. From historical accounts it is apparent that ice shelves were more extensive during the late 19th and early 20th centuries and that an ice shelf stretched along most of the northern Ellesmere Island coast (Peary 1907). England et al. (1981b) have suggested that the many ice islands of the 1940's and 1950's (Koenig et al. 1952) may be explained by the large-scale break up of Peary's ice shelf. The predominant climatic amelioration of the last 100 years (Hattersley-Smith and Serson 1970; Fisher and Koerner 1980) may be responsible for the calving of approximately 600km² of the Ward Hunt Ice Shelf in 1961 and 1962 (Hattersley-Smith 1963). Bergsma et al. (1984) have reported plant material approximately 400 years old that has recently been released from the outlet glacier of a plateau ice cap on

central Ellesmere Island. This material is thought to have been overridden during the Little Ice Age.

CHAPTER TWO

The study area

"I was now 200 feet above the sea or ice-level, and had a very good and careful look all around. No land was visible, except the coast along which we were travelling, my view of which extended about seven miles farther than our position, the trend being gradually southward and westward.

The line of hummocks was about four miles off, and appeared to incline slightly to the southward in the distance. The land itself is not high, and there being no cliffs, not a speck bare of snow visible. The hills sloped gradually from the ice, and the ridge on which we were at the extreme of our journey was a portion of undulating low land, attached to the coast, and continuing south-west with it.

I turned back and met the sledge. Halted for grog and biscuit. Hoisted the Union Jack, and drank Her Majesty's health. Extract from Lieutenant Pelham Aldrich's diary from "Voyage to the Polar Sea" by G.S. Nares. The account of the attainment of Alert Point, furthest west, May 18th, 1876.

2.1: General physiography of Phillips Inlet and the Wootton Peninsula.

Phillips Inlet and the Wootton Peninsula are located on the northwest coast of Ellesmere Island (Fig.1.1). The Inlet is a major east-west trending reentrant, 45km long with four north-south trending tributary fiords each >15km long (Fig.2.1). Four spot soundings have been made in the fiords (Canadian Hydrographic Service 1974). The Inlet mouth is 178m deep and the centres of Transition and Berg Bay fiords are 151m and 168m deep respectively. A sounding in the northern half of Ice Alley Fiord indicates a depth of only 70m.

The field area (ca.2500km²) is divisible into three geologically controlled physiographic zones (Figs.2.2 and 2.3): 1) an undulating plateau averaging 900m asl, located south of the Inlet and penetrated by the four tributary fiords; 2) a deeply fretted cirque terrain with summits >1200m on south Wootton Peninsula; and 3) a 300m plateau bounded by coastal cliffs 80-140m high on north Wootton Peninsula. Two smaller areas located at the mouth of the Inlet, around Cape's Armstrong and Woods, constitute coastal lowlands with <90m relief.

To the south of the field area the Grant Land Mountains reach >1700m

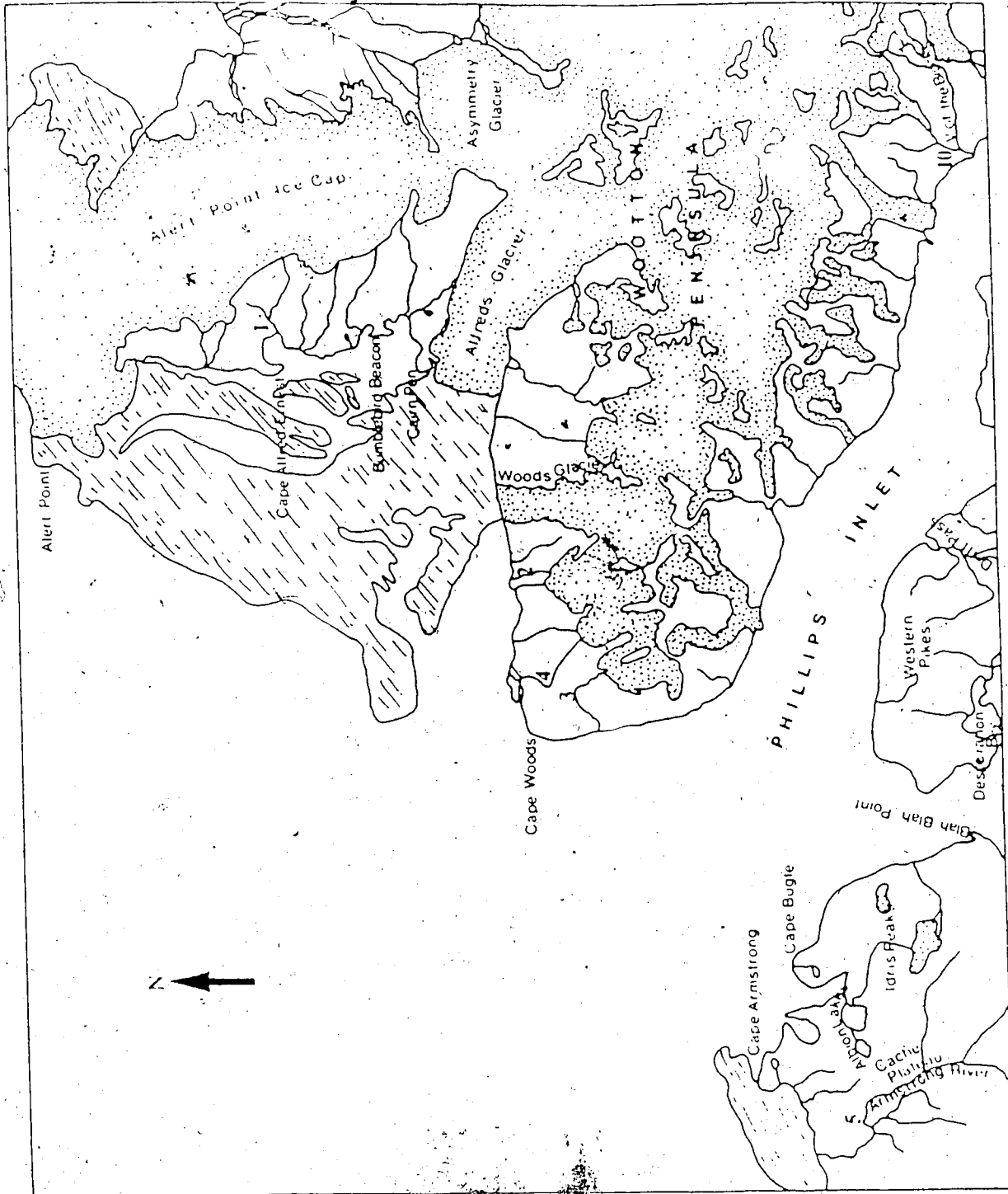


Figure 2.1a: Place names of northern Phillips Inlet and the Wootton Peninsula. Principal deltas are 1. Useless, 2. Sunkist, 3. Nightmare, 4. Cairn, 5. Armstrong and 10. Mymmshall.

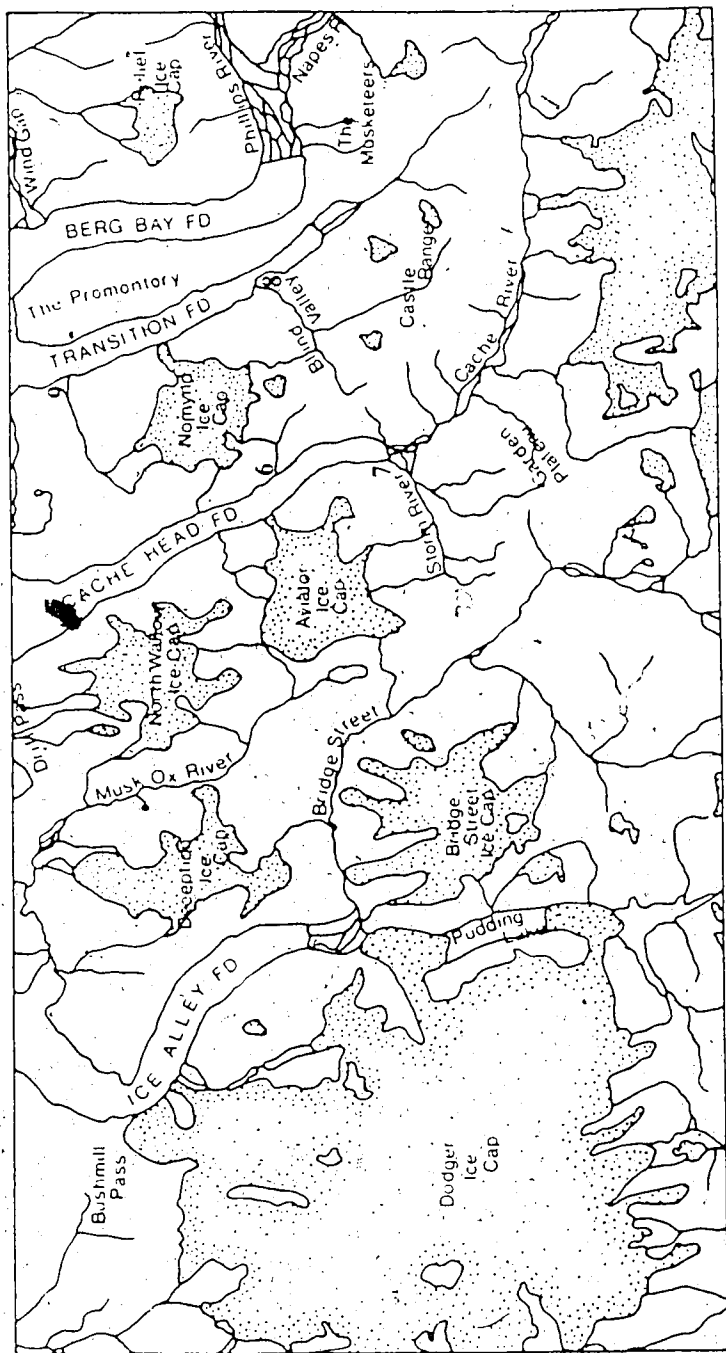


Figure 2.1b: Place names of southern Phillips Inlet. Principal deltas are Gorge, 7, Storm, 8, Blind, 9, Longmynd.

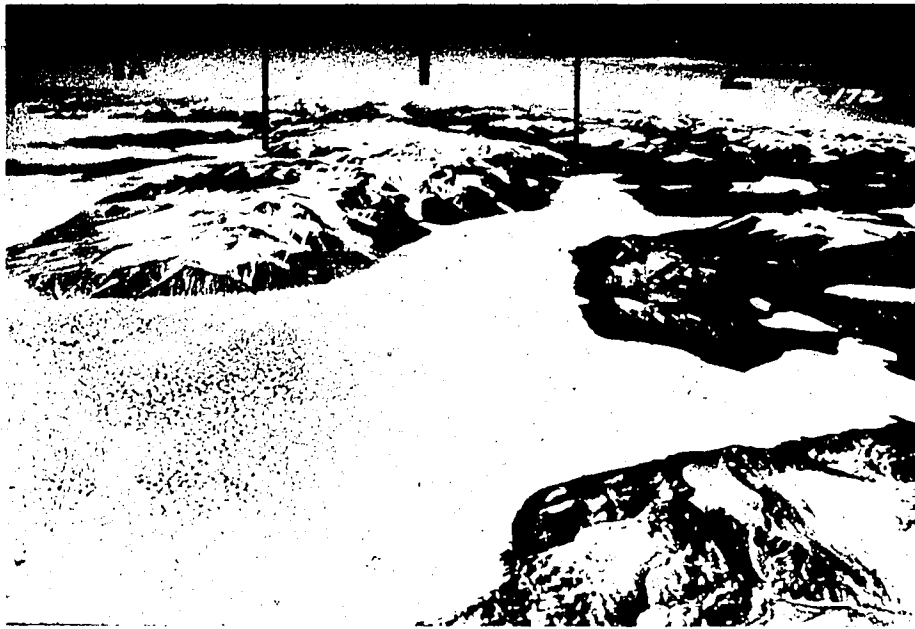


Figure 2.2: Air photograph T404R-172 of Phillips Inlet and Wootton Peninsula looking east along the Inlet. Physiographic zones 1 (fretted cirque terrain), 1A (coastal lowland) and 2 (plateau with fiords) are marked.

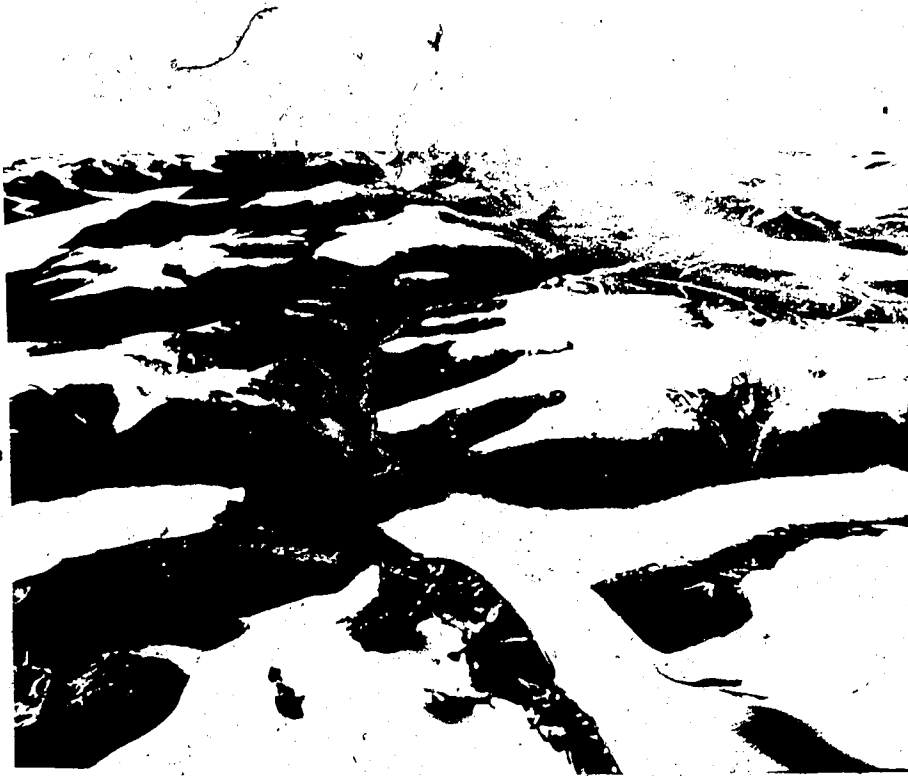


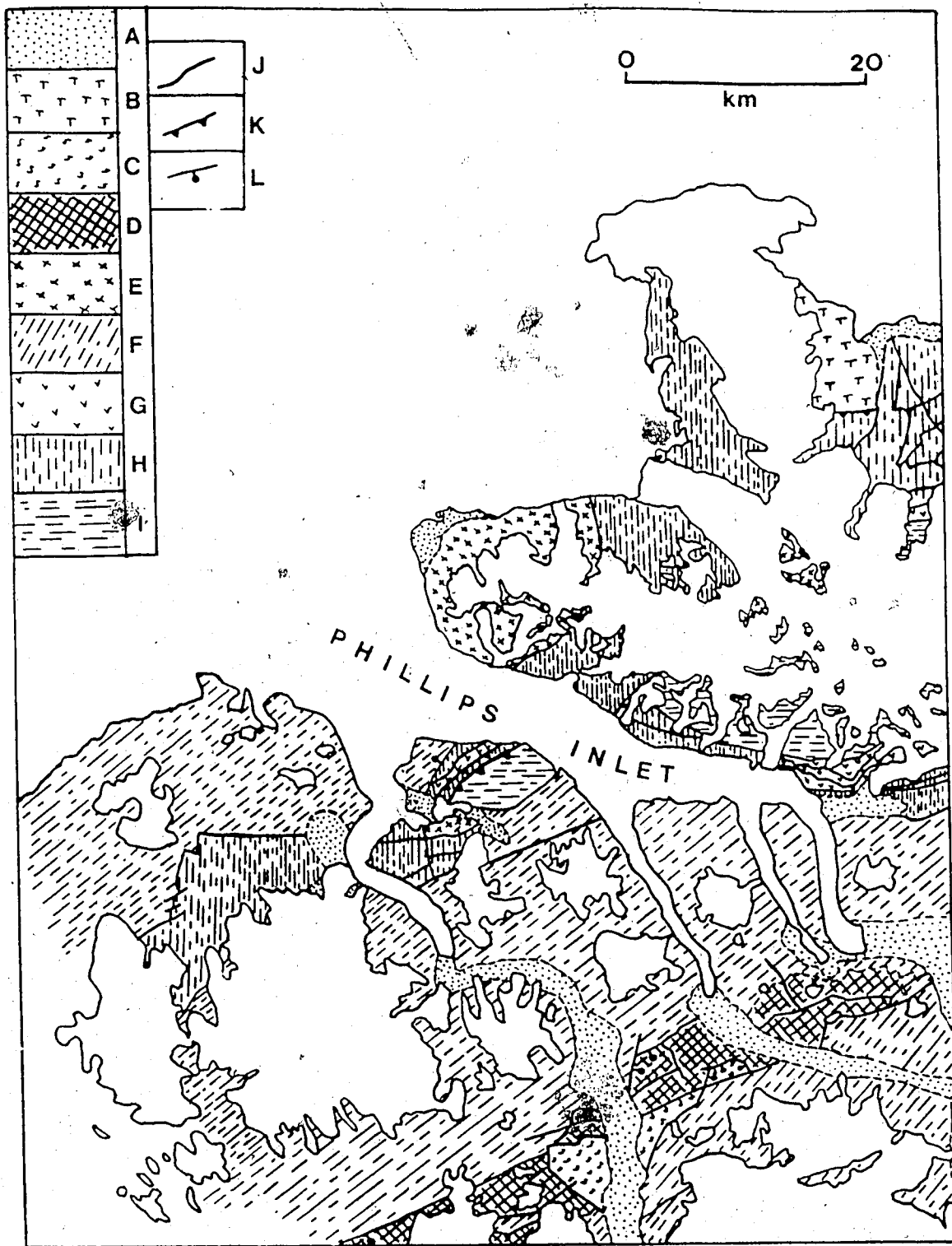
Figure 2.3: Air photograph T408R-222 looking east along Bridge Street within physiographic zone 2 (plateau with fiords). Physiographic zone 3 (Grant Land Mountains) is visible in the distance.

asl. Outlet glaciers from the mountains terminate ≤ 23 km from the fiord heads and three major rivers (Bridge Street, Cache River and Phillips River) carry meltwater from the inland ice to the north coast (Fig.2.1b). Except for three east-west oriented passes in the centre of the field area (Bushmill Pass, Drift Pass and Wind Gap; Figs.2.1a and 2.1b), the Inlet and fiords, most of the valleys in the field area have distinct V-shaped profiles despite their repeated occupancy by glaciers. Very few official names exist in the area of study, therefore many unofficial names have been adopted for ease of reference (Figs.2.1a and 2.1b).

2.2: Geology of northern Ellesmere Island.

Original interpretations for the geology of northern Ellesmere Island (cf. Thorsteinsson and Tozer 1976) included two major geosynclines bordered to the north by an older crystalline, metamorphic terrain (Pearya Geanticline). These zones have been revised by Trettin (1987) as five stratigraphic-structural zones (Fig.1.2). To the north the Pearya geanticline is a composite crystalline, sedimentary and metamorphic terrain of Middle Proterozoic to Late Silurian age. Pearya forms the north and northwest border of the Franklinian Mobile Belt (formerly Franklinian Geosyncline) which includes sediments that range in age from the Cambrian to the Devonian. The Clements Markham Fold Belt, a sedimentary and volcanic subprovince of the Franklinian Mobile Belt, is in fault contact with Pearya. Structural and stratigraphic evidence has led Trettin (1987) to conclude that Pearya is an accreted terrane sutured to the Franklinian deep water basin (Clements Markham Fold Belt) during the Late Silurian. The southern Grant Land Mountains were uplifted relative to the regions to the southeast and northwest during the Mid Palaeozoic Ellesmerian Orogeny, during which deformation of Lower Palaeozoic strata occurred (Thorsteinsson and Tozer 1976). The last geologic zone comprises the Sverdrup Basin which is Carboniferous to Early Tertiary in age (Trettin 1987). Sverdrup

Figure 2.4: Geology of Phillips Inlet and the Wootton Peninsula. A. Quaternary sediments. B. Early Tertiary, Eureka Sound Formation; sandstone, conglomerate and mudrock. C. Lower Permian ?, Esayoo Formation; basalts and pyroclastics. D. Upper Carboniferous and lower Permian, Nansen Formation; limestone, minor sandstone, mudrock and dolostone. E. Carboniferous and/or Devonian; quartz monzonite, granodiorite, quartz diorite and related rocks. F. Silurian, Lands Lokk and Imina Formation; quartzose, cherty and micaceous sandstones; compositionally immature calcareous and dolomitic sandstones; slaty and phyllitic mudrock; minor pebble, granule and intraformational conglomerate; tuff; volcanic arenite; minor volcanic flows; limestone. G. Ordovician and Silurian, Hazen Formation; pyroclastics and volcanic flows, mainly andesitic and basaltic, locally metamorphosed to greenschist facies; carbonates and mudrocks associated with volcanics; variably metamorphosed limestones associated with volcanics or schist and amphibolite. H. Proterozoic and/or lower Palaeozoic; variably calcareous phyllite and slate with minor quartzite; amphibolite schist and metamorphosed carbonates; original limestone, dolomite and dolostone variably metamorphosed to marble; recrystallized carbonates; schist; diamictic phyllite; metachert. I. Proterozoic; metamorphosed granitic intrusions and pegmatite and associated amphibolite to greenschist grade metasedimentary and meta igneous rocks (schists, amphibolites, marbles etc.). J. Fault with thrust or downthrow direction unknown. K. Thrust fault with teeth on hanging wall. L. Fault with solid circle indicating downthrow side.



Basin was the successor to the Franklinian Mobile Belt (FMB) and its sediments unconformably overlie Pearya and the FMB. Sedimentation into Sverdrup Basin was terminated by uplift during the Late Cretaceous to Oligocene (?) Eurekan Orogeny. This orogeny was responsible for the rejuvenation of the Mid Palaeozoic uplift or the Ellesmerian Orogeny. Rocks of the Sverdrup Basin outcrop in the nunataks of the Grant Land Mountains. Discussions of the Tertiary strata of northern Ellesmere Island (unit B, Fig.2.4) are contained in Tozer (1963), Wilson (1976), Miall (1979) and Trettin and Frisch (1981).

2.3: Geology of Phillips Inlet and the Wootton Peninsula.

2.3.1: Pearya

The development of Pearya has been divided into four successions by Trettin (1987). Succession I is the crystalline basement of upper Middle Proterozoic age. Succession II is made up of Upper Proterozoic and Lower Ordovician metasediments and metavolcanics. Succession III and Succession IV do not outcrop in the field area and hence are not discussed here. Several outcrops have been identified by Trettin and Frisch (1981) and Trettin and Mayr (1981) and the geology is summarized in Figure 2.4.

Succession I outcrops on the south Wootton Peninsula and the Western Pikes (Fig.2.1) as metamorphosed granitic intrusions (I on Fig.2.4). Rocks of Succession II outcrop on the north and west-central Wootton Peninsula, Wind Gap, east of the mouth of Ice Alley Fiord and in the Bushmill Pass. Two bands of Succession II rocks outcrop also within a complex fault zone in the Western Pikes (H on Fig.2.4). However, lithologies are variable from one area to another.

2.3.2: Clements Markham Fold Belt.

Sediments of the Clements Markham Fold Belt are predominantly deep water facies with volcanics and shallow marine and non marine lithologies. The Fold Belt represents that section of the Franklinian Mobile Belt originally

termed the Franklinian Eugeosyncline (Thorsteinsson and Tozer 1976). Rocks associated with this zone are Ordovician and Silurian in age (Trettin and Frisch 1981; Trettin and Mayr 1981). The Hazen Formation (both Ordovician and Silurian) represents a minor component of the bedrock of the field area (unit G, Fig.2.4). Also associated with the Clements Markham Fold Belt are the rocks of the Silurian Lands Lokk and Imina Formations (unit F, Fig.2.4). These two formations are by far the most dominant bedrock in the field area and are responsible for the high plateau that constitutes the central physiographic zone (Zone 2, Fig.1.3).

2.3.3: Sverdrup Basin.

A band of Sverdrup Basin rocks delineated by a complex fault zone occurs in the southernmost part of the field area (unit D, Fig.2.4). These have been assigned to the Upper Carboniferous and Lower Permian Nansen Formation by Trettin and Mayr (1981). The band is responsible for a distinct chain of castellated summits to the south of the fiord heads.

2.3.4: Intrusions.

Two large plutons have been mapped on the Wootton Peninsula by Frisch (1974) and Trettin and Frisch (1981; unit E, Figure 2.4). These are Early Carboniferous or Devonian in age. Many mafic dikes and sills have been mapped from air photographs by Trettin (1971), Trettin and Frisch (1981) and Trettin and Mayr (1981). Doubtless many more exist within the field area. These smaller-scale intrusions have not been dated.

2.3.5: Tectonics and structure.

Little is known about how the tectonic and structural history of northwestern Ellesmere Island controls the present physiography. Trettin (1971) outlines five periods of structural deformation for the northern Arctic

islands, the youngest of which is Late Cretaceous. The most prominent faults in the field area are included in Figure 2.4 (Trettin and Frisch 1981; Trettin and Mayr 1981). The main Inlet appears to be an extension of a major fault that extends through Wind Gap (Fig.2.1b) to Yelverton Inlet. Drift Pass, Desperation Bay and Bushmill Pass (Figs. 2.1a and 2.1b) all appear to be fault controlled. A series of passes linking the heads of the fiords and stretching from Phillips River to the valley south of the Dodger Ice Cap (Fig.2.1b) also parallels the fault contact between the Lands Lokk/Imina Formations and the Nansen Formation (Fig.2.4). The degree to which the origin of the Inlet and fiords can be ascribed to this faulting is unknown.

2.4: Climate.

2.4.1: Regional climate.

Northern Ellesmere Island is classified as a Polar Desert according to its low precipitation and net annual water balance of around zero (Bovis and Barry 1974). The area has a continental type climate where several months of total darkness cause temperatures to descend below -50°C . All of the available meteorological records on northern Ellesmere Island are from Alert on the northeast coast or from Lake Hazen in the interior. The mean annual temperature for Alert (1950 to 1970) was -18°C whereas at Lake Hazen it was -21.1°C for the 1957/1958 season (Christie 1964). Annual precipitation varies from 2.5cm at Lake Hazen (Jackson 1959) to 17cm at Alert (Bradley and England 1978a). These figures illustrate the greater continentality of inland sites on northern Ellesmere Island. This is due mainly to the availability of seasonal open water at coastal sites causing increased cloud cover, fog and cooler summer temperatures (Alt 1979). England et al. (1981b) have stated that the climate of northern Ellesmere Island has such great spatial, seasonal and annual variability that "meaningful generalizations....cannot be made".

Maxwell (1981) divided Ellesmere Island into three major zones based

upon: cyclonic activity; the sea ice-water regime; broad-scale physiographic features; and net radiation. His zone Ib is the northwestern island fringe which includes the northernmost coast of Ellesmere Island, hence Phillips Inlet. During the summer, Zone Ib is characterized by low cloud and fog which results from local puddling on the sea ice and the proximity to the Arctic Ocean. In the winter, open leads are responsible for extensive ice fog.

2.4.2: Local climate and ice cover.

Most of the land above 1100m on northern Ellesmere Island is ice covered (Hattersley-Smith 1969) but the ELA and glaciation level descend rapidly to <300m asl along the north coast (Miller et al. 1975). The glaciers of the field area are sub-polar; ie. they are frozen to their beds and undergo surface melting during summer months (cf. Ahlmann 1935; Sugden and John 1976; Paterson 1981).

The three physiographic zones of the field area are characterized by different ice covers (Fig.2.5). To the south, the Grant Land Mountains (Zone 3) host a large icefield because of their altitude (generally >1500m) and associated colder temperatures. Hattersley-Smith (1960b) reported a mean annual temperature of -24°C and an annual snow accumulation of ca.15cm in the eastern sector of these mountains. The central upland plateau (Zone 2) is characterized by small ice caps with occasional outlet lobes and several small ice carapaces. Hattersley-Smith (1969) has suggested that the reduced ice cover in such areas is due to low precipitation and a lack of upland surfaces large enough for snow accumulation. Bednański (1984) regards ice-free uplands in Clements Markham Inlet as transition areas that are too low to be glacierized and too far inland to be affected by the moisture increases associated with the Arctic Ocean. Topoclimatically, the plateau areas south of Phillips Inlet inhibit glacierization because they are windswept and without topographic lees in which snow can accumulate. Bradley and Serreze (1987) have

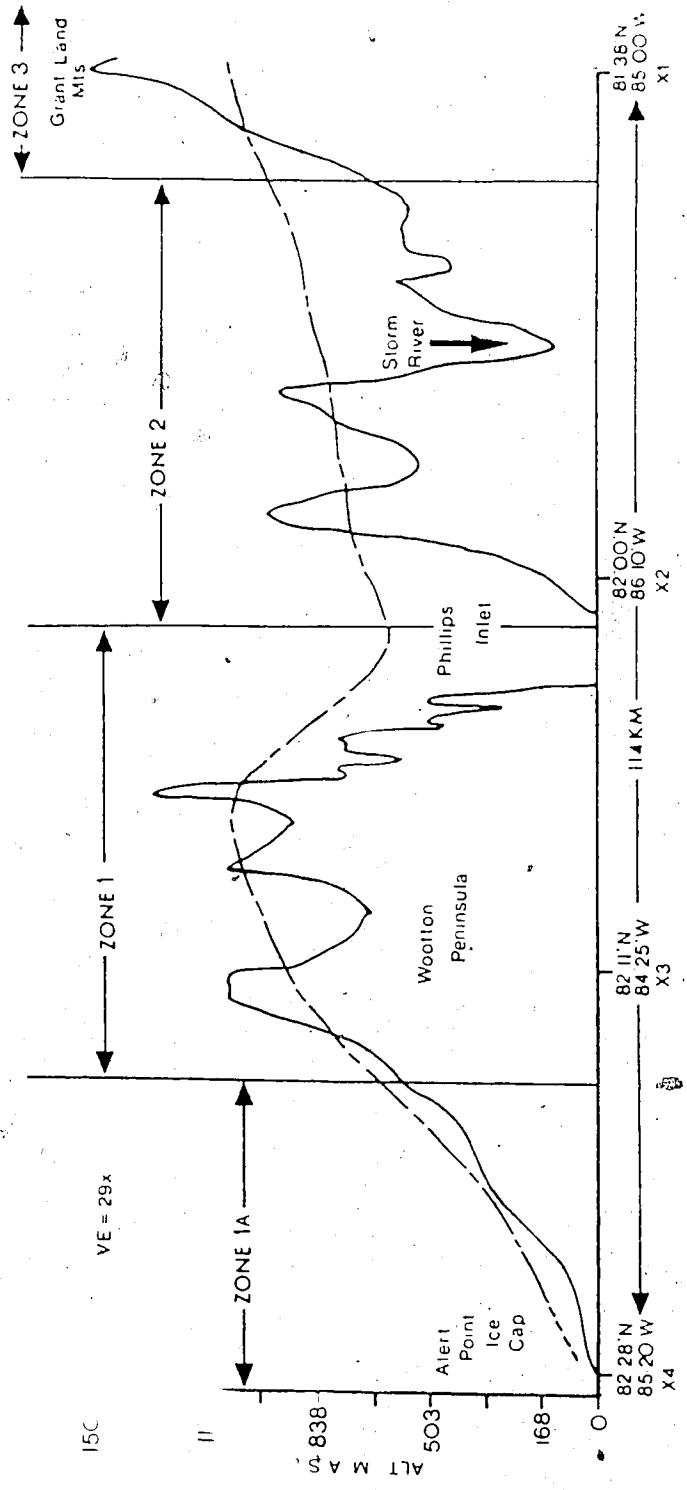


Figure 2.5: The glacial level (broken line) depicted along a transect X1 to X4 on Figure 2.6.

undertaken glacio-climatic studies on a small plateau ice cap on northeast Ellesmere Island. They conclude that the ice is a remnant of former climatic conditions and is out of equilibrium with present climate. Because some of the margins of the plateau ice caps south of Phillips Inlet are advancing, the ice caps are probably close to equilibrium with present climate. Surface conditions on these ice caps varied considerably between the summers of 1985, 1986 and 1987. During 1985 temperatures of $>10^{\circ}\text{C}$ were not uncommon and the entire snow cover on the plateau ice caps disappeared. In 1986 and 1987 temperatures rarely exceeded 6°C and accumulation areas covered approximately 60% of the surface areas of these ice caps. This occurred despite some severe temperature inversions ($>15^{\circ}\text{C}$) between the valley floor/fiord surface and the plateaux. These inversions were the result of cold Arctic Ocean air funnelling southwards along the fiords.

Finally, the northernmost coast is composed of a low coastal strip (Zone 1A) and the mountainous south Wootton Peninsula (Zone 1); cf. Fig.2.5. The proximity of the Arctic Ocean occasions a steep decline in the glaciation level in this area. The south Wootton Peninsula is heavily glacierized by cirque and transection glaciers many of which terminate in or near the sea. The north Wootton Peninsula is occupied by the Alert Point Ice Cap whose surface elevation is 300m asl. The northernmost margin of the ice cap forms a glacier ice shelf at Alert Point, the northernmost tip of the field area. Periodic open water, resulting from leads in the pack ice, causes increased cloudiness and fog on the northernmost coast, hence both increased moisture and reduced ablation (Sagar 1962). This fog occasionally penetrates the Inlet and Ice Alley Fiord (Fig.2.1b), especially if winds are from the north. Fog also persists around the Idris Peaks/Bushmill Pass area (Figs.2.1a and 2.1b) due to the orographic lifting of humid air flowing south. During the 1985-1987 field seasons fog persisted on the north coast for approximately 40% of the time. Average temperatures during 1986 and 1987 for the north coast were 0°C

and 2.9°C respectively, whereas the inland sites were 5°C for both years. Rolls on the ice shelves indicate that the prevailing winds are from the west-southwest (Hattersley-Smith 1957) and therefore there is an unhindered drift of snow across the Arctic Ocean. Because the Wootton Peninsula acts as a physical barrier to the continued western snow drift several perennial snowpatches exist at or just above sea level. The importance of cloud cover to the mass balance of the Wootton Peninsula glaciers is well illustrated by air photographs taken in August 1959. Glaciers to the south of the watershed have lost their entire surface snow cover whereas to the north ELA's are still well established at approximately 800m.

2.4.3: Glaciation level.

Isoglaciophyes (contours of equal glaciation levels, Fig.2.6) have been drawn for the field area using the summit method outlined by Andrews and Miller (1972). The glaciation level represents the long term balance between winter accumulation and summer ablation when topoclimatic characteristics are taken into account. The result is a threshold elevation above which glaciers exist on the landscape. Values of glaciation level were obtained for grids of 10km^2 within the field area. This is calculated by obtaining a mean of the highest summit without ice and the lowest summit with ice. These values are then contoured. Values of the highest elevation in each 10km^2 were also contoured in order to assess topographic controls on glaciation levels. Ice shelves are regarded as sea level glaciers because of their accumulation of iced firn (Marshall 1955). The advantage of constructing the glaciation level is that it represents local patterns that reflect present topoclimatic conditions and these, in turn, should be relevant to the style of past glaciations.

Miller et al. (1975) reconstructed a glaciation level map for the Canadian high Arctic. However, such a small scale reproduction naturally

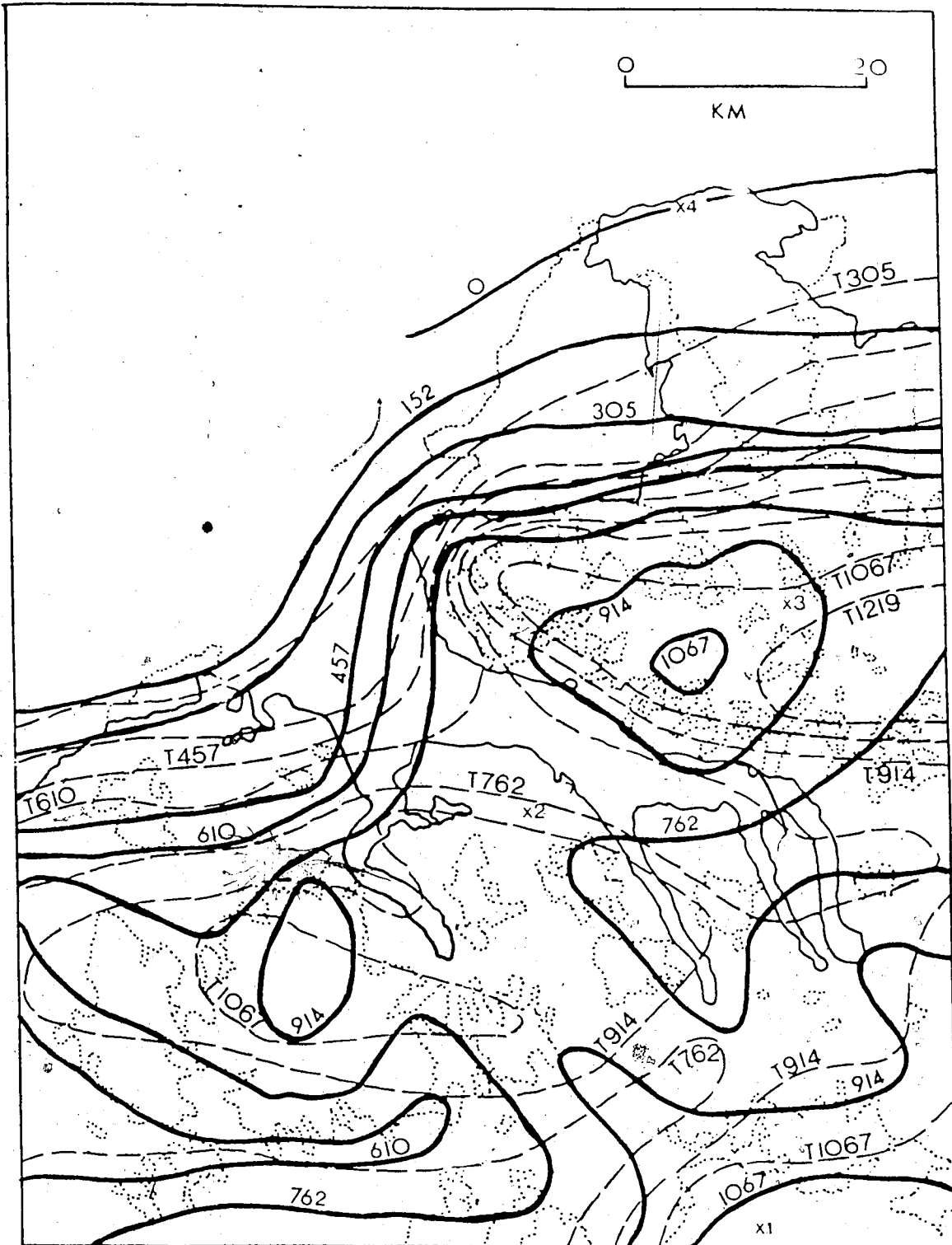


Figure 2.6: Glaciation level for Phillips Inlet and the Wootton Peninsula (solid line) and generalized topography (broken line with T prefix). Altitudes in metres.

smoothed out local patterns. Their map portrayed a decline in glaciation level from 1350m asl in the Grant Land Mountains to 400m asl on Ward Hunt Island. In Phillips Inlet and the Wootton Peninsula, the glaciation level declines from 1100m asl in the Grant Land Mountains to sea level at Alert Point. The abrupt decline in the glaciation level towards the north is interrupted by two cells of high values centred over the south Wootton Peninsula (1067m) and the Dodger Ice Cap (914m). The latter is a function of the large fault-controlled trough connecting the eastern fiord heads to the pass southwest of the field area and the main Inlet. These considerable topographic depressions contain large areas that are well below the regional glaciation level (see T contours on Fig.2.6). The Wootton Peninsula cell is especially high because of the deeply fretted relief. This precludes lower elevation summits from entering into the glaciation level calculation. The influence of the main Inlet and the south Wootton Peninsula on the glaciation level is shown in Figure 2.5.

2.4.4: Ice shelves and sea ice.

Clearly the ice shelves of the north coast of Ellesmere Island are favoured by adjacent open water, allowing accumulation at sea level and by predominant foggy or cloudy conditions, reducing ablation rates. The Cape Alfred Ernest Ice Shelf (Fig.2.1a and Fig.2.7) is approximately 200km² and is a glacier/sea ice shelf complex (cf. Lemmen et al. 1988). The ice shelf exists because of the protection offered by the natural indentation of the west Wootton Peninsula reducing the ice shelf's susceptibility to calving (cf. Hattersley-Smith 1963; Jeffries 1986). Glacier ice within the ice shelf originates from the Alert Point Ice Cap to the north and from the Woods and Alfred glacier's to the south. The sea ice and glacier ice components are recognizable on Figure 2.7. Glacier ice is delineated by morainic debris and characterized by muted crevasse patterns. The surface of the sea ice shelf is made conspicuous by its roll patterns which are oriented generally southwest-

northeast. A smaller sea ice shelf exists off Cape Armstrong and is approximately 15km^2 in size. There are no data on the depths of these ice shelves, but Prager (1983) has reported depths of 90m on the outer Milne Ice Shelf which is fed by a sea level ice cap similar to the Alert Point Ice Cap. Depths of 100m are characteristic of a floating ice tongue within the central Milne Ice Shelf and these are reduced to <20m (the critical depth for ice shelf classification) at the outer edge of the ice shelf.

Northern Ellesmere Island is surrounded by multi-year pack ice (Weeks 1976). Maxwell (1981) also reports that, during the winter, the fiords of northern Ellesmere Island contain fast ice in which second and multi-year categories predominate. Moving pack ice occurs offshore and is composed of second and multi-year ice. Maxwell describes a "good" summer as one in which the northern fiords and the Arctic Ocean contain second or multi-year sea ice with a coverage from anywhere between two and nine tenths. The presence of the moving pack ice offshore is responsible for large leads which appear at the edges of the ice shelves and at the mouth of the Inlet. These are noticeable on the 1950 and 1959 air photographs and were observed from the air in 1986 and 1987 (cf. Fig.2.7).



Figure 2.7: The Cape Alfred Ernest Ice Shelf and the Alert Point Ice Cap air photograph mosaic from 1959: 1. incipient sea ice shelf; 2. sea-ice ice shelf; 3. glacier ice shelf; 4. multi-year pack ice; 5. moraine; 6. large offshore lead.

CHAPTER THREE

Theory and methods

".....on the present glacial covering of Ellesmere and Heiberg Lands, it may be mentioned that the position of the marine-terraces with regard to now existing glaciers indicates very conspicuously that the glaciation during the last (in case there have been several) great submersion of the land- the highest sea margin in the inner part of Hayes Sound is some 600 feet- was not in any case of greater intensity than it is now, and that it has never since that period exceeded its present intensity." Extract from P. Schei; Preliminary account of the geological investigations made during the second Norwegian polar expedition in the Fram. In, Sverdrup O., New Land, Longmans, London, 1904.

3.1: Introduction.

Reconstructions of former ice margins and palaeoenvironments on a macro scale require multi-disciplinary research (cf. Andrews 1982). Theoretical data (eg. glaciology and ice dynamics) must be checked regularly by empirical data (eg. glacial geology and stratigraphy). There are two approaches to the reconstructions in this study: 1. the direct method of mapping the surficial geology, landforms and stratigraphic sections to determine glacial style and dynamics; 2. the inverse method of surveying and dating postglacial emergence to determine the pattern of glacioisostatic unloading from which one can infer the previous ice configuration. In this chapter the applicability of the first approach to a) glacial deposits and landforms and to b) glacimarine sediments will be elaborated. Then the glacioisostatic approach involving former sea level reconstructions will be discussed.

3.2: Glacial geology and geomorphology.

Extensive till sheets and well developed moraines are rare on northern Ellesmere Island (England and Bednarski, in press) hence former ice margins have been mapped using the distribution of erratics, weathering zones and meltwater channels. Such criteria are often qualitative because weathering rates in the high Arctic are unknown (Watts 1986) and erratics and meltwater

channels can be polycyclic. The most reliable chronology on past ice margins has therefore been obtained where glaciers contacted the sea, depositing sediments that contain datable marine fauna (cf. England et al. 1981a; England 1983, 1985; Bednarski 1986). Nonetheless, many aspects of past and present glacial processes remain untested in the high Arctic. These observations are critical to the understanding of past glacial style and dynamics in a topographically diverse terrain. This is especially true if the last glaciation was of a restricted nature because the glacial style would not be radically different from that observed today.

Because the Phillips Inlet/Wootton Peninsula area is 60% glacierized it represents an ideal environment in which to study contemporary glacial landform/sediment assemblages and to integrate these with parallel studies on past glacial activity. Naturally, in such a field area this involves both the terrestrial and marine environments as well as associated processes such as glacioisostasy. Evidence of former glacierization is abundant both in terms of glacial landforms and sediments as well as widespread raised marine deposits that record former changes in the regional ice load.

A Research Agreement was awarded to the author by the Department of Energy, Mines and Resources, Ottawa for mapping the surficial geology of the Phillips Inlet/Wootton Peninsula area. The surficial geology and glacial geomorphology are mapped at a scale of 1:125,000 (Fig.5.1) and the units and symbols are based upon those of the Geological Survey of Canada described in Chapter 5 (GSC Guide to Authors, 1980). Sediment assemblages from the terrestrial and marine environments, both contemporary and ancient, are described in Chapters 4 and 5 using the lithofacies code of Eyles et al. (1983) and Miall (1977). This code is used in the landsystems approach to describe and interpret glacial landscapes (Eyles 1983). Radiocarbon dates pertinent to the reconstruction of past glacial limits and deglaciation patterns are presented and discussed in Chapter 5.

3.2.1: The landsystems approach.

Based on sediments and landforms at the margins of contemporary glaciers, Eyles (1983) has identified a series of "landsystems". A landsystem is the largest unit in an ascending hierarchy of landscape classes. This hierarchy consists of: 1) a land element, which is uniform in form and material and is suitable for mapping at large scales (eg. a drumlin or kame); 2) a land facet, which is one or more land elements grouped as an homogenous landscape and mapped at scales of 1:50,000 to 1:100,000 (eg. drumlin field or outwash plain); 3) a landsystem, which is a "recurrent pattern of genetically linked land facets" mapped at scales of 1:250,000. A landsystem has characteristic topography, subsurface stratigraphy and sediments. Eyles (1983) has outlined three landsystems: the subglacial; the supraglacial; and the glaciated valley. The first two are designed for large ice sheets. The latter is most appropriate to this study because it is designed for mountainous areas where bedrock relief forces the distribution of ice to form glacial lobes. However, the glaciated valley landsystem proposed by Eyles (1983) is based upon temperate examples and should not be regarded as representative of high latitude mountainous environments. Observations around the margins of glaciers in Phillips Inlet/Wootton Peninsula were used to reconstruct sub-classifications for the glaciated valley landsystem there.

A number of high latitude locations have been used to construct the sediment assemblages for the various landsystems, but Eyles et al. (1983) make no references to high Arctic glaciers. The only Arctic examples of sediment sequences are from around glaciers in maritime Arctic environments such as Spitsbergen and Iceland. Boulton (1972a and b) has also used these sub-polar glaciers to propose a model of basal thermal regimes where debris is entrained by freezing-on (regelation) at the transition from warm- to cold-based ice. For southern Baffin Island, Dowdeswell (1986) concludes that ice in the

accumulation zones of tidewater glaciers is at pressure melt point providing a source of basal meltwater for marginal freeze-on. Lawson (1979) reached the same conclusions for the Matanuska Glacier in Alaska. Muller (1976) and Hambrey and Muller (1978) have used an extrapolated temperature curve from the White Glacier, Axel Heiberg Island, to suggest that debris-rich layers and ice-cored moraines at the snout are the product of freezing-on of debris and its upward thrusting over clean ice. These ideas originated on Greenland (Weertman 1961), were developed later on the Barnes Ice Cap (Hooke 1973) and have recently been applied to the basal ice/debris layers in the Agassiz Ice Cap (Gemmell et al. 1986). Boulton (1972a and b) suggests that thick sequences of lodgement till are only possible under warm-based or temperate conditions whereas in sub-polar or cold-based glaciers thick accumulations of basal debris lead to greater reworking and a preponderance of melt-out and "flow" tills.

Shaw (1977a and b) presents a model of entrainment and deposition from the Dry Valleys of southern Victoria Land, Antarctica. According to this model the most effective process of entrainment is by frontal apron incorporation which explains the high debris concentrations in the basal ice without invoking large scale basal freeze-on. Probably the most important constructional process for end moraines in the high Arctic is that of proglacial thrusting (Kalin 1972; Klassen 1982). The importance of this process to glacial debris entrainment has never been investigated on Ellesmere Island. Observations on four glaciers with proglacial thrust moraines are developed in Chapter 4 to construct the landsystems of Phillips Inlet and Wootton Peninsula.

This study also reports direct observations on debris within and adjacent to contemporary glacier margins. Furthermore, clast analyses, such as those undertaken by Sharp (1982, 1986) and Dowdeswell (1986), were conducted within three glaciers (twelve sampling points) in order to ascertain the mode

of clast entrainment. For example, Boulton (1978) used clast shapes as an indicator of transport paths through a glacier and concluded that the more rounded and heavily striated clasts must have been in traction at the glacier bed more than once suggesting that regelation was important. These clasts were rounded, had "stoss and lee" or bullet-shaped morphologies and typify most boulders in lodgement tills (Sharp 1982). In contrast, clasts derived from supraglacial or englacial positions are more angular because they were transported passively through the glacier. Clearly if regelation occurs on a large scale then a large percentage of striated, rounded or stoss and lee clasts would be encountered. Furthermore, tills would represent a dominant surficial unit within glaciated basins. Seventeen clast sample points were established on different surficial units in order to obtain representative clast measurements. The sampling of tills provided an opportunity to assess the subglacial conditions during previous glaciations. These measurements are then compared to the twelve samples from within glaciers in order to assess contemporary glacier bed conditions. The results of the clast analyses are discussed in Chapters 4 and 5. At each sampling point fifty stones were examined for striations, Zingg shape (Zingg 1935) and Powers roundness (Powers 1953). The lithology of each clast was noted together with stoss and lee forms and multiple striations (Appendix 2).

3.3: Glacimarine sediments.

3.3.1: Introduction.


Glacimarine stratigraphy is critical to the reconstruction of ice margins on northern Ellesmere Island because the terrestrial evidence is incomplete and rarely datable. Numerous papers on glacimarine sedimentation and stratigraphy have appeared during the last decade but only two studies have been completed in the high Arctic (Bednarski 1984; Stewart 1988). Because many glaciers in Phillips Inlet/Wootton Peninsula presently terminate in or

near the ocean, a general understanding of depositional sequences along submarine ice margins is necessary. With respect to sediment availability, a knowledge of terrestrial landsystems helps to explain depositional sequences in the marine environment.

3.3.2: Controls on glacial marine sedimentation.

Bednarski (1984) has identified two controls on the sedimentary facies of a high Arctic fiord: 1) the type and volume of sediment supply; and 2) isostatic and eustatic adjustments. Several papers deal with glacial marine sedimentation in fiord environments. Nelson (1981) constructed a model for Baffin Island fiords which involved three zones of deposition: a proximal zone where high sedimentation rates and active calving occur; an intermediate zone, 1-2km from the ice margin, characterized by diamictons from melting icebergs and gradational suspension deposits; and a distal zone, 4-6km from the ice margin, where shelf deposits and occasional dropstones predominate. The proximal zone is subdivided into inner and outer sub-zones. The inner sub-zone is characterized by melt-out tills and ice contact, subaqueous fans at or just beyond the grounding line. The outer proximal sub-zone is characterized by massive silts and fine sands with only occasional dropstones because icebergs vacate this zone before depositing their debris. In the high Arctic even the intermediate zone of Nelson (1981) could conceivably be within 1km of the ice margin because multi-year fast ice and ice shelves restrict the amount of ice berg calving and drift.

Powell (1984) has modelled a variety of glaciers from floating valley or outlet glaciers to ice sheets with frozen beds. Because cold-based glaciers are most likely to form floating glacier tongues or ice shelves these are included in Powell's model. The model recognizes a sediment assemblage or morainal bank at the grounding line which includes interbeds of massive gravels and stratified and unstratified matrix-supported diamictons with



PAGE REMOVED DUE TO COPYRIGHT
RESTRICTIONS

Figure 3.1: Lithofacies characteristics at the margin of a floating glacier/ice shelf (after Drewry 1986).

occasional massive sands. Clearly most sediment is released at the grounding line when glaciers terminate in the marine environment (cf. Drewry 1986, Chap. 13; Figure 3.1). As a result, grounding line deposits should be readily apparent in the glacial-marine record. Grounding line fluctuations are built into the sedimentary facies models of Powell (1981; 1984). Because sub-polar glaciers have low activity indexes (cf. Andrews 1975b) and may undergo only minor fluctuations during full glacial conditions, grounding line deposits may take the form of morainal banks (Powell 1984). The amount of material available for such a moraine bank is controlled by the terrestrial landscape from which the floating ice originates. Stewart (1988) has used the presence of large subaqueous fans to suggest that the main trunk glacier in Clements Markham Inlet had a tidewater front during deglaciation rather than an adjacent ice shelf. Such subaqueous fans mark the release of basally entrained debris during deglaciation and suggest that englacial streams penetrated to the glacier bed (cf. Rust and Romanelli 1975; Cheel and Rust 1982; Stewart 1988).

None of the glacial-marine depositional models discussed above considers glacioisostatic and eustatic adjustments. Geophysical models based upon different ice load histories (cf. Farrell and Clark 1976; Clark et al. 1978; Clark 1980, 1985; Quinlan and Beaumont 1981) predict two alternative scenarios that might occur on the northernmost coast of Ellesmere Island, each depending on a particular history of ice extent. On the one hand, if pervasive ice extended onto the Arctic Ocean shelf during the last glaciation the entire field area would be characterized by continuous and ongoing postglacial emergence, because glacioisostatic loading would far exceed postglacial sea level rise. On the other hand, if less extensive ice failed to inundate Phillips Inlet/Wootton Peninsula during the last glaciation initial postglacial emergence along the outer coast probably would be followed by submergence in the late Holocene as the forebulge collapsed (cf. Dyke 1979;

see Appendix 3 for definitions). Therefore, the shape of the emergence curve during the Holocene is indicative of the style of glacial unloading in a particular area and this must be applied to our understanding of glacial marine sedimentation. However, the nature of the stratigraphic sequence within a marine basin will vary considerably if glacial fluctuations have caused sea level adjustments commonly in the order of 100m.

3.3.3: Glacial marine stratigraphy.

Sediment supply and eustatic/glacioisostatic controls create complex raised marine sequences. Bednarski (1984) adapted a previous sea level model (Curry 1964) to portray a schematic section through raised marine sediments following deglaciation (Fig.3.2). Prior to the deposition of class I sediments, the site was occupied by glacier ice and therefore glacial facies were deposited. Classification I (erosional regression) includes sediments deposited when glacioisostatic uplift exceeded sea level rise following deglaciation. At this time emergence exceeded sedimentation rates resulting in the dissection of uplifted glacial deposits and no beach formation. During the deposition of sediments in classifications II (mixed erosional-depositional regression) and III (discontinuous depositional regression) there was a decrease in rebound rate. This led to a reduction in the emergence/sedimentation ratio and the occurrence of regressive wave-cut benches. Sediments in classification IV (depositional regression) are the product of marine offlap. Such sediments form regressive beaches and deltas because sedimentation rates kept up with the rate of emergence. Class V (depositional transgression) sediments are deposited in the nearshore zone during the immediate deglaciation of the site or during the later collapse of the forebulge. This involves a transgression rate equal to sediment supply resulting in a marine onlap sequence. Sediments of classes VI and VII are from deep water deposition immediately after deglaciation when transgression out-

PAGE REMOVED DUE TO COPYRIGHT
RESTRICTIONS

Figure 3.2: Transgression and regression classifications from Curray (1964) and associated sedimentary facies successions as applied to an Arctic fiord by Bednarski (1984).

paces sedimentation. Classification VI includes a thin veneer of littoral sands overlain by discontinuous marine sediments which display a normal fining-up, marine onlap sequence. Classification VII includes overstep marine deposits. In Figure 3.2 this is portrayed by an unconformity between deep water sediments and till.

The model reproduced in Figure 3.2 was used by Bednarski (1984) to explain the depositional history of Clements Markham Inlet following the last glaciation (Fig.3.3). During the last glaciation ice occupied the head of Clements Markham Inlet where typical sections reveal striated bedrock overlain by till which is overlain in turn by deepwater marine silts recording the overstep succession (section 2, Fig.3.3). These marine silts were commonly exposed to subaerial erosion after rapid emergence. At other localities the marine silts were overlapped by deltas as sea level regressed in the presence of high sediment influx (section 1, Fig.3.3). Following rapid emergence, lower-elevation littoral sediments (sands and gravels) were deposited over the marine silts (section 3, Fig.3.3). Beyond the margin of the main trunk glacier in Clements Markham Inlet the peripheral depression was occupied by the full glacial sea (England 1983). Throughout this area small outlet glaciers from adjacent uplands descended and locally terminated in the sea (Fig.3.3). Consequently, the stratigraphy in sections 4, 5 and 6 (Figure 3.3) reveal intercalated marine and glacial deposits which record fluctuating margins that either floated or calved in the full glacial sea. Such sequences are typical of long-term grounding line deposits or morainal banks (e.g. Bell 1981, 1984; McCabe et al. 1984; Drewry 1986, Chap. 13). In subsequent discussions, Bednarski's (1984) model is used as a guideline in the interpretations of the glacial marine stratigraphy in Phillips Inlet/Wootton Peninsula.

3.4: Glacioisostasy.

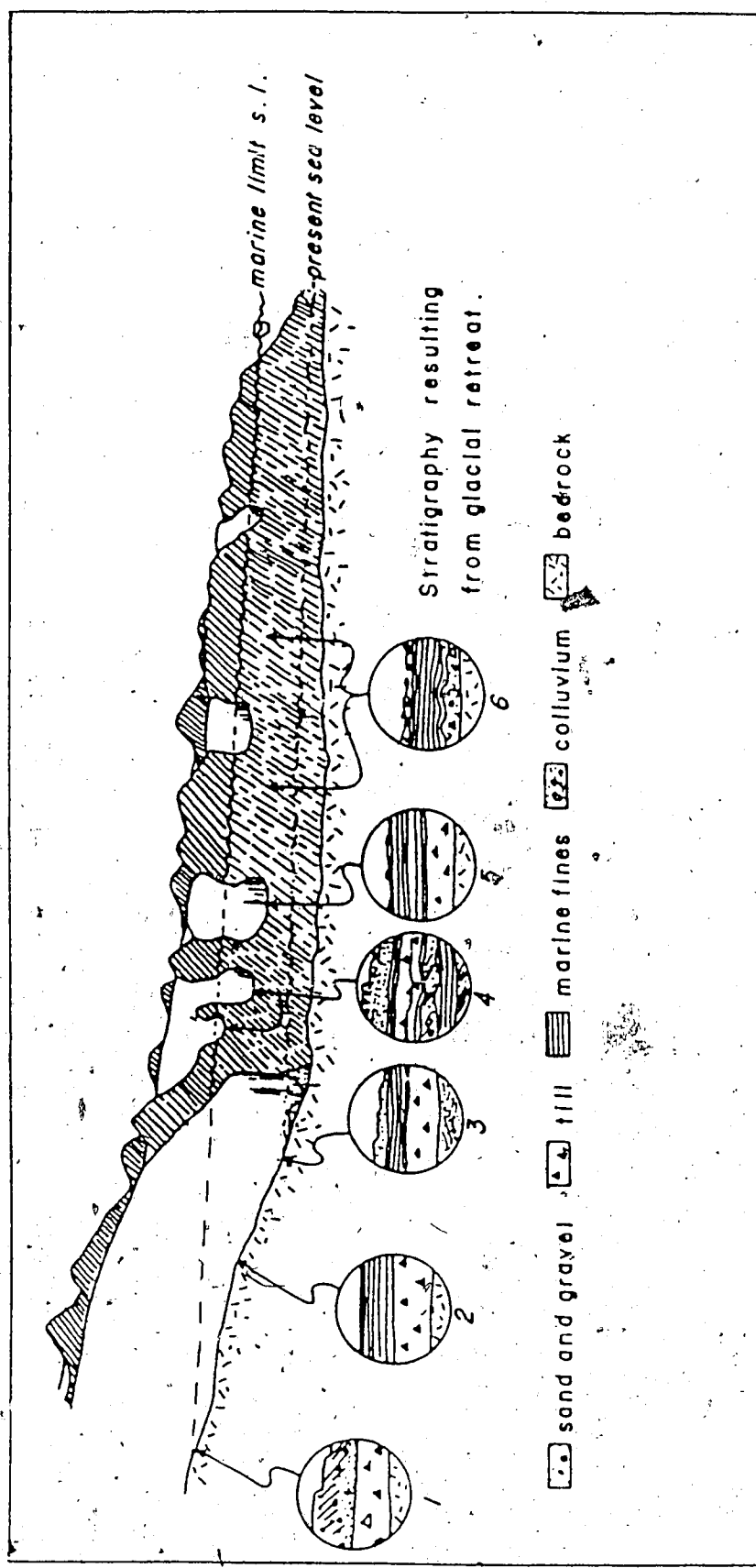


Figure 3.3: Depositional sequence resulting from the last glacial cycle in Clements Markham Inlet at 11-10ka BP (from Bednarski 1984).

3.4.1: Introduction.

Because comprehensive reviews of glacioisostasy and the interpretation of emergence patterns are available elsewhere (cf. Andrews 1970; Bednarski 1984) only a general outline is provided here. A glossary of terms relevant to this section is available in Appendix 3. This thesis, in part, constitutes an important extension of the regional sea level history of northern Ellesmere Island (see section 1.4). Such work attempts to reconstruct former ice sheet configurations through the inverse method of radiocarbon dating raised marine shorelines whose elevations record the pattern of regional, differential emergence. It is generally assumed that those areas where a given shoreline has emerged the most coincide with the greatest amount of unloading, hence the thickest ice (prior to deglaciation).

3.4.2: Methodology for reconstructing deglacial and sea level history.

3.4.2.1: Landforms.

A valid reconstruction of deglacial and sea level history relies entirely upon the correct interpretation of raised marine sediments and geomorphology. In order to construct relative sea level curves and isobases strandlines must be identified, surveyed accurately and dated. The following methods of field observation, measurement and collection were conducted in the Phillips Inlet/Wootton Peninsula field area.

Former sea levels at any site are determined by measuring the height of raised marine strandlines, washing limits or deltas. Although considerable reworking of marine sediments may occur by slope processes in areas of precipitous relief (eg. fiord walls), undisturbed raised marine landforms are often concentrated at fiord heads and other lowland embayments. The outer lip of a raised delta is often used as the former sea level. An unknown degree of error is introduced by using this approach because the lip of the delta may have retreated by back wasting during postglacial time. Bednarski (1984) has

suggested that kame terraces also may be misinterpreted as deltas. These problems are countered most effectively by using several criteria and a variety of local sites to measure marine limits. Another problem may occur if one misattributes a lower shoreline for the true marine limit. For example, a delta may be built into a lower sea level during the onset of rapid retreat, when sediments become abundant, whereas the true marine limit remains unrecorded because of limited sediments during the early stages of deglaciation (England 1987a). In this case, the lower sea level may be misinterpreted as an indication of later deglaciation or lower postglacial emergence. Similar problems may occur when a pre-existing terrace is eroded to a lower sea level and its original fauna is misattributed to the lower and younger sea level. Finally, other problems occur when one tries to assign a specific elevation to landforms which span a range of several metres and these field problems are discussed adequately in Andrews (1970).

3.4.2.2: Surveying.

A Wallace and Tiernan altimeter and a standard surveying level were used in this study to measure raised marine strandlines and deltas. Because the accuracy of an altimeter is pressure and temperature dependant, it is critical to recheck sites as many times as is logistically possible. Even though periods of stable atmospheric pressure are common in the high Arctic, and rates of change often gradual, single altimeter readings can be in serious error (>10m). Therefore pressure and temperature corrections were applied to all readings. However, it should be stressed that arctic conditions are virtually ideal for altimetry. In order to increase surveying accuracy the elevation of base camp was levelled and this provided an accurate datum at the beginning and termination of daily altimeter surveys, especially when the camp was well inland from sea level. If possible, sea level readings also were obtained for calibration of the altimeter throughout the surveys. Commonly, it

has been reported that the altimeter is within ± 2 m on levelled elevations up to 100m asl and within ± 0.5 m at 10m asl (Bednarski 1984). The altimeter provided by the Geological Survey of Canada was also calibrated in Ottawa prior to the field season. Tidal ranges are < 50 cm in Phillips Inlet and because sea level readings are usually taken from high tide there may be a small source of error when identifying the high tide mark. This is most pronounced when measuring sea level on ice-choked shorelines which have little wave action.

3.4.2.3: Determining postglacial emergence.

Once strandlines have been identified and measured they have to be dated accurately in order to reconstruct an emergence curve. Problems in the reconstruction of previous emergence curves from northern Ellesmere Island were the result of the incorrect use of dated shell samples (cf. England 1974c, 1976b). For example, the very steep emergence curves constructed by Hattersley-Smith and Long (1967) and Lyons and Mielke (1973) were obtained by plotting dated shell samples at the elevation where they were collected directly onto the emergence curve. Shells live under water and must relate to a sea level above the sample collection site (up to 165m according to the depth range of *Hiatella arctica* and *Mya truncata*, Wagner 1969). Consequently it is critical to the reconstruction of an accurate sea level history that good stratigraphic control is obtained. Shells collected from deltaic foresets or bottomsets are ideal because they can be traced to the related sea level marked by the delta surface. Otherwise shell samples in stratigraphically isolated sediments (such as silt terraces) relate to sea levels some unknown elevation above their collection height. Therefore, they can be used only as minimum dates on local deglaciation or initial emergence (in the peripheral depression).

The accuracy in dating of marine molluscs by the ^{14}C method has been

improved recently by the use of accelerator mass spectrometry (AMS); see Appendix 1). Formerly dates were obtained solely on bulk samples or extremely large single valves. With bulk samples the possibility of obtaining a blended age (from a mixed population) is high if the shells are not *in situ* (cf. England 1983). This problem is compounded when dealing with shell fragments because any reworked, older material would produce a blended and possibly anomalous age for the deposit. All of the samples submitted for ^{14}C dating in this study were analysed at the Isotracer AMS laboratory, University of Toronto, enabling the submission of single valves. Although it is desirable to submit shells collected in life position this is not always possible and fragments are dated if whole valves were unavailable at important sites. Moreover, by using AMS dating additional fragments from the same site may be dated in order to check the age of the deposit.

Driftwood is also useful both to date former sea levels and to estimate the history of sea ice severity. If driftwood is embedded in a raised beach it likely dates that level because beaches tend to experience little mass movement, thus preventing redeposition of the driftwood downslope. The usefulness of driftwood in constructing detailed emergence curves has been demonstrated on southern Ellesmere Island (Blake 1975). Because driftwood has a residence time of only 20 years in the Arctic Ocean (Haggblom 1982), it is also a good indicator of sea ice severity and can be used as a palaeoclimatic indicator regardless of height above present sea level (Blake 1972; Stewart and England 1983). Driftwood was collected throughout the field area but only those samples thought to have remained in place since their stranding were submitted for dating. Similarly, the remains of marine mammals (such as whales) are a good indicator of past sea levels because most tend to beach themselves before death or float for sufficient time after death for possible stranding (Dyke 1979, 1983, 1984).

The next chapter returns to the theme of glacial land systems based upon

observations on the contemporary glaciers of the field area. A general landsystems model is constructed and used in Chapter 5 to complement the geomorphic and stratigraphic data.

CHAPTER FOUR

Glacial geologic processes and a landsystems model for Phillips Inlet and the Wootton Peninsula.

"It was a lofty headland, and the land ice which hugged its base was covered with rocks from the cliffs above. As I looked over this ice belt, losing itself in the far distance, and covered with its millions of tons of rubbish, greenstones, limestones, chlorite slates, rounded and angular, massive and ground to powder, its importance as a geological agent in the transportation of drift struck me with great force. Its whole substance was studded with these varied contributions from the shore; and further to the south, upon the now frozen waters of Marshall Bay, I could recognize raft after raft from the last years ice belt, which had been caught by the winter, each one laden with its heavy freight of foreign material. These rafts in Marshall Bay were so numerous, that, could they have melted as I saw them, the bottom of the sea would have presented a more curious study for the geologist than the boulder-covered lines of our middle latitudes. Extract from Elisha Kent Kane's Arctic Explorations, 1898.

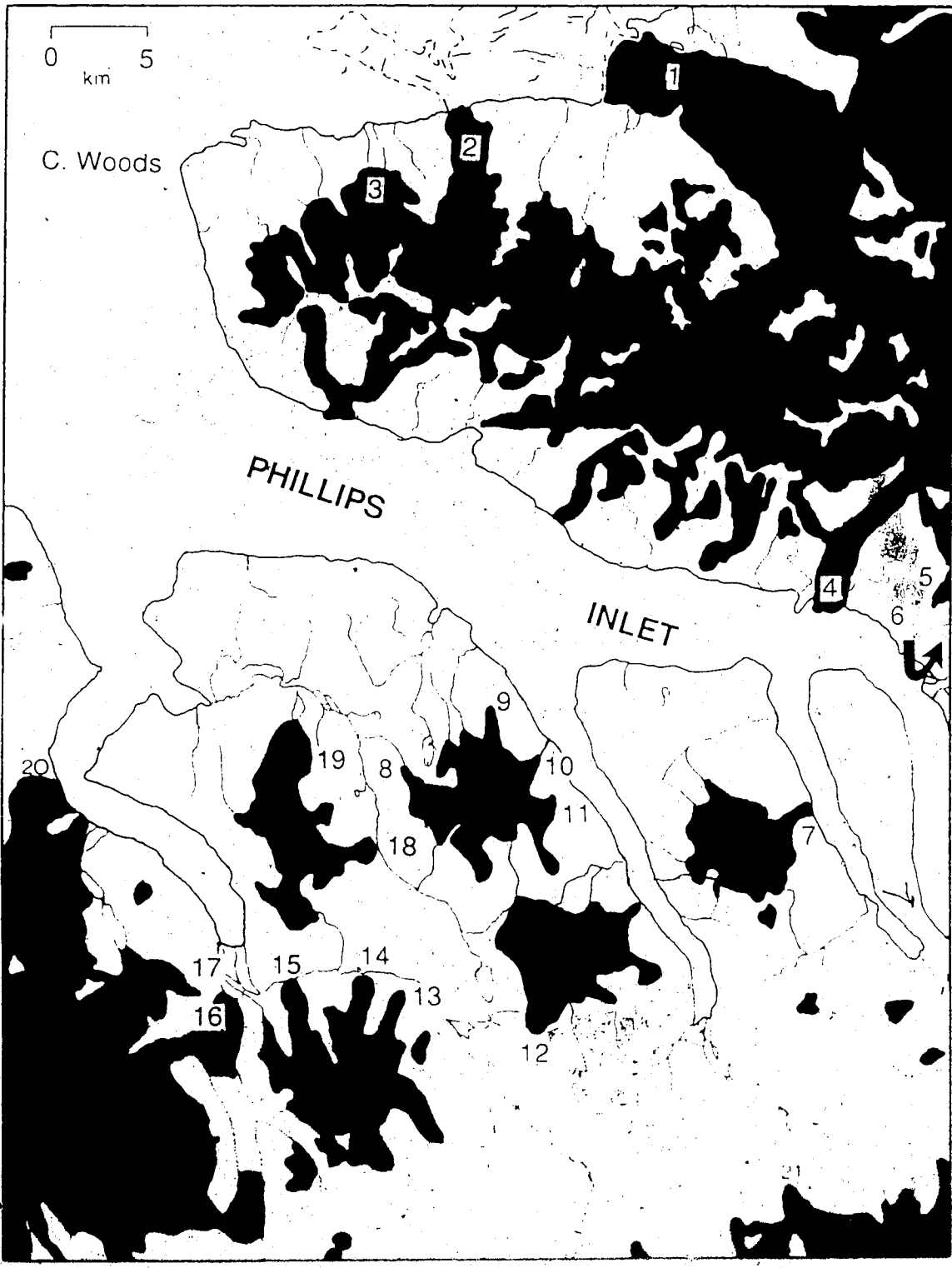
4.1: Introduction and glacier classifications.

The glaciers and physiography of Phillips Inlet/Wootton Peninsula are used to sub-classify a landsystem model (Eyles 1983) so that it is applicable to areas of high relief. The glaciers are classified as: 1. transection glaciers; 2. cirque glaciers; 3. piedmont glaciers; and 4. plateau ice caps. The distribution of these glaciers is controlled by the three physiographic zones of the field area and the regional glaciation level (Chapter 2). Transection and cirque glaciers are concentrated in Zone 1 of the south Wootton Peninsula whereas plateau ice caps and piedmont glaciers occur in Zones 1a (north Wootton Peninsula) and 2 (south of Phillips Inlet, Fig.1.3). Observations on 21 glaciers throughout the field area (Fig.4.1) are used to construct an overview of glacial geologic processes in this high latitude environment. The locations and characteristic landform/sediment associations of the different sub-landsystems are then discussed.

4.2: Observations on glacial geologic processes.

The following sections concern the nature of supraglacial debris,

Figure 4.1: Map of glaciers used in the analysis of glacial geologic processes and the construction of a landsystem model. The following are unofficially named and referred to in text: 1 Alfreds; 2 Woods; 4 Tidewater; 5 Hidden; 6 Dogleg; 14 Badweather; 15 Kipper; 16 Pudding; 17 Vienna; 18 Muskox; 19 Deception; 20 Terrible; 21 Endeavour.



mechanisms of debris entrainment and processes acting at the glacier margins. Each is discussed prior to the development of a landsystems model for the area.

4.2.1: The supraglacial system.

Although there was considerable climatic variability during the summers of 1985-1987, large amounts of supraglacial meltwater characterized all three seasons. Investigations on the surface of Tidewater Glacier (a transection/floating glacier, Fig.4.1) revealed a close relationship between its medial moraine and crevasse fillings in the ablation zone (Fig.4.2a). The glacier surface is heavily crevassed across its lower 7km and supraglacial streams are consequently short. A small tributary glacier coalesces with the floating snout forming a medial moraine some 2km long between the two glaciers. This zone of coalescence serves as a meltwater conduit and as a result the moraine has been fluvially reworked, sorted and redeposited in crevasses. In some places on the glacier surface ablation has led to topographic reversal and faulted bedding can be observed in the resulting ice-cored sediment cones (Fig.4.2b). Cones (<5m high) consisting of coarse, angular slate are present on the surface of Muskox Glacier (Fig.4.1). Here foliation and debris bands rise to the glacier surface due to compressive flow at the snout. This material is derived from steeply dipping slate bedrock which forms a 150m wall above the accumulation zone. Consequently, rockfalls are carried englacially and reappear at the glacier surface below the ELA. The deposition of supraglacial cones and kames by former glaciers is invaluable to the reconstruction of palaeo-ELA's (Andrews 1975b).

In the absence of extensive crevasses, meltwater channels meander across the glacier surfaces. Because most of the glaciers have steep or cliffed margins, supraglacial or englacial meltwater exits as waterfalls. The mode by which meltwater streams exit is important to the redistribution of debris at the snout. At the snout of Pudding Glacier (Fig.4.1) a supraglacial



Figure 4.2: Above; part of air photograph no. A 16724-76 illustrating Tidewater Glacier, its tributary and resulting medial moraine—Scale bar is 1 km. Arrow denotes position of photograph below. Below; stratified sands and gravels formerly deposited in a crevasse along the medial moraine and now topographically reversed by ablation. Pack and ice axe for scale

stream is cutting down through the ice cliff depositing large amounts of coarse bedload within tight englacial meanders (Fig.4.3). Abandonment of these bends provides small concentrations of gravel for later reentrainment which can subsequently deform the material in englacial folds.

4.2.2: Debris patterns within glacier margins.

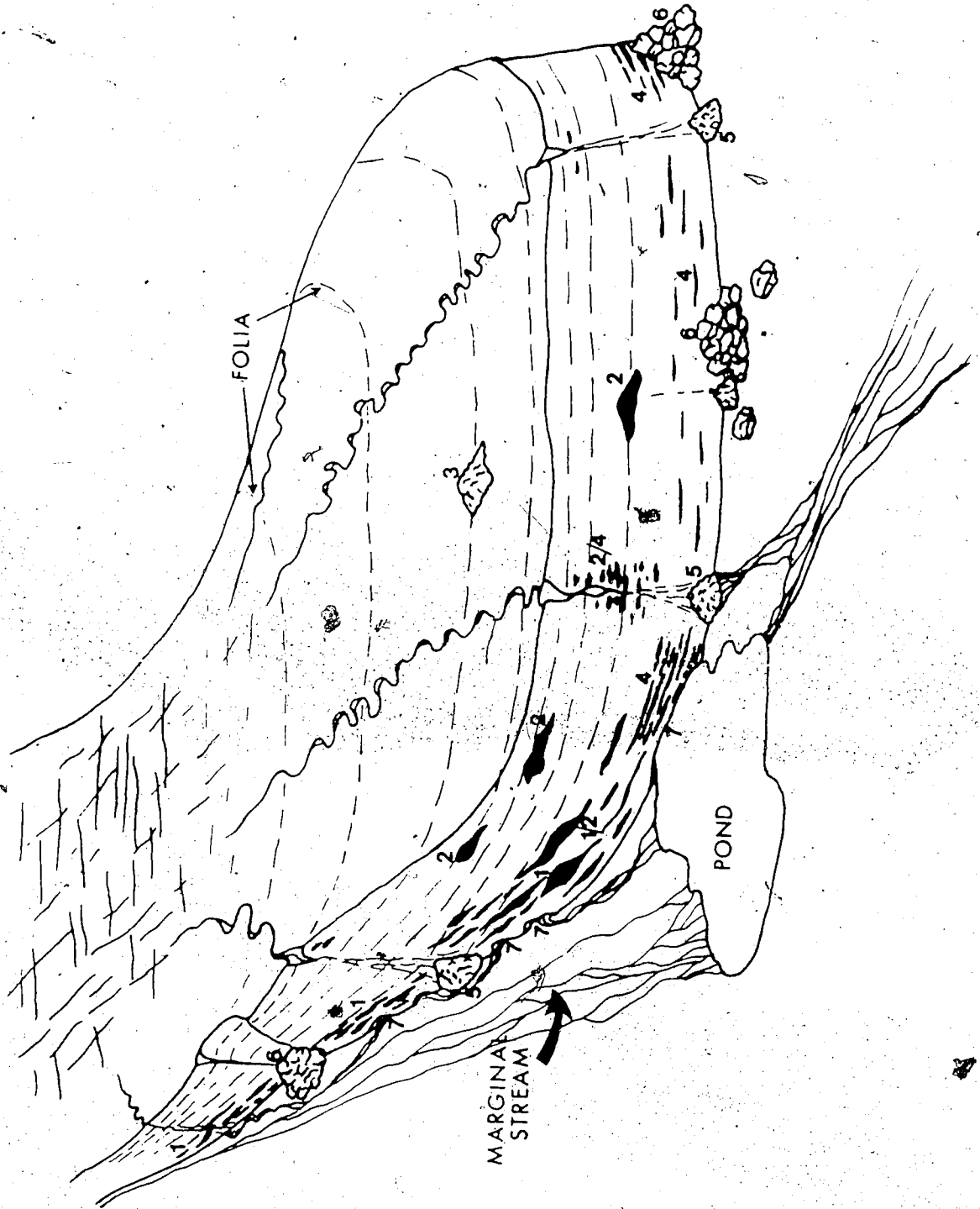
Debris concentrations at the margins of the glaciers in the field area occur as: 1. debris bands of varying thickness that become attenuated down glacier (Fig.4.4); 2. debris clots or augens which are often smeared or folded; and 3. debris-poor folia which are dispersed throughout the glaciers and express internal flow patterns. Basal ice, observed in the cliffed margins, always becomes debris-poor up glacier and coarse debris terminates well below the long-term ELA. In the snouts of many glaciers single narrow bands characterized by large concentrations of the above debris have been brought to the ice surface by compressive flow. These bands occur up to 1km up-glacier of the snout cliffs.

The debris bands (1) are concentrated predominantly in the basal ice layers. The debris bands are irregularly spaced, contain gravels, sands and silts in varying concentrations and rarely penetrate the ice cliff more than 50cm horizontally. In most glaciers the debris bands are more abundant at lateral margins (1 on Fig.4.4). Furthermore, they often cut across folia and become less abundant both with height at the snout and up-glacier. Debris concentrations in these bands are estimated at <40% volume. The debris bands constitute the basal zone in Lawson's (1979, p.6) idealized ice facies model whereas the debris-poor folia (3), with occasional discontinuous debris bands, likely represent the diffused englacial zone. Further comparisons with Lawson's model, notably the twofold subdivision of both his englacial and basal facies, are considered inappropriate for the field area because they are not readily identifiable.



Figure 4.3: Supraglacial stream cutting down through the snout of Pudding Glacier in series of tight meanders. Debris has been deposited in abandoned meanders and is now being reentrained and folded by glacier flow perturbations. Tim Fisher at left for scale.

Figure 4.4: Idealized sketch of a piedmont lobe (with no proglacial thrusting) illustrating positions of 1. lateral debris bands; 2. augens; 3. supraglacial debris cone; 4. frontal debris bands; 5. waterfall debris piles; 6. calved blocks/aprons; 7. thermo-erosional niches cut by lateral streams and an associated ice marginal pond.



Augens (2) occur at many levels in the ice but again are largely concentrated near the base (Fig.4.4). They contain a variety of sediment ranging from coarse angular debris to fine sands and silts. The degree of sorting varies considerably. The augens do not display a consistent internal structure and contain <10% ice (Fig.4.5). Material from augens and debris bands has been observed slumping or falling out of the ice face. In some cases the material has been completely removed from the ice (Fig.4.6). If this debris falls on stagnant ice then ice-cored cones form at the glacier margin.

Apron entrainment, as discussed by Shaw (1977b), is apparent where distinct re-entrained ice blocks, containing dispersed debris, occur in the basal ice zone (Fig.4.7). Above these re-entrained aprons, at the junction of the overriding ice, debris bands contain a variety of grain sizes, including cobbles and large sub angular clasts.

The amount of debris entrained varies from glacier to glacier, even between glaciers of similar proportions, substrates and basin characteristics. Possible reasons for this will be addressed in section 4.3. Twelve samples of 50 clasts were taken from ice facies within the Endeavour, Terrible and Dogleg glaciers (Fig.4.1). Another seven samples were taken from material immediately adjacent to these glaciers (Appendix 2) in order to determine possible relationships between proglacial processes and glacial entrainment.

4.2.3: Contemporary proglacial processes.

The most active processes observed at the glacier margins are fluvial (Fig.4.4). Supraglacial meltwater falling over the steep margins provides debris for proglacial meltwater streams. These streams have been observed cutting into the glacier margins and disappearing for up to 20m before exiting again. This undercutting leads to ice block detachment from the snout and ice apron accumulation causing migration of proglacial meltwater channels (Fig.4.8). It is apparent that lateral incision by meltwater streams at the



Figure 4.5: Augen structures in Pudding Glacier, both at the base (clayey silt) and high up (coarse clasts and gravels) in the snout cliff. Note the smearing above the higher augen structure which possibly represents the finer material formerly draping the sides of a crevasse. Scale bar is 1 metre.



Figure 4.6: Augen structure containing gravels and sands at the margin of Musk Ox Glacier. This structure has completely slumped out to form an ice-cored mound on the ice step. Ice hammer arrowed for scale.



Figure 4.7: Reentrained ice blocks from a former apron at the base of Pudding Glacier. Note debris band at junction of ice blocks and overriding ice.



Figure 4.8: Lateral incision and ice block collapse over ice-cored gravel terraces at the margin of Terrible Glacier.

base of the ice margin cuts an ice step over which the stream can migrate. This ice step can be buried by stream aggradation or downcut further by stream degradation. Where a part of the ice step or stream bed represents a short-lived plunge pool or slack water section, an ephemeral pond may collect sediment. Such ponds were observed in front of Muskox and Terrible glacier's where they had cut thermo-erosional niches into the snout cliffs (Fig.4.4). Providing that these ponds are large enough, pockets of sands and silts may collect. Drainage of these ponds can leave ice-cored sand/silt cones or drapes (Fig.4.9). Similar protection of underlying ice is afforded by the bedload of abandoned marginal streams. Ice-cored debris mounds also result from abandoned waterfall debris (at the margins of glaciers with considerable supraglacial debris); slumped augen structures; and the sliding of supraglacial cones onto ice steps. Such an ice-cored cone was observed partially entrained at the margin of Muskox Glacier (Fig.4.10). Ice steps are permanent features of advancing glaciers with proximal marginal meltwater channels and they are consistently buried by dry calving.

Stagnant buried ice is evident beyond several glacier snouts (Fig.4.11). A large amount of stagnant ice, deposited from recurring ice avalanches, also occurs beyond an outlet glacier draining the south Aviator Ice Cap (Evans and Fisher 1987). Because northwest Ellesmere Island is in the zone of continuous permafrost where the active layer is <1m, it would take a considerable climatic change to melt this buried ice. Buried ice is also present at the inner margins of the thrust block belt that wraps around the snout of Muskox Glacier (see below). Here, a large number of ice-cored cones on the thrust block scarps are melting out and collapsing.

4.2.4: Contemporary glacitectonic structures and associated sediments.

4.2.4.1: Definitions.

Proglacially thrust landforms are invariably termed "push moraines"

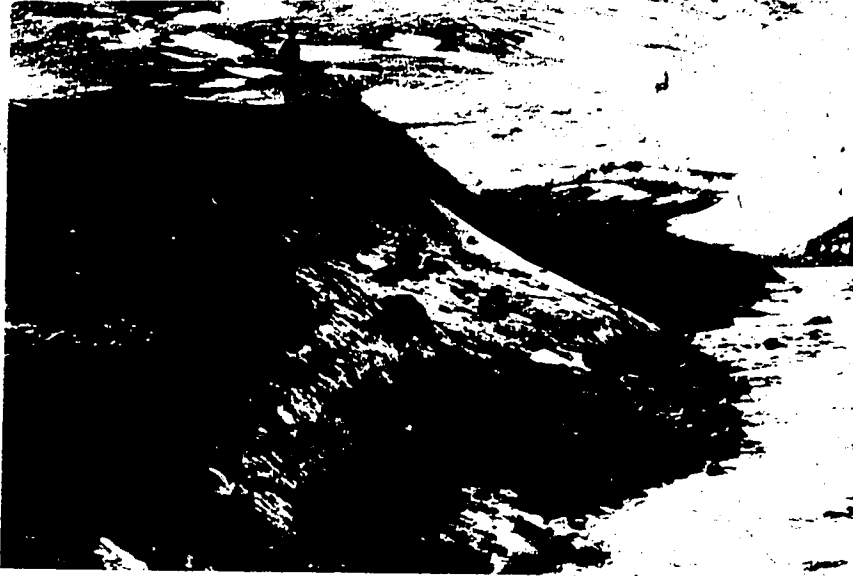


Figure 4.9: Sand/silt drape over stagnant ice at the margin of Musk Ox Glacier. Material was originally deposited in an ice marginal pond or slack water eddy on either the downwasting snout or a fluvially cut ice step.



Figure 4.10: An ice-cored debris cone in a position of partial entrainment at the margin of Muskox Glacier. Note the thin veneer of debris and its continuation into the face as an undulating debris band and the thick band of clean ice below.



Figure 4.11: Stagnant ice displaying recumbent folds and buried by alluvium at the margin of Endeavour Glacier.

in the literature (cf. Embleton and King 1975; Sugden and John 1976). A present INQUA Commission on the terminology of landform and till genesis has included "thrust moraine" as a form of "under-ice moraine" and "push moraine" as an "ice marginal" feature raised and deformed by ice edge thrusting. In the high Arctic thrust blocks are not "under ice" features. Rather, they are strictly ice marginal. Furthermore, because the dominant process involved in the construction of the high Arctic examples is proglacial block thrusting, a more appropriate morphogenetic term "thrust block moraine" is adopted here. This terminology has been used previously by Andrews (1975b) and Embleton and King (1975).

4.2.4.2: Processes.

The shear strength of a material is increased considerably when it is frozen and therefore original sedimentary structures can be preserved relatively intact within thrust block moraines. Thrusting occurs along a suitable decollement or failure plane and this may coincide with the base of permafrost where the pore water pressure is at its highest (cf. Mathews and Mackay 1960; Banham 1975). However, in the high Arctic permafrost depths exceed 450m and therefore decollement must occur along intra-permafrost beds such as clay rich-layers (which can remain plastic below freezing temperatures) or along segregated ice lenses. Thrusting can occur also through the failure of ice wedges in proglacial sandar (Klassen 1982). Shaw (1985) presented a simplified Coulomb equation to explain glacitectonic deformation:

$$S = C + (P_o - P_w) \tan \bar{\phi}$$

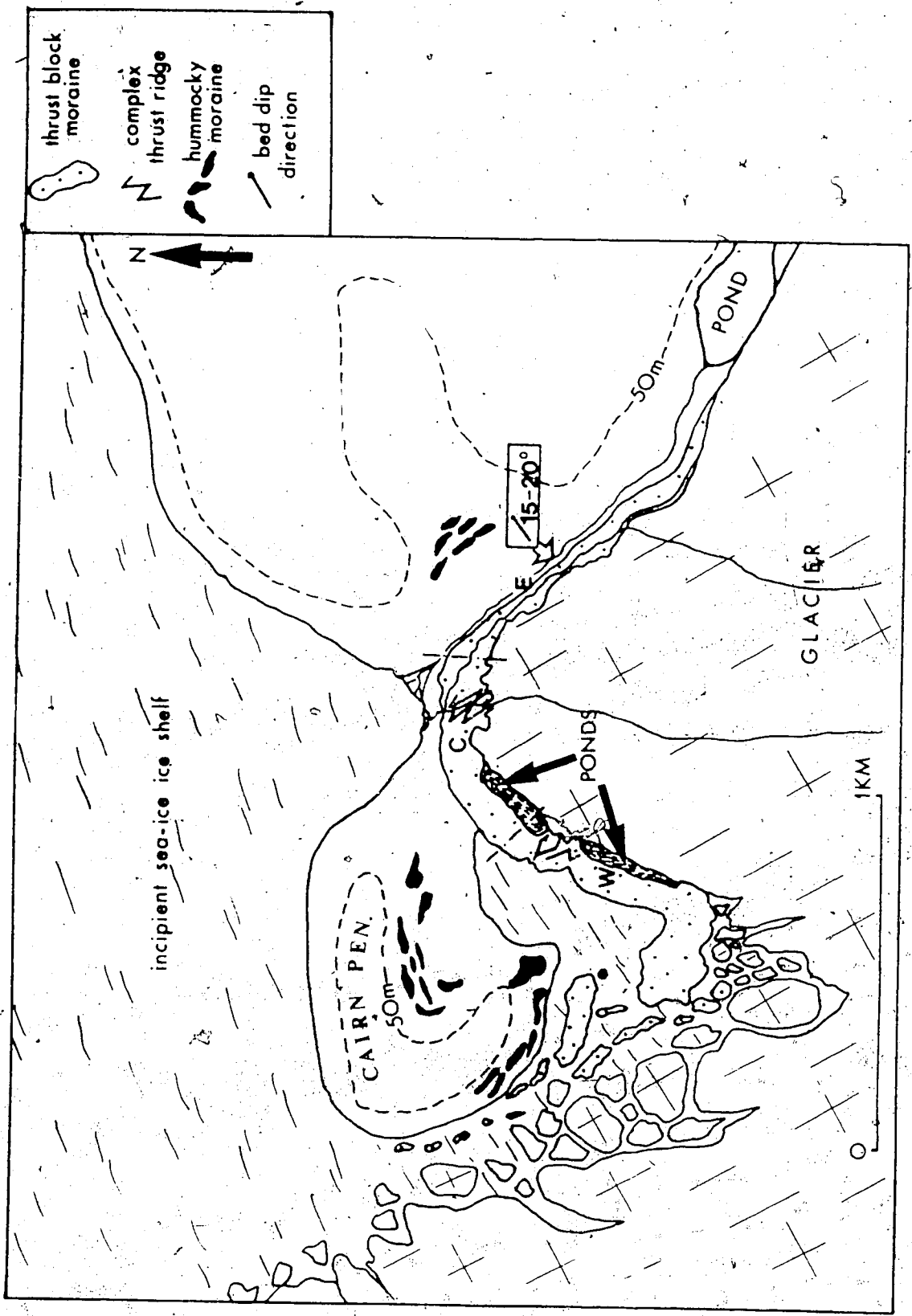
where S is shear strength (kpa), C is cohesive strength (kpa), P_o is overburden pressure (kpa), P_w is pore water pressure (kpa) and $\tan \bar{\phi}$ is the coefficient of solid friction. Applied glacier shear stress must equal or exceed S in order for failure to occur.

4.2.4.3: Observations.

Many of the piedmont glaciers act as outlets to plateau ice caps and where they descend through ice falls generate some severe longitudinal shear stress gradients. The thrust block moraines and sediment associations at four such glacier snouts are discussed here. Alfreds Glacier and Muskox Glacier are presently undergoing minor retreat from their thrust block moraines whereas Dogleg Glacier and Pudding Glacier are presently advancing over thrust blocks.

Alfreds Glacier is a transection glacier approximately 20km long and 3-4km wide (Fig.4.1). Its heavily crevassed snout debouches into the Arctic Ocean and forms the main component of the Cape Alfred Ernest Ice Shelf. The northern edge of the glacier impinges on Cairn Peninsula where it has formed a 2km long and 5-20m high, thrust block moraine comprised of a single arc (Fig.4.12). It is not known whether this moraine originally stretched along the frontal margin of the glacier, but other moraines occur at the outer edge of the glacier ice shelf (see Fig.2.7). The eastern sector of the thrust block moraine (E, Fig.4.12) contains a 15m high section of stratified glacial marine sediments with numerous dropstones and prolific *Astarte borealis* in growth position. Overlying the section is 5m of coarse, crystalline cobbles and boulders. There is little internal disturbance of the thrust block and the sedimentary beds dip 15-20° southwest. A braided stream fed by proglacial meltwater exists behind the eastern sector of the moraine. In the centre of the thrust block moraine (C, Fig.4.12) a drape of cobbles and boulders obscures the glacial marine sediments. Complex thrust ridges indicate displacement perpendicular to the ice front in addition to the overall parallel trend. The western sector of the thrust block moraine (W, Fig.4.12) is the most disrupted and lowest in relief and it is entirely covered in coarse debris. The outermost extension has been detached and displaced westward around Cairn Peninsula by glacier flow. Considerable sediment reworking is occurring between the thrust block moraine and the glacier snout.

Figure 4.12: Map of thrust block moraine and associated geomorphic features around the margin of Alfreds Glacier.



Two ponds are dammed between the ice margin and the central and western sectors of the moraine. Debris piles border the ponds and these appear to be redeposited from both the glacier and the thrust blocks.

Dogleg Glacier is approximately 8km long and 1.5km wide, occupying the upper reaches of a valley north of Wind Gap. The main lobe spills over a col into Wind Gap where it is presently overriding a 20m high block of braided outwash (Fig.4.13). No other thrust blocks occur distal to the snout. The sedimentary beds of the block dip $20-25^{\circ}$ (to the northeast) providing clear evidence for glacial thrusting. The glacier snout itself reveals a transition from relatively clean ice facies at the top to basal debris-rich ice and frozen alluvium at the bottom. Clast sample nos. 24-7-8701 to 24-7-8704 were taken from the ice cliff and from the thrust alluvium (Appendix 2). Because of the instability of the thrust blocks, mass movement is widespread (debris flows and rock falls). Furthermore, waterfalls from the ice cliff are reworking the thrust block and constructing alluvial fans on its surface. In several places ice blocks have dry-calved onto the surface and the toe of the thrust block. The northern margin of Dogleg Glacier is presently advancing over a bedrock ridge with a till veneer and thrusting is not occurring.

Muskox Glacier is a piedmont lobe 3km long and 1.5km wide at the snout (Fig.4.1). It is fed by a plateau ice cap and consequently there is strong compressive flow near its snout with folia dipping 45° up-glacier. This fact, together with the constricted nature of Muskox Valley, has produced the most extensive thrust block moraine in the field area (Fig.4.14). This moraine was originally identified by Kalin (1972) using air photographs. Two sets of arcuate thrust ridges, 10-20m high, wrap around the glacier's eastern margins (Fig.4.15). The two sets are separated by a meander in the upper Muskox River which may have disrupted a once continuous thrust block belt. The thrust blocks are composed of braided outwash and the beds dip between $15-25^{\circ}$ towards the glacier. There is considerably less overburden of coarse debris than on



Figure 4.13: Dogleg Glacier and its thrust block moraine in Wind Gap.

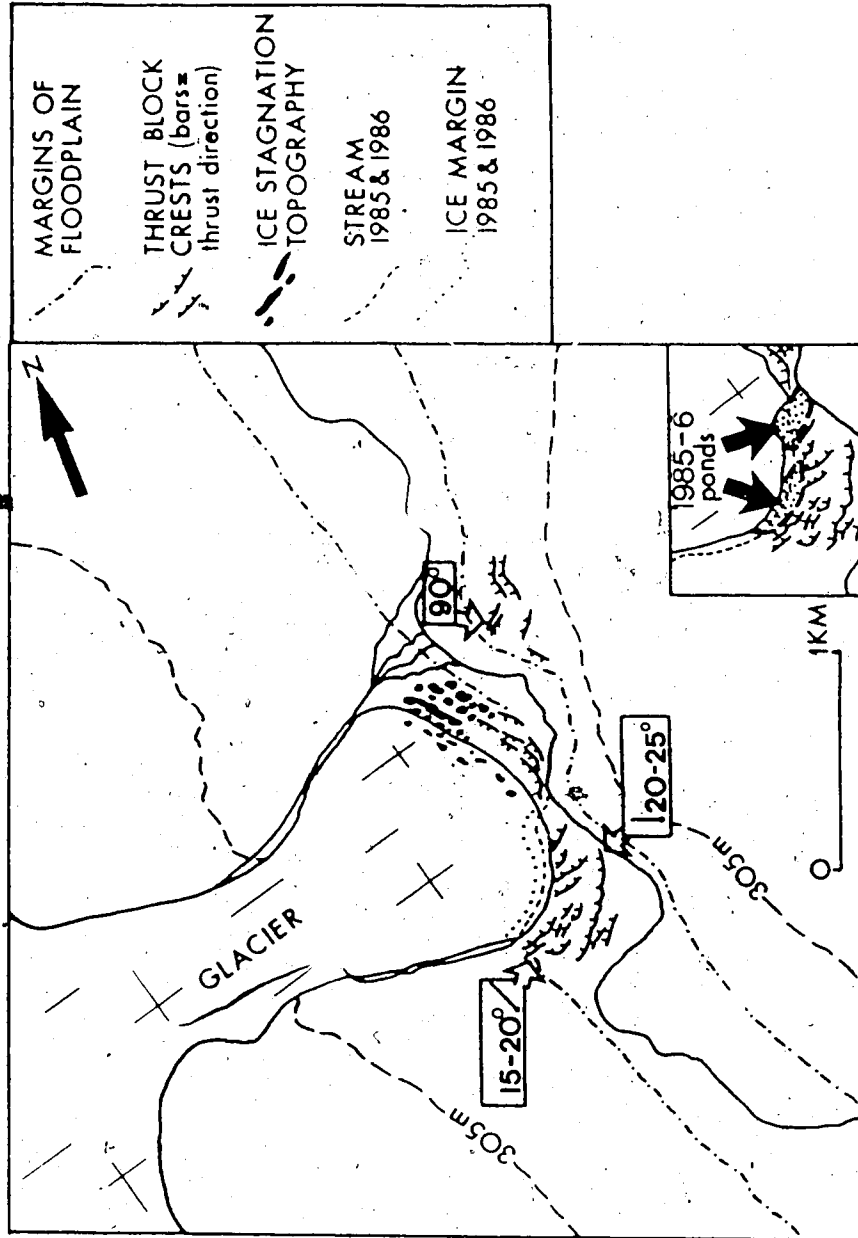


Figure 4.14: Map of thrust block moraine and associated geomorphic features around the margin of Muskox Glacier as in 1959. Inset is a map of the snout margin in 1985 and 1986.

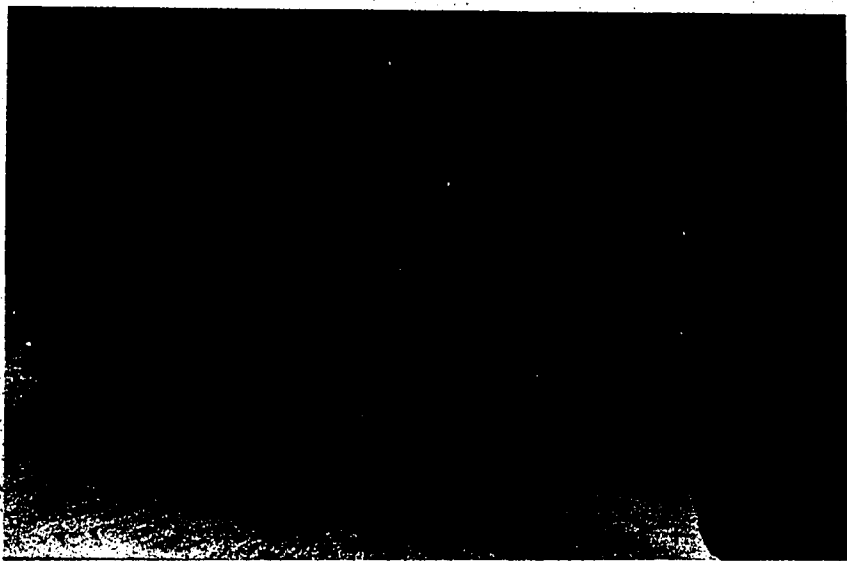


Figure 4.15: Photograph of Muskox Glacier and its thrust block moraine from the air.

the thrust block moraines of Alfreds and Dogleg glaciers. A 1959 air photograph reveals that the glacier was then in contact with the inner thrust blocks along its southeast margin. Since then the snout has thinned and a meltwater stream has cut back into the snout. During the summers of 1985 and 1986 two ponds occupied the space between the inner thrust blocks and the snout. The lower pond was the result of flooding by the main river at its peak summer discharge.

Meltwater from the upper pond has excavated a tunnel through ice within one thrust block. Previous higher water levels for the upper pond are evidenced by sand/silt drapes over stagnant ice blocks (Fig.4.9). The lower thrust block slopes have been reworked into small alluvial fans which grade into fan deltas in the upper pond. These deltas, together with debris flows derived from partially submerged ice-cored cones, send sediment out into the middle of the upper pond. The lower pond, although more ephemeral, receives more ice-rafted sediment because of the adjacent cliff in the debris-charged snout.

Puttling Glacier is a piedmont lobe 7km long with a snout 3.5km wide damming a small lake (6.25km^2). The lobe is fed by a plateau ice cap 840m above its snout. Part of the snout is overriding a series of thrust blocks,

5m high and composed of glacimarine silts with *in situ* *Hiatella arctica* shells (Fig.4.16). In contrast a 100m long section of the snout, overlying braided outwash, has failed to thrust this material. Bedrock outcrops in several places on the sandur surface thus explaining the absence of a large-scale thrust block moraine. The glacimarine silt blocks display variable disturbance and are contained within 10m of basal debris-rich ice. In this basal ice reentrained ice and silt blocks are commonly interspersed. Clots of marine silts containing shells also occur in the basal debris-rich ice. Some of the silts have been attenuated and folded in association with intense flow perturbations in the basal ice (Fig.4.17). Occasional blocks of marine silts,



Figure 4.16a: A thrust slice of marine silt, including shells in life position, at the base of Pudding Glacier. A lens of cobbles overlies the silt and could represent former outwash and/or supraglacial gravels deposited by a waterfall. The slice overlies a reincorporated apron of calved ice blocks and debris and a partially overridden thrust block of marine silts is visible in front of Tim Fisher.

Figure 4.16b: A possible explanation for the occurrence of thrust slices in basal debris-rich ice (see Fig.4.16a). T1=proglacial thrusting; T2=initiation of secondary decollement; T3=movement of thrust slice over apron.

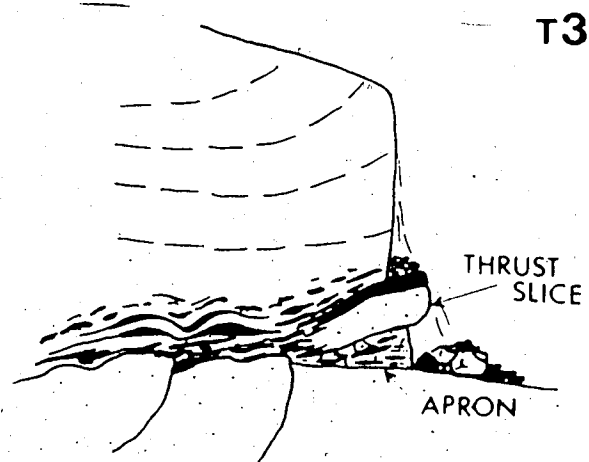
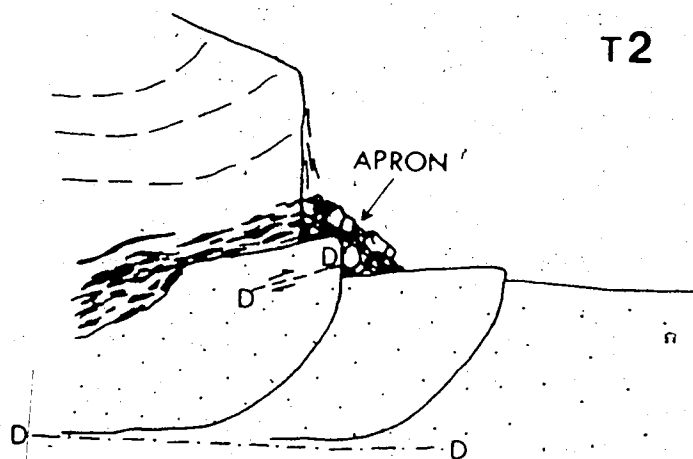
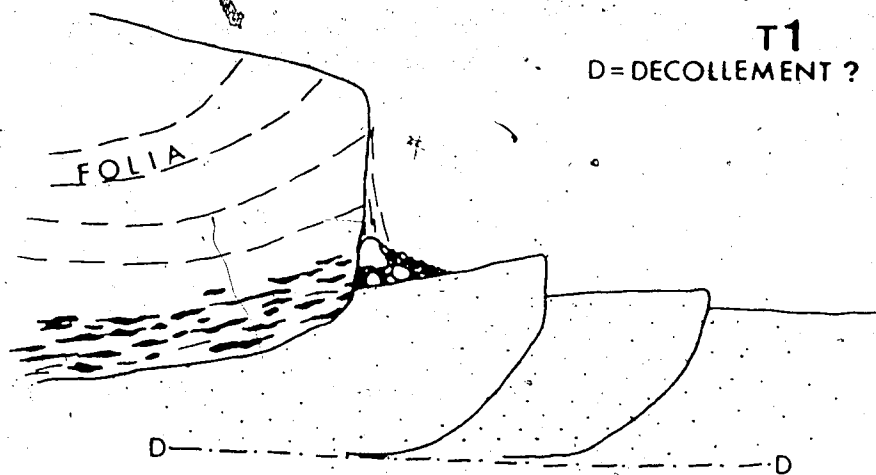




Figure 4.17: Intense folding in the basal debris-rich ice of Pudding Glacier. Glacier flow direction is from the left and out from the photograph.

with overlying gravel beds, have been thrust over stagnant ice blocks and show no signs of internal disturbance (Fig.4.16). Other blocks are heavily faulted and contorted. Other debris concentrations, generally <1m thick, are composed of grain sizes ranging from rounded cobbles to silts. These bands often penetrate the ice horizontally to depths >1m and are associated with attenuated beds of marine silt. In some places the bands have been transported upward within the glacier into faster moving ice. This is caused by compressive flow while the glacier overrides thrust blocks and ice aprons. Such irregularities at the bed set up flow perturbations which can penetrate overridden material (Hudleston 1976).

Considerable sediment reworking is occurring at the snouts of all the glaciers involved in the thrusting of proglacial debris. Debris flows, alluvial fans and rock falls from the entrained and overridden material are common. Waterfalls, from supraglacial meltwater, rework and contribute further sediment at the ice margins (Fig.4.3). Dry calving is also active and effectively buries debris at many locations. Proglacial meltwater streams are less effective in sediment reworking at the snout than they are up-ice. This is because the stream bed becomes less confined by constraining bedrock walls and water is redirected away from the ice face by calved ice blocks and debris piles.

4.3: Interpretations of glacial geologic processes and a land system model.

4.3.1: Debris entrainment.

Observations on clasts (cf. Appendix 2) are of importance to the interpretation of glacier bed conditions. For example, stoss and lee forms suggest active lodgement processes (Boulton 1978; Sharp 1982). Successive episodes of melting and regelation at the glacier bed tend to lead to greater rounding and less sphericity. There is also an increase in blades and disks

and multiple striations (Boulton 1978). Comparisons of clast shape and roundness are most appropriate within single drainage basins because clast lithology may affect both parameters considerably. In a geologically variable area like northern Ellesmere Island, comparisons between drainage basins are inadvisable. Here comparisons are made between clasts from within the glacier snouts (9 samples) and those from ice proximal or ice contact material (9 samples). Eleven of these samples were collected from within and around the snout of Terrible Glacier (Fig.4.18). Of the remaining seven samples, three were from within and around Endeavour Glacier and four from within and around Dogleg Glacier. Although there are some anomalies, the data can be summarized as follows. At the snouts there is considerable similarity in stone shapes between cones on stagnant ice, cones on the glacier surface and entrained debris. Along the glacier margins there are also striking similarities between samples from ice marginal fluvial material, partially entrained or overridden gravel terraces and basal gravel lenses. However, one sample from an augen in the englacial banded/basal dispersed ice facies of Terrible Glacier displayed some increase in angularity and a reduction in sphericity, probably as a result of derivation in the supraglacial system up-ice rather than basal traction.

Of the 1450 clasts measured, 130 (9%) had striations and 24 (1.7%) had stoss and lee forms. Of these, only 39 (2.7%) and 5 (0.4%) respectively were directly from the glacier snouts. Hence 91% of the clasts measured showed no direct evidence of glacial modification. The glacio-dynamic implications of these data will be discussed in Chapters 5 and 6. Multiple striations were noted on only 6 (0.4%) clasts, 1 being from a glacier snout. No significant increase in blades and disks was observed between ice marginal and entrained debris. These statistics suggest that there are no successive episodes of melting and regelation at the glacier bed. Moreover, all of the clast data suggest that material undergoes little modification during entrainment and

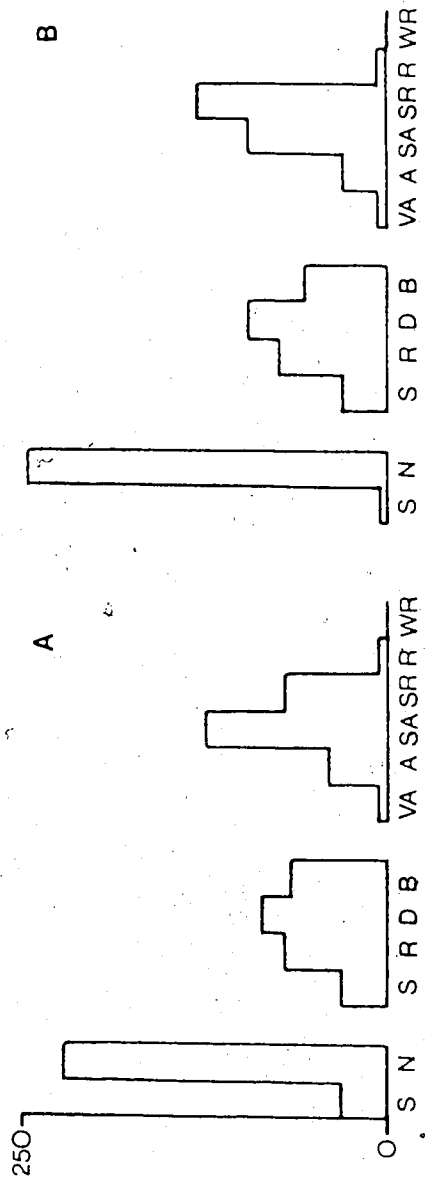


Figure 4.18: Histograms of clast analyses from Terrible Glacier (A, 5 samples) and from the marginal sediments (B, 6 samples). Abbreviations are from left to right: S=striated; N=not striated; S=spheres; R=rods; D=discs; B=blades; VA=very angular; A=angular; SA=subangular; SR=subrounded; R=rounded; WR=well rounded.

that it is transported passively by the Phillips Inlet/Wootton Peninsula glaciers. This is important when interpreting and mapping tills in the field area. Furthermore, any increase in the number of clasts displaying glacial modification within older tills would suggest that glacial thermal regimes were much different during past glaciations.

Up-glacier dipping folia, containing fine particles and occasional pockets of coarse debris (diffused and banded facies of Lawson, 1979) were observed on the Phillips Inlet/Wootton Peninsula glacier snouts. Whether or not these are a product of regelation and/or aeolian deposition and rockfall in the accumulation zone, cannot be determined from observations made in this study (Fig.4.19):

There are at least five possible origins for the augen structures observed at glacier margins. First, augens in the upper ice layers might represent sediments deposited by englacial streams (cf. Gilbert et al. 1985). Augens exposed at the ice face, may represent cross sections of such englacial pipes that are now being attenuated. Second, this debris could have been deposited by supraglacial streams and rockfalls into crevasses in the ablation zone, crevasses that have since closed. If this is correct, then a wide range of grain sizes, either internally or from augen to augen, would not be unusual. Third, debris within augens may have been deposited in meander bends that were later abandoned by migrating supraglacial streams. Fourth, augens exposed in the lower, debris-rich ice may represent accumulations within former plunge pools or the meander bends of marginal streams. These plunge pools and meanders often cut back into the ice and debris is deposited in the resulting hollows and niches. Augens originating from these sources would likely consist of poorly sorted gravels and cobbles. The relationships between marginal streams and entrainment processes is discussed below. Stewart and Bednarski (1986) have suggested that basal crevasses are important conduits for supraglacial and marginal streams and therefore these crevasses act as



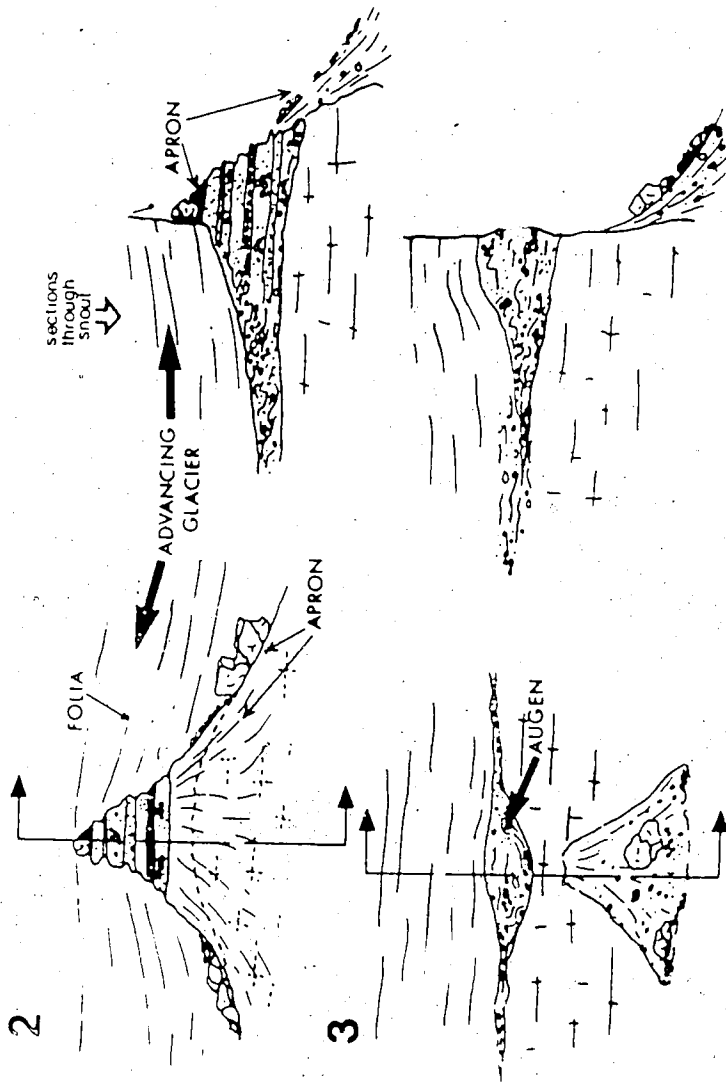
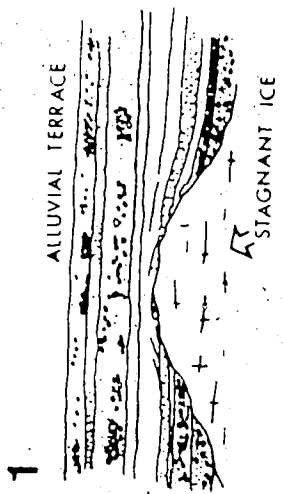
Figure 4.19: Cone of coarse, angular slate with rising folia at the snout of Muskox Glacier. Glacier flow is from the left.

sediment traps. No basal crevasses have been observed in the glaciers of the field area but this does not rule out their possible role in entrainment processes. The fifth explanation of augens involves the reentrainment of ice-cored mounds, aprons and stagnant ice. Ice-cored mounds originate at the ice margin or on ice steps where the sediments from abandoned streams, drained or frozen ponds, slumped supraglacial cones and augens, and waterfall debris accumulate.

A large cave at the snout of Endeavour Glacier revealed "clean" ice with debris-poor folia directly overlying bedrock (Fig.4.20). Elsewhere the snout has advanced onto gravel terraces which were deposited over stagnant ice during a period of glacier recession (Fig.4.11). Subsequent overriding of these ice-cored terraces has led to the incorporation of three augens, approximately 5m in diameter, in the snout cliff (Fig.4.20). Aprons composed of fallen ice blocks may accumulate debris from waterfalls or may have originally fallen on other debris. After reentrainment all of these features will appear as basal, "clean" or debris-poor ice overlain by augens and/or discontinuous debris bands, depending on the amount of debris cover (cf. Figs.4.7 and 4.16). The occurrence of such augens in a glacier snout clearly reflects glacioclimatic change.

Fluvial activity has been recognized as a dominant transport mechanism in the ice marginal environment (Maag 1969; Selby 1972; Evenson et al. 1986). Evenson et al. (1986) suggest that fluvial transport delivers more material to the glacier snout than any other process, especially in areas of moderate to high relief. Because meltwater deposits most material at the glacier margins it clearly plays a major role in the subsequent entrainment of glacial debris. This is especially true in the Canadian high Arctic where long winters without melting allow glaciers to advance and reentrain ice marginal debris. Many debris bands at the lateral margins of the Phillips Inlet/Wootton Peninsula glaciers (Fig.4.4) are interpreted as reentrained bedload because; 1) the

Figure 4.20: An explanation for the origin of gravel augens in the face of Endeavour Glacier (see text for description). The size of augen is dictated by the amount of retrogressive thaw and slumping of the ice-cored terrace before and during incorporation. The debris could be preserved in the glacier as a basal debris band.



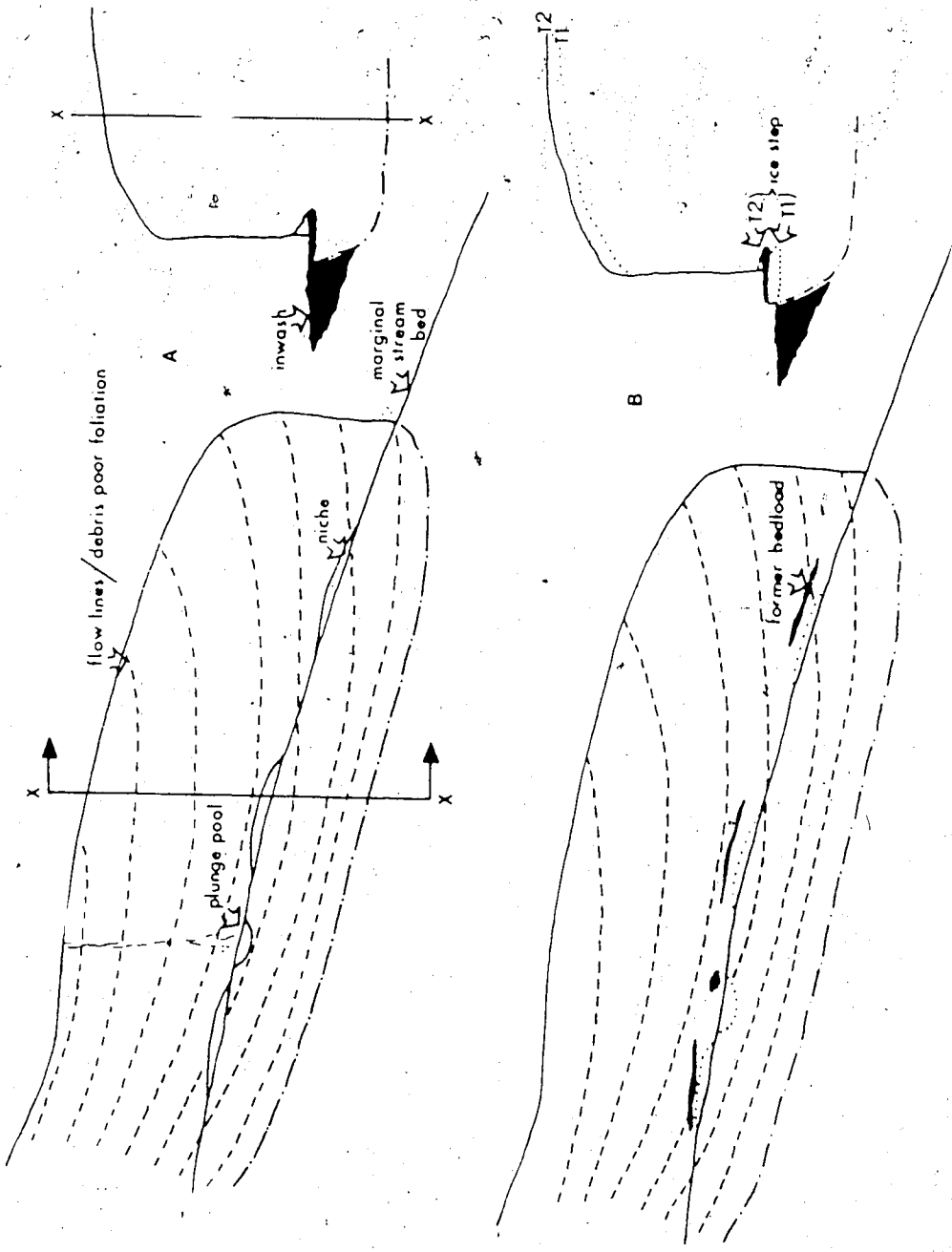
sediments are often stratified sands and gravels which show a striking similarity to proglacial material; 2) these deposits pinch and swell along their lengths; 3) they become less abundant up-glacier; 4) they are concentrated in the basal ice layers; 5) they are irregularly spaced, both vertically and horizontally; 6) they rarely penetrate the ice face by more than 50cm; and 7) they cut across the diffused and banded facies and folia at the snout (Fig.4.21). This reentrainment may involve an annual cycle caused by meltwater incision into the ice face during the summer followed by freeze up and incorporation during the winter (cf. Harris and Bothamley 1984). Large concentrations of debris may represent meander bends, abandoned terraces, ephemeral pools, or superimposed waterfall debris piles. Alternatively, these large concentrations could represent several years of accumulation along a stable ice margin and may not be annual deposits. The build up of "inwash" at the ice margin may bury and protect wasting snouts from later melting and sublimation (Evenson et al. 1986). This is a potential source of ice-cored mounds for reentrainment during any future glacial advance. The palaeoclimatic implications of these interpretations will be addressed in Chapter 6.

Apron entrainment is common at the snouts of glaciers in the field area and it takes on a variety of forms. Indeed the reentrainment of any of the deposits outlined above would constitute apron entrainment.

4.3.2: Glacial tectonic processes and sediments.

Proglacial thrusting is favoured in those areas where; 1) a suitable expanse of deformable sediment is available; 2) the snout terminates in a restricted valley; and 3) ice impinges upon a topographic high. At least one of these must be satisfied before thrusting is initiated. A two-stage model of glacitectonism proposed by Aber (1982) is considered to be the most appropriate for the Phillips Inlet/Wootton Peninsula field area. The proglacial thrusting and/or stacking at all four glaciers has occurred in the

Figure 4.21: Simplified time-sequence diagram of lateral entrainment of marginal stream bedload (vertical scale exaggerated). "A" is at the end of the summer season where the meandering stream has excavated three thermo-erosional niches/scour pools and a waterfall has excavated a plunge pool. Glacier extends below the stream bed level because of the cutting of an ice step by lateral stream erosion. "B" is at the end of the winter season. Ice flow within the snout has displaced the bedload deposited in the scour pools in the ice face upward from the stream bed level and down glacier. Note that the entrained debris cuts across debris-poor folia/flowlines. The ice step may be either destroyed or buried depending on whether the stream bed degrades or aggrades. Burying is also facilitated by dry calving if undercutting by the stream leads to slab failure of the ice cliff. Some debris may slump out from the niches or may be reworked if the stream bed aggrades. The positions of the niches and plunge pools at the end of the previous summer are shown by a dotted line in "B".



proglacial stress field (Rotnicki 1976; Van der Wateren 1985). This has been followed in some cases by overriding and therefore subglacial shearing and penetrative deformation of these sediments. Furthermore, flow perturbations have been set up in the debris-rich basal ice of Dogleg and Pudding glaciers in response to this overriding. Dogleg and Muskox glaciers have thrust coarse alluvium, the former having entirely overridden its thrust block moraine. On the other hand, Muskox Glacier is undergoing minor retreat and it has achieved only partial overriding of the inner thrust blocks after initiation of the moraine belt. Alfreds and Pudding glaciers have thrust predominantly glacimarine sediments, the latter having overridden and reworked its thrust blocks. Alfreds Glacier is undergoing minor retreat from a much larger thrust block moraine over which it deposited a blanket of coarse crystalline erratics derived from the mountains to the south. The complex thrust ridges in the centre of this moraine indicate that proglacial thrusting can disturb and reorientate blocks. The western sector of the thrust block moraine of Alfreds Glacier has been fragmented and carried into the ocean. Overriding by Alfreds and Muskox glaciers has led to the blanketing of thrust blocks by coarse debris and buried ice blocks (aprons). This leads to the disturbance of the upper sedimentary beds within the thrust blocks and a hummocky surface appearance (Fig.4.22).

The processes associated with overriding are illustrated by Dogleg and Pudding glaciers. Greater disturbance has been achieved by Pudding Glacier, in marine silts, than by Dogleg Glacier, in coarse alluvium. The vertical continuum from debris-rich basal ice to frozen alluvium within Dogleg Glacier suggests that, after initial thrusting, the glacier incorporated both apron and thrust alluvium. Clast analyses from this glacier margin did not demonstrate origin by basal freeze-on for this debris (cf. section 4.3.1.).

Differences in disturbance due to different substrata (ie. glacimarine vs fluvial) have been discussed by Boulton (1979). He also alluded to within-

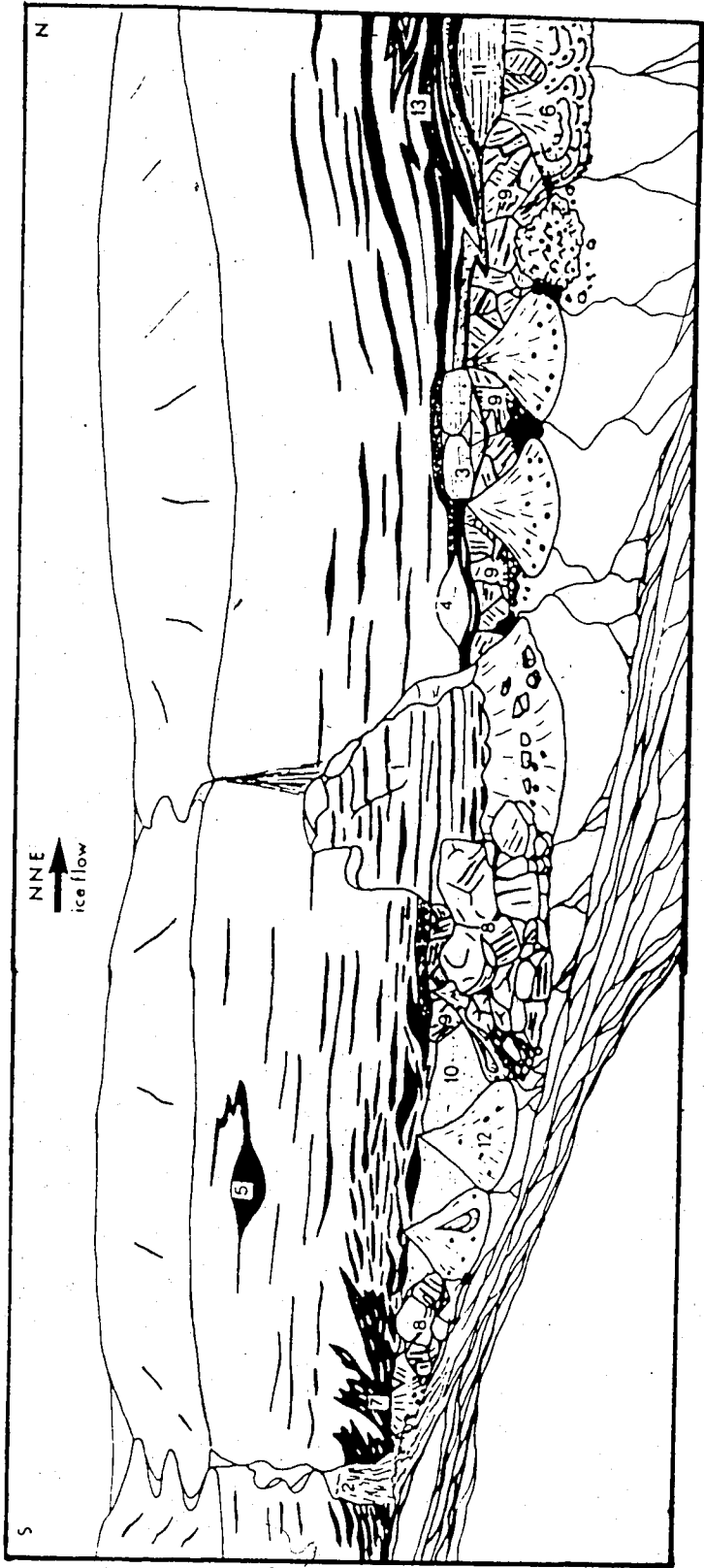


Figure 4.22: Landsystem model of piedmont lobe with thrust block moraine. 1. internally undisturbed sedimentary beds of outer thrust block ridge, not overridden by glacier; 2. innermost thrust block ridge partially overridden by glacier; 3. hummocky surface of overridden thrust block caused by veneer of melt out till and former supraglacial debris overlying former aprons and the stagnating glacier snout; 4. ice marginal pond behind thrust block moraine. Sediment is deposited in these ponds by meltwater streams, ice berg rafting and debris flows from the glacier and thrust blocks; 5. marginal meltwater stream responsible for pre- syn- and post-tectonic sediment reworking on the glacier and the thrust blocks; 6. sand/silt drape over stagnating glacier ponds. Slumping occurs from these drapes, exposing the ice core and sediment is then reworked in fluvial and lacustrine systems; 7. rising folia in the glacier snout carrying coarse and fine debris from up-ice rock falls, reentrained aprons and possible regelation. Surface ablation leads to the formation of ice stagnation topography. This debris is later lowered onto partially or entirely overridden thrust blocks (see 3); 8. buried snowpatch between the crests of thrust blocks. Reentrainment will lead to preservation of "clean" ice between debris bands; 9. ice stagnation topography on the ice-proximal faces of inner thrust blocks. If reentrained this sequence also will represent "clean" ice between debris concentrations in the base of the glacier; 10. buried ice blocks on the surface of the overridden thrust blocks. These are responsible for hummocky appearance; 11. pre- syn- and post-tectonic fluvial reworking of thrust block moraines, especially in major restricted valleys that drain inland ice.

glacier variations when unlithified frozen sediment beneath "cold" ice led to both block inclusion and subglacial deformation. For example, the differential disturbance of marine silts within the basal ice of Pudding Glacier is illustrated by sites 3, 4, 10 and 11 (Figure 4.23). The silts exposed at site 10 are undisturbed except where glacial overriding has deformed the upper beds. At site 3 a slice of the silts has been thrust over ice blocks within a former apron (cf. Fig.4.16b). At site 11 a similar block has been partially entrained and is undergoing attenuation at its margins. Finally at site 4 a clot of disturbed silts represents their complete entrainment. Further attenuation and/or penetrative deformation will disperse the silts within the glacier and may create debris-rich recumbent folds, providing slumping (ie. at site 6) does not remove the clot completely. This scenario of proglacial thrusting and overriding represents an alternative process for introducing unlithified clasts to basal ice to that proposed by Boulton (1979) and Shaw (1982).

In summary, it is apparent that fluvial processes, although important, are not solely responsible for sediment reworking at the margins of polar and subpolar glaciers (cf. Shaw 1977a, Fig.12). Fluvial, lacustrine, aeolian, melt-out and mass movement processes are all important to sediment reworking. Figure 4.22, a composite of debris entrainment, thrust block overriding and sediment reworking at the margins of Muskox Glacier, clearly demonstrates the applicability of Shaw's apron entrainment model (Shaw 1977a, Fig.12). Bands of gravels (sites 3 and 13, Fig.4.23) associated with entrained silts at the snout of Pudding Glacier, could have been derived from either waterfall debris (sites 2 and 7, Fig.4.23) or from overridden thrust blocks comprised of outwash. Other fine sediment and diamictons can accumulate in ponds dammed by thrust blocks and fed by ice marginal streams. Further observations on sedimentation and glacitectonic features along the margins of subpolar glaciers would add to our understanding of debris entrainment.

Figure 4.23: Composite of thrust block moraine, erosional and depositional processes and debris entrainment patterns at the snout of Pudding Glacier. 1. large scale detached block undergoing collapse and reworking by marginal and supraglacial meltwater; 2. supraglacial meltwater stream cutting down through the snout and depositing fluvial material in abandoned meander bends; 3. Block of marine silts, thrust, partially entrained and sliding over former apron ice blocks (see 9). The band of gravels overlying the block originates from pre- and syn-tectonic waterfalls and marginal meltwater on and around thrust blocks; 4. clot of disturbed silts representing entrained and attenuated product of 3; 5. partially smeared englacial debris clot composed of a wide range of grain sizes. These are either crevasse fillings or closed englacial stream conduits; 6. syn-tectonic debris flows from entrained sediments; 7. reentrained waterfall debris piles, predominantly gravels. These are transported vertically within the ice if perturbations are set up by bed irregularities (ie. overrun thrust blocks); 8. aprons composed of dry calved ice blocks which act as sediment traps for ice marginal meltwater, waterfalls, debris flows and rock falls; 9. reentrained ice blocks which have not undergone intense penetrative shear or deformation and thus may still be recognisable. Upper beds are deformed; 10. Overrun and largely undisturbed silts. Only upper beds are deformed by overriding; 11. entrained silt block undergoing attenuation at its margins. Intermediate stage between 3 and 4; 12. alluvial fans built out from entrained debris which is collapsing during overriding; 13. attenuated facies undergoing deformation and faulting due to overriding of bed irregularities (thrust blocks). This may set up penetrative shearing which is transmitted to underlying facies (in this case 9 and 11).



4.3.3: A landsystems model for Phillips Inlet and the Wootton Peninsula.

4.3.3.1: General model.

The glaciated valley landsystem (Eyles 1983) was designed for mid latitude environments and is inflexible to changes in topography. For the Phillips Inlet/Wootton Peninsula field area I propose four new sub-landsystems: 1) plateau ice caps without outlet glaciers; 2) plateau ice caps with outlet or piedmont glaciers; 3) extended cirque glaciers; and 4) transection glaciers (Fig.4.24). The extent and locality of these sublandsystems change with glacioclimatic conditions. For example, transection glaciers may be formed by the coalescence of piedmont lobes within the main valleys of the field area. The landform and sedimentary assemblages associated with each landsystem are critical to the recognition and mapping of former ice margins. Stratigraphic sections from the field area are described in Chapter 5 using the landsystems lithofacies code outlined in Figures 4.25 and 4.26.

Sublandsystem 1, cold-based plateau ice caps which occupy gently undulating topography, presently occurs on the north Wootton Peninsula, in the area to the south and east of the eastern fiord heads and to the southwest of the field area (Fig.4.24). The plateau ice has little potential for erosional or depositional modification of the landscape unless it develops outlet glaciers which subsequently undergo strong extending flow. In the case of the Alert Point Ice Cap, glacier advance simply leads to greater calving, especially during glaciations that are accompanied by higher relative sea level (cf. Thomas and Bentley 1978). Large areas of residuum and bedrock predominate in sublandsystem 1 and on the plateaux of sublandsystem 2. Nonetheless, the retreat of such glaciers produces abundant meltwater which cuts bedrock channels resulting in extensive fluvial modification of the landscape.

Sublandsystem 2, plateau ice caps with piedmont glaciers, is the most

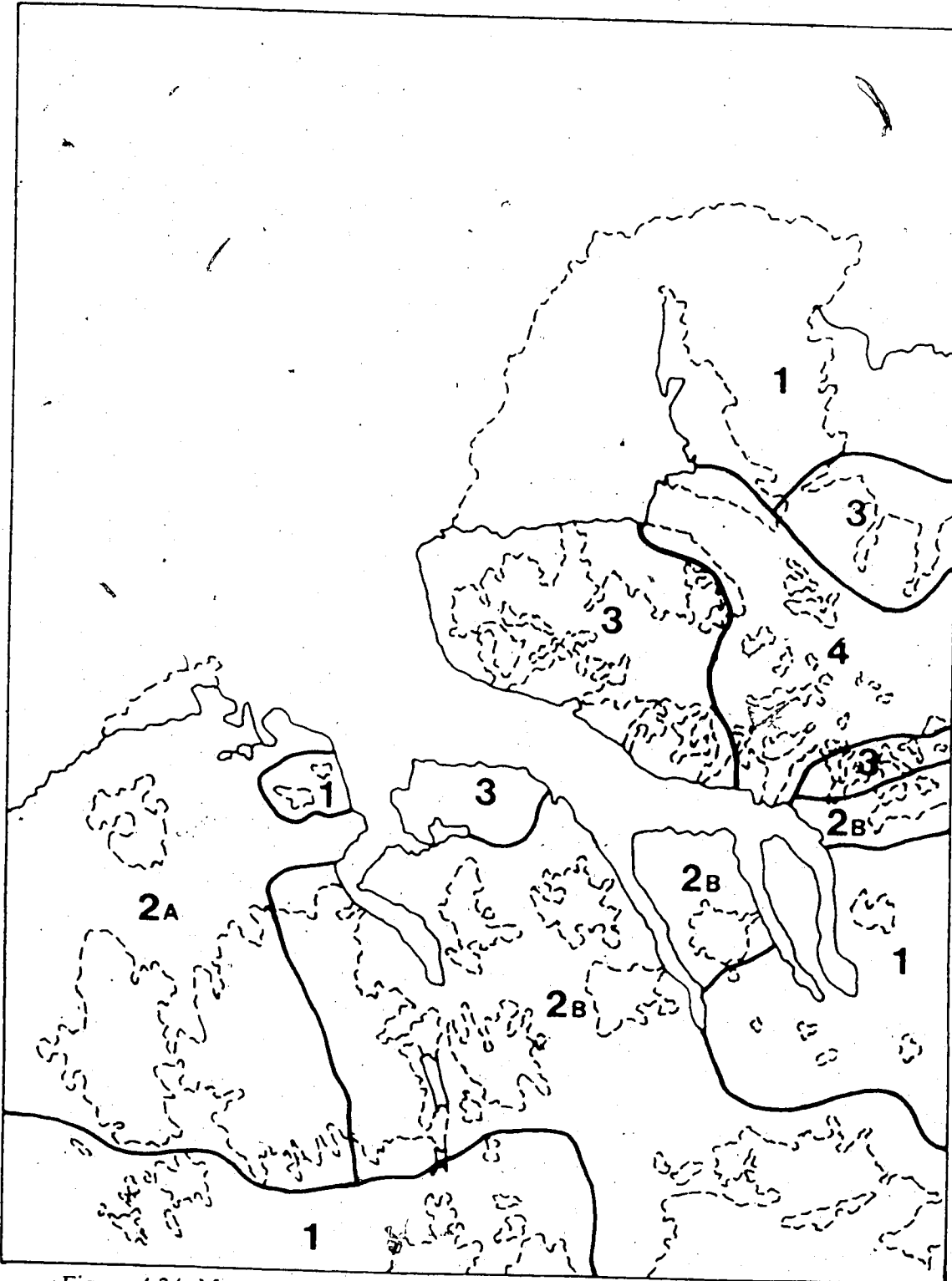


Figure 4.24: Map of present sublandsystems in Phillips Inlet/Wootton Peninsula. 1=plateau ice caps without outlet glaciers; 2a=plateau ice caps with outlet glaciers descending into extensive bedrock lowlands; 2b=plateau ice caps with outlet glaciers descending into restricted and U-shaped valleys; 3=cirque outlet glaciers; 4=transection glaciers.

PAGE REMOVED DUE TO COPYRIGHT
RESTRICTIONS

Figure 4.25: Lithofacies codes from Miall (1977) and Eyles et al. (1983).

PAGE REMOVED DUE TO COPYRIGHT
RESTRICTIONS

Figure 4.26: Coded vertical profiles showing diamicts and sediments associated with glacial landystems and principal till types. From Eyles (1983) and Eyles et al (1983).

important contemporary sublandsystem in physiographic Zone 2 (eg. the Dodger, Deception, Bridge Street, North Wallow, Aviator, Nomynd, and Relief ice caps; Fig.2.1), as well as in the northernmost Grant Land Mountains (Fig.4.24).

However, on the basis of geomorphology all the sublandsystems can be recorded in this zone through time, from former full glacial transection glaciers to modern plateau ice caps without outlet lobes (due to subsequent retreat onto the upper plateau). Further subdivision of this sublandsystem is required to account for plateau ice caps with piedmont lobes entering unrestricted bedrock lowlands (2a) and those with piedmont lobes entering restricted and U-shaped valleys (2b). Unrestricted lowlands, such as the Armstrong River area north of the Dodger Ice Cap, are unlikely to contain thick sequences of deformable sediment. This is because the river is restricted to narrow topographic depressions within the extensive undulating bedrock surface. Glacier advance in this area is unlikely to create proglacial thrusting as a result.

Furthermore, the ice would not be channeled by topography and inwash and sediment reworking at the ice margin would be restricted. Consequently, because the glaciers entrain little debris the bedrock lowlands contain patchy till veneers. In the main U-shaped valleys of the area there are large accumulations of braided outwash. For a variety of reasons (see section 4.3.2) glaciers will either 1) proglacially thrust this sediment or 2) override it without disturbance (Fig.4.27). Piedmont glaciers advancing into restricted and U-shaped valleys (eg. Muskox and Dogleg glaciers) disturb the deformable sediment in the valleys and their margins become ideal traps for extraglacial debris and inwash (kames) from upper basins. Because of the availability of sediment in sublandsystem 2b glaciers deposit extensive till veneers, till blankets and moraines upon deglaciation and glacitectonically disturbed sediments occur in many sections.

Glaciers in sublandsystems 1 and 2 are unlikely to be carrying as much supraglacial debris into the lowlands as a piedmont glacier originating in

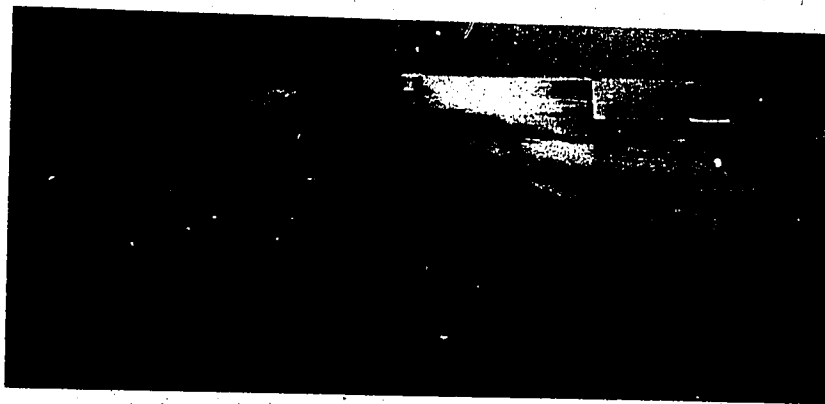


Figure 4.27: The snout cliff of Kipper Glacier illustrating clean ice overriding an alluvial fan without initiating proglacial thrusting. Ulrika Hawkins circled at right for scale.

cirque terrain (sublandsystem 3). This is because the former originate on plateaux. An example of a piedmont lobe originating in cirque terrain is Asymmetry Glacier which flows from the south Wootton Peninsula and overrides the southern margin of the Alert Point Ice Cap. Asymmetry Glacier contains abundant supraglacial crystalline debris originating from the extensive cirque bedrock walls on the south Wootton Peninsula. However, all cirque outlet glaciers in the field area terminate in extensive bedrock lowlands and therefore contain less basal debris than piedmont lobes in sublandsystem 2b. Coarse angular till veneers, till blankets and moraines, often containing megablocks, are characteristic of terrain deglaciated by extended cirque glaciers.

The contemporary transection glaciers of the field area (sublandsystem 4) are located on the south Wootton Peninsula and are generally small by northern Ellesmere Island standards (Fig.4.24). Alfreds Glacier is the longest at 20km. However, because of their length and thickness these glaciers have the greatest potential to collect supraglacial sediment from extensive confining bedrock walls and the most likelihood of creating basal melting and freeze-on of debris by regelation (cf. Hambrey and Muller 1978; Muller 1976). Because these glaciers occupy low-lying valleys, there is a large percentage of the surface area within the ablation zone and therefore a lot of reworking of supraglacial sediment into crevasses (eg. Tidewater Glacier). During past glaciations the coalescence of piedmont lobes at the main fiord heads, fed by regional ice flowing northward from the Grant Land Mountains, and the accumulation of ice in low passes created a number of transection glaciers in the field area. Upon deglaciation these glaciers deposit extensive till veneers, large kames and lateral moraines and they release large volumes of meltwater which cut abundant, deep bedrock channels.

4.3.3.2: Depositional sequences.

Idealised depositional sequences for specific landsystem types from various glacial environments have been constructed in the literature (Eyles 1983; Fig.4.26). Because Phillips Inlet and Wootton Peninsula is a topographically diverse terrain and four different sublandsystems have been identified, depositional sequences and surficial geology vary considerably. Past models of depositional sequences are discussed here with relevance to their applicability to Phillips Inlet and Wootton Peninsula.

Debris entrainment by the processes of apron incorporation and the overriding of stagnant ice and thrust blocks are recognised at the margins of the Phillips Inlet/Wootton Peninsula glaciers. On the other hand, internal thrusting and basal freeze-on or plucking of debris do not appear to be responsible for much of the basal and englacial debris-rich ice. Most debris is incorporated at the ice margin and this debris may pass through several entrainment cycles.

The preservation potential of depositional sequences in high latitude environments will vary according to site characteristics. Such potential is high for glacitectonic structures because the sediment is frozen at the time of thrusting (cf. Mackay 1956, 1959; Aber 1982; Rampton 1982). Shaw (1979) presented a model of landform and sediment associations including transverse deformation features that originated in the compressive zone of the glacier snout. He suggested that deglaciation in a permafrozen terrain led to good preservation of till structure because of the process of sublimation (Shaw 1979; Fig.3). Shaw (1977a) suggested a three-fold facies succession for sediments deposited after melt out and sublimation of a polar glacier and its incorporated apron. This upwards succession is: "Facies A, undisturbed proglacial sediments; Facies B, a complex of poorly sorted, crudely stratified flow deposits intercalated with discontinuous sorted sediments; Facies C, a body of foliated till with sub-horizontal partings representing foliation, and isolated clasts". Shaw goes on to state that hummocky moraine could be the

product of primary deposition rather than of redistribution processes.

Shaw's (1977a) succession is an appropriate working model for the Phillips Inlet/Wootton Peninsula area. However, proglacial thrusting rather than subglacial disturbance is critical to basal debris entrainment and is extremely important to moraine formation, especially in sublandsystem 2b (compare Figures 4.17 and 4.27). Furthermore, because the area where Shaw's facies succession was developed (Antarctica) is more arid than northwest Ellesmere Island, considerably more sediment reworking during ice wastage and retreat might be expected in the Phillips Inlet/Wootton Peninsula area. Thus even debris-rich basal ice may produce only a discontinuous till veneer upon melting. Supraglacial and englacial debris concentrations are often so insignificant that it would take the melting of a considerable thickness of ice to produce enough overburden to protect underlying stagnant ice from normal meltout (Shaw 1979, Fig.2). This means that Facies C or sublimation till is poorly represented in the stratigraphic record, even though buried glacier ice is evident at many locations. In high relief terrain sediment reworking during ice retreat may be accentuated where alluvial fans build out from ice margins and into river terraces. These terraces in turn grade to falling deglacial sea level. Facies A is often clearly disturbed by proglacial thrusting. Pre- syn- and post-tectonic sediment reworking at the ice margin, combined with thrusting, effectively juxtaposes Facies A and B (Boulton 1986). If ice margins fluctuate at any time then Facies B may become folded and faulted and ice blocks (some "clean" and some including Facies C) are introduced to the basal ice facies. It is possible that rafts of disturbed, homogenous alluvial or lacustrine sediment could survive as intratill concentrations after melt out and/or sublimation (Shaw 1982). The lithofacies profile produced by Eyles et al. (1983), depicting thick sequences of sublimation till (cf. Fig.4.26), is probably atypical in this high Arctic environment.

High summer discharges in the marginal streams of the field area result in large concentrations of lateral fluviglacial debris (inwash, kames) and proglacial fans, especially in the areas dominated by subland systems 2b and 4. Consequently, accumulations of paraglacial valley fill (E, Fig.4.26) are common in those areas. Despite these ice marginal accumulations, contemporary and ancient moraines are particularly rare in the field area. Their occurrence is dictated by rockfalls to lateral and medial positions on the glacier surfaces, and by supraglacial meltwater streams which rework and concentrate material in crevasse systems. These are most pronounced on the surfaces of the transection glaciers, as discussed above. Other than thrust block moraines, end moraines are absent at the snouts of the glaciers of the field area. However, where glaciers contacted the sea former ice margins are marked by distinctive glacimarine embankments (Stewart 1988). Around the snouts of the smaller cirque glaciers the moraines are large-scale proglacial ramparts. Even areas of stagnant ice are unlikely to produce hummocky moraine upon melting because there is very little debris in most glaciers. Muskox Glacier is the exception here but its moraines are still <5m high and these contain ice cores. Therefore, the former existence of thrust block moraines is important for the reconstruction of past glacial activity in the field area. A good illustration of the importance of thrusting to moraine development is at the margin of Alfreds Glacier. Moraines are only developed where the glacier impinged upon the surficial sediment of Cairn Peninsula after its emergence following deglaciation. Elsewhere in this area the glacier, the largest and most debris-charged in the field area, has deposited only a veneer of coarse debris after wastage from at least two previous advances. Thrust block moraines are not indicative of ice terminal positions *per se*, but former overriding may be deduced in some cases from the degree of disturbance and the presence or absence of till (Facies C, Shaw 1977a), reworked tills (diamictons with discontinuous sorted sediments or resedimented debris flows) or lowered

debris.

The lithofacies code outlined in Figures 4.25 and 4.26 is employed throughout Chapter 5 in the description of stratigraphic logs. Also the surficial geology and landform and sedimentary assemblages of Phillips Inlet and Wootton Peninsula are interpreted with the aid of the general landsystems model outlined above.

CHAPTER FIVE

Surficial geology, geomorphology and stratigraphy.

Everywhere occur rounded, but seldom scratched, hills of gneiss with erratic blocks in the most unstable positions of equilibrium, separated by valleys with small mountain-lakes and scratched rock surfaces. On the other hand, no real moraines were discoverable. These, indeed, seem to be commonly absent in Scandinavia, and are, generally speaking, more characteristic of small glaciers than of real inland ice. the border of the ice is everywhere sprinkled with smaller boulders, partly rounded, partly angular; but the number of these is so inconsiderable that when the ice retires they give rise only to a slope covered with boulders; not to a moraine... The small earth-bank which collects at most places at the foot of the glacier is frequently washed away again by the glacier streams and rain. At the foot of the glacier we often find ponds or lakes in which is deposited a fresh-water glacial clay, containing angular blocks of stone, scattered around by small icebergs. Extract from The Arctic Voyages of A.E. Nordenskiöld 1879.

5.1: Introduction.

This chapter presents the field observations on the surficial geology, glacial geomorphology and stratigraphy of both terrestrial and raised marine deposits. Section 5.2 introduces the units portrayed on the surficial geology map (Figure 5.1). The field area is then divided into ten sectors for ease of reference (Figure 5.2). The Quaternary deposits of each sector are described, in sequence, with a local interpretation of glacial and deglacial events (section 5.3). These interpretations are integrated in Chapter 6 where the palaeogeography of the field area is presented.

5.2: Surficial geology map.

The surficial geology of the field area was mapped at 1:125,000 in order to determine the nature and distribution of unconsolidated deposits versus bedrock. Mapping was based on air photograph interpretation and extensive field observations made during three field seasons. Even in areas of poor air photograph quality (ie. shadows or poor reflectivity), ground and helicopter traverses provided adequate data for mapping.

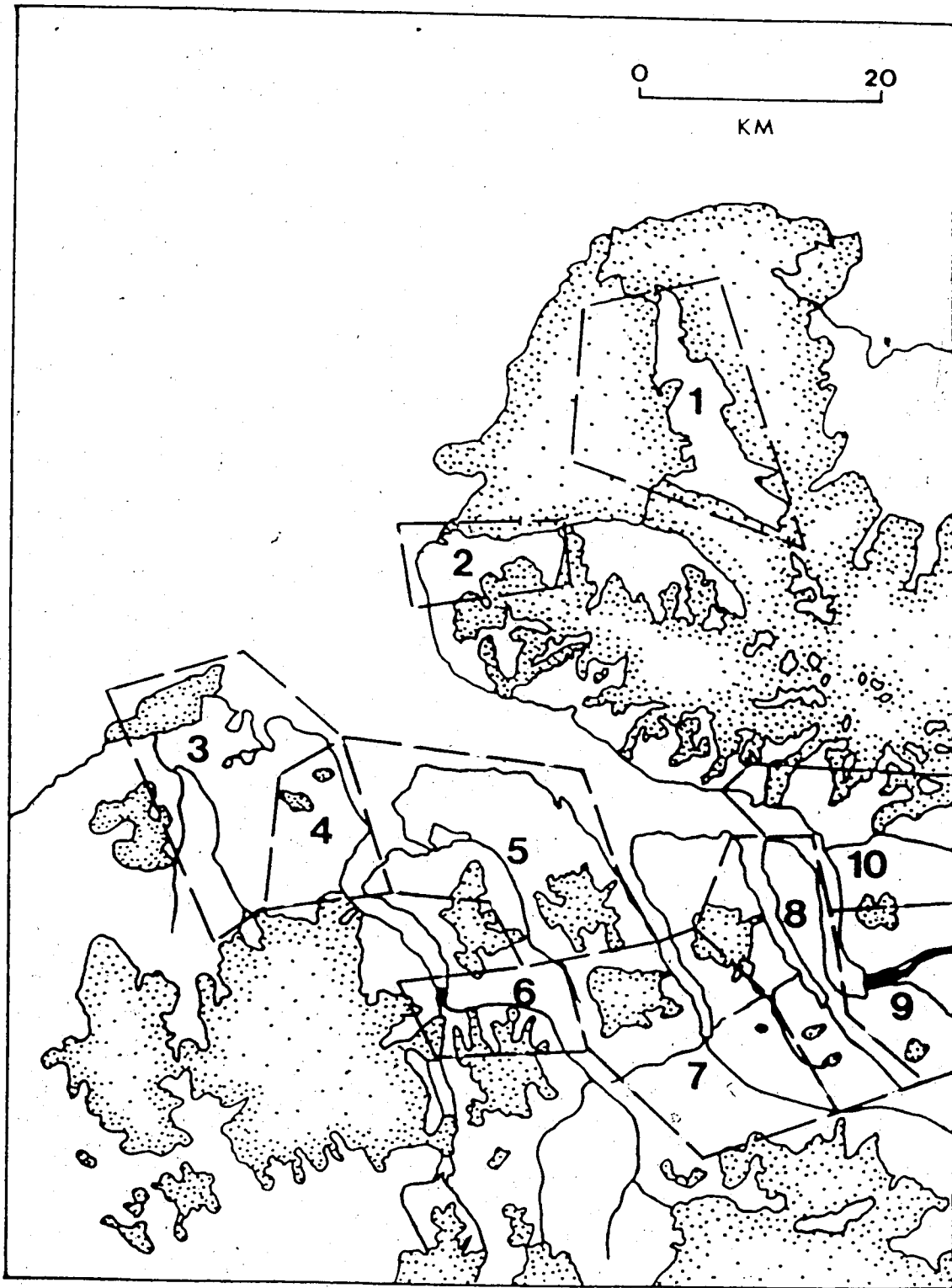


Figure 5.2: Sectors of the field area as discussed in Chapter 5.

The surficial units; geomorphologic symbols; and colours used on the surficial geology map conform to those of the Geological Survey of Canada (cf. GSC Miscellaneous Report No.29). The following nine units are differentiated in the Phillips Inlet/ Wootton Peninsula area: 1. bedrock; 2. residuum; 3. till; 4. glacialfluvial; 5. glaciallacustrine; 6. raised marine; 7. inactive alluvium; 8. active alluvium; and 9. colluvium.

5.2.1: Bedrock.

This unit includes bedrock of diverse ages and lithologies (see section 2.3). In areas of high relief bedrock constitutes the principal map unit because most slopes are too steep to support a surficial cover. Approximately 25% of the field area is mapped as bedrock. However, some areas mapped as bedrock may include pockets of surficial material too small to be portrayed at the selected scale. Likewise, small outcrops of bedrock within otherwise homogenous surficial sediments are excluded. The extent of weathering of bedrock varies with lithology. Consequently, weathering zones, diagnostic of terrains of different ages, were not discernable.

5.2.2: Residuum.

This includes well developed felsenmeer, on broad summits and gentler slopes, that still mimics the underlying geological structure (cf. Dyke 1983). Bedrock outcropping as tors is indicated by the appropriate symbol. Residuum is >50cm thick, often deeply grusified and occasionally contains scattered erratics. Other geomorphic features within this unit may include: cryoplanation terraces; nivation hollows; extensive patterned ground; and gelifluction lobes. Incipient felsenmeer, which still displays much of the original bedrock structure, is mapped as bedrock.

5.2.3: Till.

Tills and moraines are particularly rare in the field area. Tills are recognized by their erratic clasts because many sedimentary rocks weather *in situ* to grain sizes similar to till. Most commonly, tills form veneers 0.5-2m thick which mimic the underlying bedrock surface. However, some till blankets (>2m thick) completely mask the bedrock and these are mapped separately. Because many moraines represent thrust blocks of alluvium or glacialine sediment they are mapped as those sediments with the appendage of the appropriate moraine symbol. Some till veneers may be inadvertently included as residuum because locally derived glacial debris is indistinguishable from weathered bedrock. This is largely the result of a lack of striated and glacially modified clasts. If there was any doubt as to the origin of apparently weathered bedrock containing sparse erratics it was mapped as residuum.

Rare till blankets occur in valley bottoms where former piedmont lobes were sufficiently erosive due to their descent from adjacent uplands. Moraines (except thrust block moraines) are predominantly composed of colluvium that accumulated passively against the ice margin. These moraines are mapped as till because they mark a former ice margin which controlled their deposition. However, ice marginal accumulations composed of fluvial inwash are mapped as kames.

5.2.4: Glacifluvial sediments.

These are kames deposited either at the ice margin or over stagnant ice. Glacifluvial sediments also occur in association with former medial moraines as crevasse fillings, partitioning coalescent lobes within transection landsystems. Such kames are long, sinuous features; they occur in extensive till veneers; and they are interdigitated with coarse angular morainic debris (see section 4.2.1). Other kames are composed of gravels and sands and form conical mounds; chaotic hills and ridges; and former ice

marginal terraces (inwash). Although sandar represent glaciofluvial outwash in this area they are mapped as either active or inactive alluvium.

5.2.5: Glacilacustrine sediments.

These include interstratified clays, silts and sands; occasional gravelly foreset beds; and stratified diamictos deposited within former ice dammed lakes. These are common in the central part of the field area where piedmont lobes descended into large valley systems, blocking the local drainage. Occasional lake sediments were observed on plateaux adjacent to the fiords whereas most fine grained sediments in lowlands bordering the fiords are of marine origin.

5.2.6: Raised marine sediments.

These constitute the most widespread fine grained sediments in the field area (Fig.5.1). Because they were predominantly ice proximal, raised marine sediments also include a wide range of grain sizes. Massive and laminated, fine grained sediments, with varying amounts of dropstones, can record either the bottomset beds of ice contact deltas or distal sedimentation within basins of the full and deglacial marine environments. Grounding line deposits and diamictos from icebergs and glacial ice shelves are included as marine units. Appropriate symbols denote former grounding lines to which glaciers advanced during the last glaciation. Littoral sands; gravel foresets; and subaqueous sand and gravel fans commonly occur in the morainal banks adjacent to such grounding lines (cf. Stewart 1988). Because of the continuous postglacial emergence in the area many raised marine sediments have been extensively eroded as sandar downcut to progressively lower base levels. This has resulted in pockets of marine sediments well inland of the present coastline. Some thrust block moraines are composed of glacimarine sediments and consequently they are mapped as such with appropriate symbols.

5.2.7: Inactive alluvium.

These are terraced outwash gravels and sands above contemporary floodplains. These sediments are concentrated largely in major valleys but smaller accumulations are also represented by inactive alluvial fans and stream terraces at higher elevations. The valley trains extending to the topset beds of raised marine deltas are included in this category. Some thrust block moraines are also included because they are composed of fluvial sediments.

5.2.8: Active alluvium.

This includes seasonally flooded outwash gravels and sands typical of braided streams. Although these are concentrated largely in the major valleys they also occur in small alluvial fans and stream channels at higher elevations throughout the field area.

5.2.9: Colluvium.

These are scree and unsorted slope deposits >1m thick. Such sediments are widespread in high elevation terrain and are often geliflucted or rock glacierized. Geomorphic features include protalus ramparts, rock glaciers, slush avalanches/debris flows and rock avalanche tracks. Areas of modified till veneer and blanket on gentler slopes are mapped as till.

5.3: Geomorphic and stratigraphic data.

5.3.1: Introduction.

The ten sectors outlined on Figure 5.2 are related largely to camp localities and therefore the most intensive field transects. The format of this section follows that of Bednarski (1984): ie. site descriptions are followed by geomorphic and stratigraphic observations which are in turn

followed by their interpretation. This is considered to be the most comprehensive presentation of a large body of field data. The order of presentation follows the numerical order of Figure 5.2 which forms a counter-clockwise path from the west coast of the Wootton Peninsula to the fiord heads of eastern Phillips Inlet. Radiocarbon dates are also included in this section. Figures 5.3, 5.4, and 5.5 should be used for reference throughout this section.

5.3.2: Sector 1: Western Wootton Peninsula.

5.3.2.1: General description.

The west coast of the Wootton Peninsula consists of a narrow strip of land approximately 50km^2 (Fig.5.3a). This land is completely encompassed by the Alert Point Ice Cap and its ice shelf to the east and north respectively; Alfreds Glacier to the south; and the Cape Alfred Ernest Ice Shelf to the west. This small ice-free area varies from 7 to $<1\text{km}$ in width.

Physiographically, it is a gently undulating, calcareous plateau which descends from 500m asl in the south to approximately 100m asl east of Cape Alfred Ernest. South of Cape Alfred Ernest, the plateau is truncated along its western margin by coastal bedrock cliffs up to 90m high (Fig.5.6). In places these cliffs have been dissected by meltwater from the Alert Point Ice Cap forming spectacular gorges. Elsewhere, large embayments within the plateau edge, with floors $\leq 30\text{m}$ asl., resemble cirques or raised coastal coves. To the south, a thin tombolo connects the mainland to Cairn Peninsula which is 100m high and is responsible for the channeling of Alfreds Glacier to the west, causing part of the snout to thrust material to the north (Fig.5.4).

5.3.2.2: Geomorphology and stratigraphy.

The predominant surficial deposit of sector 1 is coarse crystalline outwash. This material forms a discontinuous veneer on the inner plateau and

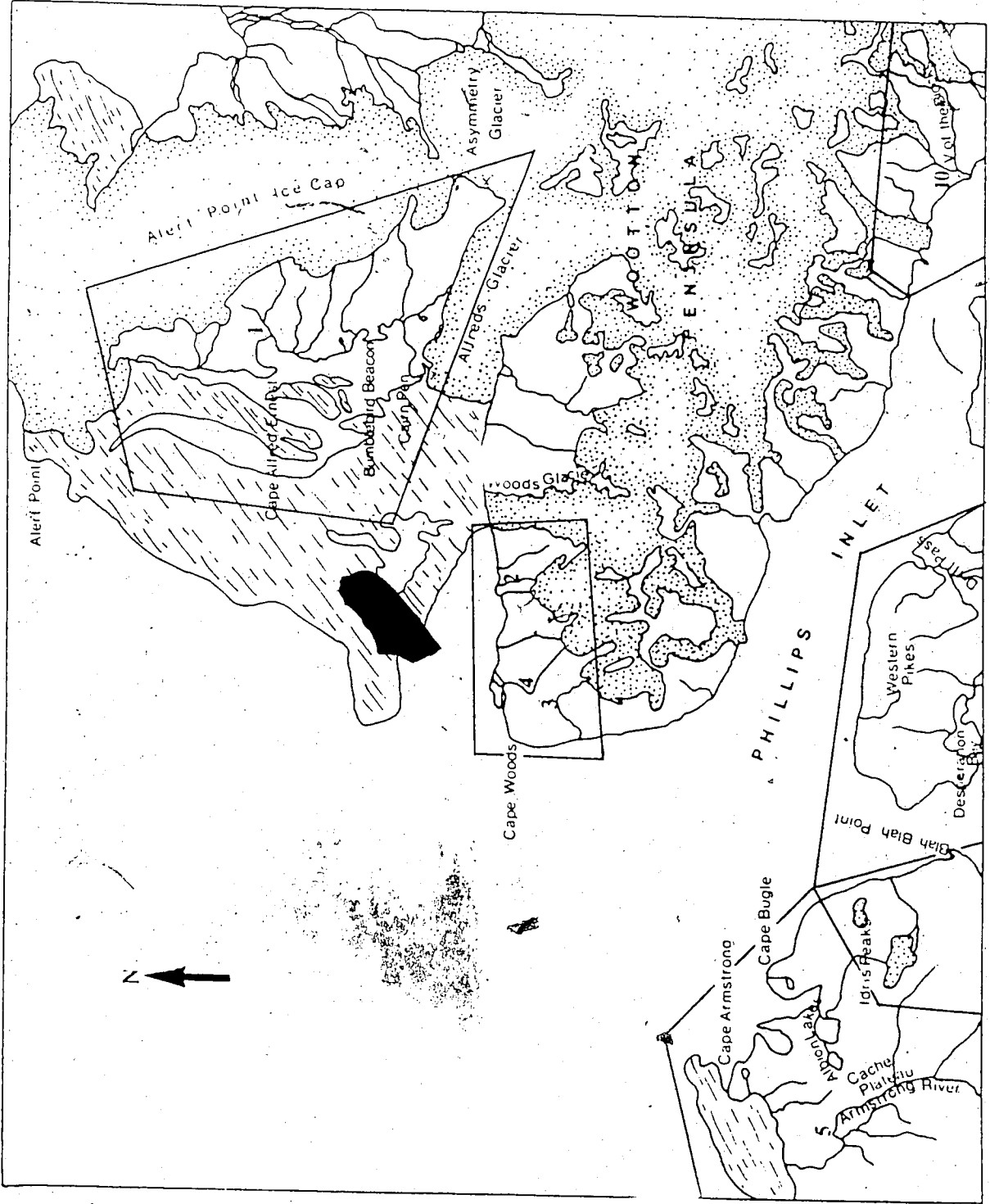


Figure 5.3a: Place names of northern Phillips Inlet and Wootton Peninsula. Principal deltas are 1. Useless, 2. Sunkist, 3. Nightmare, 4. Armstrong, and 10. Mymmshall.

Wootton Peninsula.
Cairn, 5.

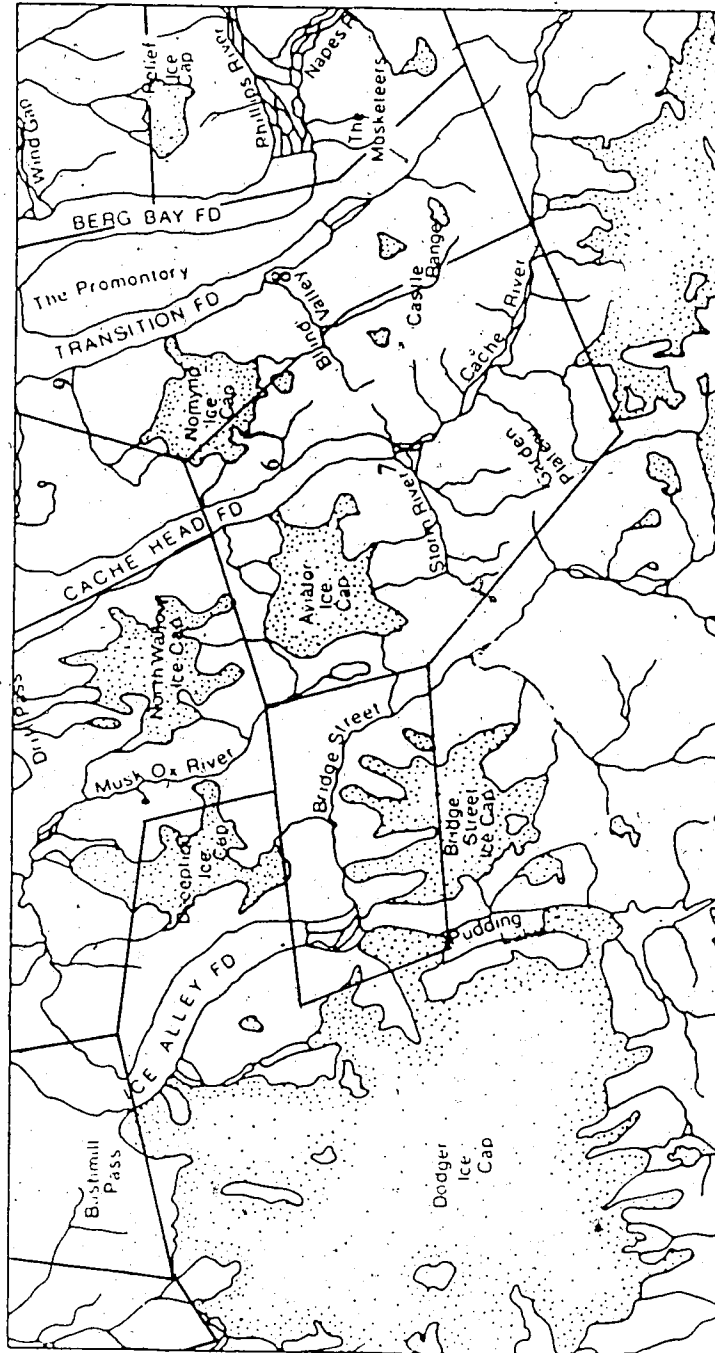


Figure 5.3b; Place names of southern Phillips Inlet. Principal deltas are 6, Gorge, 7. Storm, 8. Blind, and 9. Longmynd.

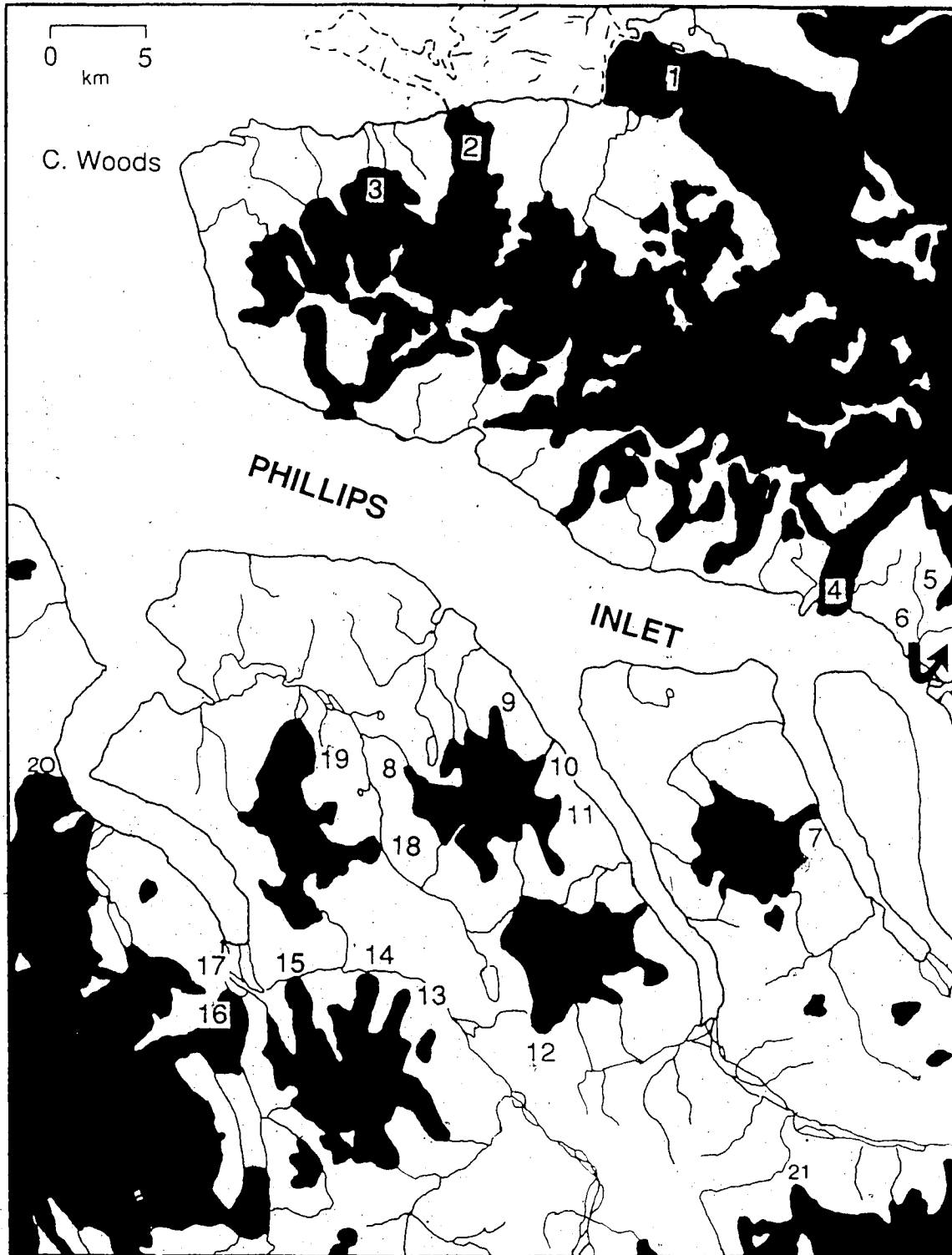


Figure 5.4: Map of glaciers used in the analysis of glacial geologic processes. Unofficial names of glaciers mentioned in this chapter are 1. Alfreds, 2. Woods, 4. Tidewater, 5. Hidden, 6. Dogleg, 14. Badweather, 15. Kipper, 16. Pudding, 17. Vienna, 18. MuskoX, 19. Deception, 20. Terrible, 21. Endeavour.

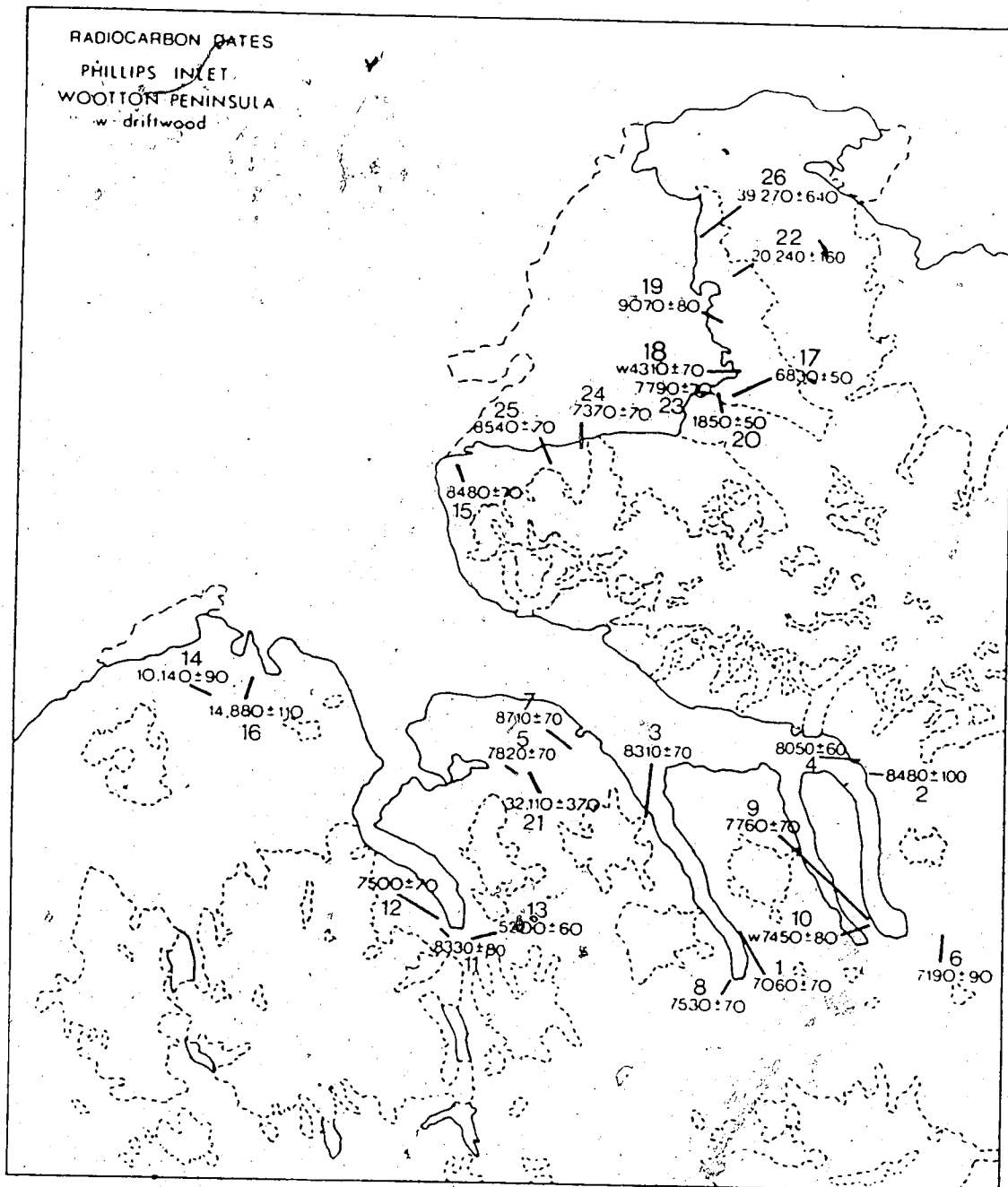


Figure 5.5: Map of radiocarbon dates from Phillips Inlet and the Wootton Peninsula.

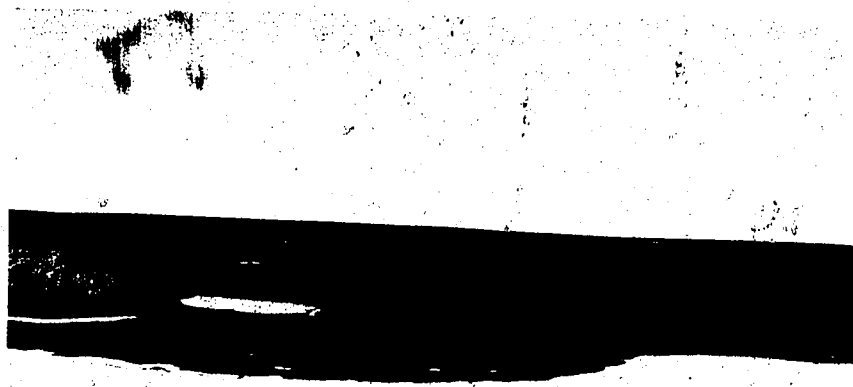


Figure 5.6: View from the air of the coastal cliffs and calcareous plateau of sector 1, west Wootton Peninsula. The best example of a large embayment with a floor 30m asl is located in the centre of the photograph.

thickens within the valleys leading to the coastal gorges (Fig.5.1). These valleys are occupied by underfit streams and, in some cases, they are dry valleys containing extensive perennial snowpatches (Fig.5.7). Larger, angular crystalline erratics are scattered on outliers of calcareous residuum on the coastal cliffs.

The only moraines in the area are located on south Cairn Peninsula where they reach 70m asl (Fig.5.8). These are former thrust block moraines (now hummocky moraine) composed of glacial marine diamicton containing abundant shell fragments. A date of 7790 ± 70 BP (TO 482) was obtained on a fragment of *Hiatella arctica* at 43m asl. An *Astarte borealis* valve in life position in glacial marine silts from the contemporary thrust block moraine of Alfreds Glacier dated 1850 ± 50 BP (TO 479); Figs.5.5 and 5.7.

The retreat of the Alert Point Ice Cap is recorded by deep meltwater channels cut through the outer plateau. These channels extend up to the margin of the ice cap (Fig.5.1). Fresh trimlines attest to the recent retreat of the ice cap and a number of perennial snowbanks occupying older meltwater channels.

Below the coastal bedrock cliffs south of Cape Alfred Ernest large raised deltas, predominantly composed of crystalline lithologies, range in altitude from 52-65m asl (marine limit). To the east of Cape Alfred Ernest, the uppermost terrace of Useless Delta (site 1, Fig.5.3a) records a sea level of 62.5m asl. Three other delta surfaces in this area, one at 52 and two at 58m asl, mark the seaward margins of large outwash trains that built out from the gorges in the plateau edge. A *Mya truncata* fragment from 47m asl in the foreset sands and gravels of the 52m delta dated $20,240 \pm 160$ BP (TO 481). Deltaic and fluvial terraces in this area are heavily pitted, suggesting delta progradation over stagnating ice. To the south, two delta surface remnants at 62m and 59m mark the seaward edge of a well developed valley train. A *Hiatella arctica* valve from foreset sands, 2m below the 59m delta, yielded a date of



Figure 5.7: Air photograph no.17456-10 of the west Wootton Peninsula, illustrating major geomorphic features. T=thrust block moraine; marine limits in metres asl; G=grounding line; X=section in Fig.5.10; s= shells dating 20,240 BP (north), 9070 BP (centre), 7790 BP (southwest) and 1850 BP (southeast); N=narwhal tusk (6830 BP); w=4310 BP driftwood.



Figure 5.8: Thrust block (hummocky) moraines on south Cairn Peninsula. These are composed of glacial marine diamictos and contain abundant shell fragments. Broken line demarcates upper limit of hummocky moraine. The contemporary thrust block moraine of Alfreds Glacier is visible in the background.



Figure 5.9: Sea-ice push ridges up to 5m in height on Bumblebird Beacon. Tim Fisher and Ulrika Hawkins circled for scale.

9,070±80 BP (TO 478). This was the only whole valve from an otherwise small sample of fragments.

Sea-ice push ridges are prominent along the northwest coast of Wootton Peninsula, reaching 5m in height and 20m in length. They exist between 8 and 50m asl on north Cairn Peninsula; between 5 and 36m asl on Bumblebird Beacon; and between 4 and 65m asl from the Beacon northwards. Hence, sea-ice push ridges exist up to marine limit on this coast (Fig.5.9). Four pieces of driftwood were collected from the sector; three undated pieces from sea level at Cape Alfred Ernest and one piece from 9m asl southeast of Bumblebird Beacon which dated 4310±70 BP (TO 477). A narwhal (*Monodon monoceros*) tusk was collected from a gelifluction lobe at 34m asl in the embayment to the west-northwest of Cairn Peninsula. A fragment from the tip of the tusk yielded a date of 6830±50 BP (TO 476).

A cliff, composed of diamicton and capped by coarse crystalline outwash, extends from Useless Delta (site 1, Fig.5.3a) to Cape Alfred Ernest and then 1.5km northwards. At Cape Alfred Ernest a bench (63m asl) has formed at the contact between a crystalline clast-rich diamicton and an underlying silt-rich diamicton. Throughout the lowlands of Cape Alfred Ernest there are widespread raised marine silts with dropstones and occasional boulders. These silts are considered to be correlative with the basal silt-rich diamicton in the cliff to the northeast.

A 1km long section has been exposed in a valley in the northernmost part of the sector (X on Fig.5.3a). Because of logistical constraints only a general overview of the stratigraphy is presented (Fig.5.10). Although large areas are obscured by colluvium, the following lithofacies are observed: 1) basal massive gravels and sands overlain in two places by; 2) matrix-supported, massive diamicton overlain by; 3) laminated silts and low angle, cross-bedded sands which coarsen into massive gravels overlain by; 4) another matrix-supported, massive diamicton capped by; 5) ca.5m of interbedded sands

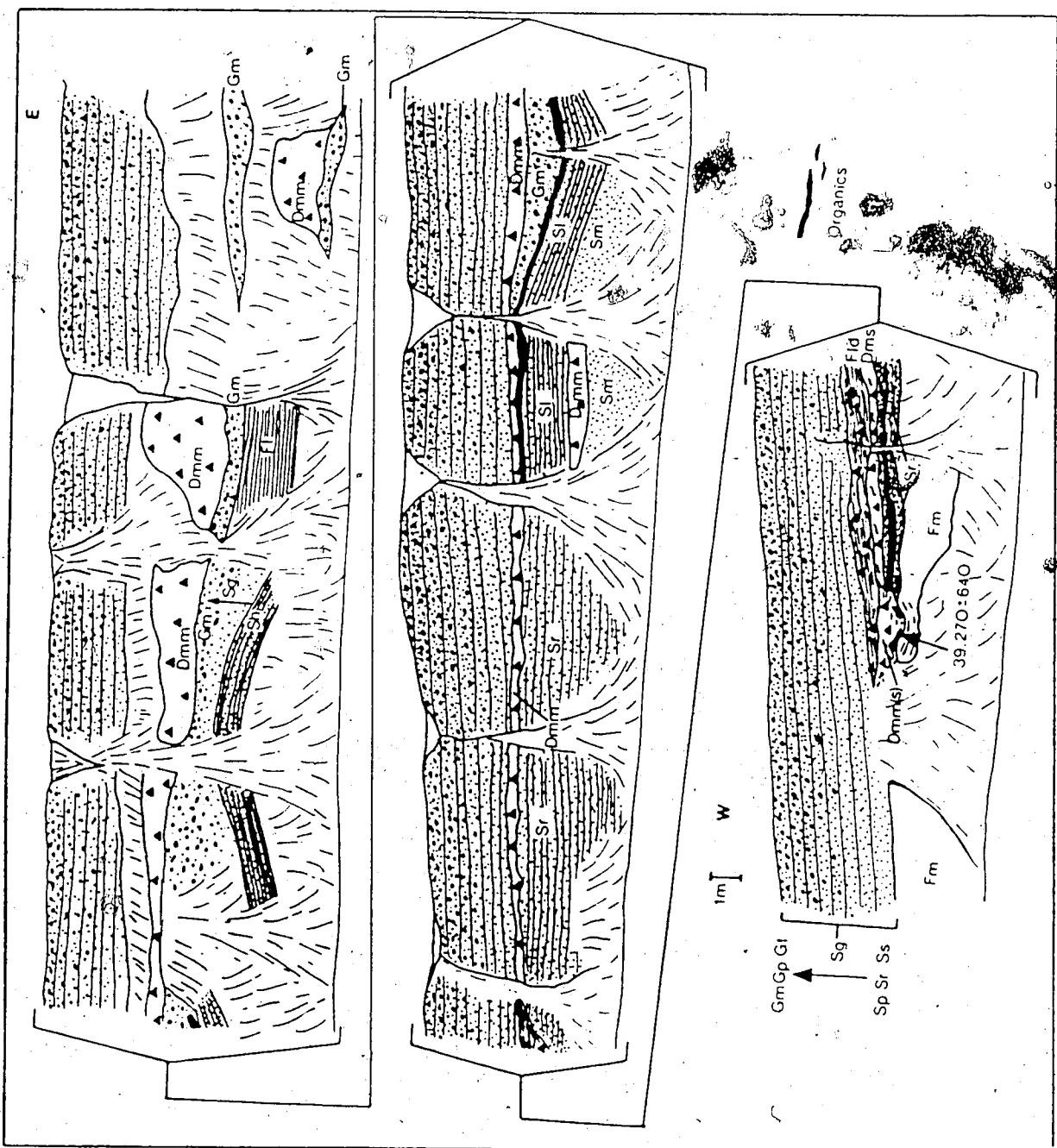


Figure 5.10: Principal units observed in the stratigraphic section south of Alert Point. For codes see Figure 4.25.

and gravels which coarsen upwards into massive gravels at the surface. The cross-bedded sands display a palaeocurrent direction from the north but the original beds appear to have undergone large scale disturbance (folding) possibly due to melt out of buried ice.

The westernmost face of the section (bottom of Fig.5.10) is composed of massive silts conformably overlain by a sequence of: rippled sands; a stratified, matrix-supported diamicton; laminated silts with dropstones; and a 5m sand/gravel sequence. An organic bed, ca.10m long and >20cm thick, occurs within the ripple bedded sands and between sands and gravels at the centre of the section. At the westernmost end of the section the stratified, matrix-supported diamicton thickens and grades laterally into a matrix-supported massive diamicton which contains shear structures and has an erosional contact with the underlying silts. The shear structures, together with several faults, continue into the underlying massive silts where the organic bed has also been sheared into stringers and lenses at 32m asl. A date of $39,270 \pm 640$ BP (TO 485) was obtained on the organics collected from one of the stringers. There is a conformable contact between the matrix-supported, massive diamicton and the overlying laminated silts with dropstones. From this point to the sea the section is devoid of diamicton and massive silts appear to grade upward into interbedded sands and massive gravels.

5.3.2.3: Interpretation.

During the last glaciation ice advanced from the central Wootton Peninsula to the coast. At the coast ice was channeled through valleys at the plateau edge, resulting in the protection of cliff top residuum by inactive ice which deposited crystalline erratics. Alternatively, the erratics are of greater age and during the last glaciation small nunataks existed along the coast. The abundance of crystalline lithologies within the plateau outwash and within adjacent raised marine deltas attests to dominant ice dispersal

from south Wootton Peninsula. This must have resulted in the overriding of the Alert Point Ice Cap by piedmont lobes from mountainous terrain to the south in the same manner as Asymmetry Glacier presently overrides the southern margin of this ice cap (cf. Fig.5.3a). Much of the erratic outwash covering this area was deposited on the Wootton Peninsula during deglaciation as indicated by the numerous valley trains. A former advance of Alfreds Glacier deposited crystalline erratics at >100m on Cairn Peninsula but the age of this advance is unknown.

Two ice advances may be represented in the section south of Alert Point (Fig.5.10). The lower matrix-supported, massive diamicton is of unknown age. However, it must predate $39,270 \pm 640$ BP, the age of the overlying organics. Because of its massive characteristics this diamicton is tentatively interpreted as a till. The upper matrix-supported, massive diamicton, displaying shearing and penetrative deformation of underlying silts, is interpreted as a till deposited during the last glaciation ($<39,270 \pm 640$ BP). The organics ($39,270 \pm 640$ BP) were redeposited in a marine environment at least 32m asl, suggesting glacioisostatic loading caused by a local ice advance. Moreover, the massive fines below the upper till suggest a marine environment prior to the arrival of the ice at this site. Because these fines grade into rippled sands and then into a stratified diamicton, without a recognizable unconformity with the till, it is concluded that these sediments are coeval. Because the westernmost face of the section is without diamicton, this suggests that the ice was floating. In contrast, the till represents a grounded ice margin now at 32m asl. Given that the full glacial sea was no higher than 70m (see bases, Chapter 6) the resulting water depth of 38m above the till would be capable of floating ice 42m thick.

In the northern part of sector 1 the silt-rich diamictons north of Cape Alfred Ernest also suggest glacialmarine sedimentation beneath or adjacent to floating glaciers. The grounding line appears to have advanced over these

silt-rich diamictos as indicated by the sharp contact between them and the overlying clast-rich diamictos at 63m. The clast-rich diamicton is interpreted as basal melt out till deposited as the glacier retreated from the shallower water. Similar sedimentary sequences to those north of Cape Alfred Ernest have been reported by Alley et al. (1987) from beneath Ice Stream B, Ross Ice Shelf, Antarctica. The coarsening upward gravels at the top of the main section south of Alert Point and the gravels overlying the sedimentary cliff north of Cape Alfred Ernest are interpreted as braided outwash grading to a fall: ... cial sea level.

During glacialiation local marine limits were recorded by deltas prograding from the gorges along the coast. The small range in delta heights along the coast suggests that deglaciation occurred almost simultaneously (Andrews 1970). Ice retreat appears to have been rapid as indicated by the extensive burying of stagnant ice in topographic depressions by outwash, especially at Useless Delta.

The shell fragment dating $20,240 \pm 160$ BP from the foreset beds of a 52m delta (which is 10.5m lower than nearby Useless Delta and 13m lower than the minimum marine limit (65m) for the sector) likely has been redeposited. Consequently, this shell date provides only a maximum age for the 52m sea level. The whole valve dating $9,070 \pm 80$ BP relates to a reworked surface (57m) of a 62m delta. Assuming that the local marine limit is 62m asl, then deglaciation of the site occurred around $9,070 \pm 80$ BP. If marine limit is in fact higher then the date provides only a minimum estimate on deglaciation. Indeed the equidistant shoreline diagram (see Chapter 6) suggests that the $9,070 \pm 80$ BP date relates to a sea level >62 m asl. Despite the fact that these two dated shell samples have been redeposited, they still record full glacial and early deglacial marine faunas in the area that are less than 5km from the contemporary ice margin. Implications of these dates and the marine limit deltas will be discussed further in Chapter 6.

Details of the Holocene sea-ice and ice shelf history may be deduced from evidence collected on the west Wootton Peninsula coast. Because the three pieces of driftwood from sea level at Cape Alfred Ernest may have been redeposited the age of this driftwood and its relevance to ice shelf history can be determined only by absolute dating. The driftwood date of 4310 ± 70 BP provides an age on the 9m sea level as well as a maximum age for the enclosure of this coastline by the Cape Alfred Ernest Ice Shelf. This reinforces other ice shelf histories along the northernmost coast of Ellesmere Island (cf. Stewart and England 1983; Jeffries 1987).

The narwhal tusk from 34m asl is an important sample for both the ice shelf chronology and Holocene zoology. The modern range of narwhal extends from Davis Strait and Disco Bay, west Greenland, in winter to the Lancaster Sound/Barrow Stra area of the central Canadian Arctic archipelago in summer. Because this range is restricted by the seasonal availability of open water (Stirling et al. 1981) it seems reasonable to conclude that its presence on northernmost Ellesmere Island (82° N) at 6830 ± 50 BP indicates more open water and restricted ice shelves at that time. Blake (1972) and Stewart and England (1983) have previously reached similar conclusions for reduced summer sea ice during this general interval (6500-4500 BP) based on driftwood abundance. The occurrence of this tusk in a gelifluction lobe strongly suggests that it has moved downslope, hence it likely relates to a sea level >35 m.

Because sea-ice push ridges exist up to marine limit they also indicate seasonally open water throughout postglacial time (cf. Kovacs 1983). This does not contradict the existence of an ice shelf since 4310 BP because open water may still exist behind the ice shelf. The presence of incipient sea-ice ice shelf or multi-year pack ice behind the Cape Alfred Ernest Ice Shelf (Fig.2.7) attests to possible periodic open water and thus the probability of onshore pile-up of sea-ice blocks. The predominant westerly winds would explain the ubiquity of sea-ice push features on this north-south orientated coastline.

Alfreds Glacier may have advanced at least twice in the Holocene. Shell fragments dating 7790 ± 70 BP and whole valves dating 1850 ± 50 BP indicate that the glacier had retreated behind its present margin at those times. Both shell samples have been ice thrust indicating at least two local readvances by Alfreds Glacier in the Holocene. During the most recent advance, the front of the thrust block moraine was transported 6km out onto the Cape Alfred Ernest Ice Shelf after its initial formation (see sections 2.4.4 and 4.2.4.3). This advance was also responsible for the formation of the fracture in the ice shelf now occupied by a suture/incipient ice shelf (Fig.2.7). Therefore, the sea-ice component of the ice shelf existed prior to the advance.

5.3.3: Sector 2: the Cape Woods coast.

5.3.3.1: General description.

Sector 2 is bordered by the Arctic Ocean to the north and west, Woods Glacier to the east and the glaciers of Wootton Peninsula to the south (Fig.5.11). A bedrock cliff (C on Fig.5.11) descends in height from 100m in the east to 0m in the west where it blends into a seaward sloping piedmont. The base of the cliff is at approximately 35m asl throughout its length. This cliff was described as a marine terrace by R.L. Christie (in Hattersley-Smith et al. 1955). A coastal lowland exists below the cliff and widens from approximately 20m in the east to 2.5km before the cliff disappears in the west. At several places the cliff has been dissected by meltwater gorges from adjacent piedmont glaciers (Fig.5.11). The cliff continues to the east and is responsible for the heavy crevassing in Woods Glacier as it descends into the Arctic Ocean (Fig.5.11).

5.3.3.2: Geomorphology and stratigraphy.

An outwash veneer, which locally thickens at the heads of large meltwater channels, descends from the glacier snouts to the coast (Fig.5.12).



Figure 5.11: Parts of air photographs A16760-88 and 93 of the Cape Woods coast illustrating major geomorphic features. M=moraine; B=Holocene beaches; marine limits in metres asl; s=shells dating 8480 BP (west), 8540 BP (centre) and 7370 BP (east); G=grounding line; C=bedrock cliff; extensive lighter toned areas are late Holocene trimlines.



Figure 5.12: The Cape Woods coastal cliff looking east. Gorges cut down through the cliff at several locations and outwash, kames and till veneer cover the cliff tops.

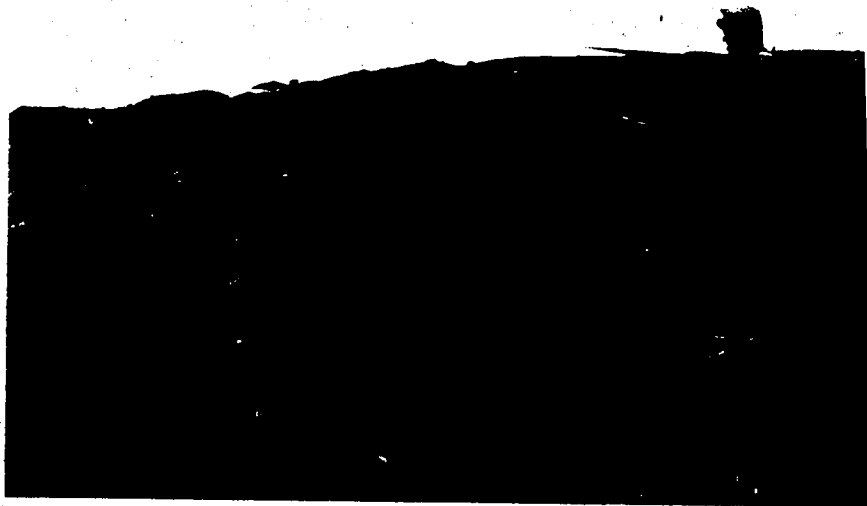


Figure 5.13: The poorly lithified sandstone and gravel conglomerate bedrock with well lithified corestones outcropping below the gently undulating coastal piedmont to the west of the Cape Woods sector.

Unlike the Cape Alfred Ernest coast, this outwash contains occasional erratic boulders or mega-blocks $>5\text{m}^3$ in size. There are also small patches of till veneer. Quartz monzonite boulders in the till and outwash are highly weathered and in some cases they have been reduced to grus. On cliff outcrops the predominant lithologies are limestone, marble and basalt which have not been mapped by Trettin and Frisch (1981). This bedrock is weathering to an incipient felsenmeer and several tors $<5\text{m}$ in height are evident. Bedrock below the cliff reveals largely incoherent, massive sandstone, and poorly- to well-lithified massive gravels that are weathering to sands and muds with occasional core stones (Fig.5.13). A sample of the gravels displays all of the characteristics of weathered and fluviially reworked quartz monzonite. These sediments display yellow/red and grey mottling.

Along the eastern half of the sector, outwash descends into gorges or extends to the cliff top which is covered with occasional cobble and boulder gravel cones and erratic mega-blocks (Fig.5.14). Below the cliff, diamicton/boulder benches and ridges extend to sea level. These grade into a large moraine, approximately 20m high, which seals off a small raised embayment from the coastal strip (Fig.5.15). Two lateral moraines approximately 5km in length mark the former margins of glaciers advancing onto the coastal piedmont from the southwest. Their retreat is demarcated by meltwater channels and sandar.

Raised marine sediments are predominantly sand-rich due to the dominance of quartz monzonite to the south. The coastal strip is characterized by raised deltas and a veneer of shelly diamicton including copious mega-blocks and boulders of quartz monzonite (Fig.5.16). A 1km long diamicton ridge exists north of the westernmost cliff section. A 48m delta to the south of the diamicton ridge and directly below the cliff is composed of sandy foresets overlain by cobble topsets (Fig.5.11). The sands are unconformably overlying the poorly- to well-lithified sands and gravels. Beneath the eastern half of



Figure 5.14: Kames on the cliff top of the eastern half of the Cape Woods coast.

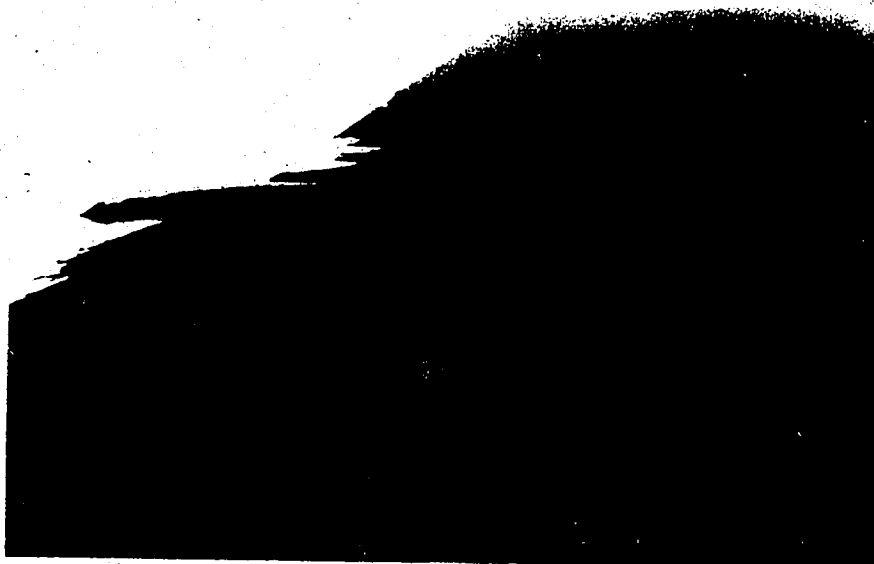


Figure 5.15: Diamicton/boulder benches and ridges are evident along the narrowest coastal strip below the cliff, west of sector 2. In this view the ridges have graded into a 20m high moraine which seals off a raised embayment from the coastal strip (see Figure 5.17).

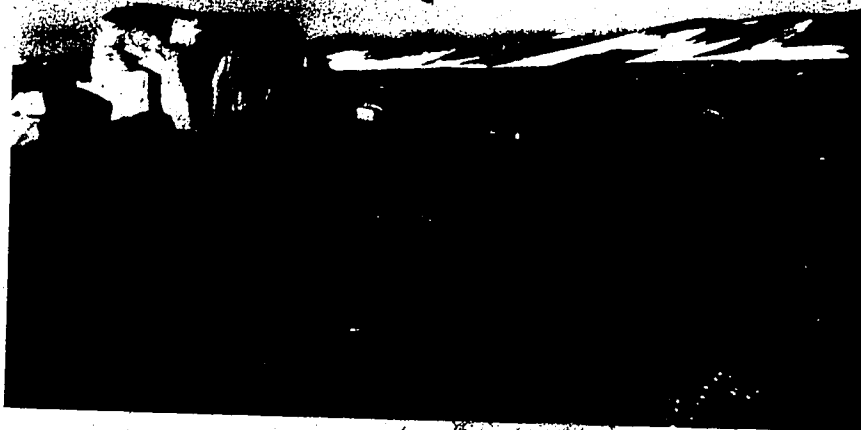


Figure 5.16: A quartz monzonite mega-block ($>5\text{m}^3$) lying on the low coastal strip of Cape Woods. The main cliff, from which sand and gravel deltas emanate, is visible in the background.



Figure 5.17: The small raised embayment to the west of Woods Glacier viewed from the lateral morainic ridge that seals it off from the coastal strip. Visible are a well defined trimline/weathering break and associated moraines/protalus ramparts. The remnant glacierette which occupies the back of the embayment is receding and exposing a glacial marine diamicton with shells in life position.

the delta a silty/sand diamicton overlies bedrock and this diamicton may be coeval with the diamicton ridge to the north. Near the cliff base, and above the delta, a sandy diamicton appears to grade into the lower silty/sand diamicton. These diamicts appear to have been overlain by the prograding delta sediments.

A small cobble terrace, 1km to the west of Sunkist Deltas, occurs at 73m asl and this is considered to provide a maximum estimate on marine limit in Sector 2. Local marine limit deltas range in height from 41-44.5 (Sunkist Deltas, site 2 on Fig.5.3a) to 65m asl (Nightmare and Cairn deltas, sites 3 and 4 on Fig.5.3a). A prominent washing limit, also at 65m asl, is marked by a gravel beach which cross-cuts outwash and links Nightmare and Cairn deltas. Raised beaches extend from this elevation down to approximately 30m asl at Cape Woods but datable material was not observed. *Hiatella arctica* valves from foreset sands below Cairn Delta dated 8480 ± 70 BP (TO 474) providing an age for the 65m sea level. At Sunkist Delta (41m asl) *Hiatella arctica* fragments from sands and gravels, overlying stratified diamicton at 35m asl dated 8540 ± 70 BP (TO 484). Mega-blocks and boulders are common on the surfaces of the Sunkist Deltas.

Retreating perennial snowbanks and glacierettes in Sector 2 record recent climatic change. Former snowbank coverage is delineated by pronounced trimlines or weathering breaks in the meltwater channels (Fig.5.11). A glacierette within the embayment west of Woods Glacier (Fig.5.3a) has retreated from a series of nested moraines extending from a prominent trimline (Fig.5.17). This glacierette has retreated considerably since the air photograph was taken in 1959 exposing a glaci-marine diamicton containing abundant shells in life position. A date of 7370 ± 70 BP (TO 483) on a *Mya truncata* valve at 23m asl was obtained on these sediments.

5.3.3.3: Interpretation.

The poorly- to well-lithified bedrock which underlies the glacimarine veneer resembles the description of the early Tertiary Eureka Sound Formation reported from eastern Wootton Peninsula (Wilson 1976; Trettin and Frisch 1981; Figure 2.2). Because of its lithification it is unlikely to be part of the upper Tertiary Beaufort Formation. This bedrock makes the identification of true glacial diamictons difficult.

The concentration of glacial debris in both the diamicton benches and the stratified diamicton underlying some deltas suggest that, during the last glaciation, the glaciers of south Wootton Peninsula extended beyond the bedrock cliff into the sea (+65m asl). Here they probably floated depositing most of their debris at the grounding line, like the present Woods Glacier (Fig.2.7). Because these glaciers originate in a deeply fretted cirque terrain, extraglacial debris is abundant and therefore moraines, till veneers and sandar are well developed. A probable morainic bank marking a former grounding line is represented by the diamicton ridge below the westernmost cliffs. Here ice was channelled through the largest of the topographic depressions that dissect the cliffs and the low delta at 48m asl demonstrates the late deglaciation of this site. Similarly, ice was channelled through the river valleys leading to the present Sunkist Deltas thus explaining their lower elevations. The 73m cobble terrace between the lower deltas of the sector marks either: 1. a kame deposited by ice coalescing around the cliffs; or 2. the height of the deglacial sea.

Retreat of the piedmont glaciers occurred prior to 8,480 BP when the sea reached 65m asl. The washing of glacial debris from marine limit down to 30m asl indicates that open water seasonally existed during the early to mid Holocene. The date of 8540 ± 70 BP from a delta at only 41m asl is more problematic. Clearly this relative sea level is younger than 8,480 BP (the assigned age of the 65m marine limit). The material dated 8540 ± 70 BP therefore must either have been redeposited from a higher elevation or the 41m delta

prograded over older deposits. The only remaining alternative is that the 41m delta was deposited subaqueously and therefore unable to grade to the relative sea level at that time. Because standard errors on both dates (8480 ± 70 and 8540 ± 70) overlap, they both are related to the local marine limit at 65m asl. Regardless of the interpretation, these shells record an environment at 8,540 BP that was amenable to marine fauna within 2km of the contemporary glacier margins.

The large moraine which seals off the embayment immediately west of Woods Glacier (Fig.5.15) is interpreted as a submarine lateral moraine of the Woods Glacier which was forced to flow westward by the increased discharge of Alfreds Glacier (Fig.5.3a). The floating tongue of Woods Glacier is presently deflected westward by Alfreds Glacier. This site was deglaciated before 7,370 BP after which the glacierette developed in the embayment, overriding the marine shells of this age. This readvance must have occurred after postglacial sea level fell below the floor of the embayment (30m asl). This puts an approximate mid Holocene age on the formation of the glacierette. A recent climatic amelioration is recorded by the extensive retreat of perennial snowpatches and glacierettes in Sector 2.

5.3.4: Sector 3: Cape Armstrong and the Armstrong River valley.

5.3.4.1: General Description.

Sector 3 includes the coastal embayments between Cape Armstrong and Cape Bugle, southward to the Armstrong River, Albion Lakes and northern Idris Peaks/Cache Plateau (Figs. 5.3a and 5.18). Two major physiographic zones of the field area occur in the sector. To the south of Albion Lakes is the undulating plateau of Zone 2 at >300m asl within which the Idris Peaks form a mountainous terrain where summits reach 600m asl.

North of Zone 2 the topography descends abruptly to the coastal lowland of Zone 1A. This zone descends from 70m asl north of Albion Lakes to sea

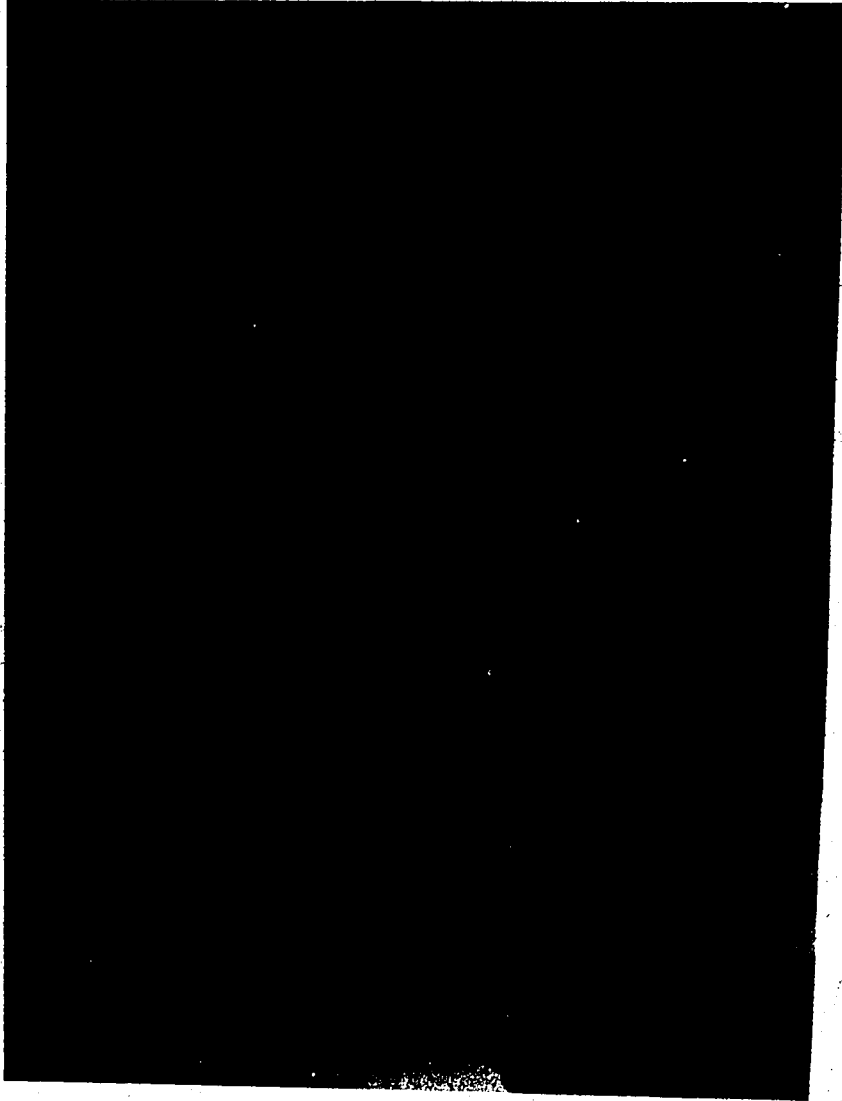


Figure 5.18: Air photograph no. A17456-27 of Cape Armstrong, the west Idris Peaks and Armstrong River illustrating major geomorphic features. Sea ice shelf is visible to the north. G=grounding line; m=meltwater channels; marine limits in metres asl; s=shells dating 10,140 BP (west) and 14,880 BP (east).

level. The 70m surface is part of a northeast-southwest oriented ridge northwest of Albion Lakes. This ridge forces the Armstrong River to flow east-west for approximately 2km before it penetrates the ridge, cutting a gorge to sea level (Fig.5.18). The Armstrong River is 18km long and is fed by meltwater from the Dodger Ice Cap to the south (Fig.5.3b). Two small ice caps exist above 300m in the Idris Peaks and a large plateau ice cap in the west descends from 200m to approximately 100m from south to north.

5.3.4.2: Geomorphology and stratigraphy.

A glaciation of unknown age is indicated by erratics of the Imina Formation (sandstones and limestones) on the metasedimentary felsenmeer of the north Idris Peaks. At lower elevations, moraines wrap around the western slopes of the Idris Peaks up to an altitude of 400m. The northern half of the Cache Plateau also hosts occasional Imina sandstones derived either from the mountains >10km to the south or from the southern Idris Peaks <5km to the southeast (Fig.2.2). The local bedrock consists of metasedimentaries, conglomerates and intrusives that outcrop as tors 5m high and as incipient felsenmeer. The southern half of the Cache Plateau is covered by either residuum, till veneer, or outwash, and spectacular meltwater channels dissect the bedrock to depths >20m (Fig.5.19). The till veneer is more extensive on the higher ground to the south whereas kames occur within the Armstrong River valley and its tributaries. Bedrock highs within the upper Armstrong River basin are notched by nested meltwater channels and their summits contain scattered erratics derived from the mountains >10km to the south. Lower bedrock knolls that protrude through the inactive alluvium of the valley are covered by till veneer. A wide meltwater channel separates the northern and southern Cache Plateau and it also contains a number of kames in its lower reaches. These kames are built out from two gorges that cut through the western shoulders of the Idris Peaks (Fig.5.1). The gorges grade upslope into



Figure 5.19: Looking south from the incipient felsenmeer of the northern Cache Plateau. The wide meltwater channel (foreground) dividing the plateau and the deep gorges cut on the southern plateau (background) are clearly visible. The Dodger Ice Cap is on the southern horizon and the upper Armstrong River is on the far right.

nested meltwater channels emanating from the highlands of the central Idris Peaks. Finally, two gorges, the largest of which is 2.5km long and 30m deep, cut through the southern half of Cache Plateau and descend towards western Bushmill Pass (Fig.5.3b).

An east-west oriented bedrock ridge at the northernmost edge of the Idris Peaks is isolated by a deep gorge draining runoff from the Peak. A 200m long kame, rising from 120-132m asl, marks the margin of ice wasting within the upper part of this gorge. The summit of the ridge has a till veneer which grades into kames, ice contact deltas, and silty, boulder-rich diamictons downslope in the easternmost cove and on Cape Bugle (Figs.5.1 and 5.3a).

A silty diamicton cloaks the bedrock ridge northwest of Albion Lakes. *Hiatella arctica* fragments from this diamicton at 55m asl dated 14,880±110 BP (TO 475). North of the ridge is a veneer of marine silts with occasional erratic boulders and clasts. Large bedrock outcrops occur in many localities (Fig.5.1). A ridge of silty diamicton loops around Cape Bugle and grades into the kames and till veneer on the bedrock ridge to the south. A hummocky diamicton surface occurs within the loop (Figs.5.1 and 5.18). Shell fragments are abundant on the ridge surface between 30 and 40m asl.

Five raised deltas occur along the south shores of Albion Lakes and the unnamed cove to the east. These emanate from gorges cutting through the north edge of Cache Plateau or from valleys draining the Idris Peaks. The deltas range from 73-80m asl, the lowest being on the south shore of the cove and the highest on the south shore of east Albion Lake. The largest raised delta in Sector 3, Armstrong Delta, is also the largest in the entire field area, covering approximately 5km² (site 5 on Fig.5.3a). The lip of the delta occurs at 61m asl whereas a prominent gravel bench at 72m asl exists to the southeast. A bedrock knoll at 91m asl, rising above the apex of the delta, is blanketed by cobble outwash. At the delta front littoral sands are unconformably overlain by gravels. *Portlandia arctica* shells in life position

from the sands at 57m asl dated $10,140 \pm 90$ BP (TO 473).

At the headland of Cape Armstrong limestone bedrock appears to have been pushed by sea-ice into ridges. A visit to the ice pushed cones offshore to the northeast reveals a preponderance of angular limestone blocks with crystalline erratics, marine silts and abundant shells of *Astarte borealis*. *Mya truncata* in a similar ice pushed ridge, collected by M. Jefferies at Cape Bourne (west of the field area), have been dated >30 ka BP (Blake 1987).

In the westernmost part of Sector 3 several perennial snowpatches and ice rises are retreating and forming trimlines. Furthermore, collapsed edges on the lower terraces (<10 m) of Armstrong Delta presumably record the retreat of ice rises over which they were deposited. Similarly, meltwater channels at the margins of the plateau ice cap to the west of Armstrong River attest to recent retreat. Finally, prominent trimlines document the melting of perennial snowpatches in the valley of the western tributary of the Armstrong River.

5.3.4.3: Interpretation.

Erratics on the felsenmeer of the Idris Peaks document a former glaciation of unknown age which flowed from south to north. During the last glaciation, ice advanced from the Dodger Ice Cap into the Armstrong Valley, probably coalescing with local ice on the higher ground to the east and west. This ice deposited moraines up to 400m asl on the western slopes of the Idris Peaks. Ice in the Armstrong River valley crossed the southern Cache Plateau depositing till veneer. Because of the sparsity of erratics and the incipient felsenmeer on the northern Cache Plateau, it is interpreted to have remained either ice-free or covered by protective, cold-based ice (cf. Dyke 1983). North of the Idris Peaks, ice advanced over the bedrock ridge onto Cape Bugle where the diamicton loop is interpreted as a grounding line. In the cove to the west, ice probably floated, locally grounding along the southern edge of the peninsula separating this cove from the next one further west. Ice also

flowed from the west Idris Peaks into Albion Lakes where it floated, abutting the 50-70m ridge on the northwest shore and depositing the bouldery diamicton at its grounding line (cf. Sugden and Clapperton 1981). The shell fragments dated at 14,880 BP were probably incorporated around the Albion Lakes by ice which grounded on the northwest shore. These shells either: 1) predate the ice advance; or 2) were coeval with it, living below floating ice and freezing-on at the grounding line during a subsequent period of ice thickening.

Beyond the grounding lines, a thin veil of marine silts with occasional dropstones was deposited, probably from a glacier ice shelf. That thin sediments exist offshore along this coast is indicated by ice thrust bedrock and shells dating >30ka BP. Thrusting of bedrock is presumably favoured by a shallow shelf and well jointed limestone. This permits the freezing of sea-ice to bedrock and subsequent block removal during onshore pile-up of ice floes. This process was presumably less active before the last glaciation otherwise *in situ* shells >30ka BP would exist.

The 80m delta bordering east Albion Lake indicates an ice-free marine enclave between ice from the Cache Plateau and from the gorge south of the Idris Peaks. Later deglaciation in these areas is recorded by slightly lower deltas at 75m and 78.5m respectively. The two meltwater gorges that cut through southern Cache Plateau, towards the western Bushmill Pass, were cut by meltwater from the Idris Peak ice cap. Clearly, ice had to be present to the west in the Armstrong River in order to prevent drainage in that direction. Drainage into western Bushmill Pass, where meltwater channels were not observed, suggests that an ice-dammed lake may have occupied the area (see section 5.3.5). The retreat of ice up the Armstrong River is marked by the pronounced meltwater channels of Cache Plateau. Because this is the main drainage route for rivers and glaciers draining north from the Dodger Ice Cap, a considerable amount of outwash was deposited in the Armstrong Delta and sandur. Moreover, if an ice dammed lake did exist in the western Bushmill Pass

then the higher meltwater channels along the west side of Cache Plateau could have been cut by its northward drainage. Fluvial erosion of the Armstrong Delta during deglaciation and initial emergence explains its low delta front (61m asl); the erosional contact between littoral sands and overlying gravels; the cobble outwash on the bedrock knoll (91m asl) at the delta's apex which indicates delta progradation to a higher relative sea level; and the 10,140 BP date from the sands which must relate to a higher relative sea level ($\leq 80\text{m}$; see Chapter 6).

The progradation of lower delta terraces ($<10\text{m}$) over the Cape Armstrong ice rises attests to the existence of ice rises prior to the mid- to late-Holocene. A recent climatic amelioration in Sector 3 is responsible for the large-scale retreat of perennial snowpatches in abandoned meltwater channels and gorges.

5.3.5: Sector 4: Bushmill Pass/Ice Alley Fiord.

5.3.5.1: General Description.

Bushmill Pass is 10km long and 2.5km wide, linking the upper Armstrong River to Ice Alley Fiord (Figs. 5.3b and 5.20). The watershed of the pass reaches ca. 250m asl and is flanked to the north by Cache Plateau and the south Idris Peaks (600m) and to the south by the highlands hosting the Dodger Ice Cap ($\leq 600\text{m}$). Bushmill Pass marks the structural boundary between the Silurian Lands Lokk and Imina Formations to the north and Proterozoic and/or lower Palaeozoic rocks to the south (see Fig. 2.2). However, there are few lithological differences between these units. The Pass appears to be the structural continuation of the southern half of Ice Alley Fiord. From Bushmill Pass northwards, the fiord mouth trends sharply southwest-northeast. Outcrops of diamicton in the centre of the fiord mouth indicate that it is very shallow. A spot sounding indicates that maximum depths are in the order of 70m (Canadian Hydrographic Service 1974).



Figure 5.20: Air photograph no. A16858-91 of Bushmill Pass, the south Idris Peaks and Ice Alley Fjord illustrating major geomorphic features. T=Terrible Glacier; m=meltwater channels; L=lateral moraine; K=kame delta; s=high shell samples; t=Holocene trimline; marine limits in metres asl.

Three small glaciers exist between the north and south Idris Peaks. These occur at 300m asl and they drain eastwards to the mouth of Ice Alley Fiord or southeastwards to eastern Bushmill Pass (Figs.5.1, 5.3a and b). To the south, Terrible Glacier (site 20 on Fig.5.4) is the main outlet of the Dodger Ice Cap, flowing northeast over a broad bedrock step and calving into Ice Alley Fiord (Fig.5.21). A number of samples were collected from Terrible Glacier and are used in the evaluation of glacial geologic processes in Chapter 4.

5.3.5.2: Geomorphology and stratigraphy.

The summits of the southern Idris Peaks are covered with felsenmeer, occasional tors and sparse erratics (Fig.5.22). Definitive erratics overlying Imina Formation sandstone and mafic dykes are calcareous, greenschist and marble clasts. On the summit shoulders, the erratics are well rounded and contrast with the angular felsenmeer (Fig.5.23). Between the Idris Peaks, the cols reach >400m asl and are covered by till veneer, which has been locally reworked by meltwater from plateau ice caps (Fig.5.1). Striated clasts exist up to 450m and shell fragments were collected from till veneer at 409m. This till descends into Bushmill Pass and onto the lower cliffs overlooking Ice Alley Fiord. Here the cliffs have been dissected by meltwater channels in excess of 50m deep and 20m wide, trending east-west. In the centre of Bushmill Pass the till veneer has been extensively reworked by slopewash and mass movement.

To the west of Sector 4, the highlands of the Idris Peaks merge with Cache Plateau of Sector 3. The two large meltwater gorges (Figs.5.1 and 5.20) that descend into western Bushmill Pass have been discussed in section 5.3.4. Further meltwater channels cut across the western flanks of the south Idris Peaks at elevations above the two gorges. Some of these higher channels also descend into Bushmill Pass.



Figure 5.21: The Dodger Ice Cap and its outlet, Terrible Glacier, viewed from the north. The glacier descends over a broad bedrock step and calves into Ice Alley Fiord. In the foreground is the felsenmeer of the south Idris Peaks with its scattered erratics. The till blanket and kames of the Bushmill Pass are in the middleground.



Figure 5.22: The north Idris Peaks (background) and small ice caps from the summit of one of the south Idris Peaks (centre) looking northwest to the Arctic Ocean. These surfaces are characterized by felsenmeer with sparse erratics and tors sculptured from more resistant mafic dikes. Till veneer, in places fluvially reworked, covers the valleys and passes between the peaks.



Figure 5.23: Well rounded erratics at 550m asl on the broad lower summit of one of the south Idris Peaks.

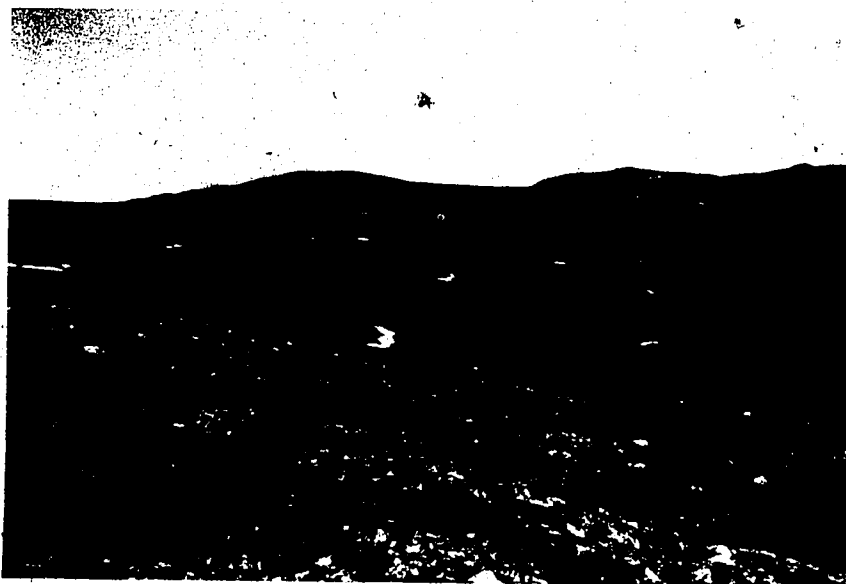


Figure 5.24: Looking north along the lateral moraine and 222m kame delta (arrowed) towards the Idris Peaks. The till blanket of east Bushmill Pass extends to the right.

A number of small gravel benches, marking the outer edges of alluvial fans emanating from the meltwater channels discussed above, occur within the centre of Bushmill Pass. These vary in altitude from 257-267m asl whereas lower, telescoping terraces emanate from the same stream outlets (Fig.5.1). In the western half of the Pass, an alluviated till veneer grades downslope into a large fan beneath which ca.3m of laminated silts outcrop. In the eastern half of the Pass, gravel hummocks and kettles have been planed at 235m asl. Further east, a former ice contact gravel terrace (50m wide) occurs at 222m asl. The 222m terrace grades upslope into a 1km long lateral moraine which wraps around the eastern slope of the mountain to the south (Figs.5.1 and 5.24). Lower telescoping terraces again occur to the east.

Eastward from the 222m terrace is an extensive area of hummocky till blanket (Fig.5.1). This extends downslope to the present margin of Terrible Glacier where meltwater has stripped the overburden and is now running on bedrock. Exposures in the till blanket are available on the north side of the stream draining Bushmill Pass. The till contains abundant boulders; numerous striated clasts (see below); and several pockets (ca.10m³) of marine silts and sands with sparse shell fragments up to an altitude of 144m. At one site, heavily faulted and contorted beds of marine silts and sands were visible at the base of a slump scar. Shell fragments were collected from till at the same altitude along the margin of Terrible Glacier.

Clast analyses were carried out on several sediment types in sector 4 and on material from Terrible Glacier and its margins. This aids the understanding of glacial debris entrainment processes in the contemporary environment and during past glaciations (see Appendix 2 and Chapter 4). Samples 17-7-873 and 17-7-874 were taken from the abandoned lateral moraine south of Bushmill Pass. Sample 17-7-874 was from a contemporary talus cone on the moraine and its increased angularity contrasts with all other samples in the sector. Samples 16-7-876 and 17-7-871 are from the till containing shell

fragments and is characterized by a relatively large number of striated clasts (33) and five stoss and lee clasts. Sample 17-7-872 is from the 222m ice contact gravel terrace and is characterized by no striated clasts.

Gravel beaches exist along the coast towards Blah Blah Point (Fig.5.3a) ranging from 72-80m asl. A 52m cobble delta, overlying marine silts, has been deposited less than 100m from the present margin of Terrible Glacier whereas a prominent 76m bench exists on the opposite shore of the fiord <1.5km from the snout. Furthermore, a 74m gravel terrace is presently emerging from the glacier snout and abundant whole *Hiatella arctica* bivalves have been collected from gravels at the base of the calving margin.

A prominent trimline and nested moraines <2m high record the recent retreat of an ice lobe in the lowland between north and south Idris Peaks. This represents a recent >1.5km retreat of the small ice caps in the basin. Similar features exist in the upper 4km of the drainage basins extending from south Idris Peaks westward to Armstrong River. This represents the recent disappearance of a perennial snowpatch comparable to the largest contemporary ice cap in the Idris Peaks. The retreat of Terrible Glacier has left cones of debris on the 52m delta and 74m gravel terrace (discussed in Chapter 4). Along the lateral margins of Terrible Glacier retreat is occurring by dry calving, caused in part by lateral incision by marginal streams.

5.3.5.3: Interpretation.

High elevation erratics exhibiting striations record former extensive glaciations in the Idris Peaks. Alternatively, those erratics that are well rounded may have been fluvially deposited (cf. England 1987b). However, if these clasts are compared to clasts sampled from the contemporary snout of Terrible Glacier and from the diamictons of Bushmill Pass their rounding is not unusual for glacially transported debris. Their present occurrence within well developed felsenmeer and tors suggests great antiquity.

The shell fragments at 409m asl. below the south Idris Peaks can be explained in two ways. First, they relate to a previous extensive glaciation when Terrible Glacier inundated the Pass and carried fossiliferous marine sediments onto the slopes of the Idris Peaks. Alternatively, they record a period of very high sea level and subsequently have moved downslope. Support for the second hypothesis comes from the glaciodynamics enforced by the local topography. During previous glaciations, the small ice caps in the Idris Peaks could advance into Bushmill Pass whereas Terrible Glacier was drawn down into Ice Alley Fiord. Therefore, ice flow directly from south to north would require a topography devoid of the fiord. Even though the fiord mouth is extremely shallow, its surface is presently >100m below the broad bedrock step at the eastern end of Bushmill Pass. During the last glaciation this caused Terrible Glacier to flow northeastward into the fiord backfilling the east end of Bushmill Pass up to an altitude of only ca. 222m asl (the altitude of the lateral moraine/kame delta; see below). Evidence for a previous higher sea level comes from the shell fragments collected at 144m at the margin of Terrible Glacier. These could be derived only from an upslope location and have been reworked by Terrible Glacier. Shells at a similar height on the north side of the stream draining Bushmill Pass have been reworked and carried upslope by Terrible Glacier as it backfilled the eastern end of the Pass during the last glaciation.

The margin of Terrible Glacier during the last glaciation is marked by the lateral moraine to the south of Bushmill Pass. This moraine grades into the gravel bench at 222m asl. This bench is interpreted as a kame delta deposited into an ice dammed lake in the Pass. Further evidence for such a lake comes from the gravel benches between 257 and 267m asl. These represent the margins of fan deltas from streams draining south Idris Peaks. To the west, lower fans are underlain by glacialustrine silts. Because gravel hummocks in the Pass are planed by a 235m asl washing limit ice must have

occupied the Pass, at least partially, prior to lake formation. The lake drained through the large meltwater channels along the east side of the Armstrong River and through gorges that mark the northern margin of Terrible Glacier, overlooking Ice Alley Fiord. The range of gravel terrace altitudes indicates that the lake had many levels. The period of most prolonged deposition is marked by the 222m kame delta that prograded westward from the margin of the expanded Terrible Glacier. Once Terrible Glacier withdrew from the eastern end of Bushmill Pass the lake drained. However, at least two lower phases marked by terraces occur below the 222m delta. This deglacial ice dammed lake in Bushmill Pass resulted from the differential response rates of local ice bodies. The smaller Idris Peaks ice caps responded first to climatic amelioration whereas Terrible Glacier maintained its maximum position for longer, damming the meltwater from the smaller catchments north and south of Bushmill Pass.

The retreat of Terrible Glacier from its last glacial limit occurred rapidly as evidenced by a 76m shoreline <1.5km from the contemporary snout. This is only 4m lower than the local marine limit south of Blah Blah Point (7km north of the glacier). The occurrence of high delta remnants at 52m and 76m underlying the snout of Terrible Glacier indicates that the glacier is presently at its maximum Holocene extent.

Results of the clast analyses have important implications with respect to present and former glacial processes. A sample taken from the active talus above the abandoned lateral moraine of Terrible Glacier reveals a high angularity which contrasts with the underlying moraine sample. The sample from the 222m kame delta shows an increase in angularity compared with two samples from the diamicton. The angularity clearly reflects a derivation from extraglacial sources and little subsequent fluvial and/or glacial reworking. The relatively high number of glacially modified clasts in the till blanket may be interpreted as indicative of former lodgement processes. As was

discussed in Chapter 4, higher concentrations of debris within glacier snouts in the field area as a whole reflect more active extraglacial, inwash and marginal meltwater activity during periods of retreat. The similarity between stone samples at the margin of, and within, Terrible Glacier (see Fig.4.18) led to the conclusions that glaciers entrained the majority of their debris during readvance over stagnant ice and aprons and that this material was redeposited after passive transportation. More debris is entrained if there is sufficient deformable proglacial sediment to disturb. Clearly the till blanket in east Bushmill Pass contains glaciectonically deformed marine sediment. Consequently, rather than invoke former lodgement, the increase in striated clasts indicates greater englacial collisions between clasts in the debris-charged basal ice as the glacier advanced over and entrained raised marine sediments. This implies that glacier bed conditions were no different during the last glaciation than today.

A considerable recent retreat of local ice caps is recorded by trimlines in the south Idris Peaks. A concomitant retreat by Terrible Glacier is recorded by its thinning over the local bedrock step and the appearance of raised deltas from beneath the snout. Considerable debris is being released also as augens and cones, some of which are stratified with clast characteristics similar to ice marginal deposits and deltas. This material was added to the surface of the glacier as it either: 1) wasted back following the last glaciation; or 2) it was proglacially thrust and entrained during readvance. As was discussed above and in Chapter 4, this material became reentrained during a climatic deterioration in the Holocene. Presumably the build up of small ice caps and perennial snow banks in the Idris Peaks relates to the same deterioration but response rates are much faster. An approximate age of <8 ka BP for the 76m delta terrace presently emerging from beneath the snout of Terrible Glacier (see Chapter 6) provides a maximum age on the deterioration.

5.3.6: Sector 5: Drift Pass/Muskox River/Desperation Bay.

5.3.6.1: General Description.

Muskox River is 16km long and drains meltwater from the North Wallow, Deception and Aviator ice caps which empties into Desperation Bay, Ice Alley Fiord (Fig.5.3a and b). The river has excavated a deep sinuous canyon approximately 1km long to the southwest of Drift Pass (Fig.5.25a). Desperation Bay is divided into an inner and outer part by a bedrock headland which rises to 75m asl (Fig.25b). Drainage from the mountains to the west of Deception Ice Cap and from the southern half of the Western Pikes also empties into Desperation Bay.

Drift Pass is 8km long and 2.5km wide linking Muskox River valley to the main Inlet. Drift Pass is as low as 125m asl at its watershed. Both flanks of the pass are fault controlled and it is occupied by a small stream fed by the easternmost valleys of the Western Pikes which drains to Cache Head Fiord.

Glaciologically the sector is flanked by the North Wallow Ice Cap to the southeast and the Deception Ice Cap to the southwest. A few small cirque glaciers exist within the deeper valleys of the Western Pikes and presumably this would be a prime area for ice build up during climatic deterioration. Due to the diverse topography of Sector 5 it would host all of the glacial landsystems during glacial conditions (section 4.3.3.1). The geology of the area is complex and the reader is referred to Chapter 2 for details (Fig.2.2).

5.3.6.2: Geomorphology and stratigraphy.

Erratics are difficult to identify in Sector 5 because most lithologies are widespread. However, erratics are easily identified on the granitic intrusions of the Western Pikes. There, Imina Formation sandstones, presumably from Drift Pass, are found up to ca.300m asl in the eastern valleys. Conversely, a small bedrock headland at the northern end of Drift Pass hosted

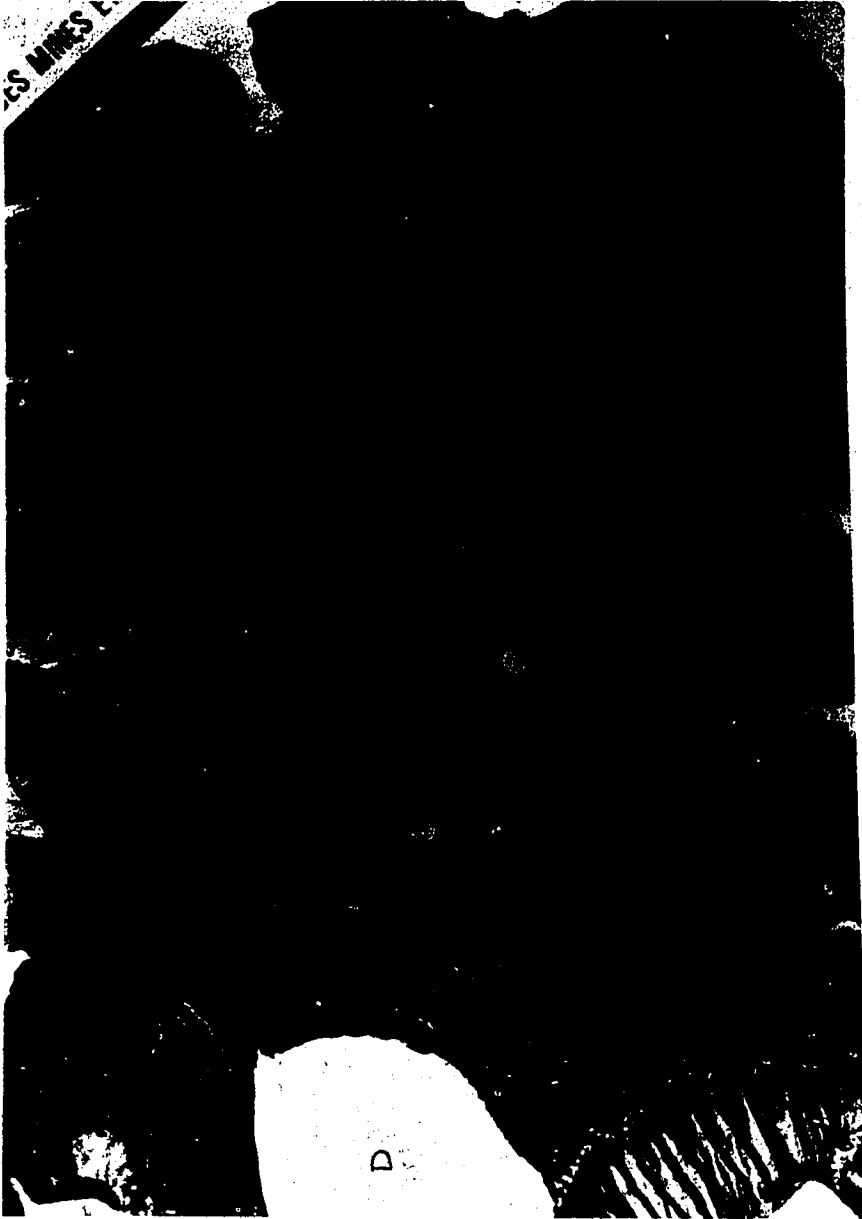


Figure 5.25a: Part of air photograph A 16866-63 illustrating Drift Pass and Muskox River and major geomorphic features of the area. m=meltwater channels; marine limits in metres asl; X=section in Fig.5.33; s=shells dating 8710 BP (north) and 7820 BP (south); L=lake sediments; H=hummocky moraine; K=sinuuous kame; G=grounding line; D=Deception Glacier.



Figure 5.25b: Part of air photograph A 16760-83 illustrating lower Muskox River and Desperation Bay and the major geomorphic features of the area. m=meltwater channels; d=74m delta; w=80m washing limit; other marine limits in metres asl; broken line=117.5m asl bench; D=Deception Glacier.

erratics up to only 150m asl. The summit of the headland (237m asl) displayed an incipient felsenmeer with tors <2m high. The summits of the Western Pikes at >900m are erratic-free and covered by well-developed felsenmeer with tors <5m high (Fig.5.26).

Drift Pass contains widespread till veneers and till blankets (Fig.5.1). The veneer extends up to 300m asl and it has been locally reworked in the valley bottom to form a sandur. The Pass also exhibits the most striking meltwater channels in the field area. The channels are nested along its southern slopes (Fig.5.27) up to 450m asl and they skirt the western slopes of the highlands hosting the North Wallow Ice Cap (Figs.5.1 and 5.25a). The upper channels cut obliquely across the meltwater gorge which drains the North Wallow Ice Cap. All of the meltwater channels document the southwesterly retreat of a glacier in the Pass to the present margin of the Deception Ice Cap (Fig.5.25a). The outermost channels extend to a sinuous ridge composed of interbedded gravels, sands and silts (Figs.5.25a and 5.28). These sediments display extensive sorting. Upslope at ca.300m asl this ridge grades into a moraine. At ca.320m asl on the southeastern slopes of the Pass this grades into a dissected moraine at 140m asl descending into Cache Head Fiord (Fig.5.28). This moraine contains striated clasts and it extends to a massive moraine at 74m asl. At 74m asl there is a sharp break marking the transition to a diamicton that has shells in life position.

Glacierized lateral moraines occupy the upper Musk Ox River valley, south of Muskox Glacier (Fig.5.1). These record the advance and coalescence of outlet glaciers principally from the Aviator and North Wallow Ice Caps (Fig.5.3b). Ice advance from the Deception Ice Cap into upper Muskox River valley would be limited to the Muskox Glacier whereas only small cirques and aretes flank the upper valley to the west. The advance of Deception Glacier (site 19 on Fig.5.4) into central Musk Ox River valley is recorded by



Figure 5.26: View to the northeast from the highest summit of the Western Pikes (915m) looking over the tors and felsenmeer developed in the granitic bedrock.



Figure 5.27: Deep meltwater channel cut into till veneer and bedrock along the southeast margin of Drift Pass.



Figure 5.28: The medial moraine/kame where it grades into the moraine loop at the northeast end of Drift Pass.

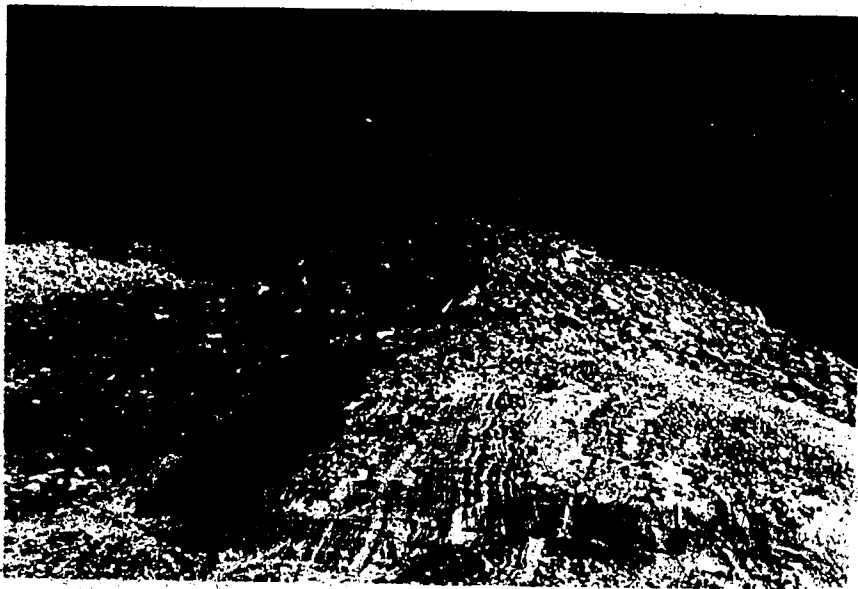


Figure 5.29: Thrust block of shallow lacustrine sediments displaying a 90° dip. Ice thrust direction was from the viewer. Note the sparse overburden in the foreground increasing to a coarse debris blanket towards Tim Fisher. Rock-glacierized scree cover the thrust blocks in the distance.

rock glacierized lateral moraines and hummocky till blanket below the bedrock cliffs to the southeast of the present glacier margin (Figs.5.1 and 5.25a).

This moraine extends 2.5km to the east where it trends across the valley floor and 3km around the cliffs to the southeast (Fig.5.1). Inside the moraine and on the valley floor proximal to Muskox Glacier is another moraine ca.20m high. This moraine extends from a number of thrust blocks <1km from the snout of Muskox Glacier. The thrust blocks are composed of sands and silts with well developed primary bedding (Fig.5.29). The inner blocks are well exposed whereas the outermost blocks have a veneer of angular cobbles and boulders and disappear under rock glacierized screes at the valley side. An inner block displays a 90° dip with a thrust direction perpendicular to the present ice margin and parallel with the valley axis.

Northeast of Deception Glacier there is an expansive outcrop of laminated silts and clays rising to 155m asl on the northeast slope of Muskox valley (Fig.5.30). Where exposed these silts and clays display intense folding and faulting (Fig.5.31) and grade upward into nondeformed silts and sands, with copious dropstones, overlain by stratified diamictons in the upper 10m. The northeast boundary of these deposits is marked by a moraine which extends into hummocky till veneer in southwest Drift Pass (Fig.5.32).

Sections southwest of Drift Pass (Fig.5.25a), although reworked by slumping, exhibit a general stratigraphy for the centre of Sector 5 (Fig.5.33). Marine silts up to 90m asl are overfolded and are unconformably overlain by 2m of matrix-supported, poorly stratified diamicton. Approximately 1m of massive gravels caps the diamicton. Shell fragments slumping from the silts yielded an age of $32,110 \pm 370$ BP (TO 480). The silts are overlapped in places by cones of massive gravels (up to 68m asl); matrix-supported, stratified diamictons with abundant evidence of current winnowing and re-sedimentation (up to 57m asl); and horizontally bedded sands with *Mya truncata* shells in life position (up to 33m asl). A date on a single valve

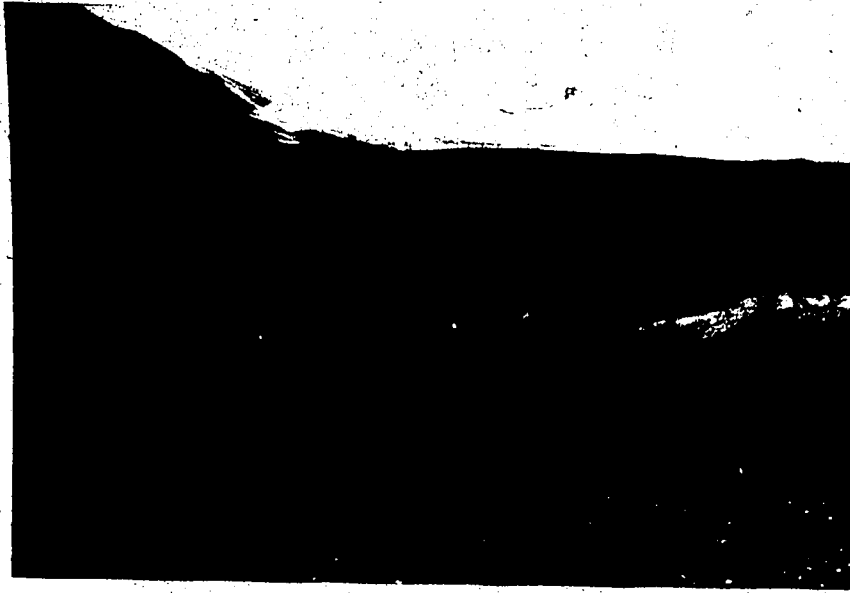


Figure 5.30: The upper outcrop of lacustrine sediments (foreground) in central Muskox River valley. In the distance is the hummocky till blanket and lateral moraine of the former Deception Glacier with associated meltwater channels and bedrock knoll.



Figure 5.31: Intense folding and faulting of lacustrine sediments of the central Muskox River valley.



Figure 5.32: The moraine immediately proximal to lacustrine sediments in central Muskox River valley. This grades into hummocky till veneer in the background.

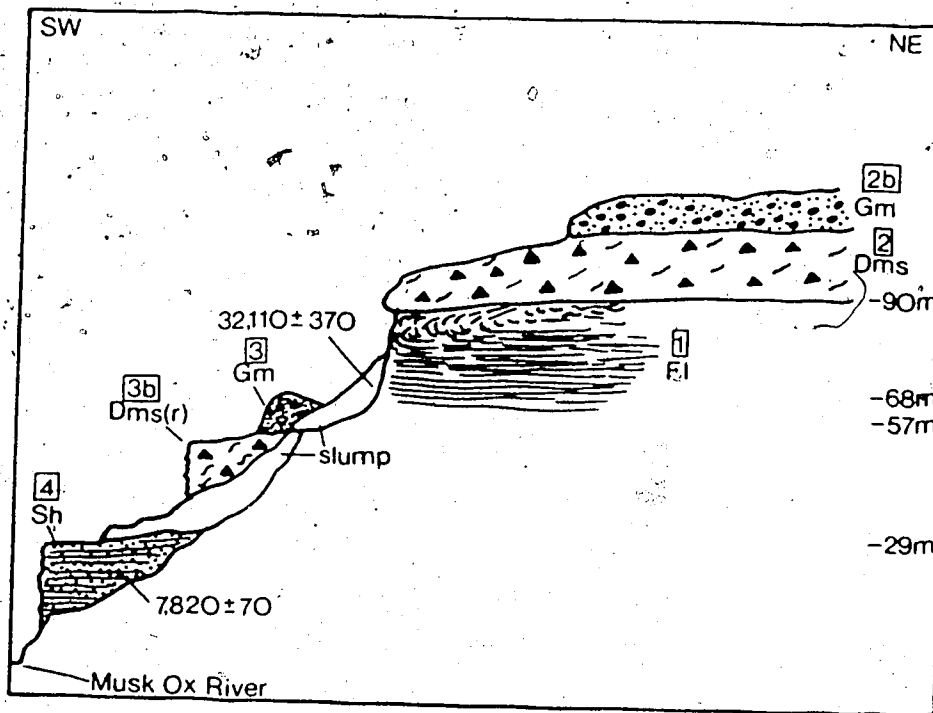


Figure 5.33: Composite stratigraphic log from the bluffs at the southwest end of Drift Pass. Facies and depositional order are indicated together with radiocarbon dates (see text for explanation).

from the sands at 29m asl is 7820 ± 70 BP (TO 255).

The surface of Drift Pass is covered by till veneer with kettles and kame terraces, numerous meltwater channels and fluvial gravels (Fig.5.1). The channels grade down to a sandur amongst rock outcrops on the floor of Drift Pass. The sandur grades to former sea levels of <89 m, marine limit at the northeast end of the Pass. The marine limit is recorded by an ice contact delta which is connected to the 237m headland by a morainal bank (Figs.5.25a and 5.34). Another prominent washing limit (88m asl) trims a moraine at the southeast end of Drift Pass, overlooking Cache Head Fiord. Inset within the 89m delta are three lower deltas; one at 85m and two at 81m asl. The 85m delta was deposited at the northeast end of the Pass from the Western Pikes after the 89m delta was abandoned. Both 81m deltas are connected to lower sandur surfaces in the Pass. A massive, matrix-supported diamicton underlies the 85m and inner 81m deltas. This diamicton is overlain by proximal bottomset sands and silts with whole *Hiatella arctica* valves. A date of 8710 ± 70 BP (TO 257) was obtained on a valve at an altitude of 40m, within the bottomset sands of the 85m delta. Along the outer, west shore of Cache Head Fiord, 3km southeast of Drift Pass, an 86m washing limit occurs within 400m of an outlet glacier of the North Wallow Ice Cap. A *Hiatella arctica* valve in life position from below this washing limit (67m asl) dates 8310 ± 70 BP (TO 253).

The retreat of the Deception Ice Cap from Desperation Bay is documented by meltwater channels nested along the southeastern slopes of the Bay (Fig.5.25b). A deeply incised meltwater gorge cuts through the headland northwest of the Bay (Fig.5.25b). Along the coast of this headland a boulder-strewn bench extends for approximately 2km at 117.5m asl (Fig.5.35). This is one of the best developed shorelines in the field area.

The summit of the bedrock headland (75m asl) which divides Desperation Bay exhibits an incipient felsenmeer developed in calcareous bedrock. A few scattered erratics occur on the summit whereas the lower slopes are blanketed



Figure 5.34: The ice contact delta at 89m asl at the northeast end of Drift Pass. The morainal bank (grounding line) connecting the delta to the 237m headland extends into the distance. Ice margin at time of delta deposition was to the left.



Figure 5.35: Geomorphology of the headland to the north of outer Desperation Bay viewed from the Idris Peaks. The 117.5m boulder-strewn bench and the deeply incised meltwater gorge (G) and nested meltwater channels within the Bay (m) are marked.

by raised marine silts containing occasional pockets of coarse debris and scattered angular boulders.

There are three prominent deltas within Desperation Bay and an extensive gravel bench that record sea level during deglaciation. Along the southeastern shore of the Bay the gravel bench prograded from the bases of meltwater channels into a former sea level at 80m asl. However, two deltas on the east and north shores of Desperation Bay record a sea level of 73.5m asl. A third (74m asl) delta prograded into the outer bay from the highlands to the south (Figs.5.25a and b).

Evidence of recent glacier retreat occurs in the sheltered valleys of the Western Pikes. Here trimlines record the thinning of cirque glaciers and perennial snowpatches (Fig.5.36). Furthermore, a freshly exposed till and outwash veneer (ca. 10m wide) occurs along the margin of Deception Glacier on the 1959 air photographs and it was also observed in the field. Muskox Glacier has retreated from its thrust block moraine and the thinning of a section of the snout has produced extensive debris covered stagnant ice. This retreat was clearly in progress on the 1959 air photographs. Finally, meltwater channels and trimlines record the retreat of the easternmost glacier in Drift Pass over a distance of ≤ 0.5 km.

5.3.6.3: Interpretation.

During the last glaciation ice advanced into Drift Pass from the Deception Ice Cap and coalesced with ice lobes from the Western Pikes and the North Wallow Ice Cap. During its advance into Drift Pass Deception Glacier overrode marine silts deforming and truncating them (Fig.5.33). If the date of $32,110 \pm 370$ BP is correct (cf. Appendix 1) then it indicates that sea level was in excess of 90m asl at that time. The medial moraine which formed between Deception Glacier and the ice from the North Wallow Ice Cap was probably reworked by fluvial processes lower down in the ablation zone. This is

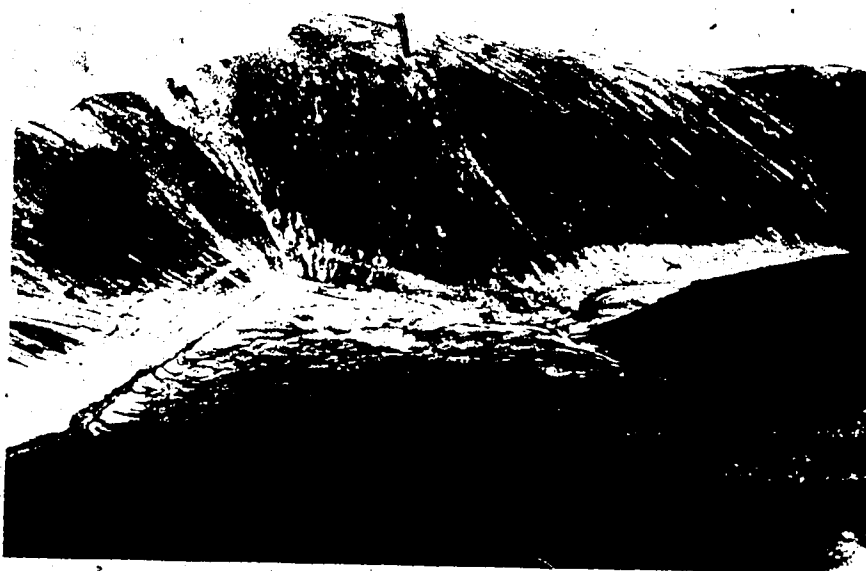


Figure 5.36: A prominent trimline in the Western Pikes representative of the extensive retreat of local cirque glaciers.

suggested by the sinuous ridge of interbedded gravels, sands and silts which is interpreted as a supraglacial kame let down onto the underlying topography after meltout, resulting in the faulting of the sediments. If this interpretation is correct, the upper elevation of this kame would mark a palaeo-ELA of 300m asl within Drift Pass during the last glaciation. This suggests a lowering of the present ELA (900m asl) by 600m.

The moraine at the downstream end of the kame represents the terminus of the glaciers advancing into Drift Pass from the North Wallow Ice Cap. The stratified diamicton at 74m, underlying the moraine, indicates that glacier ice floated in Cache Head Fiord beyond this point. The main Deception Glacier was channelled together with ice from the Western Pikes into Cache Head Fiord where it also floated. Deception Glacier also deposited a morainal bank where it grounded on the bedrock high north of the 89m ice contact delta (Figs. 5.25a and 5.34). The fact that the 89m delta emanates from the outermost meltwater channel in the pass lends support to this reconstruction. Because there are no erratics on the 237m summit at the northeast end of the pass, it is likely that the ice was thin. This is also likely from a glaciological viewpoint due to the draw-down effect of Cache Head Fiord upon a glacier in the pass.

The 8710 ± 70 BP date, underlying the 85m delta, provides a minimum age for the deposition of the 89m marine limit and initial deglaciation of Drift Pass. Because the date was from shells in bottomset sands, it provides an age for the progradation of the 85m delta. The 8310 ± 70 BP date from below the washing limit along the outer west coast of Cache Head Fiord provides an age for sea level between >67m and 86m as well as a minimum age on deglaciation at a site within 400m of a contemporary glacier.

In central Muskox River valley lateral and terminal moraines document the coalescence of Muskox Glacier and the Deception Glacier during the last glaciation. In upper Muskox River valley the Aviator and North Wallow ice caps may have advanced only as far as the rock glacierized lateral moraines in the

valley bottom where they coalesced with Muskox Glacier (Fig.5.1).

During early deglaciation drainage of the upper Muskox River was dammed by the Deception Glacier. The deformed laminated silts and clays were deposited in the resulting ice dammed lake with water depths $\leq 155\text{m}$. Rapid sedimentation caused subaqueous slumping, resulting in the intense deformation and faulting within the exposures. The moraine to the northeast of the exposures, and the stratified diamictons and abundant dropstones of the upper 10m, probably reflect the proximity of Deception Glacier. Early drainage from this lake may have been responsible for the deep excavation of upper meltwater channels at the junction of eastern Muskox valley and the Pass.

As ice retreated from Drift Pass its meltwater was responsible for cutting and/or reexcavating the deep channels on the southeast slopes (Fig.5.25a). These channels are interesting in that they cut obliquely across the gorge presently draining the meltwater of the southwest margin of the North Wallow Ice Cap. Clearly the cutting of this gorge must postdate the meltwater channels. As emergence continued during deglaciation the sandur within Drift Pass graded to successively lower sea levels. The sandur also was supplied by progressively lower discharges from the waning Deception Glacier whose drainage became largely diverted into Desperation Bay after its retreat southwest of the Drift Pass watershed. During its retreat, the Deception Glacier deposited a melt out till over glacitectonically disturbed marine silts which, in turn, were succeeded by outwash gravels (Fig.5.33). Lower cones of massive gravel between 68 and 57m asl represent kames deposited by the same process. In places ponds formed between Deception Glacier and the watershed in Drift Pass resulting in the deposition of lacustrine fines and debris flows (Dms(r) on Fig.5.33). After the final break-up of Deception Glacier in the Musk Ox River valley the ice dammed lake drained prior to the penetration of the sea around 7820 ± 70 BP. Meltwater channels and kame terraces document the above changes in drainage. Final ice stagnation at the southwest

end of the pass was responsible for the kames and kettles, and this likely progressed long after Muskox River had succeeded in breaching Deception Glacier.

In Desperation Bay, the general lack of coarse debris within the marine silts, and the sparsity of erratics on the 75m headland, suggest that the ice entering the bay floated. Nonetheless, this ice excluded the sea until considerable emergence had occurred in some areas. Numerous meltwater channels on the north shore of the bay document the retreat of ice up into the highlands of the Western Pikes (Figs.5.1 and 5.25b). The age of the meltwater gorge cutting through the headland to the north of the outer bay (Fig.5.35) is unknown. This feature could date to an earlier glaciation when ice streamed through Desperation Bay. Similarly, the 117.5m bench on the same headland is of unknown age but it could be a former sea level from an earlier glaciation (see discussion of isobase pattern in Chapter 6). The 10m gravel bench on the southeast shore of the bay suggests that glacier ice broke up rapidly leaving local ice debouching into the sea until another 6.5m of emergence had occurred. This explains local marine limits of 73.5m and 74m asl (see Chapter 6).

Evidence of considerable glacier readvance postdating the last glaciation is available in the central Muskox River valley. Here the thrust blocks, likely composed of shallow lacustrine sediments, document a 750m readvance of the northern margin of Muskox Glacier. A later readvance of the same glacier, inside the 750m margin, was responsible for the construction of the contemporary thrust block moraine from which the glacier is now retreating (cf. Fig.4.14). One of these readvances probably correlates to the build-up of small cirque glaciers and perennial snowpatches in the Western Pikes. A recent retreat of glacier snouts (up to 500m) is recorded throughout Sector 5.

5.3.7: Sector 6: Bridge Street and Ice Alley Fiord.

5.3.7.1: General Description.

Sector 6 comprises the lower Bridge Street valley and the head of Ice Alley Fiord both of which are occupied by outlet glaciers of the Dodger and Bridge Street ice caps (Figs.5.3b and 5.37). Bridge Street valley is 35km long originating in the upland plateau of physiographic Zone 2. Drainage inland from the fiord head is blocked by Pudding Glacier, and an unnamed glacier to the south, creating two ice dammed lakes. The northernmost lake is called Pudding Lake (Fig.5.3b).

5.3.7.2: Geomorphology and stratigraphy.

The 770m summit of the ridge overlooking Pudding Lake has a well developed felsenmeer without definitive erratics. Erratic lithologies (ie. those from the Nansen and Esayoo Formations to the south) are abundant extending to 176m asl on the north side of the Bridge Street valley and 205m asl on the south side. Above these elevations locally derived colluvium extends to the summit plateaux. On the north side of the valley mouth a till bench at 140m asl grades into a meltwater channel at 136m. This channel is cut into bedrock and wraps around the mountain shoulder before reaching the fiord head (Fig.5.1). Offlapping the till on the south side of the valley are pockets of silt-rich diamictons and gravel benches. Large alluvial fans, composed of coarse, sub-angular clasts with interbedded diamictons, have been deposited on the lower slopes of Bridge Street valley (Fig.5.1). These fans often exhibit steep and pitted fronts and overlie braided outwash deposits. Sections through all of these sediments are available along the main river and in extensive terraces along the lower valley slopes to the east (Fig.5.38). In some places braided outwash within the terraces is contorted and faulted (Fig.5.39). The outwash is truncated and overlain by coarse gravels that can be traced to retreating ice margins. One such section occurs across the river from the present margin of Bad Weather Glacier (site 14 on Fig.5.4).

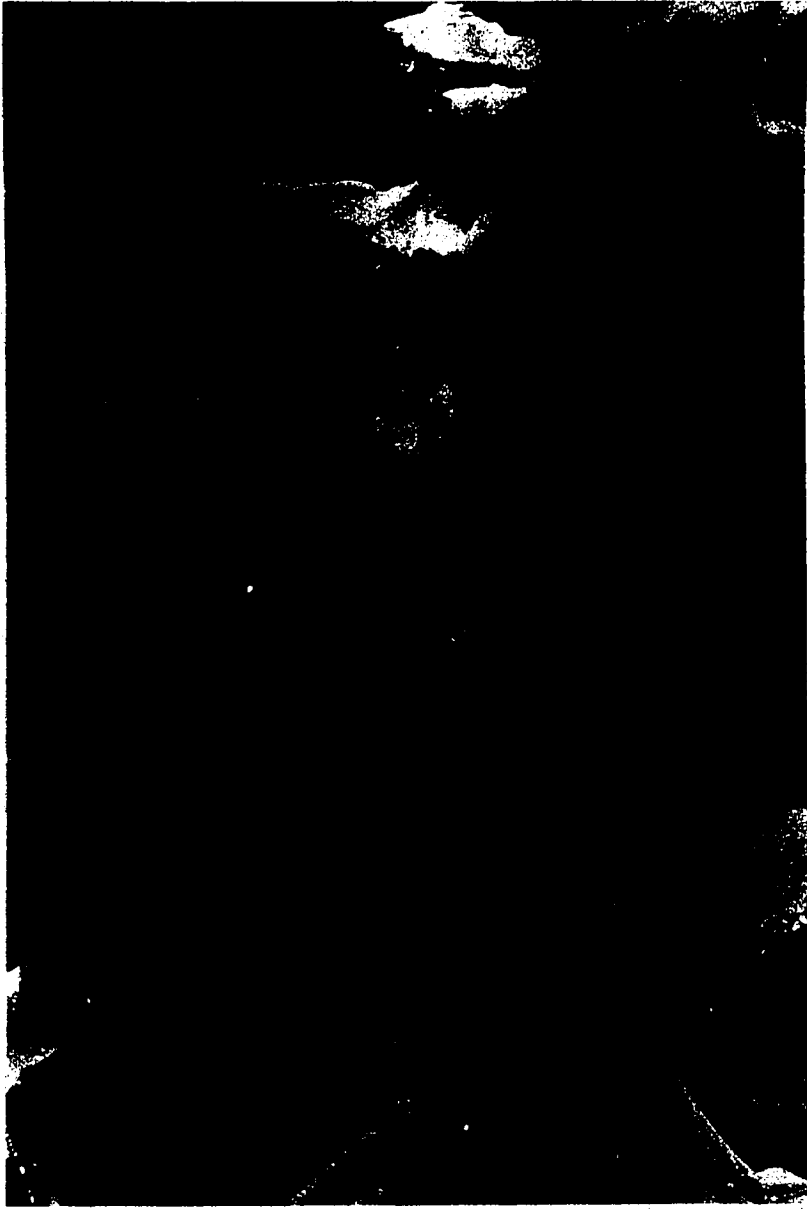


Figure 5.37: Air photograph no. A 16760-101 of the Bridge Street valley and the head of Ice Alley Fjord illustrating major geomorphic features. M=moraine; G=grounding line; marine limits in metres asl; L=lake sediments; s=shells dating 7500 BP (north), 8330 BP (centre) and 5200 BP (south); X=section in Fig.5.41.



Figure 5.38: View of upper Bridge Street valley from the west illustrating the large number of terraces cut into alluvium and lacustrine sediments (L).

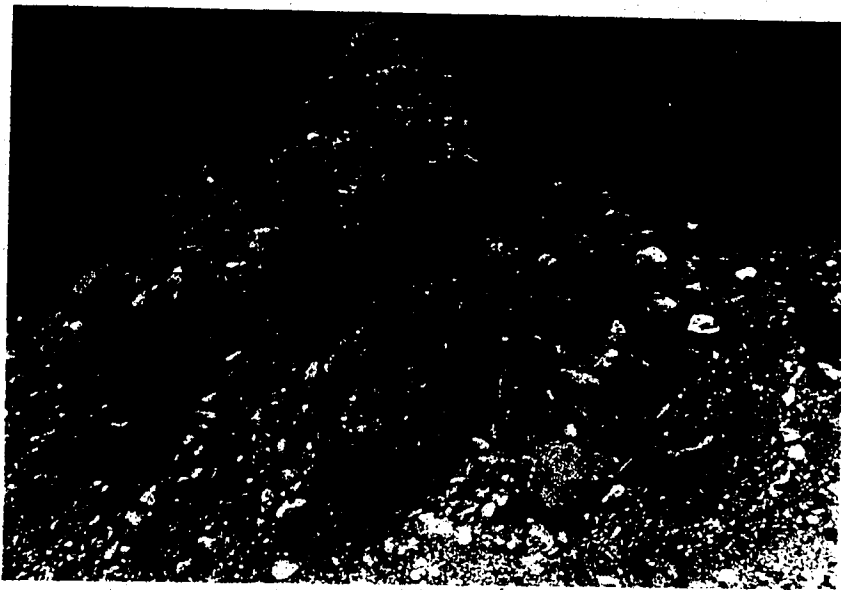


Figure 5.39: Heavily contorted and faulted braided outwash deposits on the north side of Bridge Street.

An undulating diamicton, reaching 157m asl occurs in upper Bridge Street valley (Fig.5.1). This surface is underlain by 10m of stratified diamicton. Downstream, a 10m section reveals rhythmically bedded silts and clays rising to 87m asl. These rhythmites are overlain by ≤ 2 m of diamicton including graded beds and rip-up clasts of silt/clay. A few kilometers to the southeast of the rhythmites a 20m section was visited by helicopter. This exposes steeply dipping gravel foreset beds overlain downstream by horizontally bedded fines and diamictons.

At the fiord head a number of sections, as well as marine and alluvial terraces, record deglacial events. On the north side of Bridge Street river, a prominent bench has been cut in till at 86m asl. At 54.5m asl a gravel bench (750m long) extends from the margin of Kipper Glacier westwards towards Pudding Glacier (Figs.5.1 and 5.4). Below this bench 10m of sandy foreset beds overlie 20m of massive bouldery diamicton. This diamicton is replaced abruptly downstream by laminated silts with occasional dropstones.

On the west side of the fiord head, 10m high bluffs reveal laminated marine silts with occasional dropstones. These silts are being overrun by talus from a rock glacierized lateral moraine at ≤ 86 m asl. To the south of these bluffs the silts overlie a hummock of stratified diamicton approximately 5m high (Fig.5.40). These silts contain *Hiatella arctica* in life position as well as occasional beds of gravelly diamicton. The silts are also heavily contorted and folded. A *Hiatella arctica* valve from the section at 29m asl dated 7500 ± 70 BP (TO 471).

Immediately northeast of Vienna Glacier (site 17 on Fig.5.4) a diamicton containing shells in life position, has been dissected by lateral meltwater channels. A *Hiatella arctica* valve at 52m asl from this diamicton dated 8330 ± 80 BP (TO 470).

A *Hiatella arctica* valve from one of the silt blocks entrained within the snout of Pudding Glacier (see Fig.4.16) dated 5200 ± 60 BP (TO 472). Between



Figure 5.40: The section 750m from the Ice Alley Fiord coastline exhibiting folded and contorted marine silts with occasional beds of gravelly diamicton overlying a stratified diamicton hummock (morainal bank-grounding line). The rock glacierized lateral moraine at 86m is arrowed on the slope above.



Figure 5.41: The section cut by sandar at the margin of Pudding Glacier.

20 and 50m from the glacier, a section 100m long and 10m high (Fig.5.41) can be divided into five units (Fig.5.42). From east to west these include: 1. ice-proximal stratified diamicton overlain by massive, clast-supported diamicton; 2. horizontally bedded sands and fines overlain by clast-supported, stratified diamicton; 3. contorted and folded sands and fines with occasional massive gravel beds, overlain by horizontally bedded sands and fines; 4. laminated fines with dropstones overlain by horizontally bedded sands and massive gravels which are in turn overlain by a stratified, matrix-supported diamicton; 5. interbedded sand and gravel foresets. Shells occur in life position in horizontally bedded sands and fines (Fig.5.42).

The section is overlain by massive gravels, and planar and trough crossbedded sands and gravels. The section appears to be part of an undulating fan delta dipping to the west. The overlying massive gravels at the western end of the section appear to be the topset beds to the sand and gravel foreset beds (unit 5).

Four glacially thrust blocks between 4 and 7m high exist on the lower face of the section (1-4 on Fig.5.42). Blocks 1 and 2 are composed of horizontally bedded sands and fines. Both blocks are blanketed laterally by colluvium from the section. Thrust block 3 is composed of laminated marine silts that contain *Portlandia arctica* shells in life position. The outermost edge of this thrust block is unconformably overlain by matrix-supported gravels. The sand and silt beds of thrust block 4 have undergone intense folding. Furthermore, both the ice-proximal and ice-distal faces have been extensively reworked by mass movement, specifically debris flows within the sands and silts. The remainder of the section is dominated by either stratified diamictons or bedded sands and fines of marine origin.

5.3.7.3: Interpretation.

During the last glaciation ice thickened and filled the Bridge Street

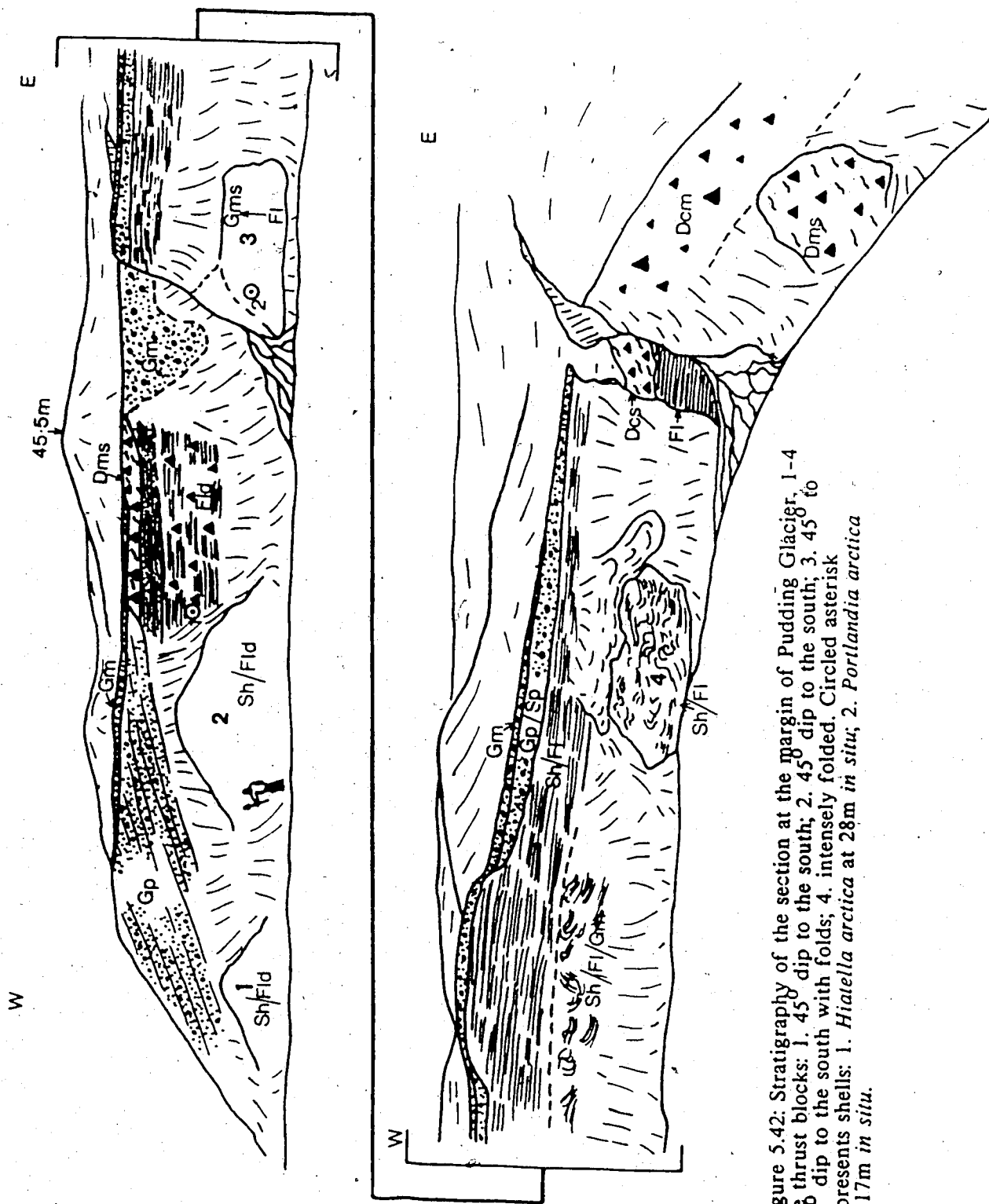


Figure 5.42: Stratigraphy of the section at the margin of Pudding Glacier, 1-4 are thrust blocks: 1. 45° dip to the south; 2. 45° dip to the south; 3. 45° to 90° dip to the south with folds; 4. intensely folded. Circled asterisk represents shells: 1. *Hiatella arctica* at 28m *in situ*; 2. *Portlandia arctica* at 17m *in situ*.

valley up to at least 205m asl. The lateral moraine at $\leq 86\text{m}$ asl and the 10m high sections along the west side of the fiord head indicate that the ice was thin enough to float. A former grounding line, marked by the hummock of stratified diamicton (morainal bank), occurs 750m from the present shoreline. Beyond the grounding line, silts with occasional dropstones probably record sedimentation beneath the ice shelf. Deformed silts, with beds of gravelly diamicton, overlying the morainal bank represent rapid deposition during ice retreat. Because the $\leq 86\text{m}$ lateral moraine has been rock glacierized, its original elevation must have been higher. At the mouth of Bridge Street valley ice was grounded at least to the westernmost point of the 54.5m gravel terrace underlain by massive diamicton.

An ice dammed lake in the upper Bridge Street valley is marked by silt/clay rhythmites that grade laterally into steeply dipping gravel foreset beds. Diamictons associated with these deposits indicate an ice contact environment. The age of the lake is unknown. Other lacustrine sediments are represented on the south side of the lower Bridge Street valley. Here pockets of stratified diamicton and gravel were deposited in lakes ponded by outlet lobes of the Bridge Street Ice Cap. These lacustrine sediments were then capped by braided outwash from the main river and by local alluvial fans which graded to a falling relative sea level.

Deglaciation of the fiord head occurred sometime before 8330 ± 80 BP when Pudding Glacier had retreated to within 500m of its present margin. The marine limit at the fiord head is probably represented by the 86m till bench on the north side of lower Bridge Street valley and it must be at least as old as the shells dated 8330 BP (see Chapter 6). The 54.5m bench relates to a later period of progradation from Bridge Street into the fiord head and may record increased discharge caused by the breaching of an ice dam in the upper or middle sections of Bridge Street. Pudding Glacier had retreated behind its present margin by 5200 ± 60 BP, the age of the overridden shells which provide a

maximum date on its readvance. This readvance was facilitated by Holocene emergence which removed the sea from the vicinity of Pudding Glacier.

The section adjacent to the snout of Pudding Glacier probably represents a former fan delta based on its marine fauna. This fan delta was subsequently capped by alluvium as streams downcut to a lower relative sea level. The lithofacies sequences within the section record deposition into an ice proximal marine environment during ice retreat. These sediments include massive, clast-supported diamictons and stratified diamictons. The gravel foreset beds near the top of the section terminated glacimarine sedimentation when sea level was $>40\text{m}$. These beds indicate a palaeocurrent from the east.

Subsequent to the deposition of the sediments in the section, and their downcutting by meltwater grading to a sea level close to present, Pudding Glacier readvanced, forming four thrust blocks (Fig.5.41). Because the silts of block C contain *Portlandia arctica* shells in life position, the sea must have penetrated inland of this site before the readvance. The marine silts presently undergoing thrusting and entrainment also contain shells in life position (*Hiatella arctica* dating 5200 ± 60 BP). There are two possible explanations for this: 1. the glacier overrode the marine silts with *Hiatella arctica* when advancing towards the fan and did not disturb them. Then the most recent advance thrust these silts into their present position; 2. the silts have been thrust and overridden twice and there has been little penetrative deformation and internal disturbance in some cases (Fig.4.23).

A readvance of glaciers in Bridge Street valley was responsible for the thrust alluvium. The disturbed alluvium was then truncated and overlain by sandar that built out from the retreating ice. These sandar have also buried bodies of stagnant ice and any future readvance could entrain these, concentrating debris within the glaciers. Pudding Glacier, because of its larger drainage basin and therefore longer response time, is still advancing as a result of a mid to late Holocene climatic deterioration. Vienna Glacier

readvanced during the Holocene past its 8300 BP limit. It is possible, therefore, that it exceeded or equalled the limit of the last glaciation at this time. Kipper Glacier has readvanced over an alluvial terrace without disturbing it and presently overlies gravel covered stagnant ice. This gravel cover grades into the 54.5m terrace downstream and suggests that the buried ice might date from the last glaciation. In summary, the glaciers of Sector 6 readvanced some time after 5200 BP and in some cases attained maximum positions beyond early Holocene margins. Although each glacier displays a somewhat different response to recent climatic amelioration, the general trend is one of retreat.

5.3.8: Sector 7: The Cache Head Fiord, Cache River and Garden Plateau area.

5.3.8.1: General Description.

Sector 7 includes the southern half of Cache Head Fiord, the northern part of Cache River and the surrounding highlands. The physiography is typical of physiographic Zone 2 (Fig.5.43). The southern half of the sector is dominated by rocks of the upper Carboniferous and lower Permian Nansen Formation (Fig.2.2) which forms the atypical castellated topography of the Castle Range (Figs.5.3b and 5.44).

The Aviator and Nomynd ice caps occupy the plateaux to the northwest and northeast respectively, whereas the Grant Land Mountains icefields occur to the south (Fig.5.3b). The outlet glaciers from these icefields either descend into the Cache River valley or occupy the upper reaches of smaller V-shaped valleys. The Storm River and Blind valleys, run east-west across the centre of the sector carrying drainage from the Aviator and Nomynd ice caps respectively. Small cirque glaciers exist in the precipitous topography of the Castle Range. The glaciation level in Sector 7 is 762m asl and summits range from 900m to 1050m asl.

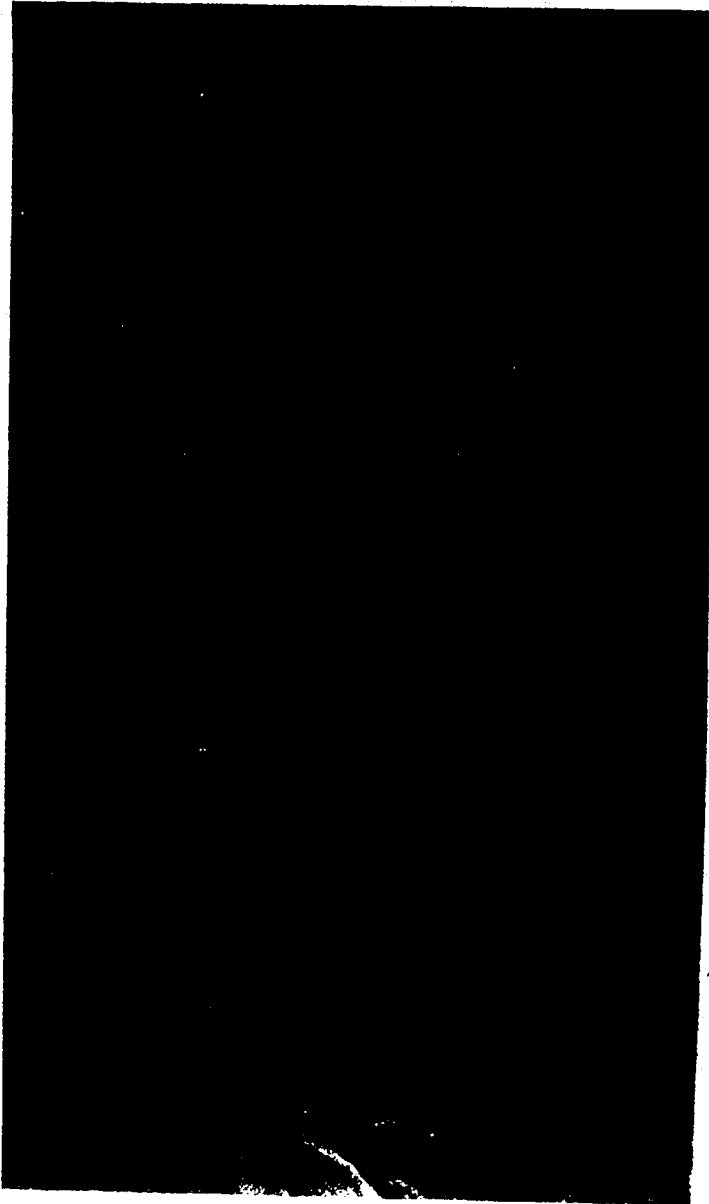


Figure 5.43: Air photograph A 16724-81 of Cache Head Fiord, Cache River and surrounding highlands with major geomorphic features. Original photograph quality is poor. K=kame; m=meltwater channels; L=rock glacierized lateral moraine; marine limits are in metres asl; s=shells dating 7530 BP. Nos. H1-5 and E1-8 are the locations of stratigraphic logs in Fig.5.48. Castle Range occupies top right half of photograph.

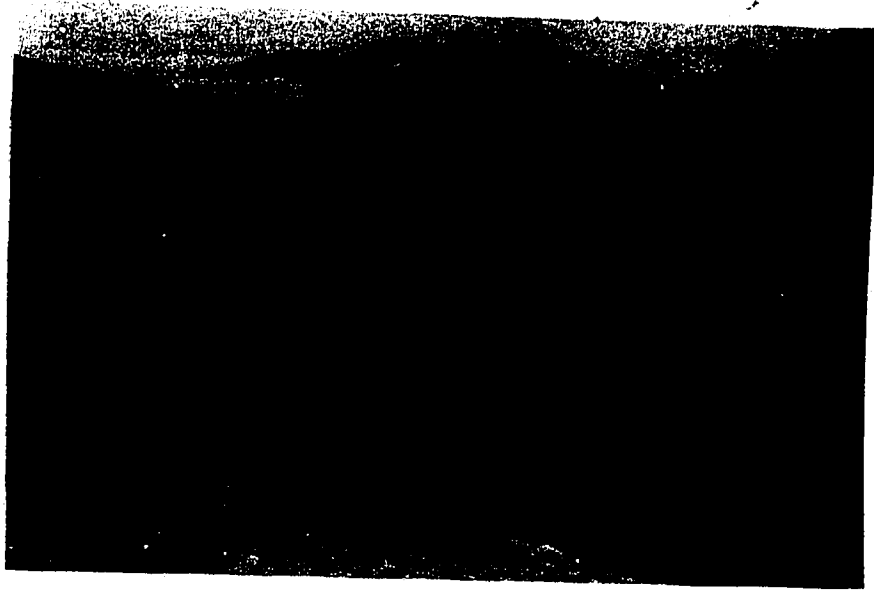


Figure 5.44: Well developed felsenmeer and tors of the Castle Range. The origin of the channel likely records the former retreat of cirque glaciers.



Figure 5.45: Looking east-southeast across the discontinuous till veneer of Garden Plateau towards Endeavour Glacier and the $\leq 600\text{m}$ ridge overlooking Cache River. The ridge contains scattered erratics from the south.

5.3.8.2: Geomorphology and stratigraphy.

Several summits were visited to determine the distribution of erratics. Erratics extend up to 433m asl on the western slopes of the Castle Range. Above this there are well developed felsenmeer and tors >5m high which have been excavated from the calcareous bedrock (Fig.5.44). Several high-elevation channels (up to 553m asl) cut into bedrock document the former retreat of cirque glaciers (Fig.5.1). Calcareous erratics from the Castle Range have been carried northwards onto the Nansen, Lands Lokk and Imina formations. Erratics descend to approximately 320m asl east of the fiord head where numerous meltwater channels cut into bedrock document the retreat of ice into the uplands of Blind Valley. Erratics were not found on either the summits of the mountain immediately southwest of the fiord head (≤ 762 m asl) or on the ≤ 450 m asl ridge above the eastern wall of the fiord. The ridge forming the eastern margin of Garden Plateau (ca.600m asl) is composed of basalts and associated volcanics which are weathering to a cindery felsenmeer with several tors <5m high (Fig.5.45). Scattered calcareous, sandstone and quartzite erratics form a discontinuous till veneer recording the former inundation by ice from the south.

Rock glacierized lateral moraines occur on the mountain slopes at the mouth of Storm River (Fig.5.3b) and demarcate the former margins of ice that advanced into the fiord head from the west. The moraine profile descends from 112m asl north of the river mouth to only 91m asl south of the river mouth. Along the Storm River valley a discontinuous till veneer extends up to ca.300m asl. Striae and roches moultonnees record former ice flow direction into the upper valley from the southwest Garden Plateau. Rock glacierized moraines occur below the Endeavour Glacier and record its advance into the Cache River valley (Fig.5.1). The cliffs of Garden Plateau are dissected by a number of large channels that were cut by meltwater from glaciers retreating onto the

plateau. These glaciers were responsible for striae and rochès moutonnees on the southwest bank of Cache River. A continuous till veneer, occasional hummocks and areas of till blanket cover the slopes east of Cache River up to ca. 350m asl (Figs. 5.1 and 5.46). Clast analyses were undertaken on this till at 79m asl (6-7-872) and 113m asl (6-7-873); see Appendix 2. There are great differences between the two samples, the most apparent being the proportion of striated clasts. The 79m sample contained eighteen striated clasts whereas the 113m sample contained only two. There is also a greater degree of rounding in the higher sample.

The pattern of deglaciation in Sector 7 is recorded by meltwater channels emanating from small valleys and by many raised deltas. Low marine limits of 61 and 60.5m asl occur at the mouths of two valleys in the central fiord whereas Gorge Delta (site 6 on Fig. 5.3b), 5km north of the fiord head, has a marine limit of 77m asl. Below the 77m delta, 10m of horizontally bedded sands and silts directly overlie bedrock. Within these sediments, at 58m asl, a single *Mya truncata* bivalve was collected in life position and dated 7060 ± 70 BP (TO 251). On the east side of the fiord head, the marine limit is recorded by a prominent gravel bench at 93m asl (Fig. 5.47). To the north a delta records a 74m sea level at the western mouth of Blind Valley. To the south two ice contact delta remnants occur at 86 and 75m asl formed by ice that retreated into a valley of the Castle Range. This ice retreat is also recorded by nested meltwater channels and moraines. Four kilometers south, inland from the fiord head, a bench cut into till records another marine limit (79m asl) at the mouth of a second outlet valley from the Castle Range (Fig. 5.43). On the opposite bank of the Cache River a large delta remnant records the same marine limit (79m asl). This marine limit represents the most inland location where a former sea level was observed. Several outcrops of marine silt occur below the gorge draining Endeavour Glacier. These silts rise to 78m asl and contain numerous boulders. The rock glacierized moraines at this location are

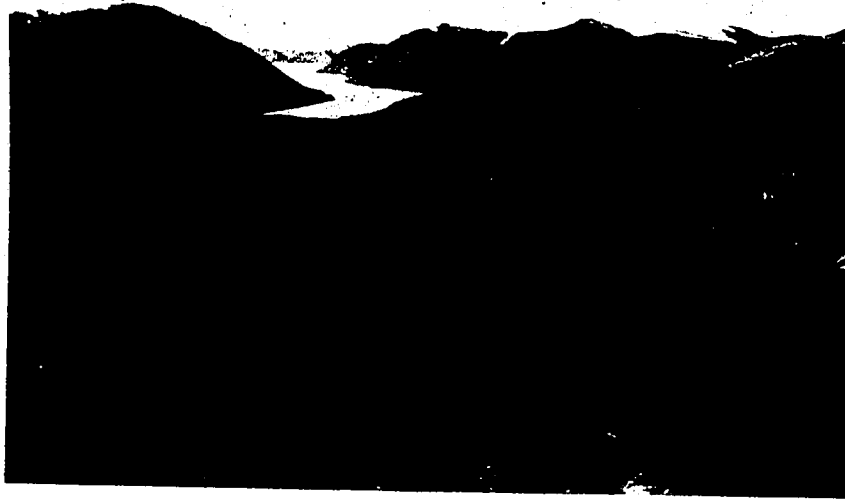


Figure 5.46: View from Garden Plateau north along lower Cache River. Till veneer/blanket occur on the east side of the valley (v).

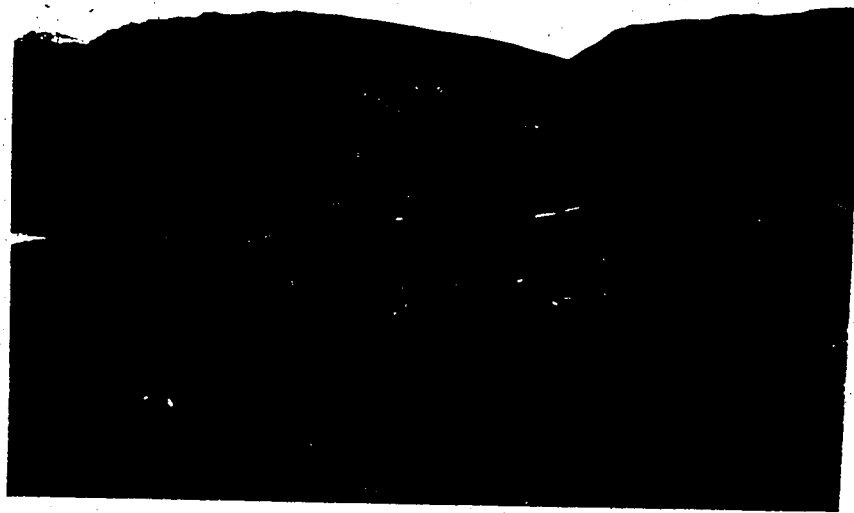


Figure 5.47: View of the east side of the fiord head from the southwest. Visible is the 93m marine limit bench (L) and the offlapping gravel outliers and raised marine sediments of sections H1-H5.

notched by gravel terraces up to 69m asl.

All of the delta remnants around the mouth of the Storm River are referred to as Storm Delta (site 7 on Fig.5.3b). The outer delta remnants are 82.5 and 85m asl. The innermost remnant measures 79m asl (Fig.5.43). Extensive kames and fluvial terraces grade to the raised deltas of the Storm River and record ice retreat to the west (Fig.5.1).

Several stratigraphic sections exist around the fiord head and along the east side of the Cache River. On the east side of the fiord head five stratigraphic logs were compiled (H1-H5, Figs.5.43 and 5.48). Section H-1 reveals 20m of diamicton containing stratified beds and striated clasts overlain by 20m of laminated fines with dropstones (Fig.5.48). These sediments are capped by the massive gravels of the 74m delta. To the south, section H-2 is similar including 25m of diamicton containing stratified beds overlain by laminated fines and offlapping gravels. Clast sample no. 6-7-874 (App.2) is from the diamicton. The sample includes a relatively high proportion of striated clasts (17) and 4 stoss and lee clasts. The diamictons pinch out to the south (inland) and are replaced in section H-3 by 20m of steeply dipping foreset sands and gravels with a palaeocurrent direction from the north. These are overlain by laminated silts with dropstones (Fig.5.48). Sample no. 6-7-871 is from the gravel foreset beds and contains 9 striated and 3 stoss and lee clasts all characterized by a high degree of rounding. In section H-4, 10-15m of the foresets are unconformably overlain by clast-supported diamictons with stratified beds. These diamictons are conformably overlain by silts with dropstones. In section H-5 the foreset beds are absent and 3m of clast-supported diamicton with stratified beds grades into 10m of laminated fines with dropstones. To the south of section H-5, towards the 86m ice contact delta, the section faces are obscured by colluvium from the offlapping gravels. However, gravels and sands appear to predominate.

From a point approximately 2.5km inland from section H-5 there are a

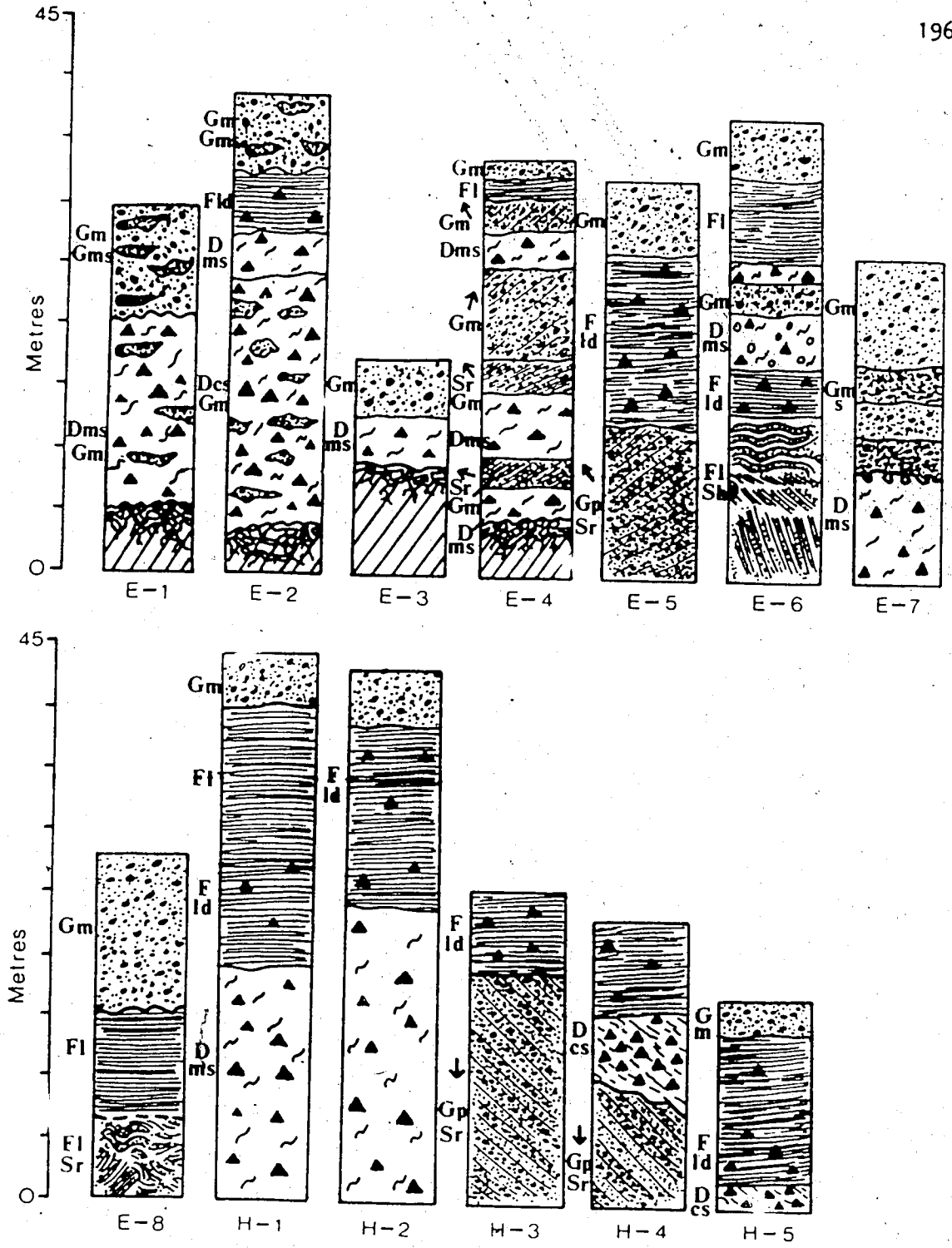


Figure 5.48: Detailed stratigraphic logs along the east bank of the Cache River. See Fig.5.43 for locations.

series of bluffs along the east bank of Cache River (Fig.5.43). Lateral facies changes within these bluffs are represented by sections E-1 to E-8 (Figs. 5.43 and 5.48). In sections E-1 and E-2, 15-20m of diamictons with stratified beds and massive gravel lenses overlie weathered calcareous bedrock. In E-1 the diamicton is unconformably overlain by 10m of massive gravels with lenses of massive, matrix-supported gravel. In section E-2, 4m of diamicton overlain by 5m of laminated fines with dropstones occur above the lower diamicton. The laminated fines are overlain by massive gravels with massive, matrix-supported gravel lenses. In section E-3, 4m of diamicton overlies weathered bedrock. The diamicton is capped by 5m of massive gravels. These gravels offlap all of the sections (E-4 to E-8) from this point southwards. Upslope from section E-3 at 146m asl is a 100m long kame terrace (Fig.5.43). Section E-4 is composed of interbedded diamictons and rippled sand and massive gravel foreset beds with a palaeocurrent direction between east-southeast and south-southwest. Two metres of laminated fines cap the foreset beds and are offlapped by massive gravels. The silts reach 66.5m asl in this part of the valley. Section E-5 is characterized by 12m of planar bedded gravels and rippled, sandy foreset beds with a palaeocurrent direction from the southeast (sample 7-7-872, App.2). These are conformably overlain by 15m of laminated silts with dropstones and then 7m of massive gravels (Fig.5.48). In section E-6, 13m of laminated fines and horizontally bedded sands have been deformed. These are overlain by laminated fines with dropstones and then by 5m of diamicton containing stratified beds and silt intraclasts (sample 7-7-871, App.2). The upper 15m of the section contains massive gravels, diamicton and laminated fines. At the base of section E-7, 10m of diamicton is overlain and loaded by massive, matrix-supported gravels that become interbedded with massive gravels in the upper 15m. Finally the base of section E-8 displays 7m of contorted and faulted laminated fines and rippled sand interbeds (Fig.5.49). These are overlain by 10m of laminated fines with an indefinite contact. The fines are

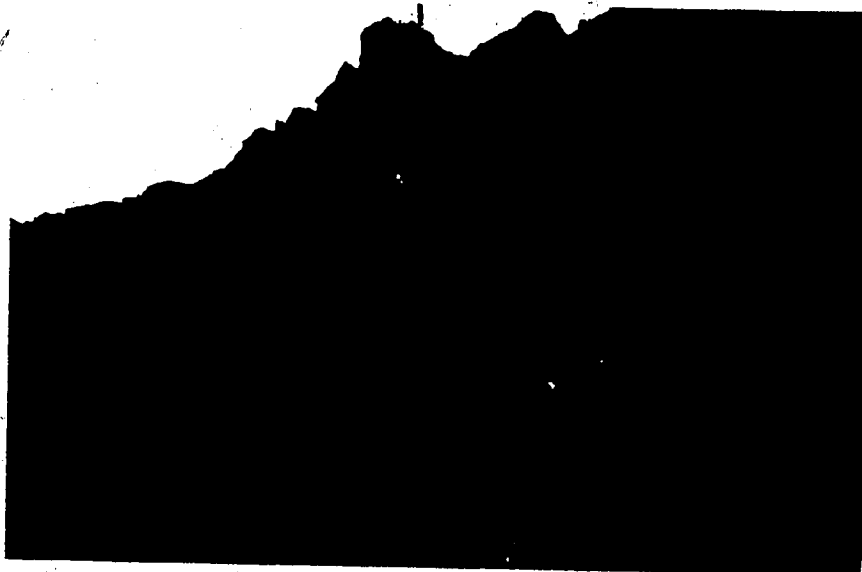


Figure 5.49: Contorted silts and sands at the base of section E-8 on the east bank of the upper Cache River.



Figure 5.50: Steeply dipping gravels and sands within subaqueous fans that are draped by laminated silts with dropstones at Storm Delta. Shell fragments from the silts at 28m asl dated 7530 ± 70 BP (TO 258).

overlain by 12m of massive gravels.

Upslope from section E-8, two large outcrops of silts and sands containing numerous, occasionally striated, clasts occur at ca.80m asl. These silts and sands are conspicuous because they do not display the characteristics of the local deep-red sandstones of the Nansen Formation. Furthermore, the sections in the river terrace below (up to 40m asl) only contain red sands in their upper 3m suggesting a non local source for the preceding silts and sands.

At Storm Delta the foreset gravels of the 79m delta have prograded over glacial marine sediments. Beds of laminated silts up to 25m thick, including abundant dropstones, drape steeply dipping interbeds of gravels and sands (Fig.5.50). The gravel and sand beds form a series of fan-like hummocks with palaeocurrent directions between northeast and northwest. *Mya truncata* fragments from the silts at 28m asl dated 7530±70 BP (TO 258).

In the upland valley to the south of Garden Plateau, cliffs >30m high contain interbedded cobble and boulder beds, stratified and massive matrix-supported gravels, diamictons, and steeply dipping gravel and sand foresets. To the east of the valley these sediments are capped by 3m of silts and fine sands. The sections form the faces of large terraces nested within the valley and the uppermost of these terraces extends from the till veneer on the southern slopes of Garden Plateau.

Evidence of Holocene and recent climatic fluctuations are available at the snout of Endeavour Glacier (see also Chapter 4). Here, 2-3m of alluvium overlies stagnant ice (Fig.4.11). This alluvium is presently being overrun and reworked by the advancing glacier (see Fig.4.20).

5.3.8.3: Interpretation.

Erratics of unknown age on the Garden Plateau (600m asl) attest to the inundation of this area by ice advancing from the Grant Land Mountains to the

south. However, erratics were not found at similar elevations at the fiord head nor along the summit ridge east of the fiord. Limestone erratics on the highlands to the northeast of the fiord head document the former advance of ice from the Castle Range to the south. This maximum distribution of erratics suggests that Cache Head Fiord was never completely inundated by ice from the Grant Land Mountains.

During the last glaciation ice originating from Storm River and the upper reaches of the Blind Valley river occupied the fiord head. Because ice retreated into these drainage basins at a later date than adjoining areas, their marine limits drop in elevation (79 and 74m asl compared to fiord head marine limit of 93m asl). The 93m gravel bench along the east side of the fiord head records the earliest deglaciation of this area rather than the height of the full glacial sea into which the piedmont lobes previously advanced (see Chapter 6). To the south of the 93m gravel bench the two ice contact delta remnants at 86 and 75m, and moraines and kames, record ice retreat from the fiord head. Deltas and benches at 79 and 80m in the lower reaches of Cache River demonstrate that the sea penetrated the Cache River valley at the same time as the inner Storm Delta (also 79m) and before the deglaciation of western Blind Valley. Therefore, the penetration of the sea into the fiord head was initially controlled by this local glacier and not a major trunk glacier in Cache River. The date of 7530 ± 70 BP from shell fragments in silts overlying the subaqueous fans below Storm Delta provide a minimum age for deglaciation of the fiord head and an age for the establishment of the 85m delta to the north (Fig.5.43). Within central Cache Head Fiord local outlet glaciers from the Aviator and Nomynd Ice Caps retreated later as indicated by local deltas at only 60.5 and 61m asl. The sands and silts containing shells below Gorge Delta (site 6 on Fig.5.3b) are interpreted as proximal bottomsets and therefore the date of 7060 ± 70 BP on a single bivalve provides an age for the delta surface (77m asl).

The terminus of ice at the fiord head is recorded by the steeply dipping foreset gravels and sands of sections H-3 and H-4 and the steeply dipping gravel and sand hummocks below Storm Delta. Because these sediments display an inland palaeocurrent, opposite to the present drainage of the Storm and Cache rivers, and because they are draped by silts containing both dropstones and shells, they are interpreted as subaqueous fans from adjacent glaciers. Further evidence of a subaqueous debris flow is the clast-supported, stratified diamicton in section H-4. These fans were probably deposited at the grounding lines of glaciers, fed by meltwater emanating from the basal debris-rich ice (Stewart 1988). Furthermore, the striated, and stoss and lee clasts from the foreset gravels of section H-3 (sample 6-7-871), lend support to a basal ice origin. The thick diamictons containing stratified beds in sections H-1 and H-2 are interpreted as melt out tills deposited behind the retreating grounding line which lay between sections H-2 and H-3 during the last glacial maximum. Because the palaeocurrents within the fans below Storm Delta are from the north, they must have been deposited by ice descending from the highlands of Blind Valley. This ice coalesced with ice from Storm River which prograded the 85m delta during its retreat. Section H-5 reveals the edge of a subaqueous fan fed by ice to the north.

The continued retreat of ice from Cache River valley was responsible for the deposition of diamictons with stratified beds and massive gravel lenses in sections E-1 and E-2. Further south, the heavily disturbed silt and sand beds of sections E-6 and E-8 likely represent glacitectonic deformation. The upper parts of sections E-1 to E-8, containing silts with dropstones, massive gravels, and diamictons with stratified beds and silt intraclasts, likely record sedimentation either within proglacial lakes dammed between the ice front and the valley wall, or into the sea. Clearly, the presence of standing water strongly influenced both the nature of sedimentation and ice retreat. In sections E-4 and E-5 gravel and sand foresets, in places

interbedded with diamictons, record the formation of subaqueous fans at the valley side. In the gravels and sands there are a greater number of striated clasts and a greater degree of rounding (sample 7-7-872, E-4) compared with the diamictons (sample 7-7-871, E-6). This suggests that basal debris-rich ice was the source of the foreset beds whereas ice rafted and/or inwash sediments contributed to the diamictons. Later build-up of alluvial fans was responsible for the overlying gravels of all the E sections. The silt/sand outcrops upslope from section E-8 were deposited into ponded water at the valley side which would require the presence of an ice front which excluded local lithologies (red sandstone) until alluvial fans were established.

The source for the ice which occupied central Cache River valley was the Garden Plateau. The abundance of slates, volcanics and associated rocks along its eastern banks supports this reconstruction. Because of the lack of large valley systems on the western slopes of the Castle Range, little ice reached Cache River valley from the east. Furthermore, striae at the base of the gorge carrying meltwater from the Endeavour Glacier (on the west side of Cache River) document the unobstructed spreading of a piedmont lobe during the last glaciation (see Fig.5.1). These piedmont lobes from the west proglacially thrust and overrode marine sediments. The age and original elevation of these marine deposits is unknown. The 146m kame terrace above section E-3 may represent the margin of an expanded Endeavour Glacier. The occurrence of a large area of till veneer/blanket on the eastern slopes of Cache River valley is the direct result of physiography. Ice advancing from the Garden Plateau area as a piedmont lobe initiated proglacial thrusting of alluvium and glacial marine sediments, thus increasing the entrained debris significantly. The higher degree of rounding and lower proportion of striated clasts in sample 6-7-873 (113m) compared to sample 6-7-872 (79m) suggests that the lower sample was derived from basal debris-rich ice which contained high concentrations of debris, increasing the likelihood of glacial clast collision.

The retreat of piedmont lobes from Cache River valley must have been rapid because marine silts extend to at least 78m asl below the Endeavour Glacier. The Endeavour Glacier must have been floating at this time as suggested by the lack of shorelines until sea level had dropped to 69m asl. The fact that the marine limit does not drop consistently from the central fiord to the centre of Cache River valley precludes the existence of a main trunk glacier during the last glaciation.

The interbedded sediments in the valley south of Garden Plateau likely relate to rapid progradation into a lake dammed by the Endeavour Glacier. The age of this lake is unknown. Endeavour Glacier would have dammed successively lower lake levels as it retreated, explaining the nested terraces.

Evidence at the margin of Endeavour Glacier suggests that two glacioclimatic fluctuations may have taken place since deglaciation. An early postglacial advance and later retreat were responsible for the buried stagnant ice at the glacier margin. Alternatively the stagnant ice dates to the last glaciation. Nonetheless, a recent readvance is documented by the overriding and reentrainment of this material. Endeavour Glacier is a major outlet of the northern Grant Land Mountains icefield and therefore likely has a response time considerably longer than the smaller, local glaciers around Cache Head Fiord.

5.3.9: Sector 8: Transition Fiord and The Promontory.

5.3.9.1: General Description.

Sector 8 includes Transition Fiord and its drainage basins. The Promontory (Fig.5.3b) is a 13km long peninsula separating the waters of Transition and Berg Bay fiords. The topography of The Promontory is precipitous and summits reach altitudes of ≤ 610 m asl. This relief declines to the south where The Promontory is attached to The Musketeers range by a low saddle of raised marine sediments (Fig.5.51). West of Transition Fiord a

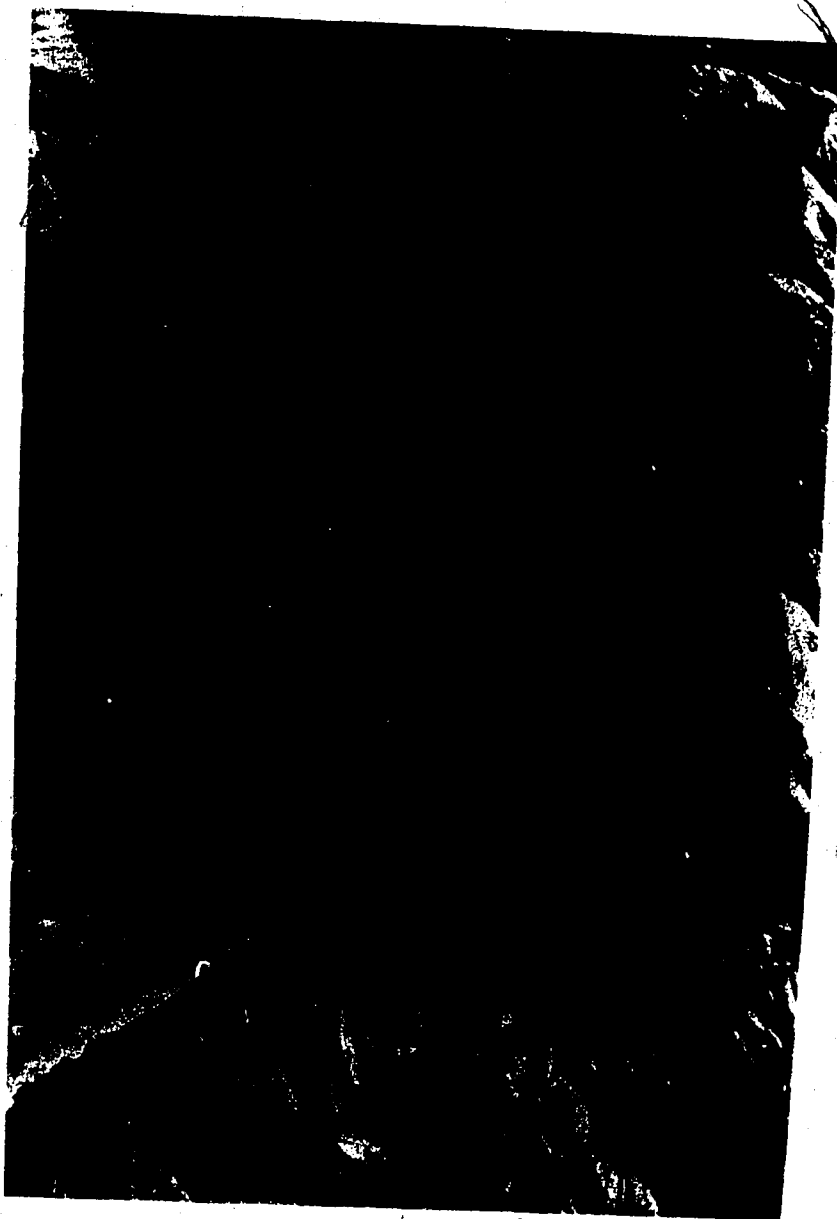


Figure 5.51: Air photograph no. A16978-35 showing the southern half of sector 8; Transition Fiord and The Promontory. Major geomorphic features are marked. G=grounding line; L=lateral moraines; R=rock glacier/lateral moraine complex; s=shells dating 7760 BP; w=7450 BP driftwood; marine limits in metres asl.

plateau hosts the Nomynd Ice Cap. The eastern river occupying Blind Valley carries meltwater from Nomynd Ice Cap and cirque glaciers in the Castle Range. The main river draining into the head of Transition Fiord is only 8km long, originating on the northern slopes of the watershed with Cache River. The only outlet glacier presently occupying the sector is Nomynd Glacier (site 7, Fig.5.4), the major outlet of Nomynd Ice Cap.

5.3.9.2: Geomorphology and stratigraphy.

The surficial geology of Sector 8 is dominated by bedrock and colluvium (Fig.5.1). Pegmatite erratics occur on residuum of Imina sandstone up to 130m asl on the southern part of The Promontory.

Large rock glaciers occur below the bedrock cliffs of Sector 8. In many places these are former lateral moraines and these occasionally contain pockets of marine sediment. On the southwest side of the fiord head coalescent rock glaciers form a bench between 86 and 92m asl (Fig.5.51). Another prominent rock glacier (1km²) occurs below the western cliffs of The Musketeers. Incomplete exposures along its outer edge (above 40m asl) provide a general stratigraphic sequence for the fiord head. At the base, a 1.5m thick discontinuous bed of diamicton, with stratified beds and numerous boulders, is overlain by 10m of interbedded sands and fine gravels. The sands and gravels are capped by \leq 5m of marine silts which are overlain in places by the rock glacier, locally wave washed into short benches 33-50m asl.

Two lateral moraines emanate from Blind Valley and descend to 120m asl above the margins of Blind Delta (site 8, Fig.5.3b; Fig.5.51). Another, sub-horizontal moraine at 110m asl marks the former margin of Nomynd Glacier (Fig.5.1). Between Nomynd Glacier and Blind Delta rock glacierized lateral moraines occur in the wider gullies leading to the Nomynd Ice Cap (Fig.5.51).

Approximately 750m from the southeast corner of the fiord coastline, a 30m high conical mound of sands and gravels is connected to a ridge (40m asl)

trending northwest-southeast along the valley side (G, Fig.5.51). Exposures in the ridge reveal sands and gravels on its eastern margin and diamictons on its western flank. To the north, the ridge and cone grade into 2.5km² of marine silts on The Promontory. The silts contain dropstones and some boulders and extend up to 65m asl on The Promontory. Large *Mya truncata* fragments from the silts at 54m asl dated 7760±70 BP (TO 259). Many *in situ* shells that were shattered by dropstones were observed in section.

Local marine limits range from 67m asl (Longmynd Delta, site 9, Fig.5.3b) to 82.5m asl (a washing limit on the southern end of The Promontory). The surface of Blind Delta occurs at 82m asl and a gravel bench 3km from the fiord head occurs at 77m asl (Fig.5.51). A driftwood log embedded in silts at 55m asl on the southern part of The Promontory dated 7450±80 BP (TO 260).

5.3.9.3: Interpretation.

Pegmatite erratics at 130m asl on The Promontory indicate that glaciers reached at least this elevation at the fiord heads. These erratics were probably ice rafted from Wootton Peninsula where they were reworked by glaciers. Today, both Transition and Berg Bay fiord's contain ice bergs derived from Tidewater Glacier on Wootton Peninsula. These bergs are the likely source of the erratic lithologies.

Diamictons are evident within sections below the rock glacier southeast of the fiord coastline and on the western flank of a local ridge (site G, Fig.5.51). The diamictons are considered to record the presence of glacier ice at the fiord head during the last glaciation. In contrast, the absence of diamicton on the southern part of The Promontory suggests that grounded ice did not extend to this area during the last glaciation. Rather, ice debouched into the fiord head from the small drainage basins of The Musketeers and Castle Range where it likely coalesced with a glacier

occupying Blind Valley fed by Nomynd Ice Cap and ice in the Castle Range. The orientation and height of the moraines at the mouth of Blind Valley suggest that ice advanced into Transition Fiord as a piedmont lobe (Fig.5.51).

Because the marine limit at the time was approximately 111m asl (see Chapter 6) compared with an ice thickness of <120m, the glacier must have floated. Similarly, Nomynd Glacier advanced approximately 1.5km and its lateral moraine at 110m indicates a gentle surface profile typical of an ice shelf (England et al. 1978). The rock glacierized lateral moraines in the gullies on the west side of Transition Fiord mark the margins of outlet lobes from Nomynd Ice Cap.

The rock glacierized screes forming a bench at 86-92m asl are likely remnants of talus cones originally deposited in the sea. The high silt content of these screes below 92m asl attests to a predominant subaqueous depositional environment. In some cases talus cones may have been deposited onto the small glacier ice shelves at the fiord head. For example, the 1km² rock glacier was likely deposited onto a glacier as suggested by its unstable surface and sharp relief, indicating buried ice. In other areas, where deeper water prevailed, the gravels and sands of the cone and the eastern margin of the associated ridge probably record a subaqueous fan along the ice front.

Ice had retreated from Blind Valley by the time sea level had dropped to 82m asl. Floating ice must also have retreated from the southern slopes of The Promontory by this time allowing the formation of a washing limit at 82.5m asl. Shortly afterwards, the sea penetrated the fiord head forming the 77m gravel bench (Fig.5.51). At this time sands and fine gravels were being deposited over diamicton. As ice retreated further south, marine silts offlapped coarser material (diamictons, subaqueous fans). The continued activity of several rock glaciers during the Holocene has buried considerable raised marine sediment. Nonetheless, short benches notched in the rock glacier during emergence are still preserved in some areas.

The low elevation of Longmynd Delta (67m asl; site 9, Fig. 5.3b) records later deglaciation. This elevation is similar to delta surfaces on the east side of Cache Head Fiord (61.7m asl) immediately to the west (Fig. 5.3b). The formation of these deltas was controlled by the late retreat of Nomynd Ice Cap (Fig. 5.3b).

The driftwood date of 7450 BP indicates that driftwood was penetrating the eastern fiord heads of Phillips Inlet during deglaciation when sea ice conditions were more open. Because this log has probably moved downslope since deposition (see Chapter 6), it is of limited importance to the history of emergence. However, it likely dates to the earliest open water conditions at the fiord heads (<82.5m) and hence records the onset of ameliorated summers. This dictates that the shells dated 7760 BP likely relate to a sea level $\geq 82.5\text{m}$, a proposition which is supported by the equidistant diagram in Chapter 6.

5.3.10: Sector 9: Phillips River and Berg Bay Fiord.

5.3.10.1: General Description.

Sector 9 includes the head of Berg Bay Fiord, the confluence of Phillips and Napes rivers, and the surrounding highlands (Fig. 5.3b). Both Phillips River (27km long) and Napes River (10km long) drain the icefield of the Grant Land Mountains to the east and south respectively. The resulting high runoff is responsible for the seasonal break up of the pack ice in Berg Bay Fiord and the penetration of icebergs from Tidewater Glacier to the north. The mouth of Phillips River contains the largest sandur of the field area (7km^2 ; Fig. 5.52).

The plateau immediately south of The Musketeers hosts a small ice cap ($\text{ca.}4\text{km}^2$) whereas the plateau to the north of Phillips River contains the larger, Relief Ice Cap ($\text{ca.}8\text{km}^2$). A 7km long piedmont glacier at the head of Napes River outlets from the icefields of the Grant Land Mountains.

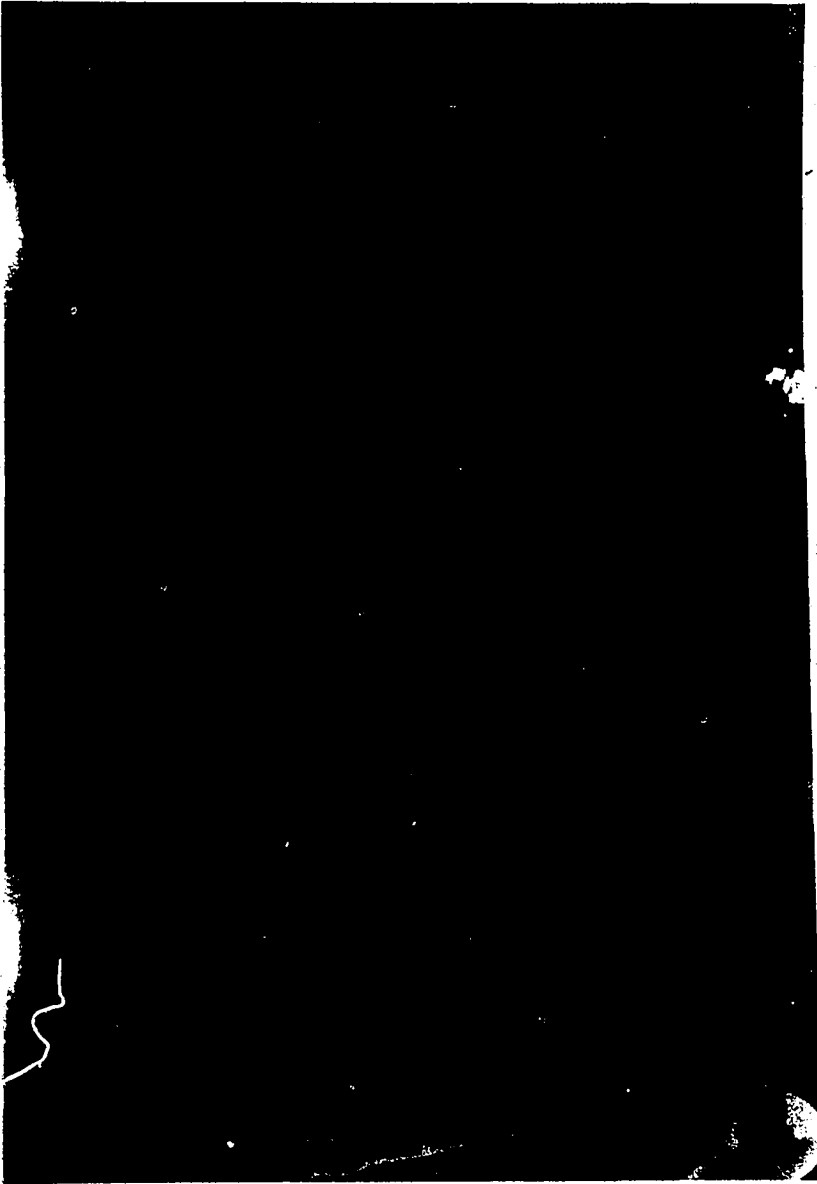


Figure 5.52: Air photograph no. A16606-15 showing Berg Bay Fiord, Phillips River, Napes River and surrounding highlands. Major geomorphic features are marked. L=rock glacierized lateral moraines; d=8.5m ice contact delta; s=shells dating 7190 BP; marine limits in metres asl. N-1 to N-4 are section logs in Figure 5.53.

5.3.10.2: Geomorphology and stratigraphy.

Incipient felsenmeer with sparse erratics occurs at $\geq 150\text{m}$ asl on the northeast shoulders of The Musketeers (Fig. 5.1). Subdued meltwater channels cut into this felsenmeer mark a former trunk glacier occupying the river confluence. Higher elevation meltwater channels and moraines document the retreat of local ice in the V-shaped valleys of Sector 9. Discontinuous till veneer/blanket occurs along the slopes of Phillips and Napes rivers up to 120m asl (Fig. 5.1).

On the western slopes of Napes River valley, till veneer/blanket extends from moraines occupying the eastern valleys of The Musketeers. A 1km^2 rock glacierized lateral moraine occurs on the eastern side of Napes River mouth. The moraine overlies pockets of silts with dropstones, clast-supported diamictons and interbedded fine gravels and sands. Immediately north of the moraine, a section contains 5m of diamicton with stratified beds and an east-southeast to west-northwest fabric. This diamicton is overlapped by silts and sands with dropstones and shells in life position. Above the section, a till blanket rises to 113m asl.

Along the south side of Phillips River and west of Napes River, rock glacierized lateral moraines range from 115m (east) to 106m asl (west) (Figs. 5.1 and 5.52). The lower moraines extend from till veneer that mantles the two northern outlet valleys of The Musketeers. Below the 115m moraine, sections are dominated by clast-supported diamictons with occasional stratification. Closer to Berg Bay Fiord, 200m west, a section includes 5m of rippled sands grading up into 50cm of stratified diamictons with dropstones and rip up clasts. Conformably overlying the diamicton are 5m of silts with sparse dropstones. A section (53m asl) below the 106m moraine (westernmost L on Fig. 5.52) contains 5m of diamicton with angular clasts and shell fragments. From here marine silts continue onto the southern part of The

Promontory.

The south side of Phillips River, east of Napes River, is dominated by colluvium, alluvium and reworked raised marine sediments. Rock glacierized scree are common at higher elevations but a large rock glacier encroaches upon the river floodplain (easternmost L on Fig.5.52). This rock glacier is immediately opposite a major outlet valley of the plateau to the north of Phillips River.

On the north side of Phillips River an ice contact delta at 85m asl (site d, Fig.5.52) extends from till blanket/veneer occupying a valley of the plateau to the north. East of this delta, several silt and fine gravel outliers rise to 57m asl and indicate that the sea extended to at least this altitude (Fig.5.1). A clast-supported diamicton underlies these sediments and ca.5km east of the Phillips/Napes River confluence, several small diamicton outcrops reach 88m asl. These diamictons contain a high proportion of striated clasts and they extend to till veneer upslope.

Several deltas and terraces occur between 67 and 90m asl throughout Sector 9 (Fig.5.53). A 90m terrace occurs below the 115m moraine on the northeast slopes of The Musketeers. A *Mya truncata* valve collected from a silt outlier (34m asl) beneath an 80m asl bench cut into till veneer dated 7190 ± 90 BP (TO 256).

Logs were compiled for extensive sections along the north bank of Phillips River (Figs.5.52 and 5.53). Only section N-1 contains a massive, matrix-supported diamicton. This diamicton contains striated clasts and has a northwest-southeast fabric. In section N-2 the diamicton gives way to 8m of steeply dipping foreset beds of massive gravels and rippled sands. This unit becomes thinner in N-3 and includes dropstones and rip-up clasts. A number of scour fills are also apparent. At the base of section N-4 there are 1m thick interbeds of massive, matrix-supported gravels, laminated fines with dropstones and clast-supported diamictons. All of the sections are overlain by

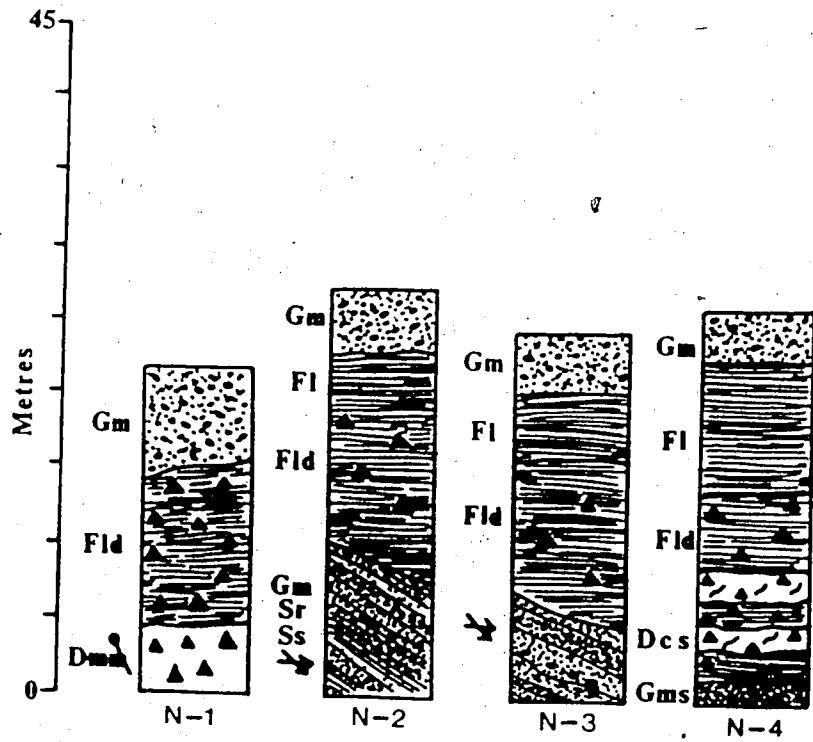


Figure 5.53: Section logs from the north side of Phillips River sandur. Locations N-1 to N-4 are denoted on Figure 5.52.

10-12m of marine silts with dropstones which contain abundant shell fragments.

5.3.10.3: Interpretation.

During the last glaciation, Napes River valley was filled by a glacier up to 115m asl (moraine altitude on northeast slopes of The Musketeers). The higher erratics and subdued meltwater channels (≥ 150 m asl) are probably older. During full glacial conditions, the floating glaciers at the Phillips/Napes river confluence coalesced in the higher sea level of Berg Bay Fiord.

The Napes River glacier deposited the 5m of diamicton with a WNW-ESE fabric at the confluence of Napes and Phillips rivers. This is likely a melt-out till or morainal bank deposited at the grounding line as the glacier impinged upon the bedrock spur. The morainal bank was subsequently offlapped by marine silts during ice retreat. Above this site, a till blanket was deposited up to 113m asl. The 1km^2 rock glacierized lateral moraine was deposited on the surface of this glacier and probably remains ice-cored.

Along the south side of the Phillips River and west of Napes River, glaciers advanced from two valleys draining The Musketeers. Rock glacierized lateral moraines on either side of these valleys have similar altitudes (~ 106 m asl). Well stratified diamictons and associated marine sediments were likely deposited below small glacier ice shelves as they debouched into the higher sea level of the fiord head. If this ice was floating at the fiord head and the lateral moraines are taken as its former surface, then the full glacial sea level would have been 93m asl (0.88×106 m ice thickness). This estimate is probably 19-24m too low, as discussed in Chapter 6, and therefore the lateral moraines may have been lowered by rock glacierization.

Ice advanced into Phillips River valley from the north. The rock glacier on the south side of Phillips River and the 85m ice contact delta represent the margin of a piedmont lobe from Relief Ice Cap. The marine limit

(79m asl) for the delta nearest the fiord head (Fig.5.52) records later deglaciation by another piedmont lobe of Relief Ice Cap (see equidistant diagram, Chapter 6). Sections N-1 to N-4 represent the facies changes associated with this ice margin. The glacier was probably grounded between sites N-1 and N-2 (Fig.5.52) and from this point eastwards a subaqueous fan prograded from the ice front. Slumps, debris flows and large-scale cut and fill, indicative of a retreating glacier (Stewart 1988), account for the interbedded stratified diamictos, sands and gravels with rip-up clasts, and silts with dropstones.

Because lower marine limits inside the last ice margin record later deglaciation (see Appendix 3), the wide range in marine limit throughout Sector 9 reflects different rates of glacier retreat into the surrounding highlands. Consequently, marine limits 80-90m asl indicate that the sea penetrated the Phillips and Napes River valleys very early. In contrast, marine limits 67-80m asl indicate that the smaller catchments around the fiord head were deglaciated much later. This is a function of water depths and the stability of the ice margins. Ice in the main valleys would be susceptible to massive calving at the onset of deglaciation. The date of 7190 ± 90 BP provides a minimum age for ice retreat into the mouths of the northern valleys of The Musketeers and an age for a sea level >80 m which is the local marine limit (see equidistant diagram, Chapter 6).

5.3.11: Sector 10: Wind Gap, Valley of the Blocks and Mymmshall Delta.

5.3.11.1: General Description.

Wind Gap occurs at the eastward end of the Phillips Inlet structural trough which extends into Yelverton Inlet to the east (Fig.5.54). The Valley of the Blocks, which has a valley-in-valley form and follows another structural boundary, parallels Wind Gap for 5km immediately to the north (Figs.5.3a and b). The upper profile of Valley of the Blocks has a broad U-



Figure 5.54: Air photograph no. A16978-38 of Wind Gap, Valley of the Blocks and Dogleg Glacier (D). Tidewater Glacier is visible on the far left. Major geomorphic features are marked. m=meltwater channels; d=85m ice contact delta; L=lateral moraine; s=shells dating 8050 BP (north) and 8480 BP (south); marine limits in metres asl.

shape which is inset by the lower profile, characterized by a deeply incised gorge (Fig.5.55). Wind Gap and Valley of the Blocks are separated by a 270m ridge over which Dogleg Glacier spills into Wind Gap (site 6, Fig.5.4).

The glaciers of Sector 10 are piedmont and transection glaciers originating in the cirques of Wootton Peninsula whereas plateau ice caps occur to the south and southeast. Mymmshall Delta (site 10, Fig.5.3a) refers to the raised delta at the mouth of Valley of the Blocks. This delta has been constructed over a broad bedrock step which marks the junction of Valley of the Blocks and Phillips Inlet.

5.3.11.2: Geomorphology and stratigraphy.

South of Sector 10, a sandstone felsenmeer with tors <5m high, occurs on the summits. Sparse greenschist and conglomerate erratics were observed at 660m asl north of Relief Ice Cap. Furthermore, the 270m bedrock ridge separating the two main valleys is covered by crystalline erratics up to 250m asl, above which there are two small areas of residuum (Fig.5.1). A former ice margin is delineated at the western end of the 270m ridge where meltwater channels and a lateral moraine descend to a prominent washing limit at 91m asl (Figs.5.54 and 5.56). Nested meltwater channels and kames document the retreat of Dogleg Glacier eastwards from its last ice limit (Fig.5.1) which occupied both lower Wind Gap and Valley of the Blocks. Other kames attest to the downwasting of Hidden Glacier while it coalesced with Dogleg Glacier near Phillips Inlet.

Two lower sea levels are recorded either side of the 91m washing limit. One is marked by an ice contact delta at 85m asl (Mymmshall Delta) and the other by a gravel bench cut into till at 82m asl at the mouth of Wind Gap (Fig.5.54). South of Wind Gap a delta emanates from the northern drainage basin of Relief Ice Cap at 74m asl. A 78m asl gravel terrace occurs 2km inland from the present shoreline (Fig.5.54). Within 1.5km of the western

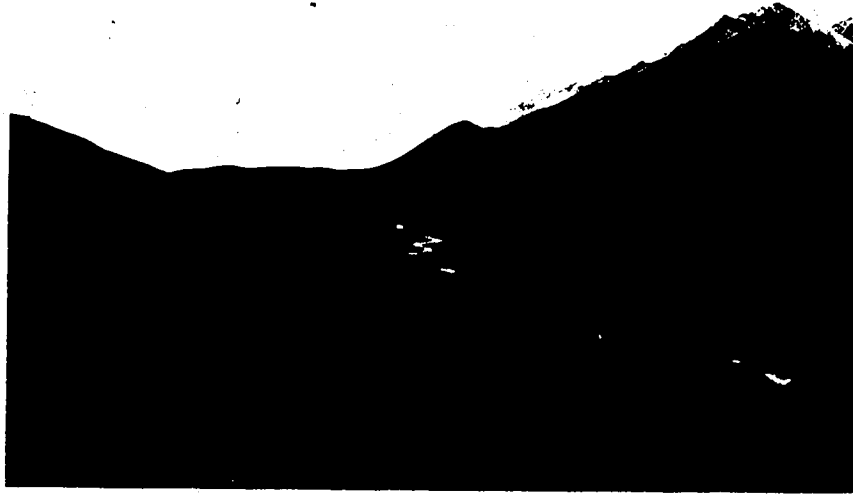


Figure 5.55: Valley of the Blocks from the east illustrating the valley-in-valley form, the steep drop into the inlet head and the transition from dissected plateau in the south to the fretted cirque landscape in the north.



Figure 5.56: Telephoto across Tidewater Glacier of the western end of the bedrock ridge separating Valley of the Blocks and Wind Gap. The 91m washing limit (arrowed), 85m ice contact delta (Mount Logan tent circled), proglacial meltwater channels (c) and lateral moraine (m) are marked.

margin of Tidewater Glacier (site 4, Fig.5.4) a delta occurs at 80.5m asl. A lateral moraine (57m asl) occurs immediately east of the delta.

At the outer lip of the 85m Mymmshall Delta, topset gravels overlie horizontally bedded sands which, in turn, overlie silts with occasional dropstones. This 10m thick fining-upward sequence is interrupted at one site by a 2m thick and 5m long wedge of diamicton with stratified beds and rip-up clasts. This wedge disturbs the horizontally bedded sands and the silts. A *Mya-truncata* valve collected from the sands (54m asl) dated 8050 ± 60 BP (TO 254). At the mouth of Wind Gap, below the 82m bench, a large bluff of silts and fine sands yielded a *Hiatella arctica* valve at 58m asl which dated 8480 ± 100 BP (TO 252). These sediments directly overlie glacially polished slate.

5.3.11.3: Interpretation.

During the last glaciation, Dogleg Glacier advanced into Valley of the Blocks and Wind Gap, overtopping much of the 270m bedrock ridge. Hidden Glacier advanced out of its confined valley, coalescing with Dogleg Glacier at the Inlet head. Dogleg Glacier probably calved at the mouth of Wind Gap, but there is no evidence for an ice shelf moraine.

Because it had an unstable calving snout, Dogleg Glacier must have retreated rapidly after the onset of deglaciation, explaining the date of 8480 ± 100 BP between the lower valleys. At this time silts and fine sands were deposited and overlapped the diamicton and glacially polished bedrock left by the retreating glacier. The 91m washing limit records the initial deglaciation of Wind Gap. Because of the wide bedrock step at the mouth of Valley of the Blocks and the direct access of Dogleg Glacier, stagnant ice persisted in this area excluding marine fauna until 8050 ± 60 BP. At this time Mymmshall Delta was deposited at 85m asl and its wedge of diamicton, interpreted as a debris flow, indicates the proximity of such stagnant ice.

Because the 8050 BP shells relate to the 85m delta, the 8480 BP shells must be associated with a sea level between 85 and 91m asl. The implications of these dates are discussed in Chapter 6.

Plateau outlet glaciers to the south had retreated from Wind Gap by the time sea level had dropped to 74m asl whereas Dogleg Glacier had retreated to within 1km of its present margin when sea level was at 78m (Fig.5.54). Because Tidewater Glacier is presently calving into the Inlet its grounding line may never have advanced appreciably further than present. Indeed its delta at 80m asl is only 11m below the highest deglacial shoreline in this area and it is within 1.5km of its present margin. The only evidence of subsequent advances by the glacier come from the 57m moraine which is on the proximal side of the delta and lateral moraines <20m higher than the contemporary margin.

Within Valley of the Blocks the river has attained at least 20m of incision through the slate bedrock which underlies 20m of alluvium. This accounts for the valley-in-valley form of Valley of the Blocks. The river is presently undercutting this bedrock and several collapses in the river cliffs were identified between the 1985 and 1987 field seasons. This evidence suggests that the river may be cutting to an unprecedented base level (England pers. comm. 1987).

5.3.12: Summary

This section highlights the principal geomorphic data and radiocarbon dates from the field area and is intended as a quick cross reference for Chapter 6.

5.3.12.1: Sector 1 Western Wootton Peninsula

Erratics (predominantly outwash) document ice advance from south Wootton Peninsula over the Alert Point Ice Cap. Tills representing two ice advances are separated by peat dating $39,270 \pm 640$ BP.

During the last glaciation, ice floated beyond the present coastline depositing sediment at well defined grounding lines. Redeposited shells dating $20,240 \pm 160$ BP record the presence of marine fauna <5km from present ice margins.

Marine limits range from 32-65m asl. Radiocarbon dates record initial deglaciation between $9,070 \pm 80$ BP and 7790 ± 70 BP. A narwhal tusk dating 6830 ± 50 BP indicates open water during the early Holocene where an ice shelf persists today. A driftwood date of 4310 ± 70 BP provides a maximum age on the formation or regrowth of the Cape Alfred Ernest Ice Shelf.

5.3.12.2: Sector 2 The Cape Woods coast

Moraines, till veneer and sandar document the advance of ice from the south Wootton Peninsula cirques into the Arctic Ocean. Glaciers floated and deposited debris as morainal banks before retreating. Marine limits range from 41-65m asl. Radiocarbon dates record initial deglaciation at 8.5ka BP and this provides an age for the 65m marine limit.

5.3.12.3: Sector 3 Cape Armstrong and the Armstrong River

Erratics occur up to 600m asl and record a glaciation(s) of unknown age flowing from south to north. During the last glaciation, ice occupied Armstrong River valley and deposited moraines at 400m asl. Glaciers floated in Albion Lakes and impinged upon a bedrock high to the north where morainal banks were deposited ($14,880 \pm 110$ BP). Marine limits range from 61-80m asl. A ^{14}C of $10,140 \pm 90$ BP records early ice retreat.

5.3.12.4: Sector 4 Bushmill Pass/Ice Alley Fiord

Erratics up to 600m asl, and till veneer with shell fragments up to 450m asl, record a glaciation(s) of unknown age. Moraines, till blanket and meltwater channels mark the last ice limit of Terrible Glacier at the east end of Bushmill Pass. This ice dammed a lake in the Pass during early deglaciation.

Marine limits range from 74-80m asl. A 74m asl delta emerging from the

snout of Terrible Glacier attests to retreat of the glacier behind its present position in the early Holocene. There are no Holocene dates presently available from the sector.

5.3.12.5: Sector 5 Drift Pass/Muskox River/Desperation Bay

Erratics were not recognised above 300m asl suggesting that large areas have escaped inundation by ice. During the last glaciation, ice advanced into Drift Pass (palaeo ELA=300m asl) and Desperation Bay deforming marine sediments dating $32,110 \pm 370$ BP. A morainal bank associated with an ice contact delta (89m asl) and the end moraine at the northeast end of Drift Pass mark the former grounding line.

Marine limits range from 73.5–89m asl. Radiocarbon dates record deglaciation between $8,310 \pm 70$ and $8,710 \pm 70$ BP in north Cache Head Fiord and before $7,820 \pm 70$ BP in central Muskox River valley. An ice dammed lake in upper Muskox River valley drained when Deception Glacier retreated from Drift Pass.

5.3.12.6: Sector 6 Bridge Street and Ice Alley Fiord

Erratics extend up to 205m asl suggesting that large areas have escaped glaciation. During the last glaciation, glacier ice floated in the fiord head depositing a morainal bank at its grounding line. An ice dammed lake occupied upper Bridge Street valley but its age is unknown.

Marine limits range from 54.5–86m asl. A ^{14}C date of $8,330 \pm 80$ BP records deglaciation of the fiord head when Pudding Glacier was <500m beyond its present margin. A ^{14}C date of $5,200 \pm 60$ BP on shells in thrust silts records a mid-Holocene readvance of Pudding Glacier.

5.3.12.7: Sector 7 Cache Head Fiord, Cache River and Garden Plateau

Erratics descend from ca. 600 to <450m asl towards the fiord head suggesting that Cache Head Fiord was never inundated by ice from the Grant Land Mountains. During the last glaciation, moraines, kames and glaciomarine sediments indicate that ice occupied the fiord head as coalescent piedmont lobes. These glaciers deformed marine and alluvial sediments. During

deglaciation, the melting of debris-charged ice led to the deposition of subaqueous fans.

Marine limits range from 60.5-93m asl suggesting early deglaciation of the fiord head but significant restrained rebound within smaller drainage basins. Radiocarbon dates of $7,530 \pm 70$ and 7060 ± 70 BP provide ages on the deglaciation of the fiord head and a small drainage basin in central Cache Head Fiord respectively.

5.3.12.8: Sector 8 Transition Fiord and The Promontory

Diamictons, a morainal bank, and subaqueous fan demarcate the last ice limit at the head of Transition Fiord. Moraine altitudes and glaci-marine sediments suggest that piedmont glaciers floated in the fiord.

Marine limits range from 67-82.5m asl. The higher marine limits at the fiord head record earlier deglaciation there than in a smaller drainage basin at the fiord mouth 13km to the north. A ^{14}C date of $7,450 \pm 80$ BP on driftwood indicates open water at the eastern fiord heads by this time. Shells of $7,760 \pm 70$ BP relate to a sea level ≥ 82.5 m asl.

5.3.12.9: Sector 9 Phillips River and Berg Bay Fiord

Meltwater channels and erratics (>150m asl) record a glaciation of unknown age. During the last glaciation, ice filled Napes River valley to ca. 115m asl and deposited a morainal bank at the river mouth. Moraine elevations of only 106m asl together with glaci-marine sediments indicate that these piedmont glaciers floated at the fiord head and deposited subaqueous fans upon deglaciation.

Marine limits range from 67-90m asl reflecting early deglaciation of the fiord head and restrained rebound within smaller drainage basins. A ^{14}C date of 7190 ± 90 BP provides a minimum age on deglaciation of the fiord head and relates to a sea level >80m asl.

5.3.12.10: Sector 10 Wind Gap, Valley of the Blocks and Mymmshall Delta

Erratics occur at 660m asl recording a former, undated glaciation

from the Grant Land Mountains. Moraines, kames, and meltwater channels indicate that Dogleg and Hidden glaciers floated at the head of Phillips Inlet during the last glacial maximum.

Marine limits range from 74-91m asl. Early deglaciation is recorded by a ^{14}C date of $8,480 \pm 100$ BP which relates to a former sea level at 85 to 91m asl. A date of $8,050 \pm 60$ BP provides an age for the ice contact Mymmshall Delta at 85m asl.

CHAPTER SIX

Discussion

*Wheels within wheels
In a spiral array
A pattern so grand
And complex
Time after time
We lose sight of the way
Our causes can't see
Their effects.*
N. Peart, *Rush*: extract
from *Natural Science* from
the album *Permanent
Waves*, 1980 (Core Music).

6.1: Introduction.

This chapter outlines the palaeogeography of Phillips Inlet and discusses it in relation to past research and the existing regional framework. The discussion will be sub-divided into four sections according to chronology: events predating the last glaciation; the last glaciation; sea level history; and Holocene (postglacial) history. Much of this pertains to objective one; determining the extent and styles of past glaciations. The second objective of the thesis was to extend the glacioisostatic data base on Ellesmere Island and therefore the sea level history of Phillips Inlet and Wootton Peninsula will be developed accordingly. Clearly the sea level record cannot be entirely separated from glacial history and therefore both are discussed when necessary.

6.2: Events predating the last glaciation.

High elevation erratics are the most common evidence for extensive glaciation in the field area. Maximum altitudes range from 600-660m asl whereas several summits up to 900m asl (ie. Western Pikes, Fig.5.3a) are erratic-free and therefore probably escaped glaciation entirely. Altitudes of erratics do not decline regularly from north to south and this is a basis for questioning the existence of a trunk glacier in the Inlet (Smith 1959, 1961; Hattersley-Smith 1961). The rounded nature of some erratics could be

indicative of fluvial deposition on a topography very different from the present (cf. England 1987b). However, clast analyses (cf. Chapter Four) indicate that glacially derived clasts are characteristically rounded due to the direct entrainment and passive transportation of proglacial sediment. The explanation of erratics on the Idris Peaks (600m asl; Fig.5.3a) requires only an increased ice thickness of 200m above the moraines of the last glaciation (400m asl). Furthermore, most of the Idris Peaks drainage basin is already above 400m asl. At the fiord heads erratics at 600m asl are still considerably lower than those reported from Clements Markham Inlet (>700m asl) Archer and Tanquary Fiords (1000m asl; cf. Hattersley-Smith 1969; Bednarski 1984, 1986).

Geomorphic and stratigraphic evidence for older glaciations is sparse, especially in topographic Zone 2 (Fig.1.3) where glaciers advanced into through-valleys as piedmont lobes. The lower massive, matrix-supported diamicton in the section to the south of Alert Point records a glaciation which was terminated prior to $39,270 \pm 640$ BP, the radiocarbon date on intertill organics (site 26, Fig.6.1).

The inclusion of striated clasts and shell fragments within till veneer at 409m asl on the southern Idris Peaks (Fig.5.20) is important to interpretations of the style of past glaciations in the area. Upslope are the restricted bedrock catchments of high elevation glacierettes. Even if these glacierettes were to expand considerably, there would be no source of deformable sediment for the creation of debris-rich basal ice; especially if the palaeoglaciation level was <400m asl, putting these slopes within the accumulation zone of these glaciers. Therefore, the striated clasts must be derived from Terrible Glacier that outlets from the Dodger Ice Cap to the south (Fig.5.20). Furthermore, the shell fragments also appear to have been transported to this site as erratics. However, arguments against a south to north flow from the Dodger Ice Cap on the present topography were already

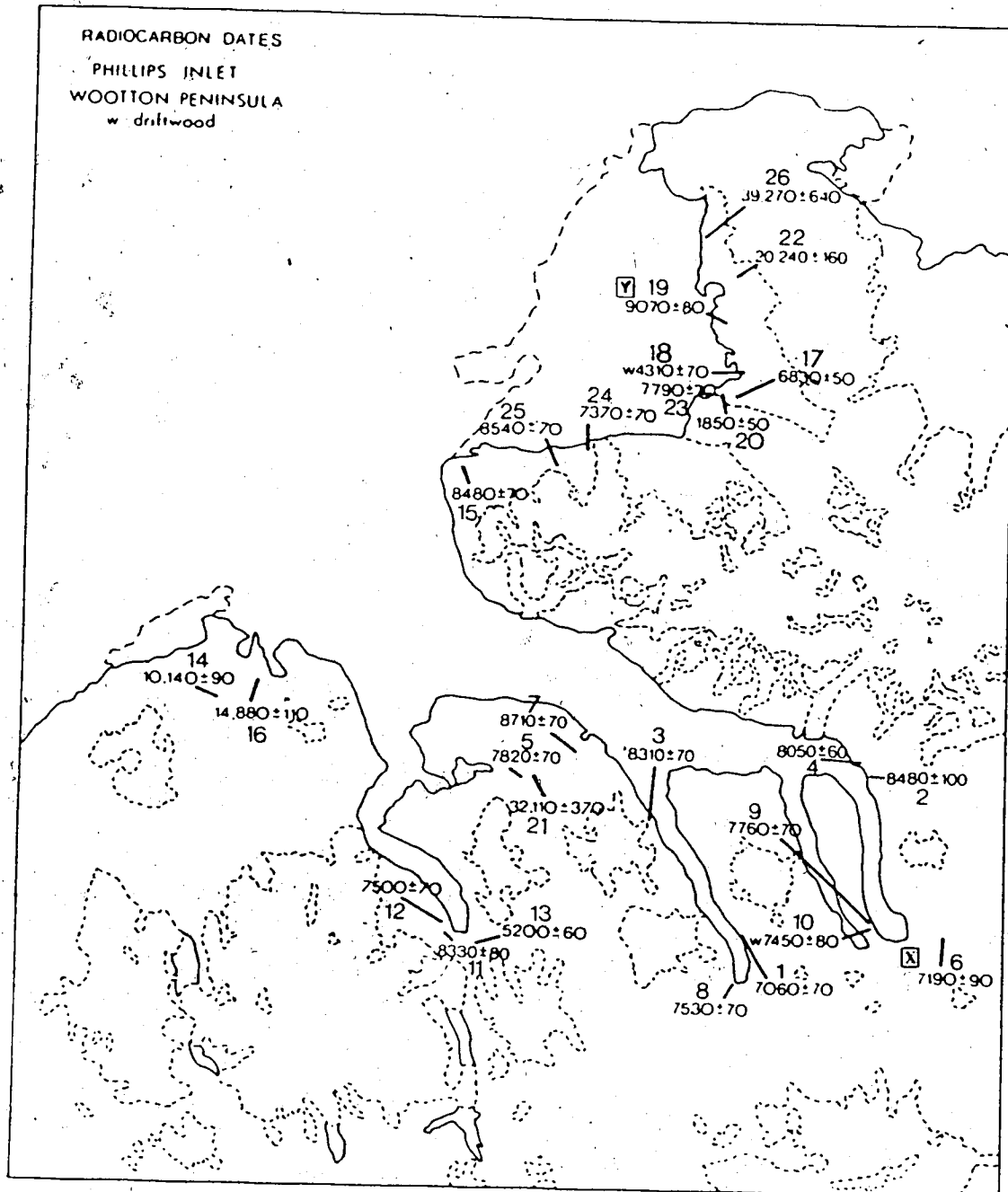


Figure 6.1: Map of radiocarbon dates of Phillip Inlet and the Wootton Peninsula.

outlined (section 5.3.5.3). Such flow would be unlikely because ice advancing from the Idris Peaks flowed into Bushmill Pass whereas Ice Alley Fiord would draw down Terrible Glacier away from the inland shell site. Another shell sample in till at 144m asl at the margin of Terrible Glacier presents a similar glaciological problem. These shells could not have been carried upslope by the glacier (in its present configuration) and therefore they may relate to a former period of higher sea level when the glacier was much reduced in size. Because these high elevation shells have not been dated, the only likely conclusion that can be made is that they predate the last glaciation. Nevertheless, because the 409m shells lie outside the last ice margins, there is a possibility that they date to a period prior to the penultimate glaciation. Shells associated with erratics at 610m asl on the Fosheim Peninsula, west-central Ellesmere Island, dated $19,500 \pm 1,100$ BP and they were originally interpreted to be ice transported (Sim 1961). On the other hand, England (pers. comm. 1987) speculates that the shells could relate to a period when relative sea level was much higher (ie. prior to considerable tectonic uplift of the site) and/or that the shells and erratics are of great age and were transported glacially on a largely prefaulted landmass. Whether or not the high elevation shells inland of Terrible Glacier were deposited on such a different landscape is unknown but they appear incompatible with the present ice configuration of the field area.

Evidence for higher sea levels, predating the last glaciation, is fragmentary. The bedrock cliffs on west Wootton Peninsula represent an intriguing geomorphic problem. These cliffs contain cove-like indentations with floors ≤ 30 m asl. At Cape Woods the marine erosion possibly responsible for the cliffs could have exploited the poorly lithified sandstone and siltstone bedrock, forming a wave-cut platform (30m asl). Clearly these features date to a period of stable sea level when sea ice cover was much reduced. Because the Holocene was a period of continued emergence, the cliffs

and platform likely predate that time even though they fall below local marine limit (65m asl).

Evidence of higher pre-Holocene sea levels is available south of Alert Point where gravels, sands and fines underlying an upper diamicton were deposited over stagnant ice of an earlier glaciation (>39ka; Fig.6.1). Piedmont lobes advancing into Cache River valley from the Garden Plateau during the last glaciation disturbed silts at the bases of sections E-6 and E-8 (Figs.5.43 and 5.48). These sediments could relate to an undated, pre-last glacial, high sea level stand that penetrated the upper valley. Alternatively, they could relate to a marine transgression immediately predating the arrival of ice in Cache River valley. A former high sea level (>90m asl) is recorded in the section at the southwest end of Drift Pass where shells dated $32,110 \pm 330$ BP. Again, these shells could relate to a marine transgression predating ice at the site. The 117.5m asl shoreline on the north side of Desperation Bay (Figs.5.25 and 5.35), because it is 24.5m higher than the maximum full glacial shoreline (93m asl; Fig.6.4), predates the last glaciation.

In conclusion it can be stated that former glaciations have been more extensive in the field area and that the evidence for associated higher sea levels is fragmentary. Indeed much of the stratigraphic evidence can be interpreted using England's (1983) hypothetical pre-last glacial sea level curve (Fig.1.5); either relative sea level fell to or transgressed to the full glacial sea.

6.3: The last glaciation.

Throughout this section reference is made to Figures 6.1-6.4 and Table 6.1. During the last glaciation many nunataks, indicated by high elevation felsenmeer, existed in the field area (Fig.6.3a). These were a result of the draw-down imparted upon advancing glaciers by the marine reentrants. The

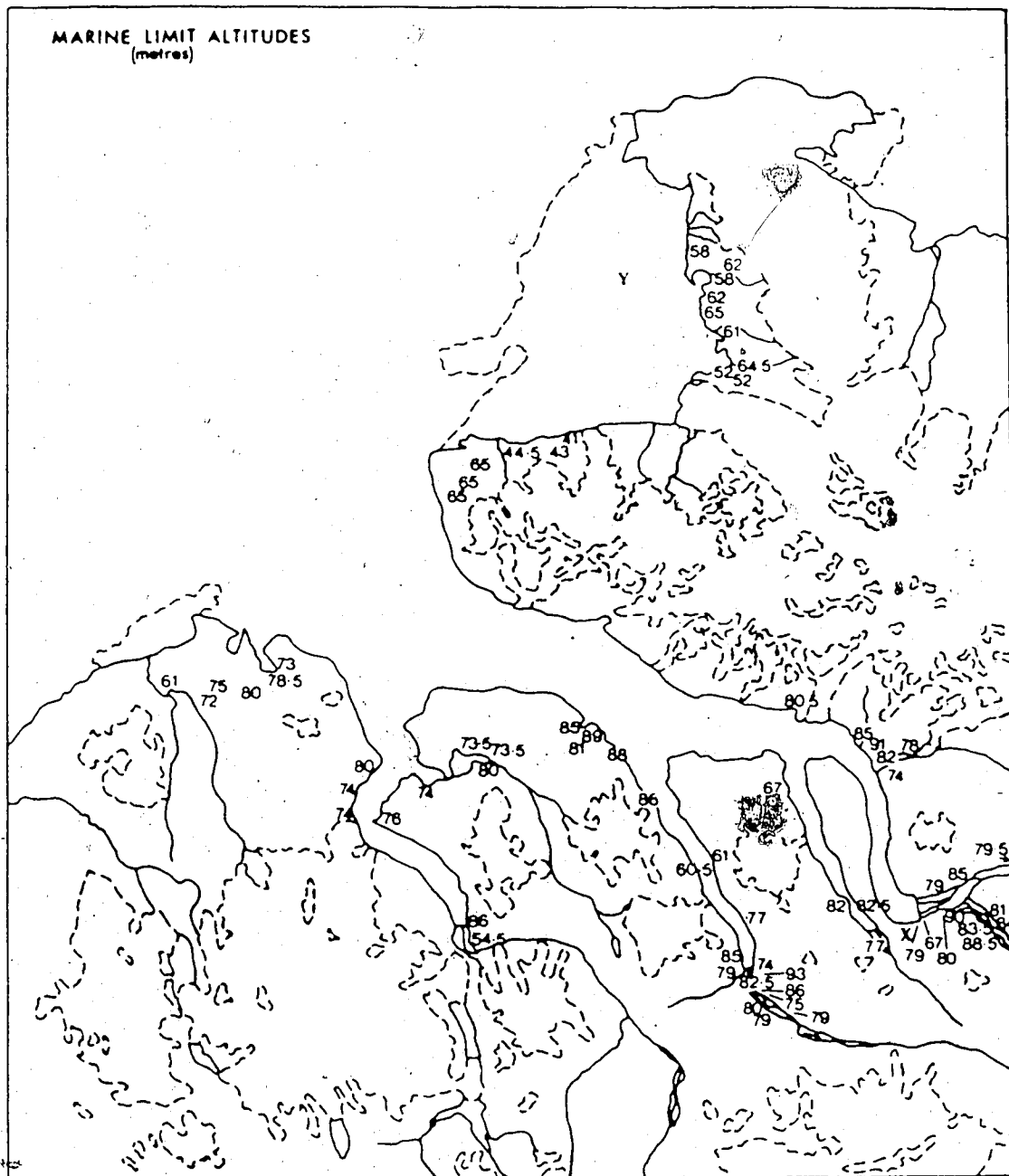


Figure 6.2: Map of marine limit altitudes of Phillips Inlet and the Wootton Peninsula.

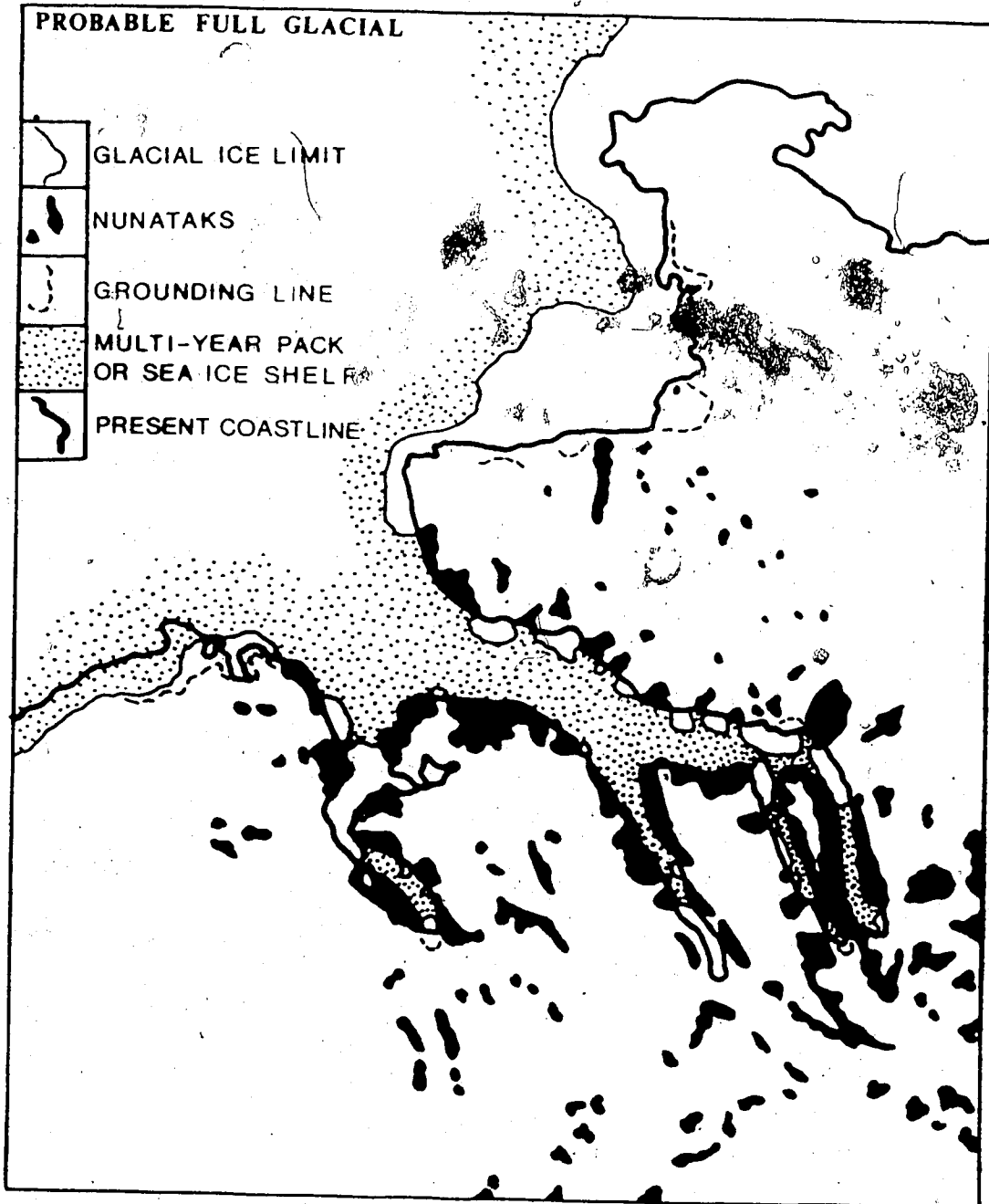


Figure 6.3a: Probable palaeogeography of Phillips Inlet and Wootton Peninsula at full glacial.

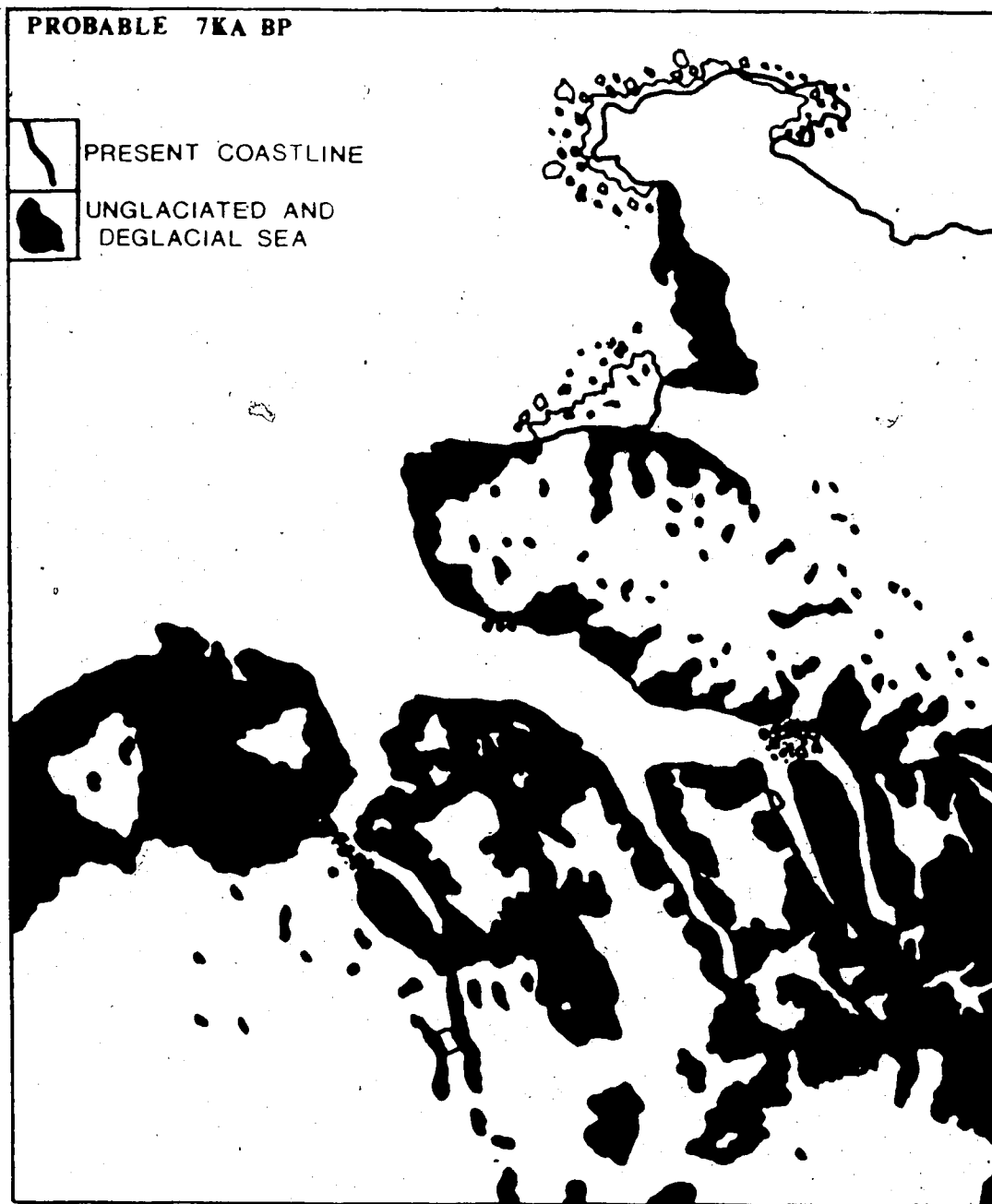


Figure 6.3b: Probable palaeogeography of Phillips Inlet and Wootton Peninsula at 7ka BP.

Figure 6.4: Equidistant shoreline diagram from Phillips Inlet and the Wootton Peninsula aligned from X-Y on Figures 6.1 and 6.2. Critical dates for construction are: 8710=85m; 8480?=85-91m; 8050=85m; 7530=85m; 7060=77m; 8540=65m; 8480=65m; 10,140=80m. The 8.5ka BP shoreline is the solid line. This is constructed to tilt at 0.85m/km and 0.73m/km according to different interpretations of related sea levels for 8480? (ie. 91m or 85m respectively). The 10.1ka BP shoreline is the broken line and this is based upon a 15% increase in tilt after Bednarski (1984).

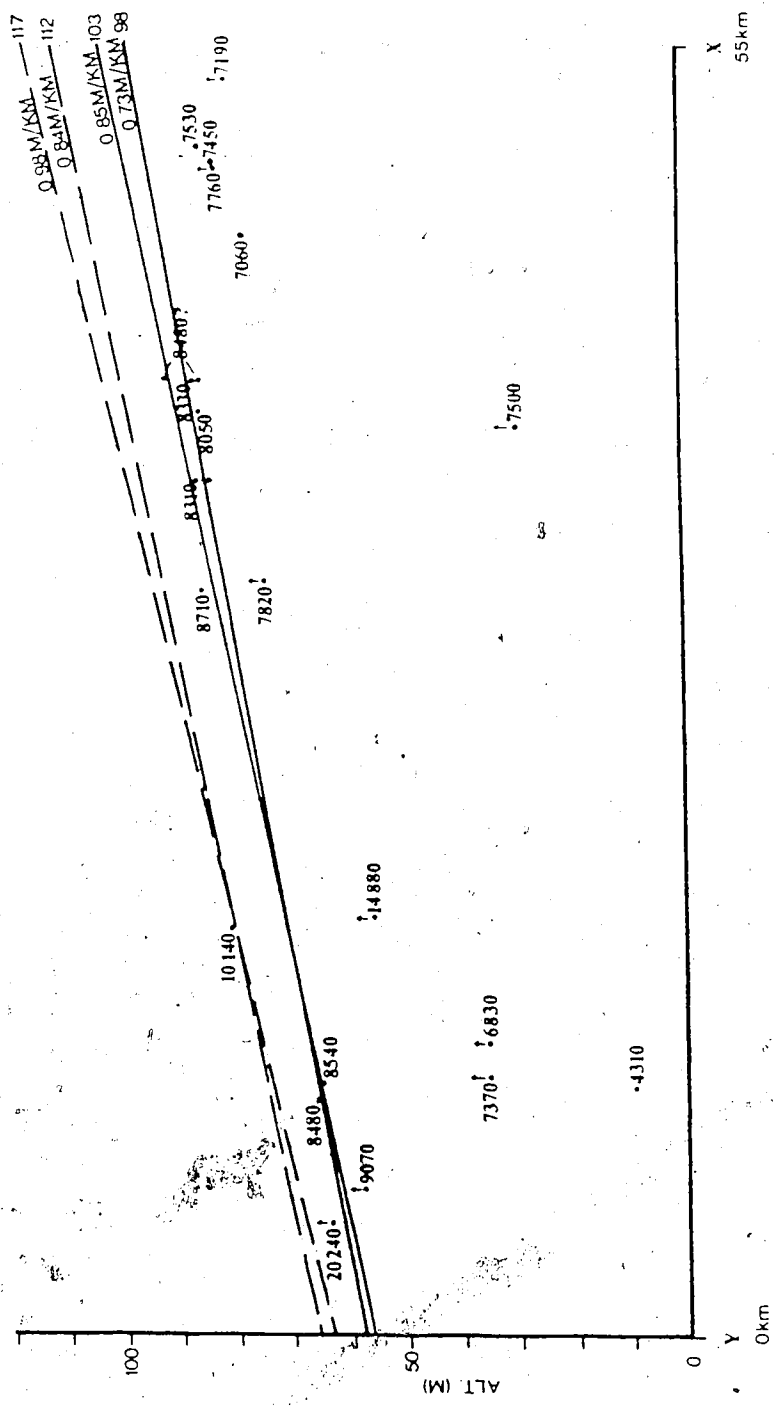


Table 6.1:

RADIOCARBON DATES FROM THE PHILLIPS INLET/ WOOTTON PENINSULA AREA

No	Location	Lab no.	Material	age years BP	Elev. (m)	Related sea level(m)	Lat.	Long.
1	Cache Head Fd	TO 251	shell	7,060±70	58	77	81°54'	85°45'
2	Wind Gap	TO 252	shell	8,480±100	58	85-91	81°58'	84°40'
3	Cache Head Fd	TO 253	shell	8,310±70	67	<86	81°57'	85°55'
4	Mygale Bay Delta	TO 254	shell	8,050±60	54	85	82°01'	84°45'
5	Musk Ox River	TO 255	shell	7,820±70	29	73.5	81°58'	86°25'
6	Berg Bay Fjord	TO 256	shell	7,190±90	34	>80	81°53'	84°20'
7	Drift Pass	TO 257	shell	8,710±70	40	85	82°02'	86°10'
8	Storm Delta	TO 258	shell	7,530±70	28	85	81°51'	85°25'
9	Berg Bay Fjord	TO 259	shell	7,760±70	54	>82.5	81°54'	84°42'
10	Berg Bay Fjord	TO 260	driftwood	7,450±80	55	82.5	81°54'	84°42'
11	Ice Alley Fjord	TO 470	shell	8,330±80	52	86	81°52'	86°50'
12	Ice Alley Fjord	TO 471	shell	7,500±70	29	>29-86	81°53'	86°50'
13	Ice Alley Fjord	TO 472	shell	5,200±60	20	---	81°51'	86°55'
14	Armstrong Delta	TO 473	shell	10,140±90	57	80	82°03'	88°08'
15	Cairn Delta	TO 474	shell	8,480±70	49	65	82°12'	86°40'
16	Albion Lakes	TO 475	shell	14,880±110	55	>55-80	82°04'	87°53'
17	Alfreds Glacier	TO 476	Narwhal tusk	6,830±50	35	35	82°16'	85°17'
18	Cape Alfred Ernest	TO 477	driftwood	4,310±70	9	9	82°16'	85°20'
19	Cape Alfred Ernest	TO 478	shell	9,070±80	57	>57	82°20'	85°25'
20	Alfred's Glacier	TO 479	shell	1,850±50	8	---	82°16'	85°25'
21	Musk Ox River	TO 480	shell	32,110±370	57	---	81°58'	86°24'
22	Useless Delta	TO 481	shell	20,240±160	47	>62.5	82°21'	85°20'
23	Cairn Peninsula	TO 482	shell	7,790±70	43	---	82°16'	85°27'
24	Wood's Glacier	TO 483	shell	7,370±70	23	>35<65	82°14'	86°04'
25	Sunkist Deltas	TO 484	shell	8,540±70	35	65	82°13'	86°10'
26	Cape Alfred Ernest	TO 485	peat	39,270±640	32	---	82°23'	85°35'

greatest ice advance was from the Grant Land Mountains and the plateau ice caps of physiographic Zone 2. Here the predominant glacial landsystems were: no.2) plateau ice caps with piedmont glaciers; and no.4) transection glaciers (see section 4.3.3.1). The latter were formed by coalescent piedmont lobes within broad valleys which lay above marine limit. At the fiord head, where large areas are below marine limit, moraines demarcating the last ice limit are <150m asl. Therefore, most piedmont glaciers were forced to float forming small ice shelves (Fig.6.3a).

As the piedmont lobes advanced into the main river valleys they proglacially thrusted and entrained debris and aprons causing disturbance of older marine sediments and outwash. These glaciers deposited till veneer and low relief hummocky moraines upon retreat. The clast characteristics of the tills closely resemble those of fluvial material suggesting passive glacial transport. Because the basal ice of these glaciers was charged with debris, thick subaqueous fans were deposited at the eastern fiord heads during deglaciation. Again, the clast analyses suggest that the fan material was transported passively by the glaciers and redeposited without undergoing much modification.

Because many of the last ice margins terminated in the sea, the raised marine record is critical to the palaeogeographic reconstructions (Fig.6.3a). Thick beds of diamicton have been cited as evidence for stable ice shelves which deposit debris over belts several kilometers wide (cf. Gravenor et al. 1984; Eyles et al. 1985). Using sedimentologic and geomorphic criteria, Stewart (1988) proposed that a tidewater glacier (without an ice shelf) occupied Clements Markham Inlet during the last glaciation. The arguments put forward by Stewart to support a tidewater glacier include: the lack of wide belts of massive diamictons; the occurrence of subaquatic outwash (fans); and the meager amount of ice rafted debris within marine silts immediately distal to the ice. The subaqueous fans and morainal banks have important

palaeogeographic implications. Stewart (1988) has pointed out that the subaquatic outwash of Clements Markham Inlet resembles Pleistocene glacial-marine lithofacies from temperate environments. Therefore, climatic conditions in the high Arctic were much warmer during the early Holocene than even today. Stewart's observations contradict Eyles et al. (1985) conclusions that the lack of coarse sediment in the Arctic Ocean basin was due to cold-based glaciers on the northern Ellesmere Island coast that released little meltwater upon deglaciation. Stewart (1988) prefers sediment entrapment in the inner fiords to explain the lack of coarse sediment in the Arctic Ocean cores.

Stewart's (1988) conclusions are based upon comparisons between Clements Markham Inlet and mid-latitude and Antarctic environments. Observations in Phillips Inlet and the Wootton Peninsula dictate a further reassessment of the sedimentologic and stratigraphic criteria for defining former ice shelves in this part of the high Arctic, especially in areas containing different glacial sublandsystems. First, there is no reason to expect all ice shelves to deposit wide belts of massive diamicton. For example, ice shelves originating as piedmont lobes at Cape Armstrong did not contain large amounts of basal debris because of the lack of deformable sediment. Second, where piedmont lobes formed ice shelves at the eastern fiord heads their basal debris may not have been released, due to basal accretion of fresh water (cf. Lyons et al. 1971). Third, multiyear fast ice and ice shelves would tend to decrease calving rates and reduce grounding line fluctuations thereby restricting deposition to a narrow belt. Therefore, thick but narrow belts of diamicton with interbedded marine sediments may represent former grounding lines outside of which are massive silts with ice rafted debris and inside of which are subaqueous fans representing retreating tidewater glaciers (Stewart 1988). Consequently, the subaqueous fans of the eastern fiord heads mark approximate positions of grounding lines and/or positions of rapid

melting at deglaciation (cf. Ringrose 1982; McCabe et al. 1986; Stewart 1988).

The amount of debris deposited at or beyond the grounding line is dictated by the glacial sublandsystem responsible for the floating ice. For example, at Cape Armstrong a low amplitude morainal bank was deposited during full glacial conditions (14.8ka) on an offshore shoal north of Albion Lakes (Figs.5.1 and 6.3a). Beyond this line a thin veil of marine silts with occasional dropstones were deposited beneath the glacial ice shelf. Coarser debris, including mega blocks, was deposited below the cliffs at Cape Woods because the ice transported medial and lateral moraines from the mountains onto the ice shelf (Fig.2.7 and 5.16).

Although there is a greater ice coverage and a much lower glaciation level on the Wootton Peninsula than elsewhere in Phillips Inlet, most glaciers on the peninsula did not advance >4km beyond their present margins during the last glaciation (Fig.6.3a). This was a result of the proximity of the Arctic Ocean and Phillips Inlet which forced the glaciers to float and calve. The largest transection glaciers (Woods, Alfreds and Tidewater glaciers, Fig.5.4) already float in the sea and because of high marine limits (65-90m asl) ranging from 7.4-7.8ka BP within 1km of their margins, it is likely that their grounding lines actually retreated during full glacial conditions, making their margins more unstable (Thomas and Bentley 1978). Similarly, the Alert Point Ice Cap floated at the present coastline and a calving bay in the cove east of Cape Alfred Ernest (Figs.5.7 and 6.3a) may explain the penetration of marine fauna to within 2km of present ice margins at 20.2ka BP (site 22, Fig.6.1). Early Holocene fauna also penetrated this coast by 9.1ka BP (site 19, Fig.6.1). Using sea level data (see section 6.4) the marine limit along the west Wootton Peninsula coast (65m asl) is dated at 8.5ka BP. Therefore, the progradation of the deltas along this coast (representing ice retreat) did not occur until 8.5ka BP. A further interpretation of the older ^{14}C dates on the Wootton Peninsula (site 19 and 22, Fig.6.1) would be that they relate to

the full glacial sea which was not recorded elsewhere in Phillips Inlet because of the presence of floating glaciers or pervasive landfast sea ice. At the head of Antoinette Bay, Greely Fiord, England (1987c) recovered shells in marine silts relating to the full glacial sea which was not represented by shorelines because of the late break up of a local ice shelf. Consequently, marine fauna of full glacial age lived beneath this ice shelf which broke up as late as 7.3ka BP. It is possible that similar conditions existed on Wootton Peninsula allowing the penetration of shells dating 20.2 and 9.1ka BP prior to initial retreat at 8.5ka BP.

In the western half of physiographic Zone 2 (Fig.1.3), glaciers retreated between 10.1 and 7.8ka BP. Retreat was underway rapidly regardless of the glacial sublandsystems. Around Armstrong River and Albion Lakes, ice had retreated by 10.1ka BP (site 14, Fig.6.1) although coarse gravels were deposited over Armstrong Delta by outwash from the retreating Dodger Ice Cap at least until sea level was at 61m asl (marine limit=80m). Ice retreated from northeast Drift Pass by 8.7ka BP (site 7, Fig.6.1) and the sea penetrated upper Muskox River valley by 7.8ka BP (site 5, Fig.6.1), isolating stagnant ice in Drift Pass and causing the final drainage of the proglacial lake in upper Muskox River (Fig.6.3b). Glaciers in Ice Alley Fiord had retreated to within 500m of present margins by 8.3ka BP (site 11, Fig.6.1) suggesting that their margins were unstable. The effect of calving was also felt at the head of Phillips Inlet where dates of 8.1 and 8.5ka BP (sites 4 and 2, Fig.6.1) document the early retreat of ice into Wind Gap and Valley of the Blocks (Fig.6.3b).

Ice persisted in the eastern fiord heads until 7.5-7.1ka BP despite the fact that ice shelf and fast ice break-up was already well underway before 7.5ka BP (Fig.6.3b). Although calving was not as pronounced in the eastern fiord heads as it was to the north and west, the coalescent glaciers had broken up into individual piedmont lobes before 7.5ka BP. At least one

piedmont lobe terminating in the sea had retreated to within 400m of its present margin by 8.3ka BP (site 3, Fig.6.1) while driftwood penetrated south of The Promontory by 7.5ka BP (site 10, Fig.6.1). Glaciers at the eastern fiord heads were depositing subaqueous fans before 7.5ka BP (site 8, Fig.6.1) and the most recent date on final ice retreat is 7.1ka BP (site 1, Fig.6.1; Fig.6.3b).

The chronology of the last glaciation in Phillips Inlet and Wootton Peninsula have broader implications, specifically for the high Arctic ice cores. For example, an abrupt isotopic shift ($\delta^{18}\text{O}$) in the Ellesmere Island, Devon Island and Greenland ice cores at 10.5ka BP has been cited as evidence of a climatic amelioration (Dansgaard et al. 1973; Koerner and Fisher 1981; England et al. 1982). However, the geologic evidence from northern Ellesmere Island can be interpreted in different ways. The isotopic shift records a specific period of climate change whereas the geologic record for initial ice retreat in the same region varies (northern Ellesmere Island retreat=10ka BP; northeastern Ellesmere Island and Greenland retreat=8ka BP; England and Bednarski 1986). The reason for this 2ka lag is that northern Ellesmere Island is characterized by contrasting glacioclimatic regimes and various topoclimatic controls affect glacier response rates to temperature/moisture change (Koerner 1977b, 1979; England and Bednarski 1986).

Deglaciation in Phillips Inlet was underway by 10.1ka BP and was well advanced by 8.3-8.5ka BP. This is similar to Bednarski's (1984, 1986) chronology for Clements Markham Inlet. To the south of the Grant Land Mountains, England (1987c) documents deglaciation at the head of Greely Fiord at 8ka BP with slow emergence from 8-7.4ka BP. Therefore, there was a lag of 2.1ka (maximum) between initial deglaciation on the northwest Ellesmere Island coast and the area directly southeast, lending further support to the differences in glacioclimatic regimes reported on either side of the Grant Land Mountains (England and Bednarski 1986). Similarly, in Otto Fiord on the

west coast Bednarski (1987) reports early deglaciation at 9.1ka BP.

The present distribution of ice on Ellesmere Island has been attributed to the effectiveness of precipitation sources (open Baffin Bay versus sea ice covered Arctic Ocean, Koerner 1977b; Maxwell 1981). The proximity of Baffin Bay has led to a thickening of ice caps on the highlands of the southeast coast during the Holocene whereas glaciers to the north have been starved of precipitation. Koerner (1977b) envisages a similar asymmetrical distribution of ice during the last glaciation. Even the larger ice masses to the south (ie. Agassiz Ice Cap) underwent a thickening of only 200m during the last glaciation (Koerner et al. 1987). This asymmetry, together with the impasse presented to advancing glaciers by the marine environment, restricted the last ice coverage on northwest Ellesmere Island. A marked climatic amelioration at 10.5ka BP could be entertained within the retreat chronology of the field area if deglaciation began as early as 10.1ka BP. The massive calving which occurred throughout the field area during the early Holocene was probably a response to more open water at that time. Any effect that this open water had upon increased precipitation (possible accumulation) was likely offset by the general warming trend and/or increased calving rates. The sedimentological evidence also suggests a change to warm-based glacial conditions during initial deglaciation in the early Holocene (cf. Ringrose 1982; Stewart 1988).

6.4: Sea level history.

Emergence curves represent the history of sea level at specific sites since deglaciation and they rely entirely upon radiocarbon dates obtained on organics that can be ascribed to former sea levels. Unfortunately driftwood was sparse in the field area and none of the dated samples could be related unequivocally to a specific sea level. Nonetheless, such dated samples are of palaeoclimatic importance because they indicate intervals of reduced summer

sea ice, in some cases at the onset of deglaciation. Most of the radiocarbon dates in the field area were obtained on marine shells collected from deglacial sediments, although many such deposits had poor stratigraphic control. In those cases where the stratigraphy was uncertain, the shells are ascribed to a range of possible sea levels. These ranges have been modified using an equidistant diagram (Fig.6.4) which is constructed principally from five ^{14}C dates with good stratigraphic control. Twenty-six ^{14}C dates have been obtained using accelerator mass spectrometry (AMS) versus conventional beta counting (see Appendix 1). The dates are summarized in Table 6.1 and their locations are shown on Figure 6.1.

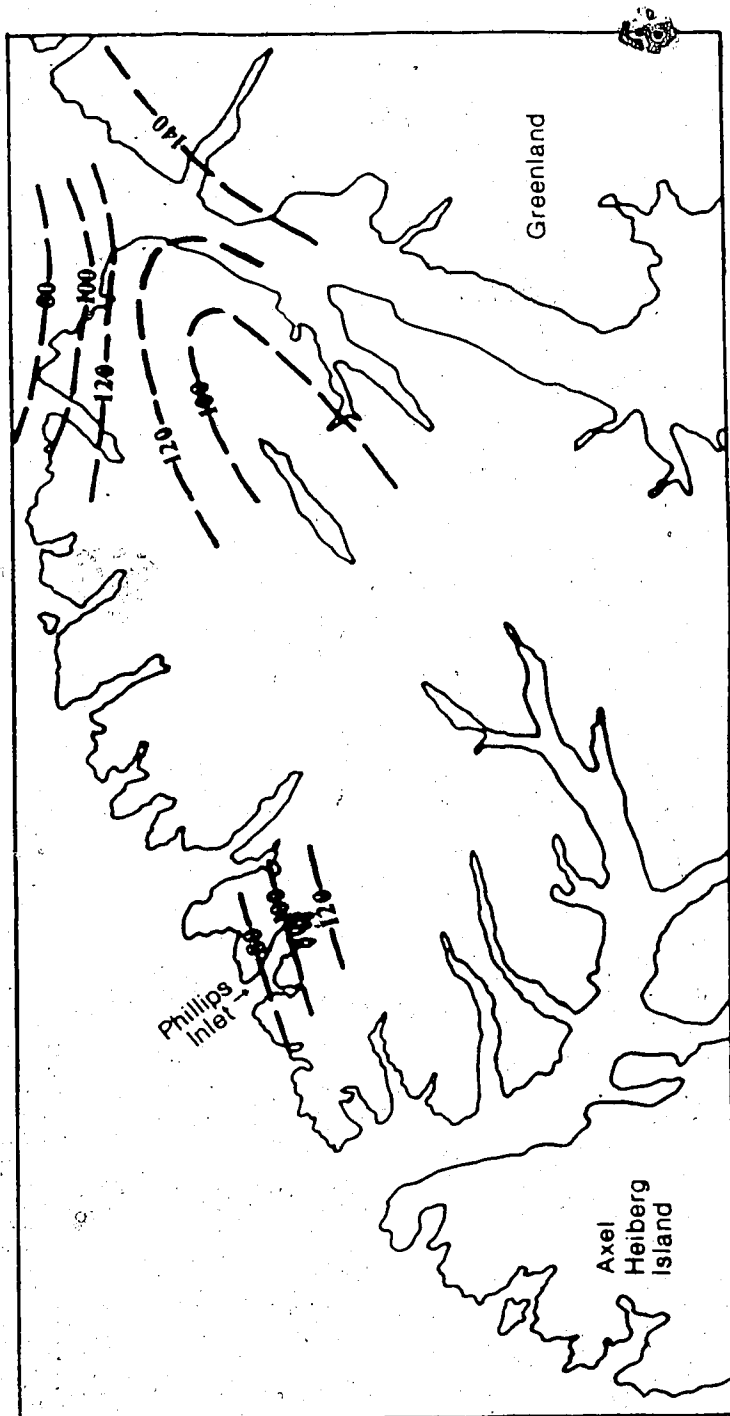
Radiocarbon dates at sites 2, 4, 7, 15 and 25 (Fig.6.1) are used to reconstruct the shoreline profile for 8.5ka BP. These dates are all clearly related to former sea levels (Table 6.1). For example, sites 15 and 25 (8480 ± 70 and 8540 ± 70 BP) dated the marine limit at 65m asl on the Cape Woods coast. Site 4 (8050 ± 60 BP) dates the ice contact Mymmshall Delta at 85m asl. Site 2 (8480 ± 100 BP) dates a sea level between 85m asl and the local marine limit (91m asl) at Wind Gap (Fig.6.2). The profile of the 8.5ka BP shoreline was then orientated until it attained a maximum tilt as defined by axis X-Y on Figures 6.1 and 6.2. A further control on the alignment occurs at site 7 (8710 ± 70 BP) which dates a marine limit of 85m asl. Site 7 cannot fall below the 8.5ka BP shoreline on the equidistant diagram. The resultant shoreline tilt reveals dominant glacioisostatic unloading toward the Grant Land Mountains to the south.

Because site 2 (8480 ± 100 BP) relates to a sea level somewhere between 85 and 91m asl, a range of tilts can be reconstructed for the 8.5ka BP shoreline (from 0.73m to 0.85m/km; Fig.6.4). Although the equidistant diagram has less control than that reported by Bednarski (1984) for Clements Markham Inlet, the tilts shown on the 8.5ka BP shoreline from both areas are similar. In Clements Markham Inlet the 8.6ka BP shoreline tilts at 0.75m/km whereas

the 11-10.5ka BP shoreline tilts at 0.88m/km. Therefore, the tilt on the full glacial sea in Clements Markham Inlet is 15% steeper than the tilt on the 8.6ka BP shoreline. In Phillips Inlet/Wootton Peninsula, the $10,140 \pm 90$ BP date on the marine limit at Cape Armstrong provides a control point for the reconstruction of a full glacial sea in this area. Based on the information from Clements Markham Inlet, two full glacial shoreline profiles have been reconstructed for Phillips Inlet using an increase of 15% above the range of tilts shown for the 8.5ka BP shoreline (Fig.6.4). Clearly these full glacial shorelines are approximations and they assume that Phillips Inlet had the same history of glacioisostatic unloading prior to 8.5ka BP as occurred in Clements Markham Inlet. Nevertheless, it is apparent that within Phillips Inlet the 10.1ka BP shoreline is some 10m higher than the 8.5ka BP shoreline. Therefore, there is no reason to believe that this is not the case along the entire length of the 8.5ka BP shoreline profile.

Using the estimated profile of the full glacial shoreline a range of 112-117m asl is obtained for the marine limit at the eastern fiord heads (Fig.6.4). The equidistant diagram also suggests that the date of 9.1ka is related to a sea level above the 65m shoreline (8.5ka BP) on Wootton Peninsula. It is also likely that the 20.2 and 14.9ka BP dates (sites 22 and 16, Fig.6.1) relate to the full glacial sea, but it is not known whether or not the sea reached its limit at these times. Figure 6.5 depicts the isobases on the >10ka BP shoreline using data from England and Bednarski (1986) and the steepest shoreline from Figure 6.4 for Phillips Inlet/Wootton Peninsula. It appears that a southerly shift occurs in the isobases between Clements Markham Inlet and the field area and an elongate (east-west) ridge of ≥ 120 m of emergence coincides with the Grant Land Mountains. Considerable sea level data from Greely Fiord/Nansen Sound, Otto Fiord and Disraeli Fiord are being analysed (J. England, J. Bednarski and D.S. Lemmen, pers. comm. 1988) and a more complete regional isobase pattern is forthcoming.

Figure 6.5: Isobase map for northern Ellesmere Island at 10.1ka BP.



All other ^{14}C dates are added to the equidistant diagram at their altitude of collection. However, it is apparent that many of these dates relate to higher relative sea levels. Some dates are plotted at specific elevations based upon the location of other samples on the equidistant diagram. For example, the date of 8310 ± 70 BP (site 3, Fig.6.1) relates to a sea level $>67\text{m} - <86\text{m}$ asl. Based upon the elevation of the 8050 ± 60 BP date (site 4, Fig.6.1; 85m Mymmshall Delta) on the equidistant diagram, the date of 8310 ± 70 BP must relate to a sea level very close to 86m and therefore the upper 8.5ka BP shoreline ($0.85\text{m}/\text{km}$) is considered to be the best reconstruction. Local marine limits, without dating control, are assigned a tentative age using the equidistant diagram (Fig.6.6) and these ages are also used in the construction of the palaeogeographical maps (Fig.6.3). Because some local marine limits (many located inside the last ice margin) occur above the 8.5ka BP shoreline (Fig.6.6), sea level could not have remained stable in this area from ≥ 10 -8.5ka BP (cf. England 1987c)

The chronology of emergence in Phillips Inlet is also relevant to the question of maximum versus minimum ice during the last glaciation (cf. Ives 1978). Although it might be argued that the restricted ice margins (interpreted as the last ice limit) are really retreat positions from a larger "classical" Wisconsinan maximum this is contradicted by the ^{14}C dates on the former sea levels. If a large outlet glacier inundated Phillips Inlet during the last glaciation, the marine limit would decrease in age from northwest to southeast. However, local piedmont lobes retreated from the fiord heads at the same time the outer inlet was becoming ice-free. For example, although ^{14}C dates as young as 7.5-7.1ka BP record deglaciation at the eastern fiord heads, shorelines of 90-93m asl adjacent to these dated sites document the break-up of coalescent ice as early as $\geq 8.5\text{ka}$ BP (Figs.6.1-6.3). This indicates the retreat from small, localized ice margins rather than the systematic, regional retreat of a trunk glacier infilling the inlet.

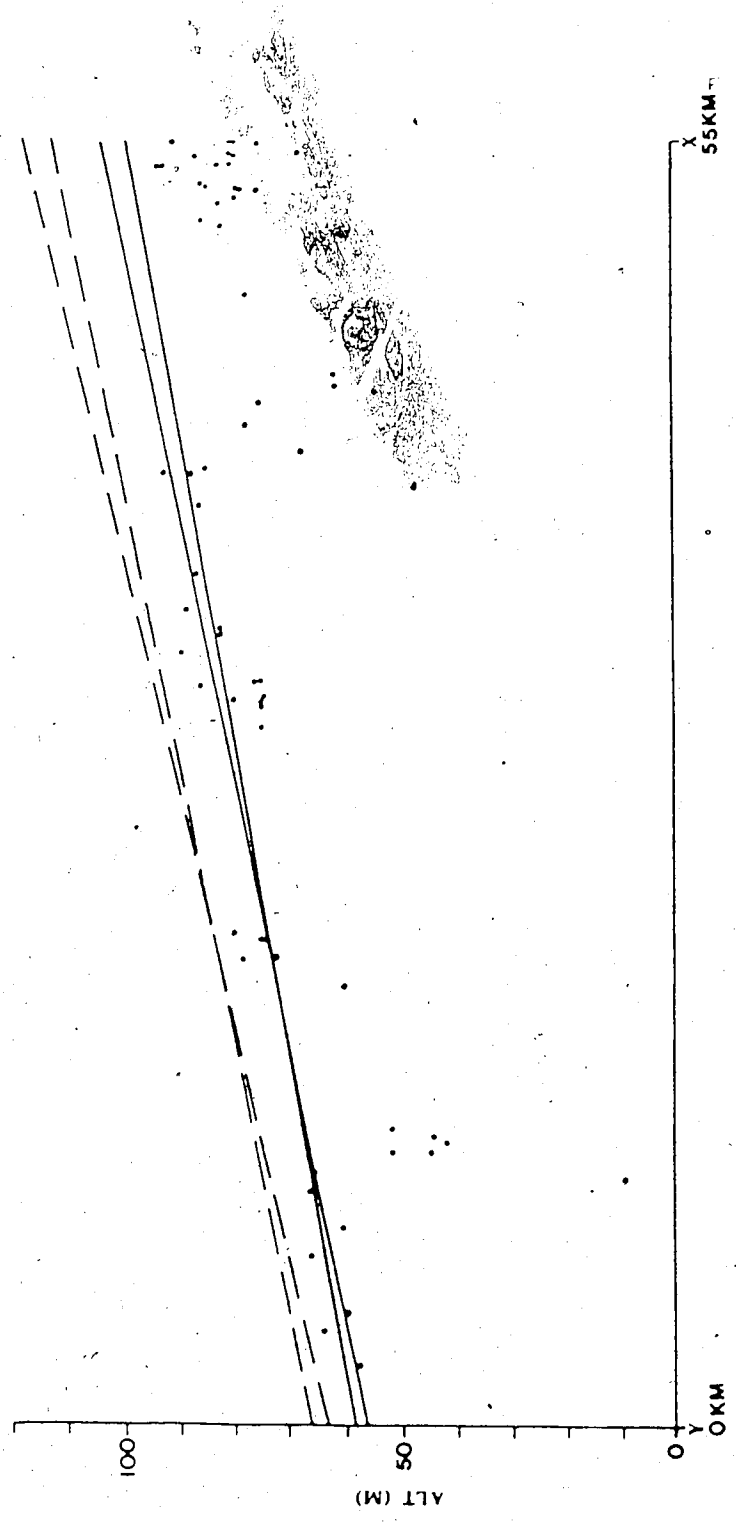


Figure 6.6: Equidistant shoreline diagram with shorelines from Figure 6.4 and the heights of all deltas and shoreline segments surveyed in the field area plotted on the X-Y axis on Figures 6.1 and 6.2.

Furthermore, there is no stratigraphic or geomorphic evidence for the retreat of such a trunk glacier beyond these local ice margins.

To the contrary, the extent of the last glaciation in Phillips Inlet and Wootton Peninsula is mapped using the distribution of distinct sediment accumulations (moraines, kames, glacial marine sediments). Retreat patterns are recorded by prominent meltwater channels and sandar. If this sediment and landform evidence represents a stillstand in overall retreat from a more extensive ice cover, then similar evidence should occur outside the margins defined in this study. Moreover, raised marine sediments associated with retreat from a more extensive "classical" Wisconsin glaciation are not evident.

Because ice cover of the field area is presently 60%, coverage during the last glaciation was almost complete (Fig. 6.3a). Nonetheless, the small range in deglacial dates (either dated directly or interpolated from the equidistant diagram) dictates a pattern of retreat that could be occasioned only by a modest adjustment in the present ice distribution rather than the break-up of a regional ice sheet. The paucity of *in situ* dates in the 11-30ka BP range is enigmatic in the high Arctic (cf. Andrews 1975a; England 1985a) but the recent discovery of full glacial flora and marine fauna has strengthened the model of minimum ice (see section 1.4.3). In the field area two such dates (20,240±160 and 14,880±110 BP) particularly strengthen the case for a full glacial sea outside the margins of the last glaciation.

6.5: Holocene (postglacial) history.

The climatic history obtained from high Arctic ice cores provides a framework for the study of glacioclimatic change in this region (Dansgaard et al. 1971, 1973; Koerner 1979; Fisher and Koerner 1980, 1983). Based on the record from the Devon Island ice core, a marked climatic amelioration began at 10.5-10ka BP and this increased steadily until 8.3ka BP (Koerner 1977a;

Koerner and Fisher 1981, 1985; England et al. 1982). The warming trend continued until 5-4.5ka BP after which a climatic deterioration from 4.5- 3ka BP was responsible for the formation or rejuvenation of the Ellesmere Island ice shelves (cf. section 1.4.4).

Independent data on high latitude climatic change during the Holocene have now been obtained in Phillips Inlet, northwest Ellesmere Island and these are summarized for its various sectors (Table 6.2). An early Holocene climatic amelioration is indicated by an enhanced calving interval (10.1-8.5ka BP) followed by the deposition of subaqueous fans from ice fronts possessing temperate characteristics (cf. Stewart 1988). Extensive open water during the early Holocene, caused by this proposed amelioration, explains the penetration of driftwood to the eastern fiord heads by 7.5ka BP as well as the existence of a narwhal <1km from the present margin of the largest transection glacier in the field area at 6.8ka BP (section 6.4). Although the narwhal could have exploited a moat behind the Cape Alfred Ernest Ice Shelf, it is unlikely that the ice shelf existed in such open water conditions. These events also coincided with increased progradation of deltas at 8.5ka BP. Sea ice push ridges up to marine limit attest to persistent open leads behind the Cape Alfred Ernest Ice Shelf from ≥ 8.5 ka BP to the present.

The early Holocene retreat for the northernmost coast contrasts with the chronology reported on the south side of the Grant Land Mountains (England 1987c) where glaciers and summer sea ice remained stable until at least 8ka BP and, in some cases, closer to 6ka BP. This difference between the north and south sides of the Grant Land Mountains questions the validity of regional generalizations concerning Holocene climatic change based solely upon ice core records.

The early Holocene climatic amelioration in Phillips Inlet was followed by a mid-Holocene deterioration during which the Cape Alfred Ernest Ice Shelf appears to have formed or redeveloped. Glaciers throughout the

Table 6.2: Chronology of Holocene geomorphic events from around the field area.

SECTOR	EARLY HOLOCENE	MID HOLOCENE	LATE HOLOCENE
1	Open water Narwhal 6.8ka BP. 8.5ka BP. Alfreds Glacier <1km beyond present margin at 7.8ka BP.	Driftwood 4.3ka BP (max. age on ice shelf). Alfreds Gl. advanced <7.8ka BP.	Formation of Cape A.E. ice shelf. Alfreds Gl. advanced <1.9ka BP. Recent retreat.
2	Beaches=open water after 8.5ka BP.	Formation of glacierette <7.4ka BP (sea level <30m)	Recent retreat of snowbanks and glacierette.
3		Formation of ice rises.	Terrace collapse and melt out of buried ice rises. Recent snowbank retreat.
4	Terrible Glacier behind present margin at approx. 8ka BP (76m ML).	Reentrainment of 52-74m deltas by Terrible Glacier.	>1.5km retreat of Idris Peaks ice. Thinning of Terrible Gl.
5		Thrust blocks=0.75km advance by Musk Ox Gl., Build up of cirque glaciers in W. Pikes.	Musk Ox Gl. thrust moraine=Little Ice Age? Retreat of cirque glaciers in W. Pikes.
6		Pudding Glacier behind present margin >5.2ka BP.	Pudding Gl. advancing. Other glaciers retreating.
7		Endeavour Gl. advanced explaining buried stagnant ice?	Endeavour Gl. advancing.
8	Penetration of driftwood at 7.5ka BP.		

field area responded in accordance with their size. Between the mid-Holocene and the present many cirque glaciers, perennial snowbanks and glacierettes have formed and retreated.

The impact of the Little Ice Age (100-400yrs BP) upon ice bodies of all sizes is unknown, although two readvances by Muskox and Alfreds glaciers may relate to mid-Holocene and Little Ice Age climatic changes. Some larger glaciers also may be responding to mid- to late-Holocene climatic deteriorations (Blake 1981; Stewart and England 1983). A number of questions remain: specifically, did any perennial snowbanks and smaller glaciers retreat and/or disappear between the mid-Holocene climatic deterioration and the Little Ice Age? Do the outermost trimlines in the field area represent mid-Holocene or Little Ice Age limits? What period does the stagnant ice beyond many snouts date from, Mid-Holocene or last glacial? The high Arctic ice cores do record a pronounced warming between 660yrs and 2.5ka BP. Therefore, the smaller glaciers and snowbanks presently undergoing retreat throughout the field area may have formed entirely during the Little Ice Age whereas the larger glacier systems may be still responding to mid-Holocene climatic deterioration upon which Little Ice Age advances were superimposed (Stewart and England 1983). The recent climatic amelioration of the last 100 years (cf. Fisher and Koerner 1980) is documented by the retreat of perennial snowbanks, glacierettes and cirque glaciers. This is particularly noticeable when comparing air photographs from 1959 and the present.



CHAPTER SEVEN

Conclusions and future research

This is not the end. It is not even the beginning of the end. But it is, perhaps, the end of the beginning.

Sir Winston L.S. Churchill, Speech on 10-11-42.

The conclusions of this thesis can be summarized as follows:

1. Older, more extensive glaciations are evidenced by high elevation erratics (600-660m), a till possibly dating >39ka BP and reworked, high-level fossiliferous marine sediments. The physiography upon which this glaciation took place is largely unknown, as are the number of events. Nonetheless, it is important to point out that regional erratics originating in the Grant Land Mountains were not found to be dispersed throughout Phillips Inlet. This argues against a pervasive ice cover at any time in the past and perhaps the hypothesis of an open Arctic Ocean (increased precipitation) during the Pleistocene (cf. Ewing and Donn 1956; Donn and Shaw 1965; Donn and Ewing 1966; Herman and Hopkins 1980; Clark 1982).
2. Evidence for higher sea levels predating the last glaciation is fragmentary and undated. Fossiliferous marine sediments were disturbed by glaciers during the last glaciation. The high-elevation shells (144 and 409m asl) inland of Terrible Glacier and within its lateral moraine are particularly enigmatic and are incompatible with the flowlines of the present glaciers. Whether these shells were ice transported by a glaciation of unknown age, or whether they represent an old high sea level remains to be established.
3. Glacial style during the last glaciation was dictated by local physiography. Four main sublandsystems, in addition to Eyles's (1983) glaciated valley landsystem, are recognized: 1. plateau ice caps with no outlet lobes; 2. plateau ice caps with piedmont glaciers; 3. extended-cirque glaciers; and 4. transection glaciers. Because glaciers were largely cold-

based, debris was incorporated by apron entrainment; proglacial thrusting; and by the overriding of stagnant, alluvium covered ice. The amount of debris entrained was a function of the availability of deformable sediment, local topography and extraglacial debris.

4. Depositional sequences were also dictated by sublandsystem type. Transection and/or piedmont glaciers at the eastern fiord heads contained abundant debris because of the availability of deformable sediment. Release of this debris during deglaciation was responsible for large subaqueous fans. Tills and moraines are also more common in areas of more extensive deformable sediment.

5. Glaciers advanced on average <10km from their present margins during the last glaciation. Most large glaciers terminated in the marine environment and their former grounding lines are identified by morainal banks. The spatially restricted nature of these grounding lines suggests that there was extensive landfast sea ice, and that glacier and sea-ice shelves existed offshore. Marine fauna dating 14.9ka BP were recovered from a morainal bank at Cape Armstrong. Full glacial fauna dating 20.2ka BP also existed beneath an ice shelf at Cape Alfred Ernest, <2km from present ice margins. Because these fauna cannot be associated with a specific relative sea level, the height of the full glacial sea during this interval remains unknown. Nonetheless, models depicting inundation of this area by large ice sheets should be abandoned (cf. Denton and Hughes 1981; Selby 1985; Hughes 1987).

6. Deglaciation started with a pronounced calving phase throughout the field area between 10.1ka and 7.8ka BP. Glaciers occupied the more sheltered eastern fiord heads until at least 7.5-7.1ka BP after which large subaqueous fans document the retreat of temperate tidewater glaciers. This chronology of deglaciation is similar to that presented for Clements Markham Inlet (Bednarski 1984, 1986) and reflects an early Holocene warming trend reported from high Arctic ice cores. However, the validity of such a regional warming

is challenged by the lag of 2.1ka between the northernmost coast and the south side of the Grant Land Mountains. This lends support to the previously suggested differences in glacioclimatic regimes on either side of the Grant Land Mountains and cautions against regional generalizations of Holocene climatic change in the high Arctic.

7. An early Holocene climatic amelioration characterized by abundant open water was followed by a mid-Holocene climatic deterioration during which the Cape Alfred Ernest Ice Shelf formed. Some of the larger glacial systems may be still responding to the mid-Holocene cooling. Evidence of a Little Ice Age advance is sparse and in many cases may be superimposed on a more dominant mid-Holocene advance. The climatic amelioration of the last 100 years has been responsible for the retreat of many large perennial snowbanks and glacierettes.

A number of very important issues remain to be addressed:

1. Amino acid ratios and even uranium-series dates are required on older shells from the field area. Younger shells should be processed similarly for calibration. Other dating techniques could also be applied. For example, the section south of Alert Point provides an ideal opportunity to investigate the palaeomagnetism of a stratigraphic sequence at this high latitude.
2. The spatial distribution of Tertiary sediments and their relationships to older erosional landforms and/or structural features remain poorly understood. Therefore, our understanding of landscape evolution is restricted to the late Quaternary.
3. More work is required on the section to the south of Alert Point. Only a reconnaissance-type log was possible in this study. The 39ka BP organics should be sampled for microfossils and the site should be revisited to enable more exhaustive sediment sampling and stratigraphic logging.
4. Similar work on the lake sediments in upper Bridge Street might be critical to the dating of ice margins inland of the inlet and fiords.

5. From the glaciological and geomorphological viewpoints, are discrete englacial debris concentrations in the glaciers of the field area the result of freeze-on or overriding by the mid-Holocene readvance? What is the age of the buried stagnant ice in the field area? Work on oxygen isotopes from basal and buried ice (cf. Boulton and Spring 1986; Sugden et al. 1987) would yield important information on glaciological history.

6. Very little is known about the tectonic history of the area. Why is there only sparse evidence of older sea levels and why is there so much postglacial emergence following such a small ice retreat (England 1987b)? The age and origin of Phillips Inlet, like most fiords in the Queen Elizabeth Islands, remains a prominent issue.

7. There is still much conjecture on the role of the Arctic Ocean as a moisture source especially given the projections of future global climatic change. Ice shelves and fast ice have been tentatively included in the reconstruction of full glacial conditions for the field area but little is known about the history of the Arctic Ocean and its role in glaciation at high latitudes. Was there ever an open Arctic Ocean in the late Tertiary or Pleistocene (cf. ~~Healy and Hopkins~~ Hopkins 1980)?

8. Future high latitude ice sheet modelling (cf. Reeh 1984) should make better use of the geological field data (which are now quite considerable for northern Ellesmere Island) and the high Arctic ice core records rather than simply using theoretical models of pervasive glaciations that are now obsolete. Geophysical models should also be working toward similar refinements of their modelling of postglacial sea levels given this expanding regional data base from northern Ellesmere Island.

BIBLIOGRAPHY

- Aber, J.S., 1982. Model for glaciotectonism. Bulletin of the Geological Society of Denmark, Vol. 30, p.79-90.
- Ahlmann, H.W., 1935. Contribution to the physics of glaciers. Geographical Journal, Vol. 86, p.97-113.
- Alley, R.B., Blankenship, D.D., Rooney, S.T. and Bentley, C.R., 1987. Sedimentation beneath ice shelves: the view from Ice Stream B. Abstract, 12th INQUA International Congress, Ottawa, p.120.
- Alt, B.T., 1979. Investigations of summer synoptic controls on the mass balance of the Meighen Ice Cap. Atmosphere-Ocean, Vol. 3, p.181-199.
- Alt, B.T., 1985. 1550-1620: a period of summer accumulation in the Queen Elizabeth Islands. In, Harington, C.R.(ed), Critical Periods in the Quaternary Climatic History of Northern North America, Climatic Change in Canada 5, Syllogeus 55, National Museums of Canada, Ottawa, p.461-479.
- Andrews, J.T., 1970. A geomorphological study of postglacial uplift with particular reference to Arctic Canada. Institute of British Geographers, Special Publication no.2, 156p.
- Andrews, J.T., 1975a. Support for a stable late Wisconsin ice margin (14,000 to ~9000 BP): a test based on glacial rebound. Geology, Vol. 4, p.617-620.
- Andrews, J.T., 1975b. Glacial Systems. Duxbury Press, Massachusetts, 191p.
- Andrews, J.T., 1982. On the reconstruction of Pleistocene ice sheets: A review. Quaternary Science Reviews, Vol. 1. p.1-30.
- Andrews, J.T. and Miller, G.H., 1972. Quaternary history of northern Cumberland Peninsula, Baffin Island, N.W.T., Canada: Part IV: maps of the present glaciation limits and lowest equilibrium line altitude for north and south Baffin Island. Arctic and Alpine Research, Vol. 4, p.45-59.
- Banham, P.H., 1975. Glacitectonic structures: a general discussion with reference to the contorted drift of Norfolk. In, Wright, A.E. and Moseley, F. (eds), Ice Ages Ancient and Modern, Seel House Press, Liverpool, p.69-94.
- Bednarski, J., 1984. Glacier fluctuations and sea level history of Clements Markham Inlet, northern Ellesmere Island. Unpublished PhD thesis, University of Alberta, 232p.
- Bednarski, J., 1986. Late Quaternary glacial and sea level events, Clements Markham Inlet, northern Ellesmere Island, Arctic Canada. Canadian Journal of Earth Sciences, Vol. 23, p.1343-1355.
- Bednarski, J., 1987. Glacial advances in Otto Fiord, Ellesmere Island, N.W.T.. Abstract, 16th Annual Arctic Workshop, Edmonton, p.4-5.
- Bennike, O., Dawes, P.R., Funder, S., Kelly, M. and Weidick, A., 1987. The late Quaternary history of Hall Land, northwest Greenland: discussion. Canadian Journal of Earth Sciences, Vol. 24, p.370-374.
- Bergsma, B.M., Svoboda, J. and Freedman, B.S., 1984. Entombed plant communities released by a retreating glacier at central Ellesmere Island, Canada. Arctic, Vol. 37, p.49-52.
- Bird, J.B., 1967. The Physiography of Arctic Canada. Johns Hopkins University Press, 336p.
- Blake, W., Jr., 1970. Studies of glacial history in Arctic Canada. 1. Pumice, radiocarbon dates and differential postglacial uplift in the eastern Queen Elizabeth Islands. Canadian Journal of Earth Sciences, Vol. 7, p.634-664.
- Blake, W., Jr., 1972. Climatic implications of radiocarbon dated driftwood on the Queen Elizabeth Islands, Arctic Canada. In, Vasari, Y., Hyvarinen,

- H. and Hicks, S. (eds), Climatic Changes in Arctic Areas During the Last Ten Thousand Years, Acta Univ. Oulu, Ser. A(3) Geol. I., p.77-104.
- Blake, W., Jr., 1975. Radiocarbon age determinations and postglacial emergence at Cape Storm, southern Ellesmere Island, Arctic Canada. Geografiska Annaler, Vol. 57A, p.1-71.
- Blake, W., Jr., 1977a. Radiocarbon age determinations from the Carey Islands, northwest Greenland. Geological Survey of Canada, Paper no. 77-1A, p.445-453.
- Blake, W., Jr., 1977b. Glacial sculpture along the east central coast of Ellesmere Island, Arctic archipelago. Geological Survey of Canada, Paper no. 77-1C, p.107-115.
- Blake, W., Jr., 1981. Neoglacial fluctuations of glaciers, southeastern Ellesmere Island, Canadian Arctic archipelago. Geografiska Annaler, Vol. 63A, p.201-218.
- Blake, W., Jr., 1985. Radiocarbon dating with accelerator mass spectrometry: results from Ellesmere Island, District of Franklin. Geological Survey of Canada, Paper no. 85-1B, p.423-429.
- Blake, W., Jr., 1987. Geological Survey of Canada, Radiocarbon dates XXVI. Geological Survey of Canada, Paper no.86-7.
- Bornhold, B.D., Finlayson, N.M. and Monahan, D., 1976. Submerged drainage at Barrow Strait, Canadian Arctic. Canadian Journal of Earth Sciences, Vol. 13, p.305-311.
- Boulton, G.S., 1970. On the origin and transport of englacial debris in Svalbard glaciers. Journal of Glaciology, Vol. 9, p.213-229.
- Boulton, G.S., 1972a. Modern Arctic glaciers as depositional models for former ice sheets. Journal of the Geological Society of London, Vol. 128, p.361-393.
- Boulton, G.S., 1972b. The role of the thermal regime in glacial sedimentation. Institute of British Geographers, Special Publication, Vol. 1, p.1-19.
- Boulton, G.S., 1974. Processes and patterns of glacial erosion. In Coates, D.R. (ed), Glacial Geomorphology, New York State University Press, p.41-87.
- Boulton, G.S., 1978. Boulder shapes and grain size distributions of debris as indicators of transport paths through a glacier and till genesis. Sedimentology, Vol. 25, p.773-799.
- Boulton, G.S., 1979. Processes of glacial erosion on different substrata. Journal of Glaciology, Vol. 23, p.15-37.
- Boulton, G.S., 1986. Push-moraines and glacier-contact fans in marine and terrestrial environments. Sedimentology, Vol. 33, p.677-698.
- Boulton, G.S. and Spring, U., 1986. Isotopic fractionation at the base of polar and sub-polar glaciers. Journal of Glaciology, Vol. 32, p.475-485.
- Bovis, M.J. and Barry, R.G., 1974. A climatological analysis of north polar desert areas. In, Smiley, T.L. and Zumberge, J.H. (eds), Polar Deserts and Modern Man, University of Arizona Press, p.23-31.
- Bradley, R.S., 1985. Quaternary Paleoclimatology. Allen Unwin, London, 472p.
- Bradley, R.S. and England, J.H., 1978. Recent climatic fluctuations of the Canadian high Arctic and their significance for glaciology. Arctic and Alpine Research, Vol. 10, p.715-731.
- Bradley, R.S. and England, J.H., 1979. Synoptic climatology of the Canadian high Arctic. Geografiska Annaler, Vol. 61A, p.187-201.
- Bradley, R.S. and Serrez, M.C., 1987. Mass balance of two high Arctic plateau ice caps. Journal of Glaciology, Vol. 33, p.123-128.
- Brassard, G., 1971. The mosses of northern Ellesmere Island, Arctic Canada. Ecology and phytogeography, with an analysis for the Queen Elizabeth Islands. The Bryologist, Vol. 74, p.234-281.
- Brigham-Grette, J., Blasco, S.M. and Miller, G.H., 1987. Discrepancies in the amino acid geochronology of Arctic Ocean cores. Abstract, 12th INQUA

- International Congress, Ottawa, p.136.
- Broecker, W.S., 1975. Floating glacial ice caps in the Arctic Ocean. Science, Vol. 188, p.1116-1118.
- Brothie, J.F. and Silvester, R., 1969. On crustal flexure. Journal of Geophysical Research, Vol. 74, p.5240-5252.
- Brown, M.P., 1985. Glaciolacustrine Sedimentation in South Piper Pass, Northern Ellesmere Island. Unpublished M.Sc. thesis, University of Alberta, 123p.
- Canadian Hydrographic Service, 1974. Map no.7954, 1:500,000.
- Cheel, R.J. and Rust, B.R., 1982. Coarse grained facies of glacio-marine deposits near Ottawa, Canada. In Davidson-Arnott, R., Nickling, W. and Fahey, R.D. (eds), Research in Glacial, Glaciofluvial and Glaciolacustrine Systems, Geobooks, Norwich, p.279-292.
- Chorley, R.J., Schumm, S.A. and Sugden, D.E., 1984. Geomorphology, Methuen, 605p.
- Christie, R.L., 1964. Geological reconnaissance of northeastern Ellesmere Island, District of Franklin. Geological Survey of Canada, Memoir no. 331.
- Christie, R.L., 1967. Reconnaissance of the surficial geology of northeastern Ellesmere Island, Arctic archipelago. Geological Survey of Canada, Bulletin no.138.
- Christie, R.L., 1975. Glacial features of the Borglum Elv region, eastern north Greenland. Rapp. Gronlands Geol. Unders., Vol. 75, p.26-28.
- Clark, D.L., 1982. Origin, nature and world climate effect of Arctic Ocean ice cover. Nature, Vol. 300, p.321-325.
- Clark, D.L., Vincent, J-S., Jones, G.A. and Morris, W.A., 1984. Correlation of marine and continental glacial and interglacial events, Arctic Ocean and Banks Island. Nature, Vol. 311, p.147-148.
- Clark, D.L., Whitman, R.R., Morgan, K.A. and Mackey, S.D., 1980. Stratigraphy and glacial-marine sediments of the Amerasian Basin, central Arctic Ocean. Geological Society of America, Special Paper, no.181, 57p.
- Clark, J.A., 1980. A numerical model of worldwide sea level changes on a viscoelastic earth. In Morner, N-A. (ed), Earth Rheology, Isostasy and Eustasy, John Wiley and Sons, London, p.525-534.
- Clark, J.A., 1985. Forward and inverse models in sea level studies. In Woldenberg, M.J. (ed), Models in Geomorphology, Allen and Unwin, Boston, p.119-138.
- Clark, J.A., Farrell, W.E. and Peltier, W.R., 1978. Global changes in postglacial sea level: a numerical calculation. Quaternary Research, Vol. 9, p.265-287.
- CLIMAP Project Members, 1976. The surface of the ice age earth. Science, Vol. 191, p. 1131-1144.
- Coleman, A.P., 1920. Extent and thickness of the Labrador ice sheet. Bulletin of the Geological Society of America, Vol. 31, p.319-328.
- Crary, A.P., 1956. Geophysical studies along northern Ellesmere Island. Arctic, Vol. 9, p.155-165.
- Crary, A.P., 1958. Arctic ice island and ice shelf studies, part 1. Arctic, Vol. 11, p.3-42.
- Crary, A.P., 1960. Arctic ice island and ice shelf studies, part 2. Arctic, Vol. 13, p.32-50.
- Curry, J.R., 1964. Transgressions and regressions. In Miller, R.L. (ed), Marine Geology, p.175-203.
- Dalrymple, R.W. and Maass, O.C., 1987. Clay mineralogy of late Cenozoic sediments in the CESAR cores, Alpha Ridge, central Arctic Ocean. Canadian Journal of Earth Sciences, Vol. 24, p. 1562-1569.
- Daly, R.A., 1902. Geology of the northeast coast of Labrador. Bulletin of the

- Museum of Comp. Zoology, Harvard, Geology Series no.5, p.203-270.
- Dansgaard, W.S., Johnsen, J.J., Clausen, H.B. and Langway, C.C., Jr., 1971. Climatic record released by the Camp Century ice core. In, Turekian, K.K. (ed), Late Cenozoic Glacial Ages, Yale University Press, p.37-56.
- Dansgaard, W.S., Johnsen, J.J., Clausen, H.B. and Gundestrup, N., 1973. Stable isotope glaciology. Meddeleser om Gronland, Vol. 197, p.1-53.
- Davies, W.E., 1972. Landscape of northern Greenland. C.R.R.E.L., Special Report no. 164, 67p.
- Dawes, P.R., 1986. Glacial erratics on the Arctic Ocean margin of north Greenland: implications for an extensive ice shelf. Bulletin of the Geological Society of Denmark, Vol. 35, p.59-69.
- Denton, G.H. and Hughes, T.J.(eds), 1981. The Last Great Ice Sheets, John Wiley and Sons, New York, 484p.
- Denton, G.H., Hughes, T.J. and Karlen, W., 1986. Global ice sheet system interlocked by sea level. Quaternary Research, Vol. 26, p.3-26.
- Donn, W.L. and Ewing, M., 1966. A theory of ice ages 3. Science, Vol. 152, p.1706-1712.
- Donn, W.L. and Shaw, D.M., 1965. The maintenance of an ice-free Arctic Ocean. In, Sears, M. (ed), Progress in Oceanography, Pergamon, p.105-113.
- Dowdeswell, J.A., 1986. The distribution and character of sediments in a tidewater glacier, southern Baffin Island, N.W.T., Canada. Arctic and Alpine Research, Vol. 18, p.45-56.
- Drewry, D., 1986. Glacial Geologic Processes, Edward Arnold, London, 276p.
- Dyck, W. and Fyles, J.G., 1963. Geological Survey of Canada radiocarbon dates II. Radiocarbon, Vol. 5, p.39-55.
- Dyke, A.S., 1979. Glacial and sea level history of southwestern Cumberland Peninsula, Baffin Island, N.W.T., Canada. Arctic and Alpine Research, Vol. 11, p.179-202.
- Dyke, A.S., 1983. Quaternary geology of Somerset Island, District of Franklin. Geological Survey of Canada, Memoir no.404, 32p.
- Dyke, A.S., 1984. Quaternary geology of Boothia Peninsula and northern District of Keewatin, central Canadian Arctic. Geological Survey of Canada, Memoir no.407, 26p.
- Embleton, C. and King, C.A.M., 1975. Glacial Geomorphology, Edward Arnold, London, 573p.
- England, J.H., 1974a. The glacial geology of northeastern Ellesmere Island, N.W.T., Canada. Unpublished PhD thesis, University of Colorado, 234p.
- England, J.H., 1974b. Advance of the Greenland ice sheet on to northeastern Ellesmere Island. Nature, Vol. 252, p.373-375.
- England, J.H., 1974c. Holocene history of a portion of northernmost Ellesmere Island. Arctic, Vol. 27, p.154-157.
- England, J.H., 1976a. Late Quaternary glaciation of the eastern Queen Elizabeth Islands, N.W.T., Canada: alternative models. Quaternary Research, Vol. 6, p.185-202.
- England, J.H., 1976b. Postglacial isobases and uplift curves from the Canadian and Greenland high Arctic. Arctic and Alpine Research, Vol. 8, p.61-78.
- England, J.H., 1978. The glacial geology of northeastern Ellesmere Island, N.W.T., Canada. Canadian Journal of Earth Sciences, Vol. 15, p.603-617.
- England, J.H., 1982. Postglacial emergence along northern Nares Strait. In, Dawes, P.R. and Kerr, J.W., Nares Strait and the Drift of Greenland: a Conflict in Plate Tectonics, Meddeleser om Gronland, Geoscience, Vol. 8, p.65-75.
- England, J.H., 1983. Isostatic adjustments in a full glacial sea. Canadian Journal of Earth Sciences, Vol. 20, p.895-917.
- England, J.H., 1985a. The late Quaternary history of Hall Land, northwest Greenland. Canadian Journal of Earth Sciences, Vol. 22, p.1394-1408.
- England, J.H., 1985b. On the origin of high Arctic fiords. Abstract, 14th

- Annual Arctic Workshop, Bedford Institute of Oceanography, Halifax, Nova Scotia.
- England, J.H., 1986a. On the instantaneous removal of the Innuitian ice sheet? Abstract, 15th Annual Arctic Workshop, INSTAAR, Boulder, Colorado, p.18-19.
- England, J.H., 1986b. A paleoglaciation level for north-central Ellesmere Island, N.W.T.. Arctic and Alpine Research, Vol. 18, p.217-222.
- England, J.H., 1986c. Glacial erosion of a high Arctic valley. Journal of Glaciology, Vol. 32, p.60-64.
- England, J.H., 1986d. The last great mythological ice sheets. Programme and Abstracts of the 9th Biennial AMQUA meeting, Champaign-Urbana, p.20-22.
- England, J.H., 1987a. The late Quaternary history of Hall Land, northwest Greenland: Reply. Canadian Journal of Earth Sciences, Vol. 24, p.374-380.
- England, J.H., 1987b. Glaciation and the Evolution of the high Arctic landscape. Geology, Vol. 15, p.419-424.
- England, J.H., 1987c. *In situ* shells of full glacial age beneath former ice shelves. Abstract, 16th Annual Arctic Workshop, Edmonton, p.20-22.
- England, J.H. and Bednarski, J., 1986. Postglacial isobases from northern Ellesmere Island and Greenland: new data. Geographie Physique et Quaternaire, Vol. XL, p.299-305.
- England, J.H. and Bednarski, J., in press. Northern Ellesmere Island. In, Fulton, R.J. and Heginbottom, J.A., Quaternary Geology of Canada, Geology and Economic Minerals of Canada, 6th Edition, Geological Survey of Canada, Ottawa.
- England, J.H. and Bradley, R.S., 1978. Past glacial activity in the Canadian high Arctic. Science, Vol.200, p.265-270.
- England, J.H., Bradley, R.S. and Miller, G.H., 1978. Former ice shelves in the Canadian high Arctic. Journal of Glaciology, Vol. 20, p.393-404.
- England, J.H., Bradley, R.S. and Stuckenrath, R., 1981a. Multiple glaciations and marine transgressions, western Kennedy Channel, N.W.T., Canada. Boreas, Vol. 10, p.71-89.
- England, J.H., Fisher, D.A. and Koerner, R.M., 1982. Reconciling glacial geology and the ice core record on northeast Ellesmere Island. Geological Society of America, Abstracts with Programs, Vol. 14, p.484.
- England, J.H., Kershaw, L., LaFarge-England, C. and Bednarski, J., 1981b. Northern Ellesmere Island: a natural resource inventory. Report to Parks Canada, Department of Geography, University of Alberta, Edmonton, 237p.
- Evans, D.J.A. and Fisher, T.G., 1987. Evidence of a periodic ice-cliff avalanche on northwest Ellesmere Island, Canadian high Arctic. Journal of Glaciology, Vol. 33, p.68-71.
- Evans, D.J.A. and Lemmen, D.S., 1987. Indicators of Holocene climatic change from Wootton Peninsula/ Phillips Inlet and Marvin Peninsula/ Disraeli Fiord, northern Ellesmere Island. Abstract, 12th INQUA International Congress, Ottawa, p.163.
- Evenson, E.B., Clinch, J.M. and Stephens, G.C., 1986. The importance of fluvial systems in debris transport at alpine glacier margins. Programme and Abstracts of the 9th Biennial AMQUA Meeting, Champaign-Urbana, 1986, p.58-60.
- Ewing, M. and Donn, W.L., 1956. A theory of ice ages. Science, Vol. 123, p.1061-1066. Ewing, M. and Donn, W.L., 1958. A theory of ice ages 2. Science, Vol. 126, p.1157-1162.
- Eyles, C.H., Eyles, N. and Miall, A.D., 1985. Models of glaciomarine sedimentation and their application to the interpretation of ancient glacial sequences. Palaeogeography, Palaeoclimatology, Palaeoecology, Vol. 51, p.15-84.
- Eyles, N., 1983. Glacial geology: a landsystems approach. In, Eyles, N.(ed);

- Glacial Geology: An Introduction for Engineers and Earth Scientists. Pergamon, Oxford, p.1-18.
- Eyles, N., Eyles, C.H. and Miall, A.D., 1983. Lithofacies types and vertical profile models; an alternative approach to the description and environmental interpretation of glacial diamict and diamictite sequences. Sedimentology, Vol. 30, p.393-410.
- Fairchild, H.L., 1905. Ice erosion theory a fallacy. Bulletin of the Geological Society of America, Vol. 16, p.13-74.
- Farrell, W.E. and Clark, J.A., 1976. On postglacial sea level. Geophysical Journal of the Royal Astronomical Society, Vol. 46, p.647-667.
- Fisher, D.A. and Koerner, R.M., 1980. Some aspects of climatic change in the high Arctic during the Holocene as deduced from ice cores. In, Mahaney, W.C. (ed), Quaternary Paleoclimate, GeoBooks, p.249-271.
- Fisher, D.A. and Koerner, R.M., 1983. Ice core study: a climatic link between the past, present and future. In, Harington, C.R. (ed), Climatic Change in Canada, Syllogeus 49, p.50-69.
- Flint, R.F., 1971. Glacial and Quaternary Geology, John Wiley and Sons, 892p.
- Fortier, Y.O. and Morley, L.W., 1956. Geological units of the Arctic Islands. Royal Society of Canada Transactions, Vol. 50, p.3-12.
- Frisch, T.O., 1974. Metamorphic and plutonic rocks of northernmost Ellesmere Island, District of Franklin. Geological Survey of Canada, Bulletin no. 229.
- Funder, S., Bennike, O., Mogensen, G.T., Noe-Nygaard, B., Pedersen, S.A.S. and Petersen, K.S., 1984. The Kap Kobenhavn Formation, a late Cainozoic sedimentary sequence in north Greenland. Rapport Gronlands Geologiske Undersogelse, Vol. 120, p.9-18.
- Gemmell, A.M.D., Sharp, M.J. and Sugden, D.E., 1986. Debris from the basal ice of the Agassiz Ice Cap, Ellesmere Island, Arctic Canada. Earth Surface Processes and Landforms, Vol. 11, p.123-130.
- Geological Survey of Canada, 1980. Guide to Authors, Miscellaneous Report no.29.
- Gilbert, R., Syvitski, J.P.M., and Tatlor, R.B., 1985. Reconnaissance study of proglacial Stewart Lakes, Baffin Island, District of Franklin. In Current Research, Geological Survey of Canada, Paper no.85-1A, p.505-510.
- Gravenor, C.P., Von Brunn, V. and Dreimanis, A., 1984. Nature and classification of waterlain glacial sediments, exemplified by Pleistocene, late Palaeozoic and Precambrian deposits. Earth Science Reviews, Vol. 20, p.105-166.
- Gregory, J.W., 1913. The Nature and Origin of Fjords, J. Murray, London, 542p.
- Grosswald, M.G., 1980. Late Weichselian ice sheet of northern Eurasia. Quaternary Research, Vol. 13, p.1-32.
- Haggblom, A., 1982. Driftwood in Svalbard as an indicator of sea ice conditions. Geografiska Annaler, Vol. 64A, p.81-94.
- Hambrey, M.J. and Muller, F., 1978. Structure and ice deformation in the White Glacier, Axel Heiberg Island, N.W.T., Canada. Journal of Glaciology, Vol. 20, p.41-66.
- Harris, C. and Bothamley, K., 1984. Englacial deltaic sediments as evidence for basal freezing and marginal shearing, Leirbreen, southern Norway. Journal of Glaciology, Vol. 30, p.30-34.
- Hattersley-Smith, G., 1957. The rolls on the Ellesmere Ice Shelf. Arctic, Vol. 10, p.32-44.
- Hattersley-Smith, G., 1960a. Some remarks on glaciers and climate in northern Ellesmere Island. Geografiska Annaler, Vol. 42, p.45-48.
- Hattersley-Smith, G., 1960b. Glaciological studies: snow cover, accumulation

- and ablation. Defence Research Board, Ottawa, Hazen 10.
- Hattersley-Smith, G., 1961. Some glaciological studies in the Lake Hazen region of northern Ellesmere Island. In, Raasch, G.O.(ed), Geology of the Arctic 2, p.791-808.
- Hattersley-Smith, G., 1963. The Ward Hunt Ice Shelf: recent changes of the ice front. Journal of Glaciology, Vol. 4, p.415-424.
- Hattersley-Smith, G., 1969. Glacial features of Tanquary Fiord and adjoining areas of northern Ellesmere Island, N.W.T.. Journal of Glaciology, Vol. 8, p.23-50.
- Hattersley-Smith, G., 1972. Climatic change and related problems in northern Ellesmere Island, N.W.T., Canada. In, Vasari, Y., Hyvarinen, H. and Hicks, S. (eds), Climatic Changes in Arctic Areas During the Last Ten Thousand Years. Acta Univ. Oulu, A3 Geol. 1, p.137-148.
- Hattersley-Smith, G., Crary, A.P. and Christie, R.L., 1955. Northern Ellesmere Island, 1953 and 1954. Arctic, Vol. 8, p.3-36.
- Hattersley-Smith, G., Fuzesy, A. and Evans, S., 1969. Glacier depths in northern Ellesmere Island: airborne radio-echo sounding in 1966. Defence Research Board, Ottawa, Technical Note no.69-6, Hazen 36, 23p.
- Hattersley-Smith, G. and Long, A., 1967. Postglacial uplift at Tanquary Fiord, northern Ellesmere Island, N.W.T.. Arctic, Vol. 20, p.255-260.
- Hattersley-Smith, G. and Serson, H., 1970. Mass balance of the Ward Hunt ice rise and ice shelf: a ten year record. Journal of Glaciology, Vol. 9, p.247-252.
- Herman, Y. and Hopkins, D.M., 1980. Arctic Ocean climate in late Cenozoic time. Science, Vol. 209, p.557-562.
- Hodgson, D.A., 1985. The last glaciation of west-central Ellesmere Island, Arctic archipelago, Canada. Canadian Journal of Earth Sciences, Vol. 22, p.347-368.
- Hooke, R. LeB., 1973. Flow near the margin of the Barnes Ice Cap and the development of ice-cored moraines. Geological Society of America Bulletin, Vol. 84, p.3929-48.
- Horn, D.R., 1963. Marine geology, Peary Channel, District of Franklin, N.W.T.. Geological Survey of Canada, Paper no.63-11, 33p.
- Hudleston, P.J., 1976. Recumbent folding in the base of the Barnes Ice Cap, Baffin Island, N.W.T., Canada. Geological Society of America Bulletin, Vol. 87, p.1684-1692.
- Hughes, T.J., 1987. The marine ice transgression hypothesis. Geografiska Annaler, Vol. 69A, p.237-250.
- Hughes, T.J./ Andrews, J.T., 1980/1981. Genes and glacial history: a letter to the editor./ Big and small ice. Boreas, Vol. 9, p.149/ Vol. 10, p.52.
- Hughes, T.J., Denton, G.H. and Fastook, J.L., 1985. The Antarctic ice sheet: an analog for northern hemisphere paleo-ice sheets? In, Woldenberg, M.J.(ed), Models in Geomorphology, p.25-72.
- Hughes, T.J., Denton, G.H. and Grosswald, M.G., 1977. Was there a late Wurm Arctic ice sheet? Nature, Vol. 266, p.596-602.
- Hunkins, K., Be, A.W.H., Opdyke, N.D. and Mathiew, G., 1971. The late Cenozoic history of the Arctic Ocean. In, Turekian, K.K. (ed), The Late Cenozoic Glacial Ages, Yale University Press, p.215-237.
- Idso, S.B., 1980. The climatological significance of a doubling of the Earth's atmospheric carbon dioxide concentration. Science, Vol. 207, p.1462-1463.
- Idso, S.B., 1982. An empirical evaluation of Earth's surface air temperature response to an increase in atmospheric carbon dioxide concentration. In, Reck, R.A. and Hummel, J.R. (eds), Interpretation of Climate and Photochemical Models. Ozone and Temperature Measurements. American Institute of Physics, p.119-134.
- Ives, J.D., 1974. Biological refugia and the nunatak hypothesis. In, Ives,

- J.D. and Barry, R.G. (eds), Arctic and Alpine Environments, Methuen, p.605-636.
- Ives, J.D., 1978. The maximum extent of the Laurentide ice sheet along the east coast of north America during the last glaciation. Arctic, Vol. 31, p.24-53.
- Jackson, C.I., 1959. The meteorology of Lake Hazen, N.W.T., Part 1: analysis of observations. Operation Hazen, Defence Research Board, Ottawa, Report no.8.
- Jeffries, M.O., 1986. Ice island calvings and ice shelf changes, Milne Ice Shelf and Ayles Ice Shelf, Ellesmere Island, N.W.T.. Arctic, Vol. 39, p.15-19.
- Jeffries, M.O., 1987. The growth, structure and disintegration of Arctic ice shelves. Polar Record, Vol. 23.
- Kalin, M., 1972. The active push moraine of the Thompson Glacier, Axel Heiberg Island. Research Report (Glaciology), no.4, McGill University, Montreal, 68p.
- Kellogg, W.W., 1975. Climatic feedback mechanisms involving the polar regions. In, Weller, G. and Bowling, S.A. (eds), Climate of the Arctic. University of Alaska Press, p.111-116.
- Kelly, M., 1980. The status of the neoglacial in western Greenland. Gronland Geologiske Undersogelse Rapport, no. 96, 24p.
- Kerr, J.W., 1980. Structural framework of Lancaster aulacogen, Arctic Canada. Geological Survey of Canada, Bulletin no.319, 24p.
- King, L., 1983. Contribution to the glacial history of the Borup Fiord area, northern Ellesmere Island, N.W.T., Canada. In, Schroeder-Lanz, H., Late and Postglacial Oscillations of Glaciers, A.A. Balkema, Rotterdam, p.305-323.
- Klassen, R.A., 1982. Glaciotectonic thrust plates, Bylot Island, District of Franklin, Canada. In, Current Research, Geological Survey of Canada, Paper 82-1A, p.369-373.
- Koenig, L.S., Greenaway, K.R., Dunbar, M. and Hattersley-Smith, G., 1952. Arctic ice islands. Arctic, Vol. 5, p.67-103.
- Koerner, R.M., 1977a. Devon Island ice cap: core stratigraphy and paleoclimate. Science, Vol. 196, p.15-18.
- Koerner, R.M., 1977b. Ice thickness measurements and their implications with respect to past and present ice volumes in the Canadian high Arctic ice caps. Canadian Journal of Earth Sciences, Vol. 14, p.2697-2705.
- Koerner, R.M., 1979. Accumulation, ablation and oxygen isotope variations on the Queen Elizabeth Islands ice caps, Canada. Journal of Glaciology, Vol. 22, p.25-41.
- Koerner, R.M. and Fisher, D.A., 1981. Studying climatic change from Canadian high Arctic ice cores. In, Harington, C.R. (ed), Climatic Change in Canada 2, National Museum of Canada, Ottawa, Syllogus 33, p.195-218.
- Koerner, R.M. and Fisher, D.A., 1985. The Devon Island ice core and the glacial record. In, Andrews, J.T. (ed), Quaternary Environments: Eastern Canadian Arctic, Baffin Bay and West Greenland, Allen and Unwin, p.309-327.
- Koerner, R.M., Fisher, D.A. and Paterson, W.S.B., 1987. Wisconsinan and pre-Wisconsinan ice thicknesses on Ellesmere Island, Canada: inferences from ice cores. Canadian Journal of Earth Sciences, Vol. 24, p.296-301.
- Koerner, R.M. and Paterson, W.S.B., 1974. Analysis of a core through the Meighen Ice Cap, Arctic Canada and its paleoclimatic implications. Quaternary Research, Vol. 4, p.253-263.
- Kovacs, A., 1983. Shore ice ride-up and pile-up features, part 1: Alaska's Beaufort Sea coast. Cold Regions Research and Engineering Laboratory, Hanover, Report no.83-9, 51p.

- Krumbein, W.C., 1941. Measurement and geological significance of shape and roundness of sedimentary particles. Journal of Sedimentary Petrology, Vol. 11, p.64-72.
- Lawson, D.E., 1979. Sedimentological analysis of the western terminus region of the Matanuska Glacier, Alaska. Cold Regions Research and Engineering Laboratory, Hanover, Report no.79-9, 112p.
- Leech, R.E., 1966. The spiders (Areneida) of Hazen Camp, 81°49'N, 71°18'W. Questiones Entomologicae, Vol. 2, p.153-212.
- Lemmen, D.S., Evans, D.J.A. and England, J.H., 1988. Glaciers and the morphology and structure of the Milne Ice Shelf, Ellesmere Island, N.W.T., Canada: discussion. Arctic and Alpine Research, in press.
- Linton, D.L., 1955. The problem of tors. Geographical Journal, Vol. 121, p.470-487.
- Long, A., 1967. Age of trapped seawater at the bottom of Lake Tuborg, Ellesmere Island, N.W.T.. Transactions of the American Geophysical Union, Vol. 48, p.136.
- Lowden, J.A. and Blake, W., Jr., 1979. Geological Survey of Canada radiocarbon dates XIX, Geological Survey of Canada, Paper no. 79-7, 58p.
- Lyons, J.B. and Mielke, J.E., 1973. Holocene history of a portion of northernmost Ellesmere Island. Arctic, Vol. 26, p.314-323.
- Lyons, J.B., Ragle, R.H. and Tamburi, A.J., 1972. Growth and grounding of the Ellesmere Island ice rises. Journal of Glaciology, Vol. 11, p.43-52.
- Lyons, J.B., Savin, S.M. and Tamburi, A.J., 1971. Basement ice, Ward Hunt Ice Shelf, Ellesmere Island, Canada. Journal of Glaciology, Vol. 10, p.93-100.
- Maag, H., 1969. Ice dammed lakes and marginal glacial drainage on Axel Heiberg Island. Axel Heiberg Island Research Report, McGill University, 147p.
- Mackay, J.R., 1956. Deformation by glacier ice at Nicholson Peninsula, N.W.T., Canada. Arctic, Vol. 9, p.218-228.
- Mackay, J.R., 1959. Glacier ice thrust features of the Yukon coast. Geographical Bulletin, No. 13, p.5-21.
- Marshall, E.W., 1955. Structural and stratigraphic studies on the northern Ellesmere Island ice shelf. Arctic, Vol. 8, p.109-114.
- Mathews, W.H. and Mackay, J.R., 1960. Deformation of soils by glacier ice and the influence of pore pressures and permafrost. Transactions of the Royal Society of Canada, Vol. 54, Series 3, p.27-36.
- Maxwell, J.B., 1981. Climatic regions of the Canadian Arctic islands. Arctic, Vol. 34, p.225-240.
- McCabe, A.M., Dardis, G.F. and Hanvey, P.M., 1984. Sedimentology of a late Pleistocene submarine-moraine complex, County Down, Northern Ireland. Journal of Sedimentary Petrology, Vol. 54, p.716-730.
- McCabe, A.M., Haynes, J.R. and Macmillan, N., 1986. Late Pleistocene tidewater glaciers and glaciomarine sequences from north County Mayo, Republic of Ireland. Journal of Quaternary Science, Vol. 1, p.73-84.
- Mercer, J.H., 1970. A former ice sheet in the Arctic Ocean? Palaeogeography, Palaeoclimatology, Palaeoecology, Vol. 8, p.19-27.
- Miall, A.D., 1977. A review of the braided river depositional environment. Earth Science Reviews, Vol. 13, p.1-62.
- Miall, A.D., 1979. Tertiary fluvial sediments in the Lake Hazen intermontane basin, Ellesmere Island, Arctic Canada. Geological Survey of Canada, Paper no.79-9.
- Miller, G.H., Bradley, R.S. and Andrews, J.T., 1975. The glaciation level and lowest equilibrium line altitude in the high Canadian Arctic: maps and climatic interpretation. Arctic and Alpine Research, Vol. 7, p.155-168.
- Morris, T.H., Clark, D.L. and Blasco, S.M., 1985. Sediments of the Lomonosov Ridge and Makarov Basin: a Pleistocene stratigraphy for the North Pole.

- Geological Society of America Bulletin, Vol. 96, p.901-910.
- Muller, F., 1976. On the thermal regime of a high Arctic valley glacier. Journal of Glaciology, Vol. 16, p.119-133.
- Nelson, A.R., 1981. Quaternary glacial and marine stratigraphy of the Qivitu Peninsula, northern Cumberland Peninsula, Baffin Island, Canada: summary. Geological Society of America Bulletin, Vol. 92, p.512-518.
- Odell, N.E., 1938. The geology and physiography of northernmost Labrador. In, Forbes, A.(ed), Northern Labrador Mapped from the Air, American Geographical Society Special Publication no.22, p.187-216.
- Paterson, W.S.B., 1977. Extent of the late Wisconsin glaciation in northwest Greenland and northern Ellesmere Island: a review of the glaciological and geological evidence. Quaternary Research, Vol. 8, p.180-190.
- Paterson, W.S.B., 1981. The Physics of Glaciers, Pergamon, Oxford, 380p.
- Paterson, W.S.B., Koerner, R.M., Fisher, D., Johnsen, H.J., Dansgaard, W., Bucher, P. and Oeschger, H., 1977. An oxygen isotope climatic record from the Devon Island Ice Cap, Arctic Canada. Nature, Vol. 266, p.508-511.
- Peary, R.F., 1907. Nearest the Pole. A Narrative of the Polar Expedition of the Peary Arctic Club in the S.S. "Roosevelt", 1905-1906. Doubleday, Page and Company, New York.
- Pelletier, B.R., 1966. Development of submarine physiography in the Canadian Arctic and its relation to crustal movements. In, Garland, G.D.(ed), Continental Drift, University of Toronto Press, p.77-101.
- Pelletier, B.R., 1979. Review of surficial geology and engineering hazards in the Canadian offshore. Maritime Sediments, Vol. 15, p.55-91.
- Powell, R.D., 1981. A model for sedimentation by tidewater glaciers. Annals of Glaciology, Vol. 2, p.129-134.
- Powell, R.D., 1984. Glacimarine processes and lithofacies modelling of ice shelf and tidewater glacier sediments based on Quaternary examples. Marine Geology, Vol. 57, p.1-52.
- Powers, M., 1953. A new roundness scale for sedimentary particles. Journal of Sedimentary Petrology, Vol. 25, p.117-119.
- Reh, B.T., 1983. Digital signal processing of UHF radio-echo sounding data from northern Ellesmere Island. Unpublished M.Sc. thesis, University of British Columbia, 88p.
- Reh, B.T., Selby, M.J. and Smith, C.J.R., 1981. A comparison of observed and theoretical postglacial relative sea level in Atlantic Canada. Canadian Journal of Earth Sciences, Vol. 18, p.1146-1163.
- Reh, B.T., Selby, M.J. and Smith, C.J.R., 1981. Polar desert sandar in Antarctica. New Zealand Journal of Geology and Geophysics, Vol. 23, p.595-604.
- Reh, B.T., 1982. Quaternary geology of the Yukon coastal plain. Geological Survey of Canada, Bulletin no. 317, 49p.
- Reeh, N., 1982. A plasticity theory approach to the steady-state shape of a three dimensional ice sheet. Journal of Glaciology, Vol. 28, p.431-455.
- Reeh, N., 1984. Reconstruction of the glacial ice covers of Greenland and the Canadian Arctic islands by three-dimensional, perfectly plastic ice sheet modelling. Annals of Glaciology, Vol. 5, p.115-121.
- Retelle, M.J., 1986. Glacial geology and Quaternary marine stratigraphy of the Robeson Channel area, northeastern Ellesmere Island, N.W.T.. Canadian Journal of Earth Sciences, Vol. 23, p.1001-1012.
- Ringrose, S., 1982. Depositional processes in the development of eskers in Manitoba. In, Davidson-Arnott, R., Nickling, W. and Fahey, B.D. (eds), Research in Glacial, Glacio-fluvial and Glacio-lacustrine Systems.

- GeoBooks, Norwich, p.117-137.
- Rotnicki, K., 1976. The theoretical basis for and a model of the origin of glaciotectionic deformations. Quaestiones Geographicae, Vol. 3, p.103-139.
- Rust, B.R. and Romanelli, R., 1975. Late Quaternary subaqueous outwash deposits near Ottawa, Canada. In, Jopling, A.V. and McDonald, B.C. (eds), Glaciofluvial and Glaciolacustrine Sedimentation, SEPM Special Publication no.23, p.177-192.
- Sagar, R.B., 1962. Meteorological and glaciological studies: ice rise station, Ward Hunt Island, May to September 1960. Arctic Institute of North America, Research Paper no.24.
- Schei, P., 1904. In, Sverdrup, O., New Land, Four Years in the Arctic Regions, Vol.2, Longmans, London, Appendix 1, p.455-465.
- Schneider, S.H., Kellogg, W.W. and Ramanathan, V., 1980. Carbon dioxide and climate. Science, Vol. 210, p.6-7.
- Selby, M.J., 1972. The termini and moraines of glaciers in the McMurdo Dry Valleys, Antarctica. Proceedings of the 7th New Zealand Geography Conference, Hamilton, 1972, p.247-257.
- Selby, M.J., 1985. Earth's Changing Surface, Oxford University Press, 607p.
- Sharp, M., 1982. Modification of clasts in lodgement tills by glacial erosion. Journal of Glaciology, Vol. 28, p.475-481.
- Sharp, M., 1986. Sedimentation and stratigraphy at Eyjabakkajokull- an Icelandic surging glacier. Quaternary Research, Vol. 24, p.268-284.
- Shaw, J., 1977a. Till body morphology and structure related to glacier flow. Boreas, Vol. 6, p.189-201.
- Shaw, J., 1977b. Tills deposited in arid polar environments. Canadian Journal of Earth Sciences, Vol. 14, p.1239-1245.
- Shaw, J., 1979. Genesis of the Sveg tills and Rogen moraines of central Sweden: a model of basal melt out. Boreas, Vol. 8, p.409-426.
- Shaw, J., 1982. Melt out till in the Edmonton area, Alberta, Canada. Canadian Journal of Earth Sciences, Vol. 19, p.1548-1569.
- Shaw, J., 1985. Subglacial and ice marginal environments. In, Ashley, G.M., Shaw, J. and Smith, N.D. (eds), Glacial Sedimentary Environments, SEPM Short Course No.16, p.7-84.
- Sim, V.W., 1961. A note on high level marine shells on Fosheim Peninsula, Ellesmere Island, N.W.T.. Geographical Bulletin, Vol.16, p.120-123.
- Smith, D.I., 1959. Geomorphology. In, Operation Hazen Narrative and Preliminary Reports, 1957-1958, Defence Research Board
- Smith, D.I., 1961. The glaciation of northern Ellesmere Island. Folia Geographica Danica, Vol. 9, p.224-234.
- Sobczak, L.W., 1982. Fragmentation of the Canadian Arctic archipelago, Greenland and surrounding oceans. In, Dawes, P.R. and Kerr, J.W. (eds), Nares Strait and the Drift of Greenland: A Conflict in Plate Tectonics, Meddeleser om Gronland, Geoscience 8, p.221-236.
- Stewart, T.G., 1981. The Holocene Paleoenvironments of Clements Markham Inlet, northern Ellesmere Island, N.W.T., Canada. Unpublished M.Sc. thesis, University of Alberta, 135p.
- Stewart, T.G., 1988. Deglacial-marine sediments from Clements Markham Inlet, Ellesmere Island, N.W.T., Canada. Unpublished PhD thesis, University of Alberta, 229p.
- Stewart, T.G. and England, J.H., 1983. Holocene sea ice variations and paleoenvironmental change, northernmost Ellesmere Island, N.W.T., Canada. Arctic and Alpine Research, Vol. 15, p.1-17.
- Stirling, I., Cleator, H. and Smith, T.G., 1981. Marine mammals. In, Stirling, I. and Cleator, H. (eds), Polynas in the Canadian Arctic, Canadian Wildlife Service, Occasional Paper no.45, p.45-58.
- Sugden, D.E., 1977. Reconstruction of the morphology, dynamics and thermal

- characteristics of the Laurentide ice sheet at its maximum. Arctic and Alpine Research, Vol. 9, p.21-47.
- Sugden, D.E., 1978. Glacial erosion by the Laurentide ice sheet. Journal of Glaciology, Vol. 20, p.367-391.
- Sugden, D.E. and Clapperton, C.M., 1981. An ice shelf moraine, George VI Sound, Antarctica. Annals of Glaciology, Vol. 2, p.135-141.
- Sugden, D.E. and John, B.S., 1975. Glaciers and Landscape. Edward Arnold, London, 376p.
- Sugden, D.E., Knight, P.G., Livesay, N., Lorrain, R.D., Souchez, R.A., Tison, J.-L. and Jouzel, J., 1987. Evidence for two zones of debris entrainment beneath the Greenland ice sheet. Nature, Vol. 328, p.238-241.
- Taylor, A., 1956. Physical geography of the Queen Elizabeth Islands, Canada. Volume II Glaciology, Volume III Ellesmere Island-Grant Land. American Geographical Society, New York.
- Tedrow, J.C.F., 1970. Soil investigations in Inglefield Land, Greenland. Meddeleser om Gronland, Bd. 188, 93p.
- Thomas, R.H. and Bentley, C.R., 1978. A model for Holocene retreat of the West Antarctic Ice Sheet. Quaternary Research, Vol. 10, p.150-170.
- Thorsteinsson, R. and Tozer, E.T., 1976. Geology of the Arctic archipelago. In, Douglas, R.J.W. (ed), Geology and Economic Minerals of Canada, Geological Survey of Canada, Ottawa, p.549-590.
- Tozer, E.T., 1963. Mesozoic and Tertiary stratigraphy, western Ellesmere Island and Axel Heiberg Island, District of Franklin. Geological Survey of Canada, Paper no.63-30.
- Trautman, M.A., 1963. Isotopes Inc., radiocarbon measurements III. Radiocarbon, Vol. 5, p.62-79.
- Trettin, H.P., 1969. Geology of Ordovician to Pennsylvanian rocks, M'Clintock Inlet, north coast of Ellesmere Island, Arctic archipelago. Geological Survey of Canada, Bulletin no.183.
- Trettin, H.P., 1971. Geology of Lower Paleozoic Formations, Hazen Plateau and southern Grant Land Mountains, Ellesmere Island, Arctic archipelago. Geological Survey of Canada, Bulletin no. 203.
- Trettin, H.P., 1972. The Innuitian Province. In, Price, R.A. and Douglas, R.J.W. (eds), Variations in Tectonic Styles in Canada, Geological Association of Canada, Special Paper no.11.
- Trettin, H.P., 1987. Pearya: a composite terrane with Caledonian affinities in northern Ellesmere Island. Canadian Journal of Earth Sciences, Vol. 24, p.224-245.
- Trettin, H.P. and Frisch, T.O., 1981. Preliminary geological map and notes, Yelverton Inlet map area, District of Franklin. Geological Survey of Canada, Open File Report no.758.
- Trettin, H.P. and Mayr, U., 1981. Preliminary geological map and notes, parts of Otto Fiord and Cape Stallworthy areas, District of Franklin. Geological Survey of Canada, Open File Report no.757.
- Volk, H.R., 1980. Records of emergence around Gobleayah Bay and Neil Peninsula in connection with the Wisconsin deglaciation pattern, Ellesmere Island, N.W.T., Canada: a preliminary report. Polarforschung, Vol. 50, p.29-44.
- Wagner, F.J.E., 1969. Faunal study, Hudson Bay and Tyrell Sea. Geological Survey of Canada, Paper no.63-53, p.7-48.
- Walcott, R.I., 1970. Flexural rigidity, thickness and viscosity of the lithosphere. Journal of Geophysical Research, Vol.75, p.3941-3954.
- Wateren van der, D.F.M., 1985. A model of glacial tectonics applied to the ice pushed ridges in the central Netherlands. Bulletin of the Geological Society of Denmark, Vol. 34, p.55-74.

- Watts, S.H., 1986. Intensity versus duration of bedrock weathering under periglacial conditions in high arctic Canada. Biuletyn Peryglacjalny, Vol. 30, p.141-152.
- Weeks, W.F., 1976. Sea ice conditions in the Arctic. AIDJEX Bulletin, no.34, p.173-205.
- Weertman, J., 1961. Mechanism for the formation of inner moraines found near the edge of cold ice caps and ice sheets. Journal of Glaciology, Vol. 3, p.965-978.
- Weidick, A., 1976. Glaciations of northern Greenland - new evidence. Polarforschung, Vol. 46, p.26-33.
- Weidick, A., 1977. C^{14} dating of survey material carried out in 1976. Gronlands Geologiske Undersogelse Rapport, no. 85, p.127-129.
- Wilson, D.G., 1976. Eureka Sound and Beaufort Formations, Yelverton Bay, Ellesmere Island, District of Franklin. Geological Survey of Canada, Paper no.76-1A, p.453-456.
- Zingg, Th., 1935. Beitrag zur Schtteranalyse. Schweizerische Mineralogische und Petrologische Mitteilungen, Vol. 15, p.38-140.

APPENDIX 1

Radiocarbon dating

Previous dates from northern Ellesmere Island have been obtained almost exclusively by the conventional bulk sample method using a proportional gas counter. This technique involves the conversion of carbon to a gas and then the counting of β particles thus measuring the quantity of ^{14}C indirectly. The major problem with the conventional technique is that it requires a large volume of carbon and therefore very small but nonetheless important samples cannot be dated. Recent advances in mass spectrometry have enabled the accurate dating of very small samples by measuring the concentrations of individual ions. All of the dates in this thesis were obtained by accelerated mass spectrometry in the Isotrace Laboratory at the University of Toronto.

There are three main advantages to AMS dating: first, the size of the sample required; second, the shorter time required for dating; third, the possible extension of the range of ^{14}C dating from 45,000 to 90,000 years (cf. Blake 1985). However, there are problems in dating marine shells regardless of technique. Because shells are composed primarily of calcium carbonate in the metastable crystal form of aragonite, they are most susceptible to contamination by modern carbon. The aragonite can dissolve and then be redeposited as the stable crystal, calcite. During this process an exchange of modern carbon takes place. Therefore, shells >25,000 years old are generally regarded as infinite even though there is a remote possibility that the date is accurate (cf. Bradley 1985).

To account for fractionation effects all ^{14}C dates are usually normalized to -25‰ for $\delta^{13}\text{C}$ which remedies an age anomaly of approximately 400 years. However, for marine shells another correction is usually made for the apparent age of sea water which for high latitudes is averaged at 750 ± 50 years. This correction is made in the opposite direction to the $\delta^{13}\text{C}$

correction thus reducing the correction deficiency to 350 years. The Geological Survey of Canada correct to $\delta^{13}\text{C}=0.0\%$ for marine shells and to $\delta^{13}\text{C}=-25\%$ for other material. Because the majority of ^{14}C dates from the high Arctic originate from the G.S.C., the same corrections were made to the dates from the Isotrace Laboratory thus enabling regional correlation. Clearly dates within the field area are internally consistent.

APPENDIX 2
Clast analyses.

Fifty clasts from specific sample sites were analysed for the following: Zingg shape in which clasts were measured along their three principal axes; A the longest axis, B the largest cross section perpendicular to axis A, and C the short diameter of the pebble also perpendicular to axis A. Zingg's (1935) particle shape analysis is discussed in Krumbein (1941).

Zingg's shape classifications.

Class	B/A	C/B	Shape
I	$>2/3$	$<2/3$	Disks
II	$>2/3$	$>2/3$	Spheres
III	$<2/3$	$<2/3$	Blades
IV	$<2/3$	$>2/3$	Rods

Powers-roundness which is a visual scale where photographs of clay models are used to classify clasts in the field. There are six roundness classifications: very angular; angular; sub-angular; sub-rounded; rounded; and well-rounded. This scale is discussed in Powers (1953).

Striations were noted for each clast in order to ascertain the percentage of glacially modified clasts per sample set. Clasts with stoss and lee (bullet) forms and/or multiple striations were also noted (cf. Boulton 1978; Sharp 1982).

Twenty-nine sample sets were recorded in the field and they are arranged here by location and sample number. Descriptions of site and material/englacial position are noted also. All samples are then reproduced

graphically. For discussion see Chapters 4, 5 and 6.

Abbreviations: S= striated, N= non-striated. Dark shade= stoss and lee.

ms= clasts with multiple striations.

S, R, D, B = sphere, rod, disk, blade.

VA, A, SA, SR, R, WR= Powers roundness classes.

Lith %= lithology percentages. SS= sandstone, CG=

conglomerate, SL= slate, Q= quartz, B= basalt, C=

calcareous, M= marble, D= diorite, G= greenschist, P=

pegmatite, SC= schist, GB= gabbro.

Endeavour Glacier.

5-7-871 Diamicton flows in front of Endeavour Glacier. Lith.%: SS 68, CG 12, SL 10, Q 8, B 2.

5-7-872 Gravels overlying stagnant ice in front of Endeavour Glacier. Lith.%: SS 70, SL 22, Q 6, C 2.

5-7-873 Augen structure in snout cliff of Endeavour Glacier. Lith.%: SS 28, SL 60, Q 10, C 2.

Sediments.

6-7-871 Subaqueous fan sediments in section at Cache Head Fiord. Lith.%: SS 16, CG 4, SL 48, Q 8, M 16, D 8.

6-7-872 Till veneer at 79m above Cache River, south of Cache Head Fiord. Lith.%: SS 26, SL 18, Q 6, M 14, D 36.

6-7-873 Till veneer at 112.5m above sample 6-7-8702. Lith.%: SS 32, CG 8, SL 4, Q 8, B 12, C 8, M 8, D 6, G 2.

6-7-874 Diamicton/till below marine sediments at Cache Head Fiord, north of sample 6-7-8701. Lith.%: SS 22, CG 6, SL 16, Q 6, B 6, M 38, D 6.

7-7-871 Diamicton overlying silts, sands and gravels in alluvial fan

- section, east bank of Cache River. Lith.%. CG 16, SL 22, B 12, C 6, M 36, D 8.
- 7-7-872 Subaqueous fan sediments, east bank of Cache River. Lith.%. CG 2, SL 38, Q 2, M 52, D 4, GB 2.
- 17-7-871 Diamicton with shell fragments at >140m, lower Bushmill Pass. Lith.%. SS 16, SL 34, B 4, M 40, SC 6.
- 17-7-872 From kame delta in Bushmill Pass. Lith.%. SS 26, SL 18, Q 6, M 36, SC 12, GB 2.
- 17-7-873 Abandoned lateral moraine of Terrible Glacier, Bushmill Pass. Lith.%. SS 22, SL 30, B 4, M 38, SC 4, GB 2.
- 17-7-874 Talus cone on lateral moraine of sample 17-7-8703. Lith.%. SS 4, B 16, C 10, M 66, SC 4.
- Terrible Glacier.
- 14-7-871 From basal ice facies with small augens in snout cliff of Terrible Glacier. Lith.%. SS 12, SL 70, Q 4, M 12, SC 2.
- 14-7-872 From cone on wasting snout of Terrible Glacier in englacial ice facies. Lith.%. SS 22, CG 2, SL 74, M 2.
- 14-7-873 From stratified cone on wasting snout of Terrible Glacier in englacial ice facies. Lith.%. SS 12, SL 64, Q 4, B 2, C 2, M 2, SC 14.
- 14-7-874 Augen structure in snout cliff of Terrible Glacier, from basal ice facies. Lith.%. SS 2, SL 92, Q 4, B 2.
- 14-7-875 From diamicton cone slumping from augen structure in englacial ice facies in cliff of Terrible Glacier. Lith.%. SS 14, SL 44, Q 2, B 4, M 28, SC 8.
- 14-7-876 From cone overlying dead ice adjacent to sample 14-7-8705. Lith.%. SS 8, SL 56, Q 4, B 2, M 20, SC 6, GB 4.
- 16-7-871 From gravel terrace at lateral margin of Terrible Glacier. Lith.%. SS 18, SL 42, Q 2, B 4, M 18, SC 16.

16-7-872 From augens in englacial ice facies in lateral cliff of Terrible Glacier. Lith. %: SS 10, SL 80, Q 2, B 2, C 2, SC 4.

16-7-873 Gravel lens between overridden stagnant ice and englacial ice facies, lateral cliff of Terrible Glacier. Lith. %: SS 14, SL 38, B 4, M 36, P 2, SC 6.

16-7-874 From gravel bench partially overridden by Terrible Glacier, upstream of sample 16-7-8703. Lith. %: SS 6, SL 54, M 36, SC 6.

16-7-875 Gravel bed in basal ice facies above large meltwater cave in lateral cliff of Terrible Glacier. Lith. %: SS 6, SL 54, B 4, M 32, P 2, SC 2.

16-7-876 Slumping diamicton with shell fragments at >140m, margin of Terrible Glacier. Lith. %: SS 16, SL 60, Q 4, M 16, P 2, SC 2.

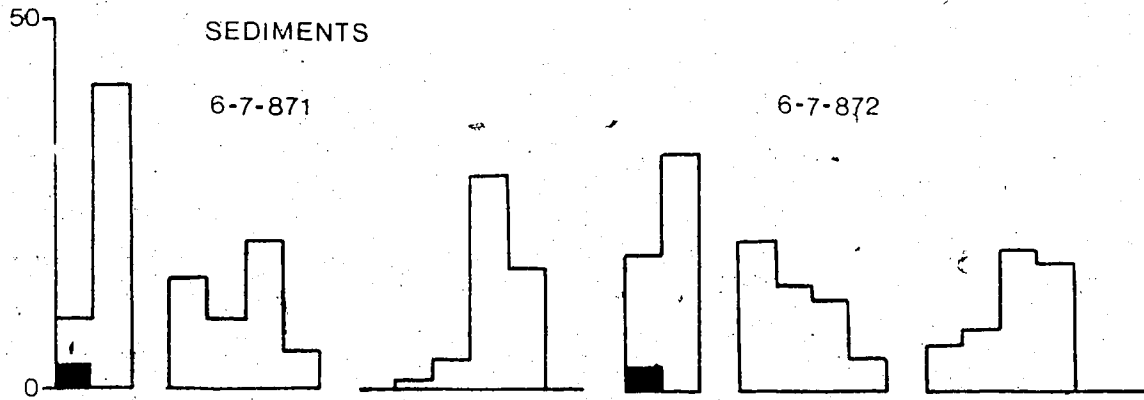
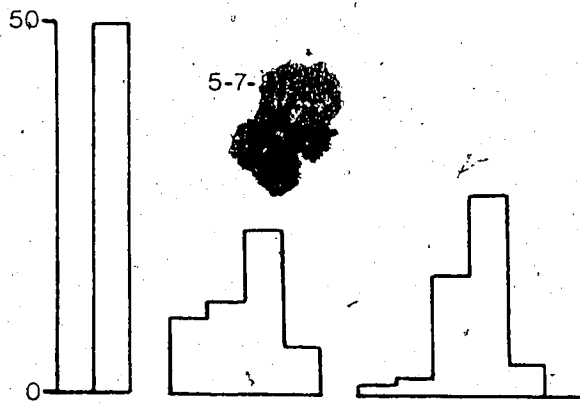
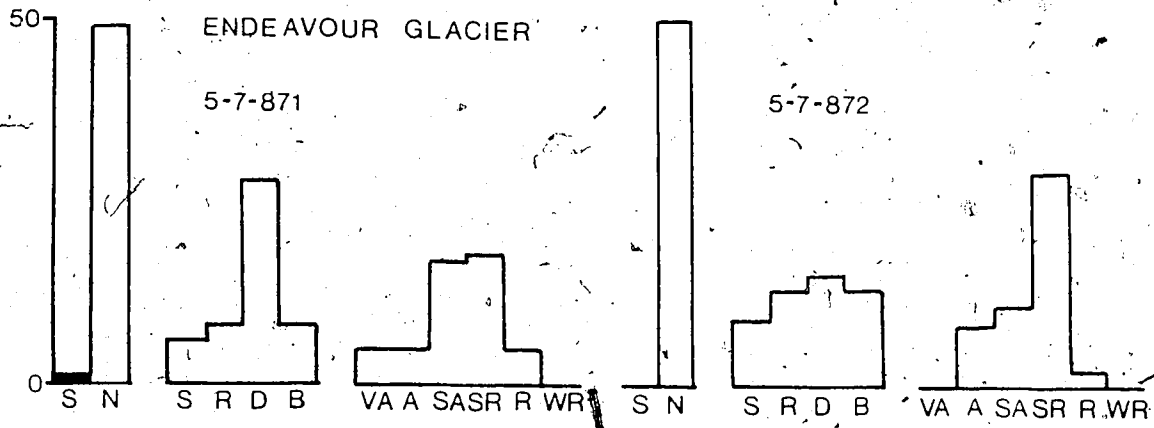
Dogleg Glacier.

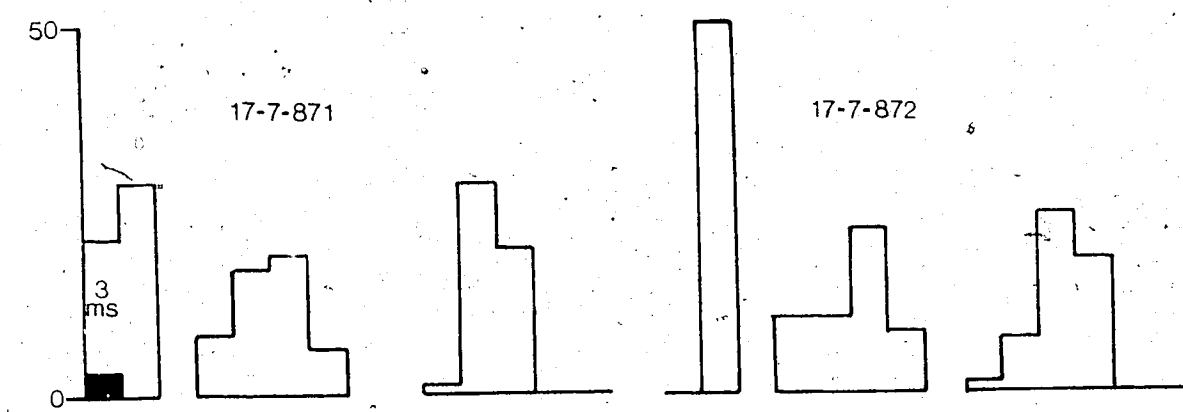
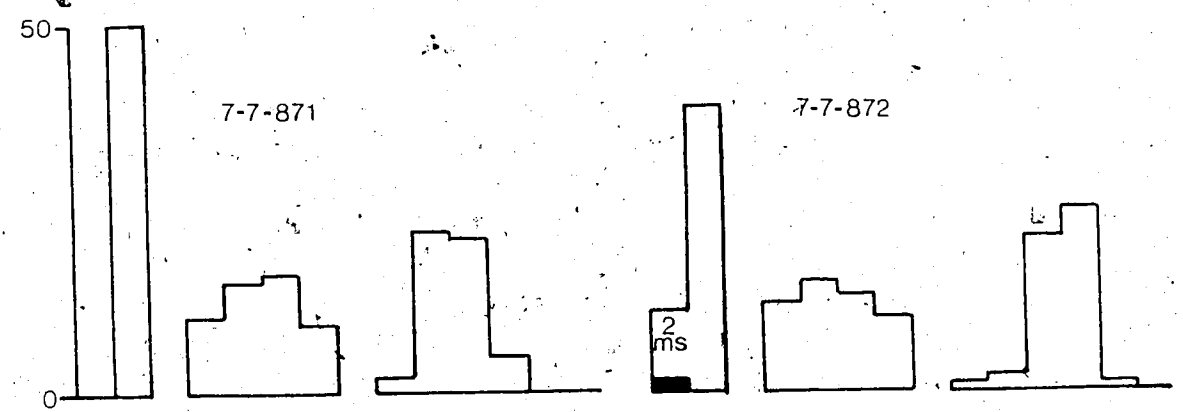
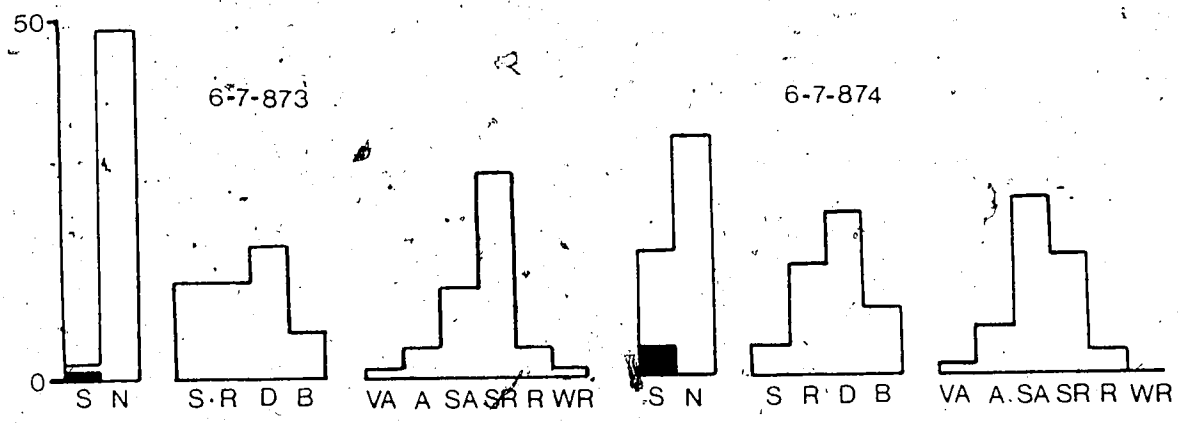
24-7-871 From basal ice facies, Dogleg Glacier. Lith. %: SL 12, M 4, P 84.

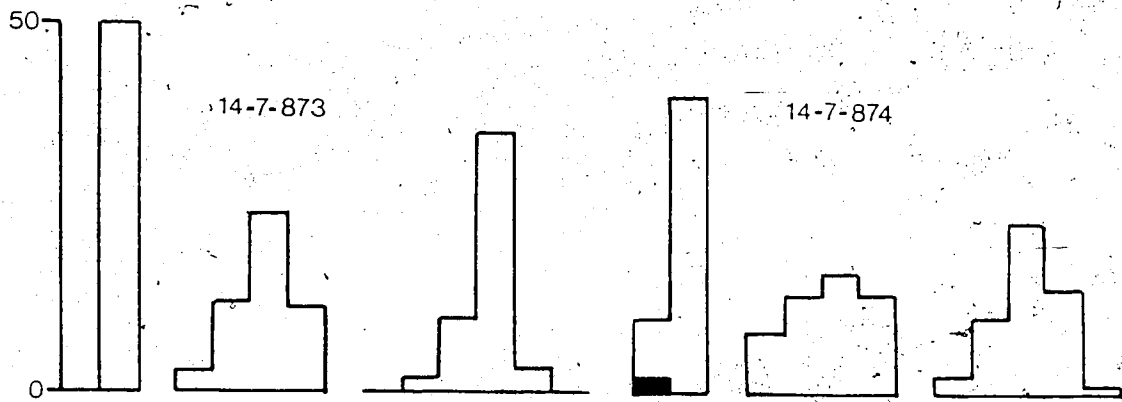
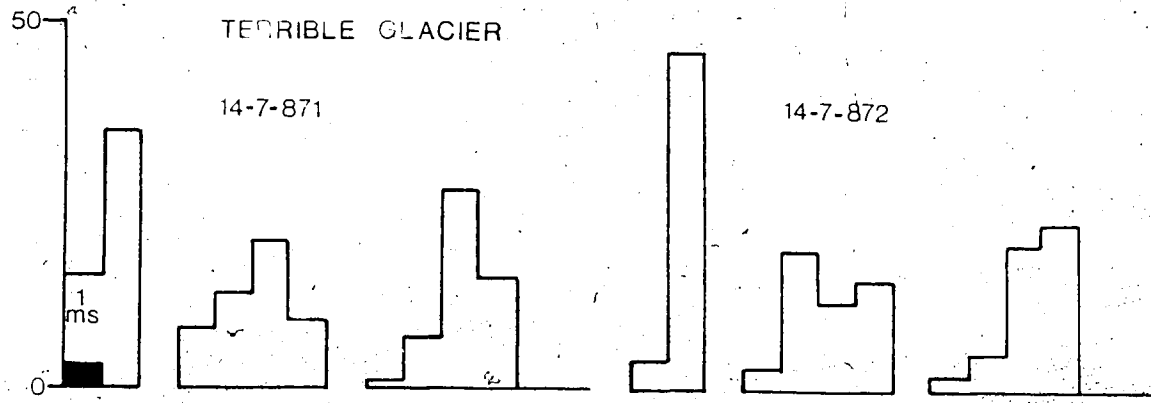
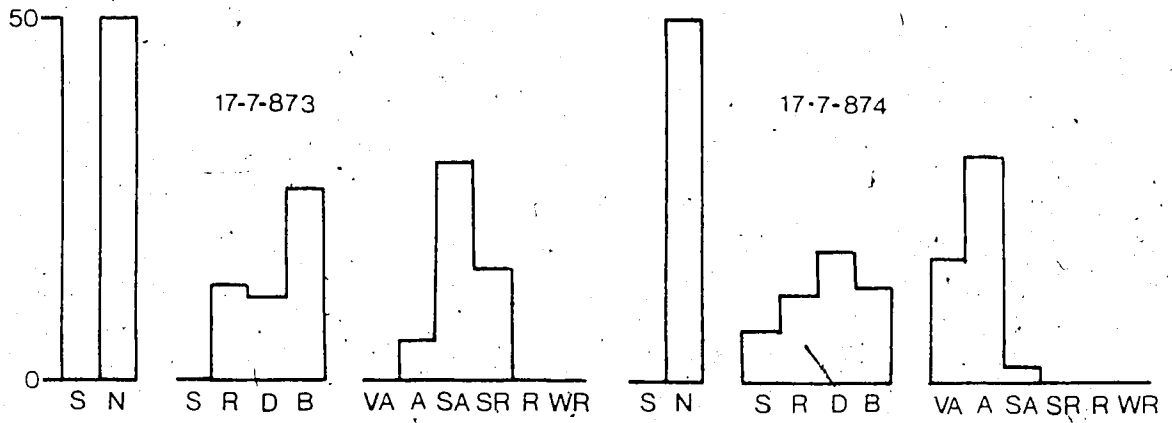
24-7-872 From basal ice facies at lateral margin of Dogleg Glacier. Lith. %: SL 2, B 8, M 16, P 70, SC 4.

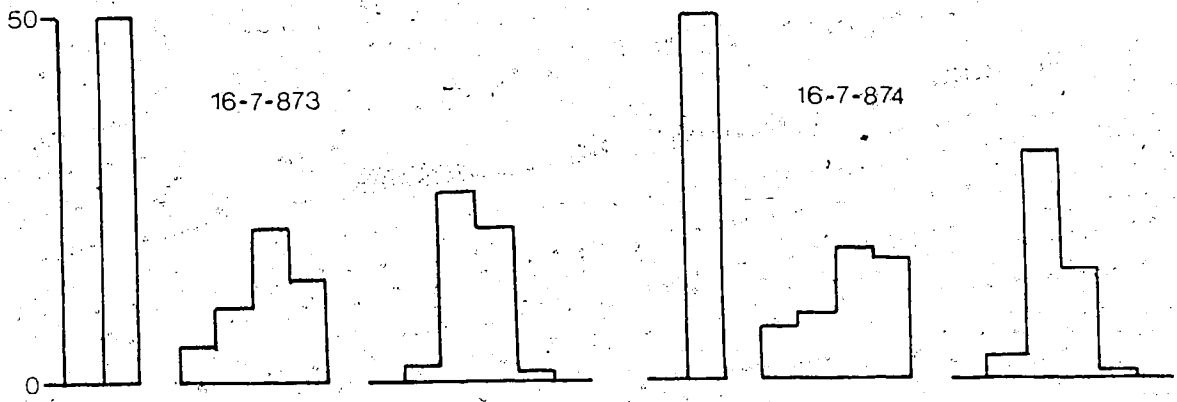
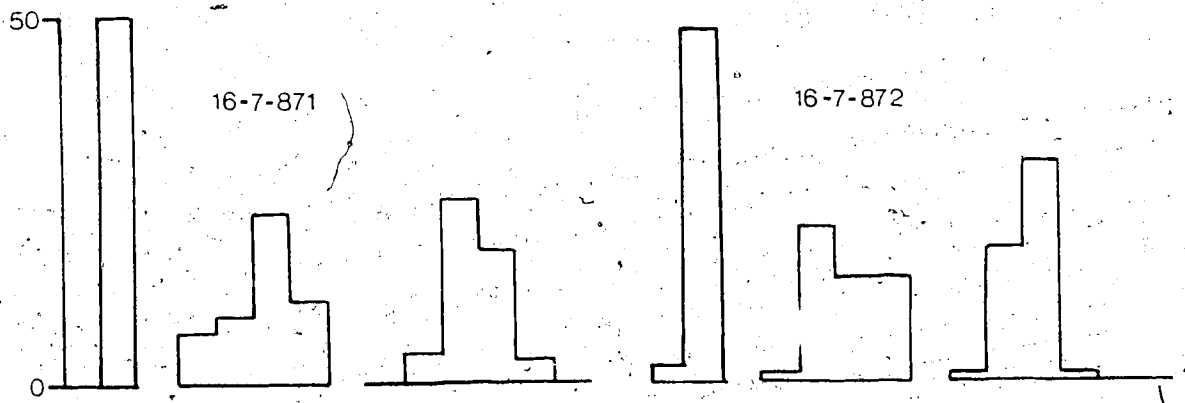
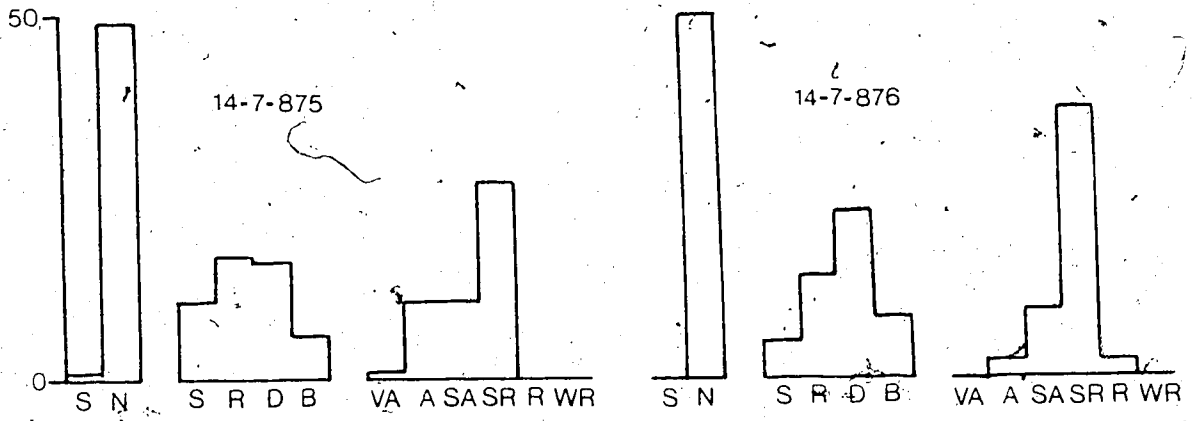
24-7-873 From thrustured alluvium in front of Dogleg Glacier. Lith. %: SS 2, SL 60, Q 2, B 2, M 4, P 26, SC 4.

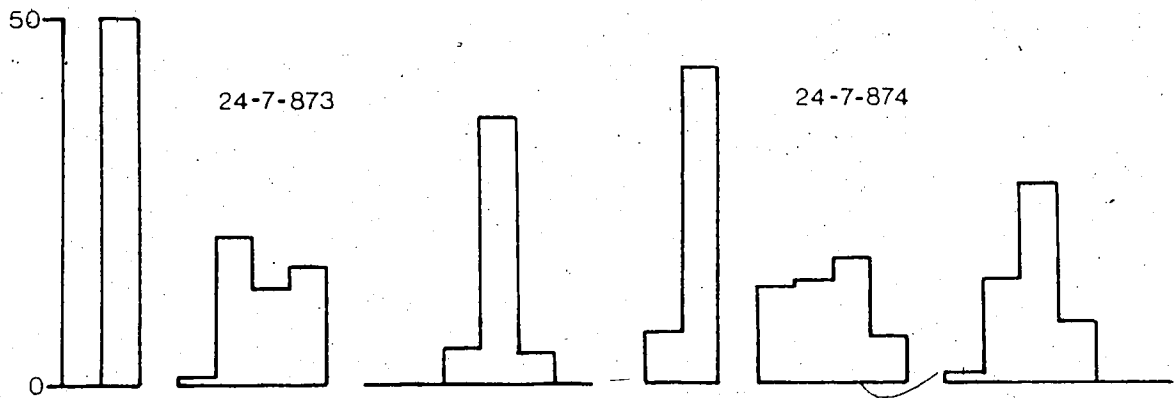
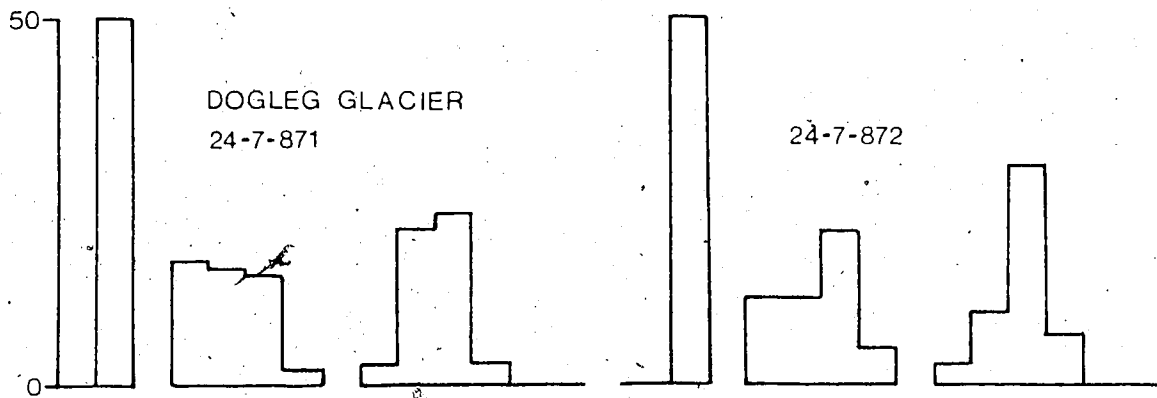
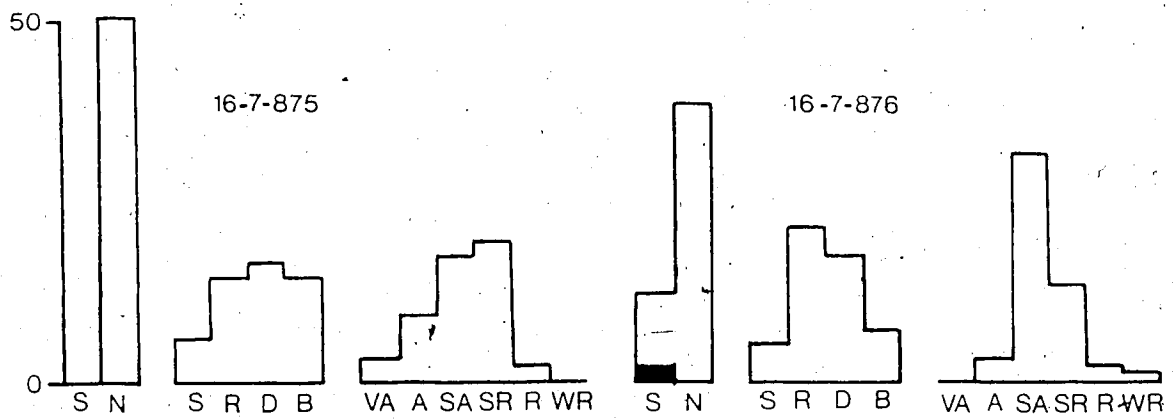
24-7-874 From basal ice facies at snout of Dogleg Glacier. Lith. %: SL 34, Q 4, B 8, M 10, P 34, SC 10.











APPENDIX 3

Glossary of glacioisostatic terms

Equidistant diagram: a diagram drawn orthogonal to the local isobases with the elevations of dated shorelines plotted against distance. This shows the extent and geometry of crustal rebound. Such a diagram can be reproduced only if shorelines are well dated at progressively lower elevations. It is assumed that a synchronous shoreline rises in the direction of maximum former ice thickness, hence such diagrams are relevant to determining the style of the last glaciation.

Eustatic sea level change: a sea level change caused by variations in the water stored on the land by ice sheets. This was originally thought to be globally uniform hence a universal correction was adopted for specific time intervals. This has since been abandoned after the work of Clark et al. (1978) who reconstructed zones of differential sea level change around the globe based on a hydroisostatic model that took the deformation of the ocean basins into consideration. Northern Ellesmere Island lies within their Zone I and I/II transition (see section 3.3.2).

Forebulge: an area of positive displacement extending ca.200km beyond an ice sheet margin due to the rigidity of the crust. The distance at which this occurs is a product of the flexural parameter (α)x1.89 (Walcott 1970). The forebulge beyond the Laurentide Ice Sheet was estimated to be ca.18m in height and ca.200km in width occurring beyond the outer edge of the peripheral depression. During deglaciation the forebulge collapses and migrates slowly towards the former ice centre (cf. Brotchie and Sylvester 1969; Walcott 1970; Clark et al. 1978; Quinlan and Beaumont 1981). At any site the migration of the forebulge can cause either emergence followed by submergence or continuous submergence, depending on location relative to the forebulge crest.

Ice-contact delta: a delta exhibiting characteristics of an ice-contact

environment. For example, a pitted surface suggests deposition over stagnant ice and a steep up-stream slope or escarpment indicating an ice-contact face. Intercalated glacial diamictos and delta sediments also indicate ice contact conditions. These deltas record sea level either at full glacial or immediate deglacial conditions at a specific site (ie. increased sediment influx as a result of increased ablation).

Isobase: an line joining points of equal emergence over an equal amount of time. Isobases are normally drawn on shorelines of a specific age and they contour the differential emergence of them towards the area of maximum former ice thickness. See also equidistant diagram. The amount of rebound shown by isobases on northern Ellesmere Island is minimal between 11 and 8ka BP, slow between 8 and 6.2ka BP and rapid after 6.2ka BP (see Figs.1.4 and 1.5).

Marine limit: the maximum elevation attained by the sea on a glacioisostatically depressed coastline. This can be recorded by beaches, deltas or other landforms such as washing limits or the lowermost elevation of glacially perched boulders. The regional marine limit marks the highest level reached by the sea in the whole field area while the local marine limit refers to the sea level attained on a deglaciated terrain (ie. deglacial shoreline). Generally the elevation of marine limit decreases in elevation and age as one crosses from the full glacial sea to sites inside the last ice limit. Those sites inside the last ice limit are lower because some emergence occurred beneath the thinning ice prior to its retreat and the entry of the sea.

Peripheral depression: the depression of the lithosphere extending ca.200km beyond an ice sheet margin. This occurs during glacioisostatic loading of the crust because the lithosphere is rigid. If glacioisostatic equilibrium is attained at the coastal margin of an ice sheet then the marine fauna within the peripheral depression would cover a wide range of ages corresponding to the duration of the loading. England (1983) refers to this occupancy of the peripheral depression as the "full glacial sea". Within the

area of the peripheral depression the marine limit rises in elevation towards the former ice margin. Behind the ice margin the marine limit falls due to restrained rebound. Within the peripheral depression the transgression to the marine limit caused by glacial loading during ice advance occurs much more slowly than the later transgression inside the ice limit where it is dictated by the sudden retreat of ice. Therefore, in the full glacial sea a complete transgressive sedimentary sequence should be preserved (ie. onlap not overstep). However, sediments tend to be retained within terrestrial drainage basins during full glacial conditions due to the decrease in runoff *vis-a-vis* reduced ablation. Also, whether the sea transgressed to marine limit in the peripheral depression during the last glaciation of the high Arctic remains to be documented (England 1983).

Postglacial emergence: the upward displacement of the land relative to the sea following deglaciation. This is dependent upon ice thickness and the distance of the site from the ice margin (cf. Andrews 1970).

Relative sea level curve: a diagrammatic representation of emergence or submergence throughout postglacial time in relation to present sea level. These are constructed using datable strandlines and marine limits at a specific site.

Restrained rebound: a term referring to the amount of glacioisostatic unloading that occurred beneath an ice mass prior to deglaciation of a site. Therefore, this emergence is not recorded by sea level. Behind former ice margins the marine limit will fall in elevation accordingly because it records successively smaller amounts of unloading.

Strandline: the trimline of a former water body indicated by various landforms including beaches, deltas and washing limits. Because these require some time to form, sea level has to be either stationary with respect to the land and/or sediment influx has to be high. In Arctic Canada it is usually the latter. Although strandlines have been used to indicate progradation of

U
sediments during glacial stillstands (cf. Andrews 1970) it has been demonstrated that proglacial sedimentation is reduced during a glacial advance in arid high latitude environments (cf. Rains et al. 1981). The principal climatic control in these environments is aridity, hence glacial advance requires reduced ablation/run off. However, ice contact deltas and strandlines associated with a moraine provide good chronologic indicators of initial deglaciation and emergence.